รายงานการวิจัย

ระบบนิเวศวิทยาเชิงคณิตศาสตร์ Mathematical Ecology

ยงค์วิมล เลณบุรี ภาควิชาคณิตศาสตร์ คณะวิทยาศาสตร์ มหาวิทยาลัยมหิดล

รายงานการวิจัย

ระบบนิเวศวิทยาเชิงคณิตศาสตร์ Mathematical Ecology

ยงค์วิมล เลณบุรี ภาควิชาคณิตศาสตร์ คณะวิทยาศาสตร์ มหาวิทยาลัยมหิดล

กิตติกรรมประกาศ

โครงการวิจัยได้รับทุนอุดหนุนการวิจัยจากสำนักงานกองทุนสนับสนุนการวิจัย

ประเภท ทุนพัฒนานักวิจัย

ประจำปี 2538 - 2540 (รอบที่ 1)

ปีที่พิมพ์ 2540

บทคัดย่อ

แบบจำลองทางคณิตศาสตร์ของระบบนิเวศน์ของสิ่งมีชีวิตประเภทเคียว (single species) หรือสองประเภทในลักษณะของผู้ล่าและเหยื่อ (predator-prey) ได้ถูกนำมาดัดแปลง เพื่อคำนึงถึง ผลกระทบของแฟกเตอร์ตัวที่สาม เช่น ผลกระทบจากการแปรเปลี่ยนของสนามแม่เหล็กโลกต่อความ สามารถในการส่งผ่านสารอาหารของเนื้อเยื่อเซล หรือผลกระทบจากพยาธิต่อความสามารถในการล่า เหยื่อ หรือผลกระทบจากสารพิษต่อความสามารถในการสืบพันธุ์ และคำรงชีวิตอยู่ของสิ่งมีชีวิตใน สิ่งแวดล้อมปิด

แบบจำลองที่ได้เป็นสมการเชิงอนุพันธ์ไม่เชิงเส้น 3 สมการ โดยการวิจัยแบ่งเป็นสี่ขั้นตอน คือ ขั้นตอนแรก คำนึงถึงการเปลี่ยนแปลงในแฟคเตอร์ที่สามเมื่อเวลาเปลี่ยนแปลงไป จึงมีสมการ อนุพันธ์ของแฟคเตอร์ที่สามรวมอยู่ด้วย เป็นหนึ่งในสามสมการ ซึ่งประกอบขึ้นเป็นแบบจำลอง

ขั้นตอนที่สอง ไม่มีสมการของการเปลี่ยนแปลงในแฟกเตอร์ที่สาม แต่เบ่งกลุ่มของเหยื่อออก เป็นสองกลุ่ม คือ กลุ่มของ susceptible prey กับกลุ่มของ infective prey

ขั้นตอนที่สาม ไม่มีสมการของการเปลี่ยนแปลงในแฟคเตอร์ที่สาม แต่แบ่งกลุ่มของผู้ล่าออก เป็นสองกลุ่ม คือ กลุ่มของ susceptible predator กับกลุ่มของ infective predator

ขั้นตอนที่สี่ คำนึงถึงการเปลี่ยนแปลงของแฟคเตอร์ตัวที่สาม ซึ่งเป็นปริมาณของสารพิษ โดย แบ่งออกเป็นสองกลุ่ม คือ ปริมาณของสารพิษในสิ่งแวดล้อม กับปริมาณของสารพิษในประชากร

การวิเคราะห์กระทำโดยใช้ทฤษฎีทาง bifurcation และเทคนิคของ singular perturbation ซึ่ง ทำให้เราสามารถเข้าใจการทำงานของระบบที่กำลังศึกษาได้ดีขึ้น ทั้งเพิ่มความสามารถในการควบคุม ดูเล และจัดการระบบนั้น ๆ ให้ดำเนินไปตามที่เราต้องการ ผลของการวิจัยจึงจะสามารถมีประโยชน์ อย่างมากในเชิงสิ่งแวดล้อม

Abstract

Mathematical models of ecosystems involving single species or two species, namely a predator-prey system, are modified to incorporate the effect of an external force or a third factor. This can be the effect of the geomagnetic field variation on the cell membrane permeability in an activated sludge process, or the effect of parasite invasion of a predator-prey system, or the effect of toxicants on the population in a closed environment.

The resulting models consist of three nonlinear ordinary differential equations. The research project is organized into mainly 4 stages. In the first stage, variation in the third factor with time is taken under consideration in the form of one of the three differential equations which comprise the model.

In the second stage, the variation in the third factor is not taken into the model, while the prey population is divided into two groups; namely, the susceptible prey and the infective prey.

In the third stage, the variation in the third factor is still not taken into the model, while the predator population is divided into two groups; namely, the susceptible predator and the infective predator.

In the fourth and final stage, the third factor, which is the level of toxicants in this case, is divided into two groups; namely, the level of toxicant in the environment, and that in the population.

Analysis of the models are carried out using either the bifurcation theory or the singular perturbation technique. The study allows us to better understand the systems under study as well as learn how to manage and control them more efficiently. The results of our study should therefore yield valuable insights which has far reaching repercussions on the environmental problems we are facing today.

สารบัญเรื่อง

		หน้า	
กิตติกรรมประกาศ		ก	
บทคัดย่อ (ภาษาไทย)		ข	
บทคัดย่อ (ภาษาอังกฤษ)		ค	
สารบัญเรื่อง	.*	1	
สารบัญภาพ		3	
บทนำ		4	
รายละเอียคและผลการวิจัย		12	
การวิจัยช่วงที่ 1 ผลงานที่ได้ตีพิมพ์เรื่อง	Dynamic Behavior of a Membrane Permeability Sensitive Model for a Continuous Bio-Reactor Exhibiting Culture Rhythmicity	13 17	
ผลงานที่ได้ตีพิมพ์เรื่อง	Bifurcation and Chaos in a Membrane Permeability Sensitive Model for a Continuous Bioreactor	21	
ผลงานที่เสนอในการประชุมเรื่อง A Singular Perturbation Analysis of a Product			
	Inhibition Model for Continuous Bio-Reactors	23	

			หน้า
ผลงานที่ submi	tted for p	publication เรื่อง Modelling Effects of High Product and	
		Substrate Inhibition on Oscillatory Behavior in Continuous	
		Bioreactors	24
การวิจัยช่วงที่ 2			25
ผลงานที่ได้ตีพิว	มพ์เรื่อง	Singular Perturbation Analysis of a Model for a Predator-prey	
		System Invaded by a Parasite	27
ผลงานที่เสนอใ	นการประ	ะชุมเรื่อง How Can Nonlinear Dynamics Elucidate Mechanisms	
		Relevant to Issues of Environmental Managemant and	
		Global Change	28
ผลงานที่เสนอในการประชุมเรื่อง Singular Perturbation Analysis of a Model for the			
		Effect of Toxicant in Single-Species Systems	38
ผลงานที่ใค้ตีพิว	มพ์เรื่อง	Dynamical Modelling of the Effect of Toxicants on a	
		Single-Species Ecosystem	39
สรุปและข้อเสนอแ	นะ		40
สรุป Output ของโ	ครงการ		41
บรรณานุกรม			43
ประวัตินักวิจัย			53

สารบัญภาพ

		หน้า
รูปที่ 1	คำตอบของ LV equations ซึ่งมีลักษณะกวัดแกว่ง (oscillation)และเป็นคาษ	. 9
รูปที่ 2	คำตอบของ LV equations ซึ่งมีสักษณะกวัดแกว่ง (oscillation)และเป็นคาบ	10
รูปที่ 3	คำตอบของแบบจำลองของ food web สามารถมีลักษณะของ limit cycle	
	์ ซึ่งมีความถี่ต่ำ และเกิด burst ของการกวัดแกว่งความถี่สูงขึ้นภายในทุก ๆ	
	รอบของความถี่ต่ำ (จาก Y. Lenbury and C. Likasiri, Mathl. Comput.	
	Modelling 20 (1994) 71)	11
รูปที่ 4	คำตอบเชิงตัวเลขของระบบสมการ (5)-(7) บนระนาบ (x,y)	
	ซึ่งแสคงลู่ทาง(trajectory)ซึ่งมุ่งเข้าสู่การหมุนเวียนบนผิวของ 2-torus โคย	
	$M = 1$, $\gamma = 1$, $\beta = 1.5$, $\theta = 0.6$, $y_s = 1.5$, $d = 0.375$, $\delta = 2.1$,	
	$x_s = 7.875, \; \rho = 1.3125, \; Z_0 = 5.7, \; \omega = 1/12$	15
รูปที่ 5	แสดงคำตอบ x(t) ของระบบสมการ (5)-(7) โดย	
	$M = 1$, $\gamma = 1$, $\beta = 1.5$, $\theta = 0.6$, $y_s = 1.5$, $d = 0.375$, $\delta = 2.1$,	
	$x_s = 7.875, \; \rho = 1.3125, \; Z_0 = 5.7, \; \omega = 1/12 \; \text{uat } \alpha = 1$	16
รูปที่ 6	Bifurcation diagram	20
รูปที่ 7	รูปร่างของ equilibrium manifolds ของระบบสมการ (42)-(44) ใน 5 กรณี	
	ที่กล่าวไว้ในเนื้อหา	32
รูปที่ 8	คำตอบเชิงตัวเลขของระบบสมการ (42)-(44) เมื่อเลือกค่าพารามิเตอร์	
	ให้สอคคล้องกับเงื่อนไขของกรณีที่ 1	33
รูปที่ 9	คำตอบเชิงตัวเลขของระบบสมการ (42)-(44) เมื่อเลือกค่าพารามิเตอร์	
	ให้สอคกล้องกับเงื่อนไขของกรณีที่ 2	34
รูปที่ 10	คำตอบเชิงตัวเลขของระบบสมการ (42)-(44) เมื่อเลือกค่าพารามิเตอร์	
	ให้สอดคล้องกับเงื่อนไขของกรญีที่ 3	35

บทน้ำ

ความสำคัญและที่มาของปัญหาที่ทำการวิจัย

ประเทศไทยเป็นหนึ่งในหลาย ๆ ประเทศที่กำลังพยายามพัฒนาทางเศรษฐกิจและเทคโนโลยี ให้ก้าวรุคหน้าไปอย่างรวดเร็ว และต้องประสบกับปัญหาของสิ่งแวคล้อมที่กำลังจะเสื่อมลงอย่างน่า เป็นห่วง รวมทั้งปัญหาการจัดการกับปฏิกูลของเสีย (waste management) ซึ่งเป็นผลพวงของความ เจริญก้าวหน้าทางเศรษฐกิจและอุตสาหกรรม ดังที่ประเทศที่เจริญแล้วหลาย ๆ ประเทศได้ประสบมา แล้ว และต่างก็ยอมรับว่าเป็นปัญหาสำคัญที่ต้องให้ความสนใจอย่างจริงจัง ก่อนที่จะสายเกินไป

นักวิชาการย่อมประจักษ์ดีว่า เราต้องทำการวิจัยค้นคว้าในเรื่องระบบต่าง ๆ เชิงนิเวศวิทยาไป พร้อม ๆ กับการพัฒนาทางเทคโนโลยี เพื่อที่ประเทศชาติจะไม่ต้องเผชิญหน้ากับปัญหาด้านสิ่ง แวดล้อมที่ร้ายแรงในภายหน้า โดยที่ไม่มีการตระเตรียมไว้ล่วงหน้าเพื่อรับสถานการณ์ดังกล่าวอย่างมี ประสิทธิภาพ เนื่องจากมิได้สนับสนุนให้มีการวิเคราะห์วิจัย เพื่อให้เกิดความเข้าใจที่คีพอเกี่ยวกับ ระบบนิเวศวิทยาต่าง ๆ ที่จะได้รับผลกระทบจากการพัฒนาด้านเทคโนโลยีและอุตสาหกรรม ทั้งมิได้ มีการค้นคว้าหาวิธีการขจัดปัญหาต่าง ๆ ที่จะเกิดขึ้นนั้นอย่างมีประสิทธิภาพ

การวิจัยด้านแบบจำลองทางกณิตศาสตร์ของระบบต่าง ๆ ในเชิงนิเวศวิทยา เป็นวิธีหนึ่งที่จะ ทำให้เราสามารถเกิดความเข้าใจที่ดีขึ้น เกี่ยวกับระบบที่เรากำลังศึกษา ทั้งยังทำให้เราได้ภาพรวมของ เหตุการณ์ และความเป็นไปได้ทั้งหมดที่อาจจะเกิดขึ้นในระบบที่กำลังศึกษาอยู่

ขบวนการที่เป็นหัวใจสำคัญขบวนการหนึ่ง ของการศึกษาด้านนิเวศวิทยา คือ ระบบซึ่งสิ่งมี ชีวิตสองชนิดล่าจับเหยื่อหรือสารอาหาร (prey) ชนิดเดียวกันเป็นอาหาร (competition) ระบบดัง กล่าวจะพบใด้ในธรรมชาติสิ่งแวดล้อมรอบตัวเราโดยทั่วไป ไม่ว่าจะเป็นเสือกับสิงโตที่ต่างก็ล่ากวาง เป็นเหยื่อ หรือเหยี่ยวกับนก magpie ที่ต่างก็กินหนอนและแมลงเป็นอาหาร ตัวอย่างตั้งเดิมของ competition ระหว่าง 2 species คือ feeding process ของ barnacles สองชนิด คือ Chthamalus และ Balanus (J. Connell, Ecology 42 (1961) 710) ซึ่งพบว่ามีพฤติกรรมที่น่าสนใจหลาย ๆ แบบ

แบบจำลองของ competing species นี้ มีรากฐานมาจาก model ของ feeding process ระหว่าง 2 species ซึ่งเป็นระบบผู้ล่ากับเหยื่อ (predator-prey) โดยมีกลไกของการจับกินเหยื่อที่ขึ้นอยู่กับความ หนาแน่น (density dependent) ซึ่งได้มีผู้อธิบายโดยใช้สมการซึ่งเรียกกันว่า Lotka-Volterra (LV) equations (A.J. Lotka, Essays on Growth and Form, Oxford U. Press, New York (1945)). สมการ ดังกล่าวสามารถอธิบายและกำหนดเงื่อนไขที่ species หนึ่งจะสูญพันธุ์ หรือเงื่อนไขที่ทั้งสอง species

สามารถอยู่ร่วมกันได้ (persistence) นอกจากนั้น ยังสามารถหาเงื่อนไขที่สมการคังกล่าวจะมีคำ ตอบที่เป็นคาบ (limit cycle behavior)

ผลงานเกี่ยวกับระบบที่ 2 species แย่งกินเหยื่อชนิดเดียวกันเป็นอาหาร ที่สำคัญและเป็นที่อ้าง ถึงโดยทั่วไป คือผลงานของ Volterra (V. Volterra, R. Commun. Talassografico Italiano. (1927)1-142) หากแต่ Volterra model นั้นมีขีดจำกัดหลายประการ เช่น amplitude of oscillation ของคำตอบ จะไม่แน่นอน ทั้งยังมีความไม่เสถียร (structurally unstable) อีกด้วย

ภายใต้เงื่อนไขบางประการ Hopf bifurcation จะสามารถเกิดขึ้นใน LV equations ได้ ก่อให้ เกิดเป็น limit cycles ดังที่เห็นได้ในรูปที่ 1 และรูปที่ 2 ซึ่งระบบ predator - prey นี้มักจะใช้กล่าวถึง สัตว์บก เช่น แมวป่ากับกระต่ายในประเทศแคนาดา (C. Elton and M. Nicholson, J. Anim. Ecol. 11 (1942) 215) แต่ก็สามารถใช้อธิบายปรากฏการณ์ระหว่างสัตว์น้ำกับ algae (M.L. Rosenzweig, Science 175 (1972) 564) หรือนกกับแมลง หรืออื่น ๆ อีกได้มากมาย รวมทั้งสามารถใช้อธิบายระบบ เชิงชีววิทยา ที่ใช้ในการขจัดของเสีย (สารอาหาร-แบคทีเรีย-โปรโตซัว) ซึ่งเป็นวิธีขจัดของเสียในน้ำ ทิ้ง จากโรงงานต่าง ๆ ที่มีผู้หันมานิยมใช้มากขึ้นกว่าการขจัดโดยขบวนการทางเคมี เนื่องจากการใช้ ขบวนการทางเคมีเพื่อขจัดของเสียจะทำให้เกิดปฏิกูลจากสารเคมีที่ใช้ในขบวนการนั้นเพิ่มขึ้นในสิ่ง แวคล้อม อันเป็นสิ่งที่เราไม่พึงประสงค์เป็นอย่างยิ่ง

ได้มีผู้ทำการวิจัยถึงแฟกเตอร์ตัวอื่น ๆ ที่มีผลกระทบกับระบบ predator-prey มาเป็นเวลา นานพอสมควร เช่นผลกระทบจากยาฆ่าแมลง (insecticides) ปุ๋ย (fertilizer) ซึ่งเปลี่ยนแปลงความทรง ตัวที่ดี (balance) ระหว่าง predator (ผู้ล่า) และ prey (เหยื่อ) ไม่นานมานี้ Freedman (H.I. Freedman, Math. Biosc. 99 (1990) 143) ได้ทำการศึกษาระบบ predator-prey โดยปรับเปลี่ยนเพื่อคิดถึงผลของ พยาธิ (parasites) ซึ่ง infect ทั้ง predator และ prey ในเวลาเดียวกัน ซึ่ง Freedman ได้ทาเงื่อนไข ซึ่ง ทำให้ประชากรทั้งหมดอยู่ร่วมกันต่อไปได้ (persistence) และเงื่อนไขที่ประชากรบาง species จะ สูญพันธุ์ (extinct) หลังจากนั้น Nhung และ Anh (T.V. Nhung and T.T. Anh, preprint IC/93/391 ICTP) นำผลของ Freedman ไปปรับเปลี่ยนโดยคิดว่าแต่ละเผ่าพันธุ์ (population) สามารถแบ่งได้เป็น 2 กลุ่ม คือ susceptible group และ infective group นั่นคือ กลุ่มที่ยังไม่โดน infect โดย parasites จะ มีความสามารถในการล่าเหยื่อ (หรือเจริญเติบโต) แตกต่างไปจากกลุ่มที่โดน infect แล้ว ดังปรากฏ ใน model system ต่อไปนี้

$$\begin{split} \dot{S}(t) &= B(X) - \frac{D(X)S(t)}{X(t)} - \left[\beta_0 + \beta_1 Y_2(t)\right] S(t) - \frac{Q_1(X)SY_1(t)}{X(t)} - \frac{P_1(X)SY_2(t)}{X(t)} \\ \dot{I} &= \left[\beta_0 + \beta_1 Y_2(t)\right] S - \frac{D(X)I(t)}{X(t)} - \frac{Q_2(X)I(t)Y_2(t)}{X(t)} - \frac{P_2(X)I(t)Y_2(t)}{X(t)} \\ \dot{Y}_1 &= -\Gamma(Y)Y_1 - \gamma_0 IY_1 - \gamma_1 Y_1 Y_2 + C \frac{Q_1 SY_1}{X} + C_1 \frac{P_1 SY_2 + Q_2 IY_1 + P_2 IY_2}{X} \\ \dot{Y}_2 &= -\Gamma(Y)Y_2 + \gamma_0 IY_1 + \gamma_1 Y_1 Y_2 + (C - C_1) \frac{P_1 SY_2 + Q_2 IY_1 + P_2 IY_2}{X} \end{split}$$

โดยที่ $S(t), I(t), X(t) = S(t) + I(t), Y_1(t), Y_2(t), Y(t) = Y_1(t) + Y_2(t)$ คือ susceptible prey, infective prey, prey ทั้งหมด, susceptible predator, infective predator, และ predator ทั้งหมด ตาม ลำคับ

Nhung และ Anh. ก็ได้กำหนดเงื่อนไขที่ทำให้เกิด persistence และ extinction ของแต่ละ กลุ่ม เช่นเคียวกัน ทั้งนี้เขากล่าวว่า model นั้นควรเหมาะสมที่จะใช้กับระบบ predator-prey ที่พบได้ ในประเทศเวียตนาม เช่น เหยี่ยว กับ magpie ซึ่งต่างก็มีพยาธิ flukes หรือ เสือกับหมูป่า ซึ่งต่างก็มี พยาธิ Tapeworms เป็นต้น ทั้งนี้ model system ของ Nhung และ Ahn ประกอบด้วยสมการของอัตรา การเปลี่ยนแปลงของ prey และ predator เท่านั้น โดยไม่ได้คิดถึงการเปลี่ยนแปลงใน factor ตัวที่สาม แต่ประการใด

ในผลงานที่กล่าวมาข้างต้นนี้ ยังไม่ได้มีการศึกษาหาความเป็นไปได้ที่จะเกิด limit cycle behavior จาก bifurcation analysis แต่อย่างใด ซึ่งการที่มีแฟคเตอร์ที่สามมาเป็นอีกแรงหนึ่งที่เปลี่ยน แปลง dynamics ของระบบ predator-prey นี้ ควรจะก่อให้เกิด limit cycle behavior ในลักษณะต่าง ๆ ที่น่าสนใจยิ่งกว่าที่พบในรูปที่ 1 และรูปที่ 2

ในผลงานชิ้นหนึ่งของผู้วิจัย ซึ่งได้รับตีพิมพ์ในวารสารนานาชาติแล้ว (Y. Lenbury and C. Likasiri, Mathematical and Computer Modelling, 20(1994)71) ผู้วิจัยได้ศึกษาระบบห่วงโซ่อาหาร ซึ่งมี species ที่สามเป็น superpredator จับกินทั้ง prey และ predator เป็นอาหาร ซึ่งมี model เป็น ระบบสมการต่อไปนี้

$$\begin{split} \dot{p} &= -\mathrm{D}p + \nu(b)p + \eta(s)p \\ \dot{b} &= -\mathrm{D}b + \mu(s)b - \frac{1}{X}\nu(b)p \\ \dot{s} &= \mathrm{D}(s_0 - s) - \frac{1}{V}\mu(s)b - \frac{1}{Z}\eta(s)p \end{split}$$

โดยที่ p(t), b(t), s(t) คือ superpredator, predator, และ prey ตามลำดับ

ผู้วิจัยได้ใช้ singular preturbation method และ separation conditions หาเงื่อนไขที่กำตอบ ของแบบจำลองจะมีลักษณะเป็นคาบ โดยมีความถี่ต่ำ และหาเงื่อนไขที่กำตอบ จะมีลักษณะเป็น limit cycle ที่มีความถี่ต่ำ แต่แทรกด้วย oscillations ที่มีความถี่สูง เป็นช่วง ๆ (bursts of high frequency oscillations) ดังที่เห็นได้ในรูปที่ 3 คำตอบที่มีลักษณะที่สับสนเช่นนี้ สามารถอธิบายปรากฏการณ์ ของ eco-systems ต่างๆ ที่เราต้องการศึกษาได้เป็นอย่างคื โดยมันบอกให้เราเข้าใจยิ่งขึ้นถึงการที่ใน วงจรหนึ่งจะแบ่งได้เป็น 2 ฤดู คือ rich season กับ poor season

ในระหว่าง rich season นั้น prey (เหยื่อ) มีอยู่เป็นจำนวนมาก ผู้ล่าทั้ง predator และ superpredator สามารถล่าเหยื่อเป็นอาหารได้อย่างสะควกสบาย ทำให้มีการเพิ่มจำนวน หรือลด จำนวนลงอย่างคล่องตัว (high - frequency) เกิดเป็น oscillations ที่มีความถี่สูง จนกระทั่ง prey ลด จำนวนลงไปอย่างมาก เกิดเป็น poor season prey มีจำนวนน้อยมากและสามารถเพิ่มจำนวนขึ้นได้ อย่างเชื่องช้า (low-frequency) predator และ superpredator ก็จะลดจำนวนลงด้วย เนื่องจากขาด แคลนเหยื่อที่เป็นอาหาร เมื่อเวลาผ่านไปเหยื่อได้มีเวลา regenerate ก็จะกลับเข้าสู่ rich season และ fast dynamics อีกครั้งหนึ่ง

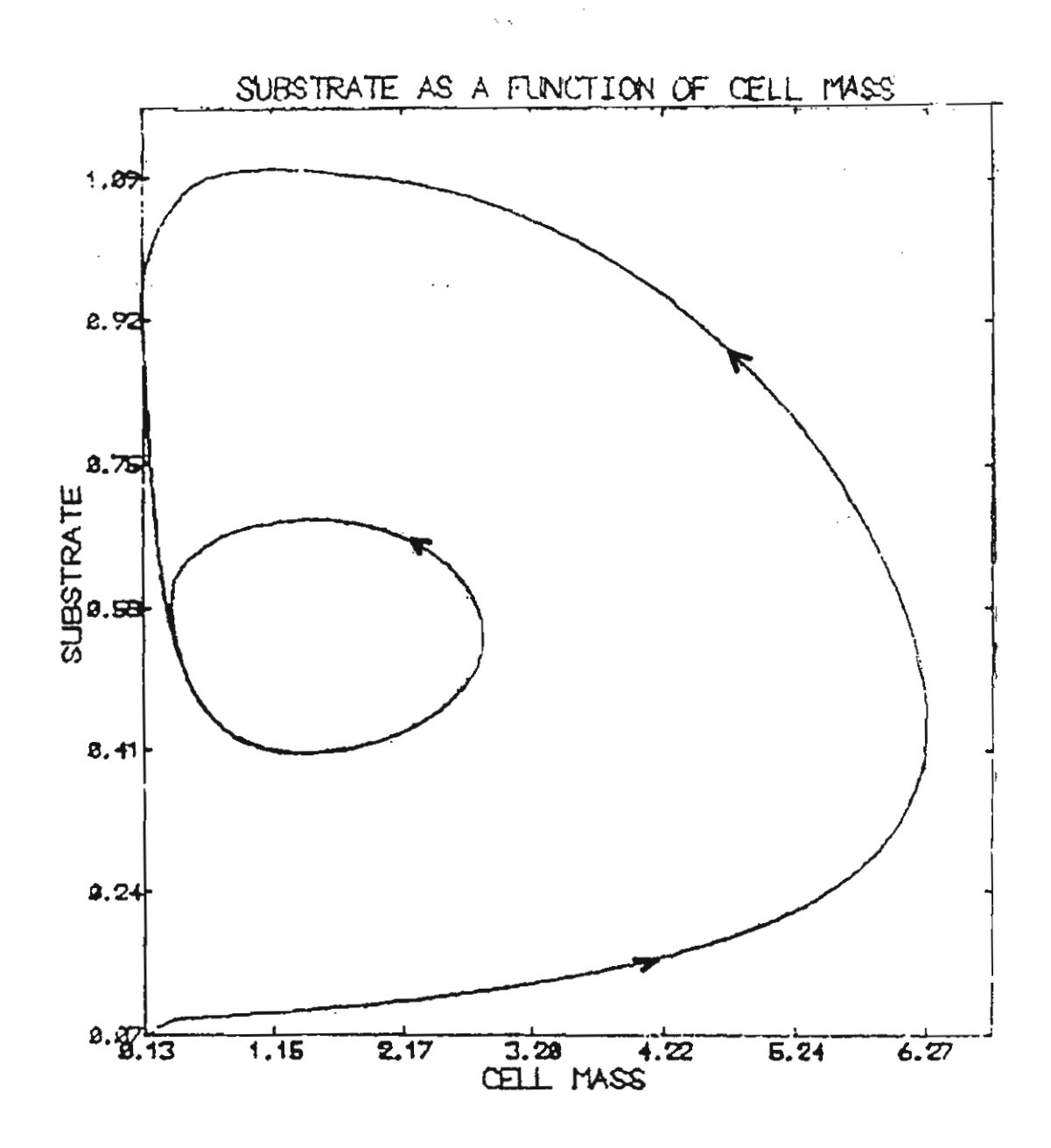
ความเข้าใจที่ได้จากการวิเคราะห์แบบจำลองทางคณิตศาสตร์เช่นนี้ มีประโยชน์ในหลาย ๆ ด้าน ถ้าเราจะสามารถคาดได้ว่า poor season นั้น จะมีขึ้นในช่วงใด เราจะสามารถทิ้งระยะการล่าเหยื่อ ในช่วงดังกล่าว เพื่ออำนวยให้ species ที่ใกล้จะสูญพันธุ์ได้มีเวลา regenerate นอกจากนั้นเรา อาจสามารถใช้กลไกของ species ที่สาม ซึ่งใช้ทั้ง prey และ predator เป็นอาหาร กับเรื่องของการ ปลูกข้าว (prey) ซึ่ง ถูกบ่อนทำลายด้วยตัวแมลง (predator) ชนิดใดชนิดหนึ่ง เราอาจจะสามารถนำ superpredator ซึ่งกินทั้งแมลงและข้าวเป็นอาหารมาช่วยขจัดแมลง โดยกำหนดเงื่อนไขให้แมลงถูก ขจัดหมดไปก่อนที่ข้าวจะถูก superpredator ใช้เป็นอาหาร จนหมดไป เช่นนี้เป็นต้น ทั้งนี้แบบจำลอง ของคลื่นอาหารที่เคยทำการศึกษาที่ผ่านมาข้างต้น ยังไม่ได้คิดถึงลักษณะที่ poputation มีการแบ่งแยก เป็น susceptible และ infective group แต่ก็จะเห็นได้ว่า การวิเคราะห์วิจัยแบบจำลองทางคณิตศาสตร์ ของระบบต่าง ๆ เช่นนี้ จะเพิ่มขีดความสามารถในการจัดการ (manage) สิ่งแวดล้อมอย่างมี ประสิทธิภาพมากขึ้น

บทพื้นฐานของ model ของ Nhung และ Anh ผู้วิจัยจึงทำการวิเคราะห์ แบบจำลองของ ระบบ predator-prey ซึ่งมีลักษณะการแบ่งแยกเป็น susceptible และ infective group โดยใช้ Singular Perturbation Method เพื่อศึกษาลักษณะคำตอบต่าง ๆ ของ model system โดยใช้ response functions ลักษณะต่าง ๆ เช่น เป็น function เชิงเส้น (linear) หรือเป็นฟังก์ชัน แบบ Holling เป็นต้น เพื่อจะสามารถนำ model ดังกล่าวไปดัดแปลงให้รวมถึงผลกระทบของการเปลี่ยนแปลงจำนวนของ factor หรือ force ตัวที่สามต่อไป

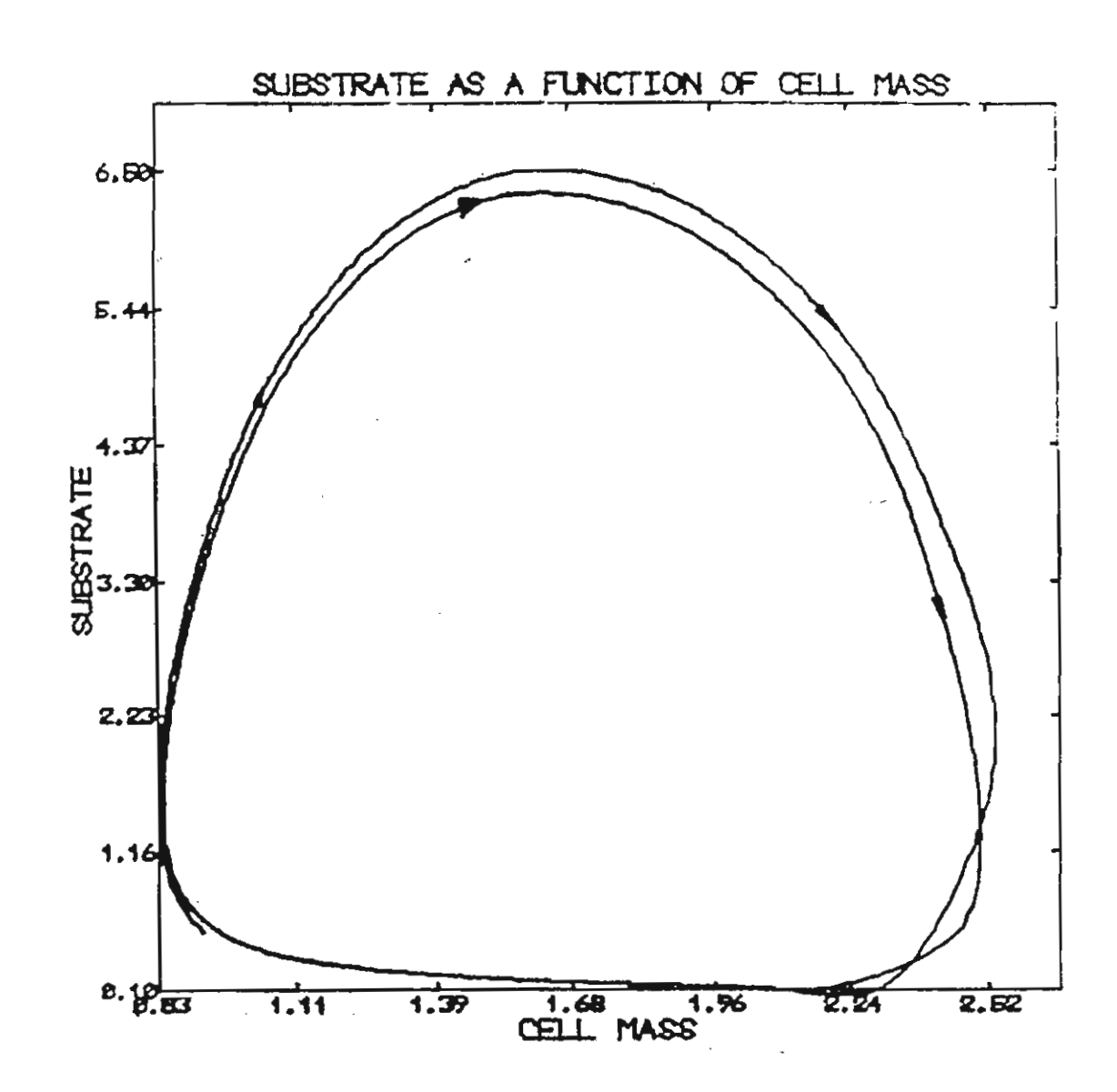
นอกจากนั้นยังได้ดัดแปลง ปรับปรุง model predator-prey เพื่อรวมผลกระทบของการ เปลี่ยนแปลงใน "third force" ซึ่งอาจจะเป็น parasites หรือ พันธุ์สัตว์ชนิดที่ 3 (superpredator) หรือ third force อื่น ๆ ที่จะมีผลทำให้ขีดความสามารถในการล่าเหยื่อและการขยายพันธุ์ ของ 2 species แรกนั้นเปลี่ยนแปลงไป โดยที่ susceptible และ infective groups จะมี dynamics ที่ต่างกัน ทั้งนี้ จะ พิจารณาการ incorporate ผลจาก force ที่ 3 นี้ ในลักษณะต่าง ๆ กัน เพื่อพิจารณาสร้าง model ให้ เหมาะสมกับระบบ eco-systems ที่เราสนใจ

หลังจากนั้นจึงคำเนินการวิเคราะห์แบบจำลองที่พัฒนาขึ้น ด้วยทฤษฎีทางคณิตศาสตร์
(Theory of Differential Equations, Singular Perturbation Method, Bifurcation Theory) เพื่อหา เงื่อนไขของความอยู่รอดของทุก species และเงื่อนไขที่คำตอบในลักษณะต่าง ๆ จะเกิดขึ้นได้

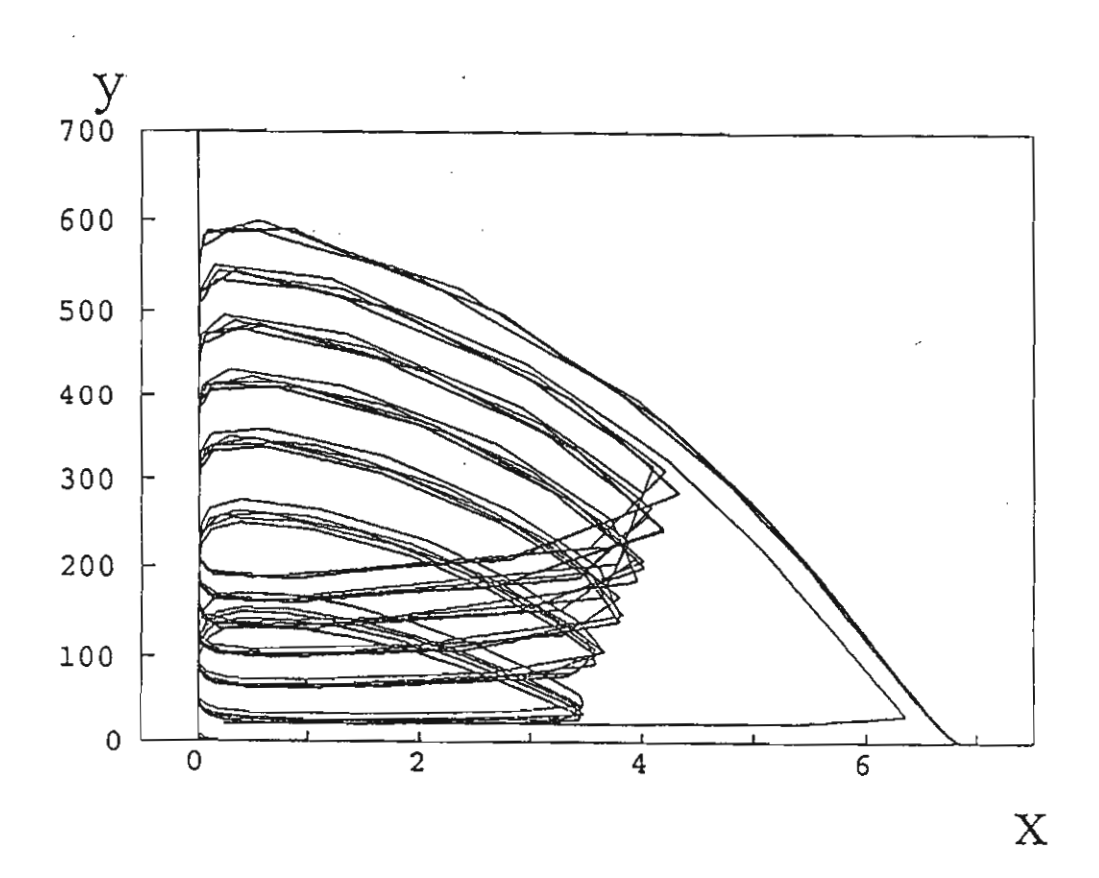
ในขั้นสุดท้ายจึงหาคำตอบเชิงตัวเลข (numerical simulation) ของแบบจำลอง เพื่อทดสอบ ผลการวิจัยทางทฤษฎีว่าถูกต้องหรือไม่ แล้วนำผลการวิเคราะห์ทางทฤษฎีไปแปลผลเพื่ออธิบาย eco-systems ที่ทำการศึกษา



รูปที่ 1 คำตอบของ LV equations ซึ่งมีลักษณะกวัดแกว่ง (oscillation)และเป็นคาบ



รูปที่ 2 คำตอบของ LV equations ซึ่งมีลักษณะกวัดแกว่ง (oscillation)และเป็นคาบ



รูปที่ 3 คำตอบของแบบจำลองของ food web สามารถมีลักษณะของ limit cycle ซึ่งมีความถี่ต่ำ และเกิด burst ของการกวัดแกว่งความถี่สูงขึ้นภายในทุก ๆ รอบของความถี่ต่ำ (จาก Y. Lenbury and C. Likasiri, Mathl. Comput.

Modelling 20(1994) 71)

รายละเอียดและผลการวิจัย

โครงการวิจัยนี้แบ่งออกเป็น 4 ช่วงย่อย ช่วงละประมาณ 9 เคือน โดยงานวิจัยในแต่ละช่วง เริ่มจากรากฐานของแบบจำลองทางคณิตศาสตร์ของระบบการแพร่พันธุ์ของสิ่งมีชีวิตหรือประชากร (population growth) อย่างง่าย ๆ ดังนี้

$$\frac{\mathrm{dx}}{\mathrm{dt}} = \mu \,\mathbf{x} - \mathbf{D}\,\mathbf{x} \tag{1}$$

โดยที่ x(t) คือ จำนวนประชากร ณ เวลา t ใด ๆ

μ คือ อัตราการเจริญเติบโตสัมพัทธ์ของประชากร x

D คือ อัตราการตายของประชากร x

ถ้าเราคิดถึงระบบของผู้ล่ากับเหยื่อ (predator-prey systems) และให้ S(t) เป็นปริมาณของ เหยื่อ หรือสารอาหรที่ x จับกินเป็นอาหาร ก็อาจจะเขียนแบบจำลองของระบบคังกล่าวได้คังนี้

$$\frac{dS}{dt} = D(S_F - S) - \frac{\mu(S)x}{v}$$
 (2)

$$\frac{\mathrm{dx}}{\mathrm{dt}} = \mu(S)x - Dx \tag{3}$$

โดย S_F คือความเข้มข้นหรือความหนาแน่นของ S ที่นำมาเพิ่มให้กับระบบที่กำลังศึกษาด้วย อัตราที่คงที่ ซึ่งอาจคิดได้ว่าเป็นอัตราการเคลื่อนย้าย (migration) ของ S เข้าสู่สังคมนิเวศน์ที่กำลังทำ การศึกษา

Monod เป็นผู้มีชื่อเสียงในการเสนอให้ specific growth rate μ(S) เป็นฟังก์ชันต่อไปนี้

$$\mu(S) = \frac{\mu_m S}{K + S} \tag{4}$$

โดยที่ µm คือ maximum specific growth rate

K คือ Monod constant

Y คือ yield coefficient ซึ่งเท่ากับอัตราการลคลงของ S ต่ออัตราการเพิ่มขึ้นของ x

ผู้วิจัยได้นำสมการ (1) หรือสมการ (2) และ (3) มาปรับปรุงเพิ่มเติมในลักษณะต่าง ๆ เพื่อ กิดถึงผลกระทบของแฟคเตอร์ภายนอก หรือแฟคเตอร์ตัวที่สาม โดยได้แบ่งการวิจัยเป็น 4 ช่วง ดังกล่าวแล้วข้างต้น ดังต่อไปนี้

การวิจัยช่วงที่ 1

1.1 ในช่วงนี้ผู้วิจัยได้นำแบบจำลองต้นแบบ (2) และ (3) มาปรับเปลี่ยนเพื่อคำนึงถึง ผลกระทบของ external force เช่น การแปรเปลี่ยนของ geomagnetic field ซึ่งมีผลทำให้ permeability P ความสามารถในการส่งผ่านสารอาหารผ่านผิวของเซล เปลี่ยนแปลงไปตามเวลา t และจะมีผลต่อ การใช้สารอาหาร S เพื่อการเจริญเติบโตของเซล x ทำให้ได้เป็นสมการอนุพันธ์ไม่เชิงเส้น 3 สมการ ดังนี้

$$\frac{dS}{dt} = -\frac{(c_1 x P + c_2)S}{(S + K_m)y} - D(S_F - S)$$
 (5)

$$\frac{\mathrm{dx}}{\mathrm{dt}} = \frac{(c_1 x P + c_2)S}{S + K_m} - Dx \tag{6}$$

$$\frac{dP}{dt} = -\gamma \cos(w_0 t) P - \frac{(\gamma_2 - P)(c_1 x P + c_2) S}{S + K_m}$$
 (7)

โดยที่ เทอมแรกในสมการ (7) เป็นอัตราการเปลี่ยนแปลงของ P ในลักษณะเป็นคาบ ซึ่ง derive ได้ จากการสังเกตความสัมพันธ์ระหว่าง P กับการเปลี่ยนแปลงใน geomagnetic field (Yerushalmi et al., 1989)

โดยใช้ bifurcation analysis ผู้วิจัยสามารถพิสูจน์ทฤษฎีบทต่อไปนี้ได้ ทฤษฎีบทที่ 1 ถ้า

$$\gamma > 0$$
 (8)

$$\beta \ge 1$$
 (9)

$$\frac{1}{\beta} > \theta > \frac{1 - \sqrt{\frac{\gamma}{\gamma + 1}}}{\beta} \tag{10}$$

$$\gamma > M > \frac{1 - \theta}{\theta} \tag{11}$$

โดยที่

$$\gamma = \frac{(z_S + d) M}{z_S^2 - M d}$$

$$\beta = \frac{\gamma_2 c_1}{D}$$

$$\theta = \frac{z_{S}}{M + z_{S}}$$

$$M = k_m$$

และ z_S คือค่าของ S ที่ steady state แล้วระบบสมการ (5)-(7) จะมีคำตอบเป็นคาบ ซึ่ง bifurcate จาก non-washout steady state สำหรับค่าของ δ ในช่วง (δ_c , δ_c + ϵ) โดยที่

$$\delta = \frac{(\beta x_S + \rho) M}{(M + z_S)^2} \tag{12}$$

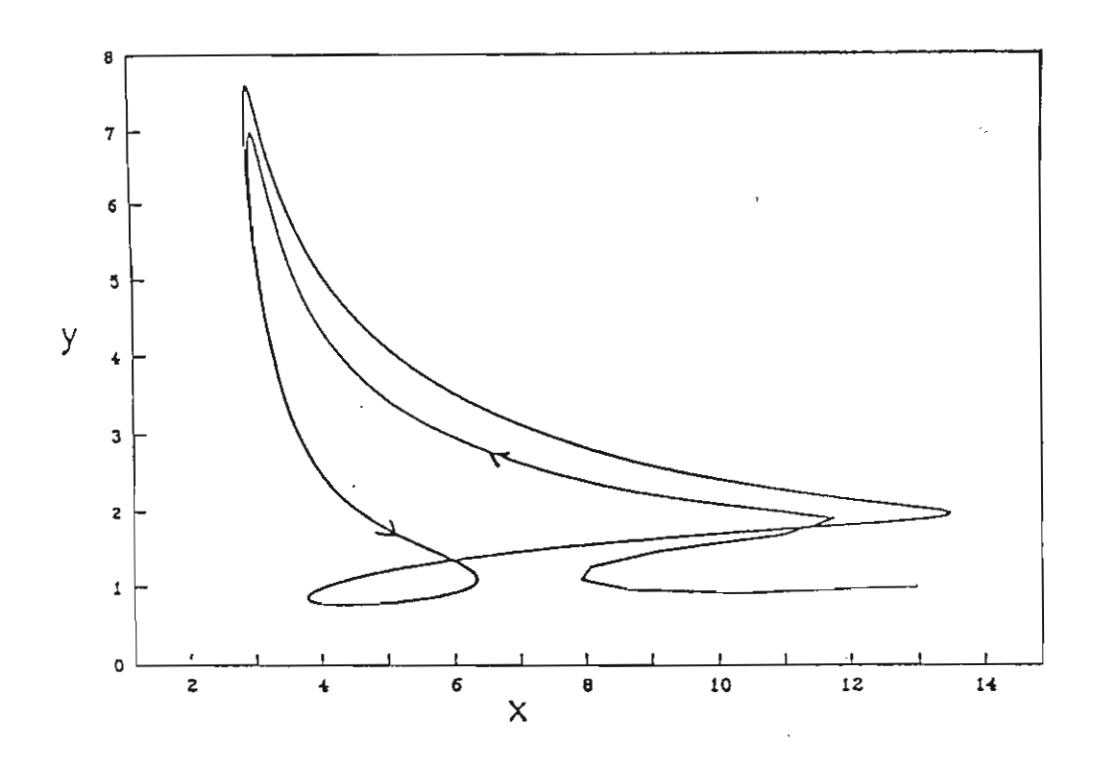
$$\delta_{c} = (2 - \beta \theta)(z_{S} + d)\gamma \tag{13}$$

$$\rho = \frac{c_2}{a D_2} \tag{14}$$

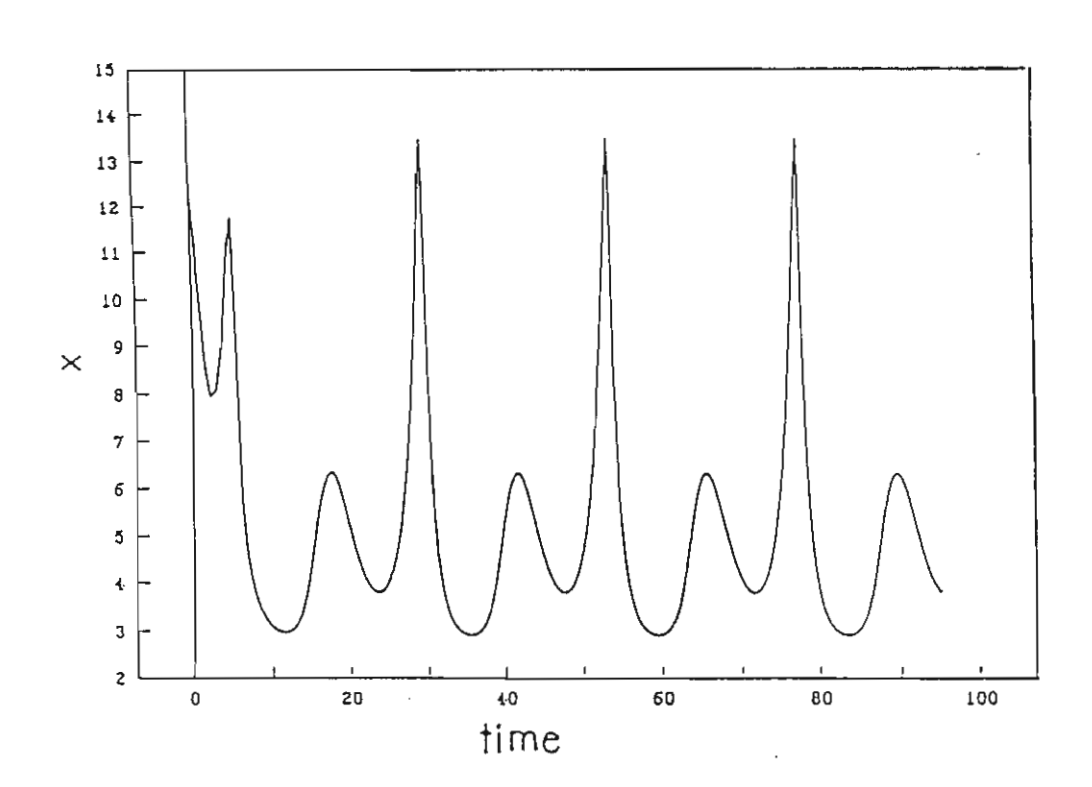
โดย bifurcation ที่เกิดขึ้นนี้จะซ้อนกับ periodic solution ที่ได้จาก eigenvalues $\pm w_0$ i ที่เกิดจากการ ที่ geomagnetic field มีการเปลี่ยนแปลงอย่างเป็นคาบอยู่แล้ว จึงจะได้คำตอบของระบบสมการ (5)- (7) เป็น periodic solution บนผิวของ 2-torus ดังที่แสดงในรูปที่ 4 และ 5 ซึ่งเทียบกับข้อมูลจากห้อง ทดลองแล้วมีลักษณะใกล้เคียงกันมาก แสดงว่าแบบจำลองที่ทำการวิจัยสามารถจำลองสิ่งที่เกิดขึ้นจริง ได้เป็นอย่างดี

การวิเคราะห์ด้วยทฤษฎีบทของ Hopf และผลของการหาคำตอบเชิงตัวเลขทำให้เราสามารถ บอกได้ว่า operating zone ใด เราจึงจะสามารถดำเนินงานปฏิกรณ์ (reactor) ได้อย่างปลอดภัย และ หลีกเลี่ยงบริเวณที่จะมีคำตอบแบบยุ่งเหยิงสับสนซึ่งไม่เป็นที่ต้องการได้ ทั้งนี้ reactor ในปฏิกรณ์ขจัด ของเสียซึ่งเป็นสารพิษมีอันตรายต่อสิ่งมีชีวิตได้เป็นอย่างมาก ทำให้ผลการวิเคราะห์วิจัยในลักษณะนี้ มีประโยชน์มากในการ monitor และ control ปฏิกิริยาใน reactor ให้ดำเนินการไปอย่างปลอดภัยและ มีประสิทธิภาพมากที่สุด

ผู้วิจัยได้นำผลงานวิจัยระบบสมการ (5), (6) และ (7) เขียนขึ้นเป็น paper และได้รับ published เรียบร้อยแล้วใน *J. Sci. Soc. Thailand* ซึ่งจะสามารถอ่านรายละเอียดของการวิจัยได้ใน manuscript ที่แนบมาด้วยต่อไปนี้



รูปที่ 4 คำตอบของระบบสมการ (5) - (7) บนระนาบ (x,y) ซึ่งแสดงลู่ท่าง (trajectory) ซึ่งมุ่งเข้าสู่การหมุนเวียนบนผิวของ 2-torus โดย $M=1,\ \gamma=1,\ \beta=1.5,$ $\theta=0.6,\ y_s=1.5,\ d=0.375,\ \delta=2.1,\ x_s=7.875,\ \rho=1.3125,\ Z_0=5.7,$ $\omega=1/12$ และ $\alpha=1$



รูปที่ 5 แสดงคำตอบ x(t) ของระบบสมการ (5)-(7) โดย $M=1,\,\gamma=1,\,\,\beta=1.5,\,\,\theta=0.6,$ $y_s=1.5,\,\,d=0.375,\,\,\delta=2.1,\,\,x_s=7.875,\,\,\rho=1.3125,\,\,Z_0=5.7,\,\,\omega=1/12$ และ $\alpha=1$

Dynamic Behavior of a Membrane Permeability Sensitive Model for a Continuous Bio-Reactor Exhibiting Culture Rhythmicity

DYNAMIC BEHAVIOR OF A MEMBRANE PERMEABILITY SENSITIVE MODEL FOR A CONTINUOUS BIO-REACTOR EXHIBITING CULTURE RHYTHMICITY

YONGWIMON LENBURY, SOMSAK ORANKITJAROEN

Department of Mathematics, Faculty of Science, Mahidol University, Rama 6 Rd., Bangkok 10400, Thailand.

(Received April 3, 1995)

ABSTRACT

A modified Monod model of a continuous microbial culture in which the yield term depends linearly on the substrate concentration is extended to incorporate the effect of external forces on the cell membrane permeability. Bifurcation analysis of the new mathematical model, which consists of three non-linear ordinary differential equations, shows that the model can simulate the oscillatory behavior observed in experimental data for certain ranges of the system parameters. Computer simulation of the model is presented in support of our theoretical predictions.

INTRODUCTION

Sustained oscillations in the patterns of microbial growth and product formation have been frequently observed in continuous cultures when the feed conditions and the culture conditions remain constant [1, 2]. According to Yerushalmi et al. [2], these oscillations are even more pronounced in the long term fermentations or in the cell-retention fermentations where the cells stay in the bio-reactor for long periods of time.

Although the mechanism for these oscillations is not yet fully understood, it is clear that occurrence of such oscillatory behavior has adverse effects on the efforts to optimize the operation of continuous bio-reactors. It also effects productivity of the process and complicates its proper design. It is therefore most important to investigate in depth the factors that cause such rhythmicities, the explanations for which range from experimental errors to the changing microbial physiological behavior often attributed to changes in the cellular metabolic pathway under certain conditions. Recent studies of the parameter affecting the cell physiology of *C. acetobutylicum* showed a high sensitivity of growth and solvent production to the cytoplasmic membrane permeability [2]. A high permeability of the cytoplasmic membrane promotes the growth of the microbial culture, the utilization of the substrate and the biosynthesis of the solvents. The opposite result is obtained with a low permeability of the cell membrane.

The controlling action of the cellular membrane permeability on the activities in many anaerobic processes has been frequently observed. Examples include the influence of plasma-membrane lipid composition and membrane fluidity on growth and solute accumulation by S. cerevisiae [3], growth of Clostridium thermccellum [4], and growth and production of ethanol and glycerol by yeast cultures [5].

In this paper, we consider a mathematical model which incorporates this sensitivity to the cellular membrane permeability, the specific rate of change of which is assumed to vary in a sinusoidal fashion. One physical controlling factor which has been proposed to exert its biological effect on the cytoplasmic membrane permeability is the geomagnetic field variation. This concept has been extensively investigated and is well supported by experimental evidence [6, 7]. Attempts to incorporate such effects into a model of the continuous microbial culture was carried out by Yerushalmi et al. [2]. We consider a modification of their model based on an adaptation of the Monod model in which the yield term is assumed to vary linearly with the substrate concentration. Through bifurcation analysis, the model is shown to simulate different oscillatory behavior observed in experimental data.

SYSTEM MODEL

Basically, microbial kinetics have varied in diverse ways from a model due to Monod fashioned after Michaelis-Menten kinetics for single enzyme-substrate reactions. This simple but valuable model views microbial growth as conversion of a fixed amount of substrate (or nutrient) to biomass occurring autocatalytically in the presence of preexisting biomass [8]. The yield coefficient Y in the Monod's model is constant. The most obvious departure of the predictions of Monod's model, apparently, is in the variation of the stoichiometric coefficient Y. Theoretical studies of models in which the yield term varies linearly with the substrate concentration can be found in the work of Agrawal et al. [8] and that of Lenbury et al. [9]. In [8], Agrawal et al. carried out an extensive theoretical investigation of the dynamic behavior of isothermal continuous stirred tank biological reactors modelled by the following mass balance equations on cells and the limiting substrate:

$$\frac{dS}{dt} = -\sigma(S)X + D(S_0 - S) \tag{1}$$

$$\frac{dX}{dt} = \mu(S)X - DX \tag{2}$$

where X denotes the cells concentration; S the substrate concentration; $\mu(S)$ the specific growth rate; $\sigma(S)$ the specific substrate consumption rate; S_0 the feed substrate concentration; and D the dilution rate.

In their work, the function $\sigma(S)$ was assumed to have the form

$$\sigma(S) \equiv \frac{\mu(S)}{Y(S)} \equiv \frac{\mu_{m}S}{(K_{m}+S)Y(S)}$$
 (3)

where μ_m is the maximum specific growth rate and K_m is the Monod constant while the yield term Y(S) has the form

$$Y(S) = \frac{\text{amount of blomass formed}}{\text{amount of substrate consumer}} = aS + b$$
 (4)

which reflects the increase in the yield in response to an increase in the substrate concentration S. This also includes the case of constant yield when a = 0.

The model equations (1) and (2) do not take into account the variation of the membrane permeability with time. Since studies have confirmed high sensitivity of culture growth and production to membrane permeability, it is suggested in [2] that the influence is incorporated into the system model so that the mass balance equation on the limiting substrate is given by

$$\frac{dS}{dt} = -\frac{n'SX}{S+K_m} + D(S_0 - S)$$
 (5)

where n' = kn, with k a proportionality constant, and n the number of active nutrient transport sites. According to Yerushalmi et al. [2], permeation dynamics is the major factor responsible for the formation of the active sugar (nutrient) transport sites, especially in the aging cells. This is in turns due to the accumulation of the non-active deposits in the cytoplasm which make the permeation control the incorporation of the protein in the lipid skeleton of the cytoplasmic membrane. This relationship may be described by the equation:

$$\frac{d}{dt}(nX) = k_p \frac{d}{dt}(PX) \tag{6}$$

where P measures the membrane permeability and k_p is a constant of variation. Integrating equation (6), we obtain the relation

$$nX = k_p XP + k_1 \tag{7}$$

where k₁ is a constant of integration.

Using (7), equation (5) may be cast in the following form:

$$\frac{dS}{dt} = -\frac{(C_1XP + C_2)S}{(S + K_m)Y} + D(S_0 - S)$$
 (8)

where $C_1 = kk_pY$ and $C_2 = kk_1Y$ are constants. In other words, assuming that the yield term is constant, the specific growth rate has the form

$$\mu = \frac{(C_1 P + C_2 / X)S}{(S + K_m)}$$
 (9)

so that the mass balance equation for X becomes

$$\frac{dX}{dt} = \frac{(C_1XP + C_2)S}{(S + K_m)} - DX$$
 (10)

in which the effect of permeability variation has been taken into account. On the other hand, it is reasonable to expect the yield coefficient Y to reflect the varying amount of nutrient mass required to produce a unit of biomass, as has been argued in [8] and [9] for example. We therefore combine both effects by letting Y assume the form in (4) so that the mass balance equation for S becomes

$$\frac{dS}{dt} = -\frac{(C_1XP + C_2)S}{(S + K_m)(aS + b)} + D(S_0 - S)$$
 (11)

Experimental evidence has shown that external forces such as electrical or magnetic fields can contribute to permeability by introducing an 'order' in the composition of the cytoplasmic membrane (see [2] for more detail). As a result, the cellular membrane permeability can follow an oscillatory pattern which can be described by the following equation:

$$\frac{dP}{dt} = -K\cos(\omega_0 t)P \qquad (12)$$

where K is a proportionality constant. Equation (12) describes the periodic changes in the cytoplasmic membrane permeability when there is no cells growth. If there is cells growth, the newly formed cells posses thin cell membrane with high permeability which contributes to an increase in the apparent permeability of the cells population. In the case of influence from the geomagnetic field variations, the period is found to be approximately 24 hours, so that $\omega_0 = 2/24$. However, to include other factors which may effect membrane permeability in the similar manner, we let ω_0 be an arbitrary constant frequency of oscillation of the applied field.

Thus, the variation in the permeability of the cells population, based on the overall cells mass, can be described by the following equation:

$$\frac{d}{dt}(PX) = -\gamma_1 \cos(\omega_0 t)PX + \gamma_2 \frac{dX}{dt}$$

in which the first term on the right was directly obtained from equation (12), describing the periodic changes in the membrane permeability, while the second term describes the increase in the apparent permeability of the cells population due to the growth of the culture and the formation of new cells, assuming that the inhibitory effect of other factors such as the butanol level is neglegible.

Eliminating X from both sides of the above equation results in the following expression:

$$\frac{dP}{dt} = -\gamma_{1}\cos(\omega_{0}t)P + (\gamma_{2} - P)\mu \qquad (13)$$

where μ is given by equation (9).

Therefore, our system model consists of equations (10), (11), and (14) with (9). We are interested in the dynamic behavior and, in particular, the existence of different types of oscillatory behavior in the system described by these three equations.

BIFURCATION ANALYSIS

For the following analysis, it is convenient to introduce new variables. Namely, we define $T=Dt,~x=X/a,~y=PC_1/D$, $z=S,~\rho=C_2/aD$, $M=k_m,~d=b/a,~z_0=S_0$, $\alpha=1/D$, $\beta=\gamma_2C_1/D$, $u=\cos\left(\omega_0t\right)$, $v=\gamma_1\sin\left(\omega_0t\right)$, and $\omega=\omega_0/D$.

In these variables, our model equations becomes

$$\frac{dx}{dT} = (xy + \rho) \frac{z}{M + z} - x \tag{14}$$

$$\frac{dy}{dT} = -\alpha uy + (\beta - y) \left[y + \frac{\rho}{x} \right] \frac{z}{M + z}$$
 (15)

$$\frac{dz}{dT} = -(xy + \rho)\frac{z}{(M+z)(z+d)} + (z_0 - z)$$
 (16)

$$\frac{du}{dT} = -\omega v \tag{17}$$

$$\frac{dv}{dT} = \omega u \tag{18}$$

The above system has a steady state solution $(x_s, y_s, z_s, u_s, v_s)$ obtained from equating the right sides of equations (14) - (18) to zero, namely

$$y_s = \beta \qquad (19)$$

$$-(\beta x_s + \rho) \frac{z_s}{(M + z_s)(z_s + d)} + (z_0 - z_s) = 0$$
 (20)

$$x_s = (z_s + d) (z_0 - z_s)$$
 (21)

and

$$u_{s} = 0, \quad v_{s} = 0 \quad (22)$$

If we let

$$\theta = \frac{z_s}{M + z_s} \tag{23}$$

$$\delta = \frac{(\beta x_s + \rho)M}{(M + z_s)^2}$$
 (24)

then the Jacobian matrix J of the system of equations (14) - (18) evaluated at the steady state (x_s , y_s , z_s , u_s , v_s) can be written as

$$\int_{0}^{\beta\theta-1} \frac{\theta x_{s}}{0} \frac{\delta}{0} \frac{\delta}{0} \frac{\delta}{0} \frac{\delta}{0} \frac{\delta}{0} \frac{\delta}{0} \frac{\delta}{0} \frac{\delta}{\delta} \frac{(z_{s}^{2} - Md)}{\delta} \frac{\delta}{\delta} \frac$$

The 5 eigenvalues of J are found to be

$$\lambda_{1,2} = \frac{1}{2}\Gamma(\delta) \pm \frac{1}{2}\Lambda^{1/2}(\delta) \tag{25}$$

$$\lambda_3 = -1$$

$$\lambda_{4.5} = \pm i\omega$$

where

$$\Gamma(\delta) = \beta\theta + \frac{\delta(z_s^2 - Md)}{M(z_s + d)^2} - 2$$
 (26)

$$\Lambda(\delta) = \Gamma^{2}(\delta) - 4\{(\beta\theta - 1) \left| \frac{\delta(z_{s}^{2} - Md)}{M(z_{s} + d)^{2}} - 1 \right| + \frac{\theta\beta\delta}{z_{s} + d} \} \qquad (27)$$

Due to the complex conjugate eigenvalues \pm iw, therefore, the model will have a periodic solution for appropriate parametric values. In particular, by the theory of ordinary differential equations, if the parametric values are such that all ligenvalues other than $\alpha_{4,5}$ have negative real parts, then the simulated solution trajectories close to the steady state will approach a closed cycle surrounding the critical point (x_s , y_s , z_s , u_s , v_s) in the five dimensional phase space. In this case the profile of x(T) will be periodic with time closely resembling the regular rhythmicity found in many experimental data. However, such closed cycles lying on a plane in the phase space cannot simulate more irregular oscillatory patterns also observed in other data, such as that taken from the work of Paruleka et al.[10] presented in Figure 1. Here, alternatively low and high peaks can be observed in the growth pattern. Such characteristics appear in all their runs under different operating parameters.

To investigate the possibility of such higher dimensional oscillations in our model, we consider the system of equations (14) - (16) with $\alpha = 0$, and let

$$\delta_{\rm b} = (\beta \theta - 1)^2 (z + d) / \beta \theta \tag{28}$$

$$\delta_{c} \equiv (2 - \beta \theta)(z_{s} + d) \gamma$$
 (29)

where

$$\gamma = \frac{(z_s + d)M}{z_s^2 - Md}$$
 (30)

According to Hopf bifurcation theory [11], if a value δ_c can be found such that

- i) Re $\lambda_1(\delta_c) = 0$,
- ii) $\lambda_1(\delta_c)$ and $\lambda_2(\delta_c)$ are complex conjugates,
- iii) Im $\lambda_1(\delta_c) \neq 0$,
- iv) Re $\lambda'_1(\delta_c) \neq 0$, where λ' denotes the derivative of λ ,
- v) all other eigenvalues have negative real parts,

then the system of equations (14) - (16) with $\alpha=0$ will have a family of periodic solutions for values of δ in some open interval (δ_c , $\delta_c+\epsilon$). The result is stated in the following theorem.

Theorem If

$$\gamma > 0$$
 (31)

$$\beta \geq 1$$
 (32)

$$1/\beta > \theta > \frac{1 - \sqrt{\gamma/(\gamma + 1)}}{\beta} \tag{33}$$

and

$$\gamma > M > \frac{1-\theta}{\theta} \tag{34}$$

then the system of equations (14) - (16) with $\alpha=0$ will have periodic solutions bifurcating from a non-washout steady state for values of δ in some open interval (δ_c , $\delta_c+\epsilon$) where is given by equation (29).

Proof First, we show that with θ so chosen, $\delta_b < \delta_c$ by considering the equation

$$F(\theta) = (\beta\theta)^2 - 2(\beta\theta) + \frac{1}{\gamma + 1} = 0$$

The function $F(\theta)$ is quadratic in θ and has two real roots:

$$\theta_{1,2} = \frac{1 \pm \sqrt{\gamma / (\gamma + 1)}}{\beta} \tag{35}$$

Thus, for $\theta_1 > \theta > \theta_2$, we have $F(\theta) < 0$, that is

$$(\beta\theta)^2 - 2(\beta\theta) + \frac{1}{\gamma+1} < 0$$
 (36)

Rearranging (36), we find

$$(\beta \theta)^2 - 2(\beta \theta) + 1 < (2\beta \theta - \beta^2 \theta^2)^{\gamma}$$
 (37)

Multipying both sides by zs+d, we have

$$\frac{(\beta\theta-1)^2(z_s+d)}{\beta\theta} < (2-\beta\theta)(z_s+d)\gamma \qquad (38)$$

That is, we have

$$\delta_{\rm b} < \delta_{\rm c}$$
 (39)

if $\theta_1 > \theta > \theta_2$. However,

$$\theta_1 = \frac{1 + \sqrt{\gamma / \gamma + 1}}{\beta} > 1/\beta$$

so that if θ satisfies inequality (33) then

$$\theta_1 > 1/\beta > \theta > \theta_2$$

which implies (39) as claimed.

Now, we observe that

$$\Gamma (\delta_{c}) = 0 \qquad (40)$$

and
$$\Lambda(\delta_c) = -4\left[-(\beta\theta - 1)^2 + \frac{\theta\beta\delta_c}{z_s + d}\right]$$
 (41)

which is negative because of inequality (39). Thus,

Re
$$\lambda_1$$
 (δ_c) = Γ (δ_c)/2 = 0

and λ_1 (δ_c) and λ_2 (δ_c) are complex conjugates. Also, since we have strict inequality in (39),

$$\operatorname{Im} \lambda_1(\delta_c) = \frac{1}{2} \left[-\Lambda(\delta_c) \right]^{1/2} \neq 0$$

These are requirements i), ii), and iii), respectively.

Moreover, from (26) we have

$$\Gamma'(\delta_c) = \frac{(z_s^2 - Md)}{M(z_s + d)^2} = \frac{1}{\gamma(z_s + d)} \neq 0$$

and therefore Re λ_1' (δ_c) $\neq 0$ which is requirement iv). Finally, the remaining eigenvalue is $\lambda_3 = -1 < 0$.

Thus, all requirements for Hopf bifurcation are met. For δ in some open interval $(\delta_c, \delta_c + \epsilon)$, the system of equations (14) - (16) with $\alpha = 0$ will have a periodic solution bifurcating from its steady state (x_s, y_s, z_s) . For the system of equations (14) - (18) with $\alpha \neq 0$, this means that if conditions (31) - (34) are satisfied a Hopf bifurcation occurs on top of the existing periodic solution (due to the eigenvalues $\pm i\omega$) giving rise to solution trajectory on a 2-torus in the five dimensional phase space.

With the above choice of parametric values, Hopf bifurcation occurs at a non-washout steady state (x_s , y_s , z_s), namely $y_s = \beta \ge 0$ and from (23),

$$z_s = \frac{M\theta}{1-\theta} > 0 \tag{42}$$

since $\frac{M\theta}{1-\theta} > 0$, with θ chosen to be less than $1/\beta = 1$. Then, the value of d can be determined from (30) as

$$d = \frac{\gamma z_s^2 - z_s M}{M(\gamma + 1)}$$
 (43)

Since

$$(\gamma z_s^2 - z_s M)$$
 $(Mz_s^2 - z_s M) = M(z_s^2 - z_s)$

and $z_{\epsilon} > 1$ by the second inequality in (34), we have d > 0.

With these values of γ , β , θ , z_s , and d, the critical value δ_c can be found from (29). It is important to note that with our choice of γ ,

$$\theta < \theta_1 = \frac{1 + \sqrt{\gamma / (\gamma + 1)}}{\beta} < \frac{2}{\beta}$$

since $\frac{\gamma}{(\gamma+1)} \le 1$. Therefore $2 - \theta \beta > 0$ so that the value of δ_c given by (29) will be positive.

The parametric value $\delta>0$ is then chosen to be in the interval (δ_c , $\delta_c+\epsilon$) for some small $\epsilon>0$ so that Hopf bifurcation may occur. Then, x_s can be determined from (20) and (24) as

$$x_{c} = \delta(\Lambda_{c} + z_{c}) z_{c}/(\Lambda_{c}) > 0$$
 (44)

Then, from (20) and (21) we find that

$$\rho = \frac{x_s(M + z_s)}{z_s} - \beta x_s$$

That is,

$$\rho = x_{s} (1 - \theta \beta) / \theta \qquad (45)$$

which is positive since $\theta < 1/\beta$.

Finally, from (21), we have

$$z_0 = \frac{x_s}{z_s + d} + z_s > 0$$
 (46)

using the values of x_s , y_s , z_s and d found previously

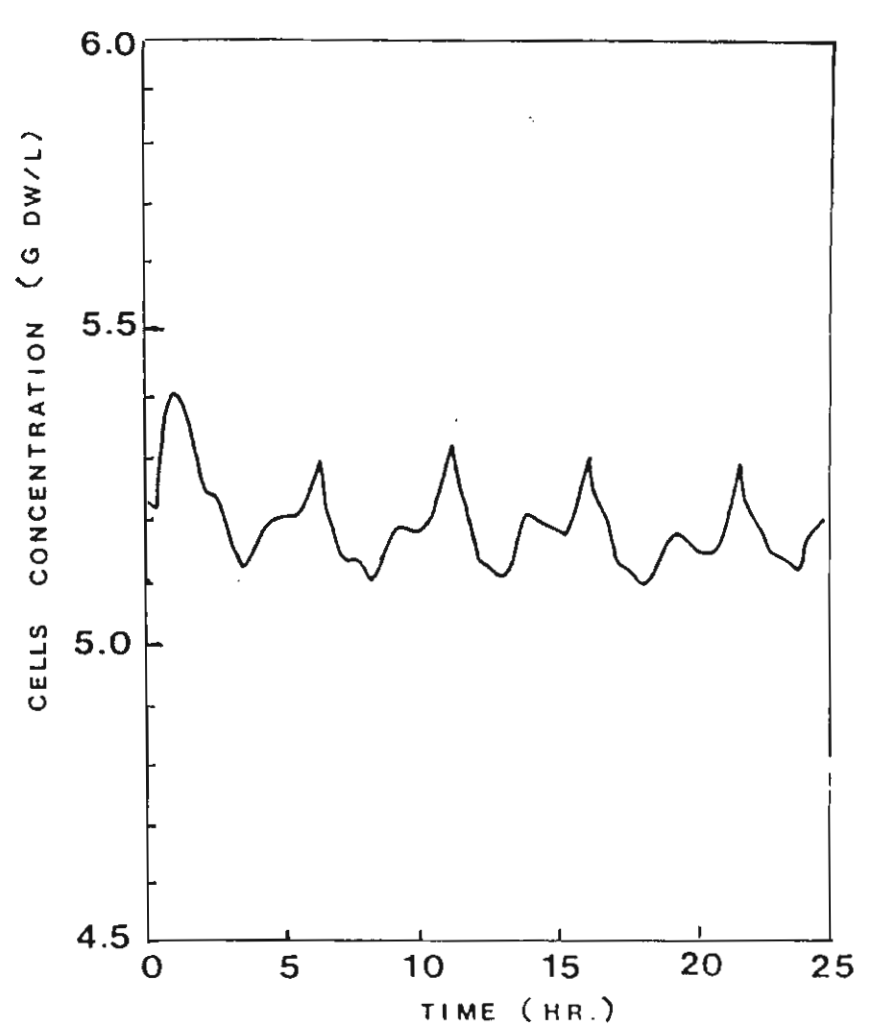
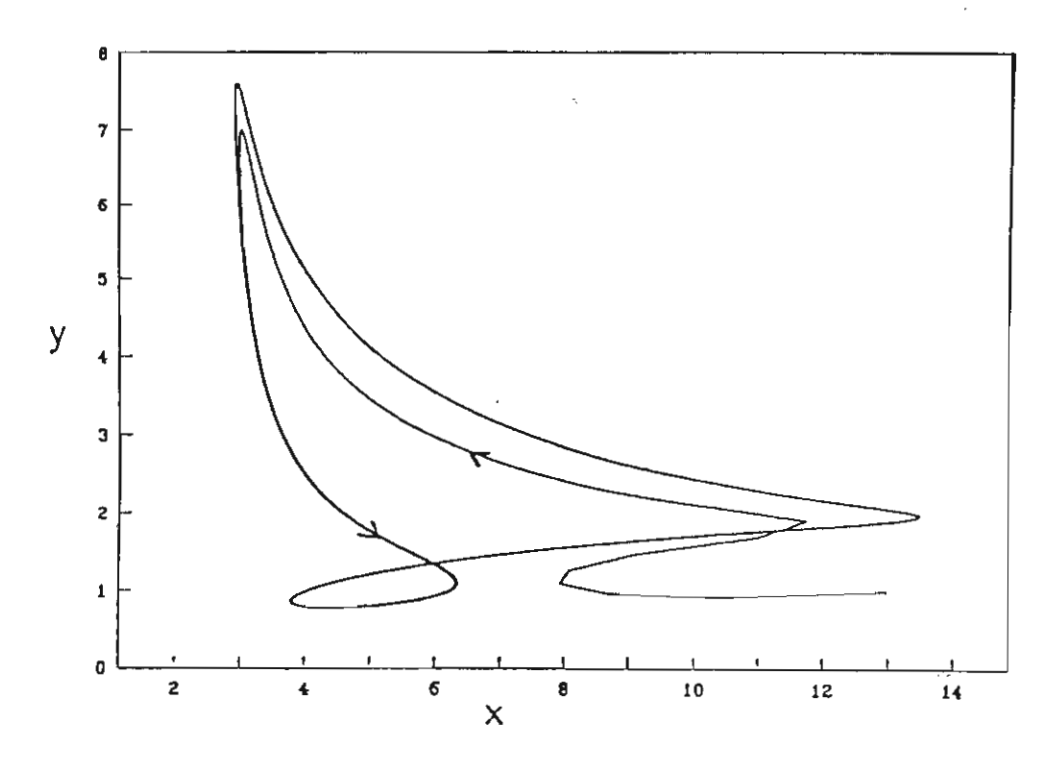


Fig. 1. Alternatively low and high peaks can be observed in the profile of cells concentration (x), for which the data points have been taken from reference [10] of continuous culture with fixed dilution rate: D=0.2 hr¹, pH = 5.5, Temp = 30° C



J.Sci.Soc.Thailand, 21(1995)

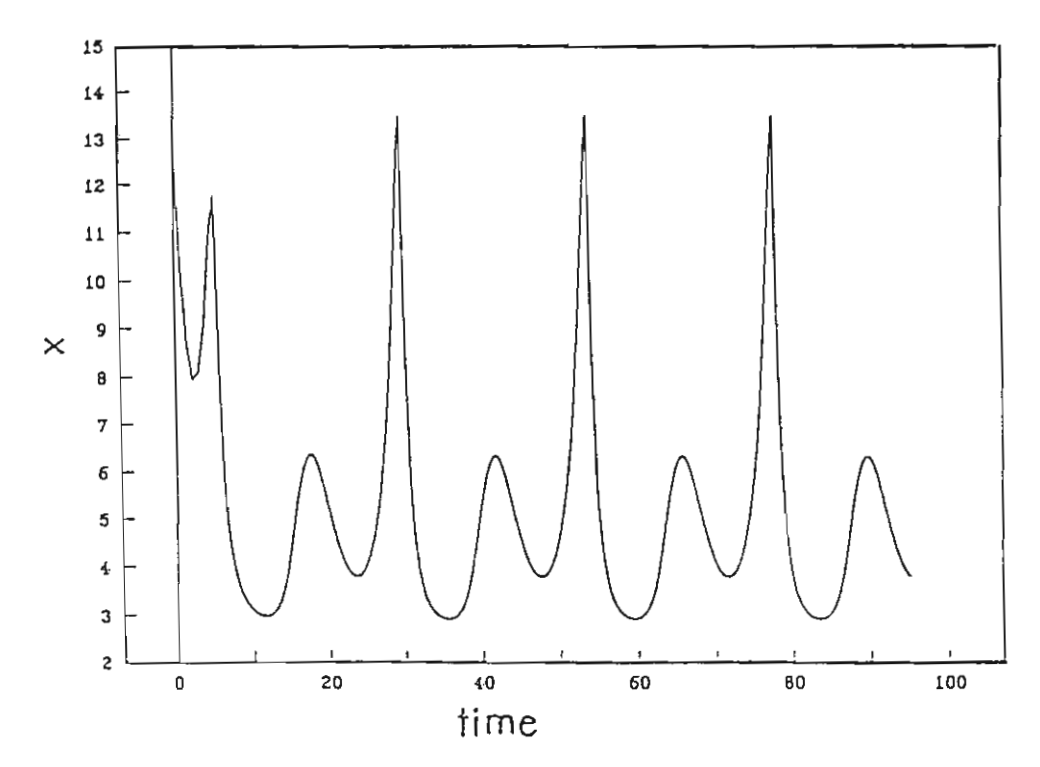


Fig. 3. The simulated time course of cells concentration | x | of Fig. : exhibiting alternatively low and high peaks resembling those observed in experimental data.

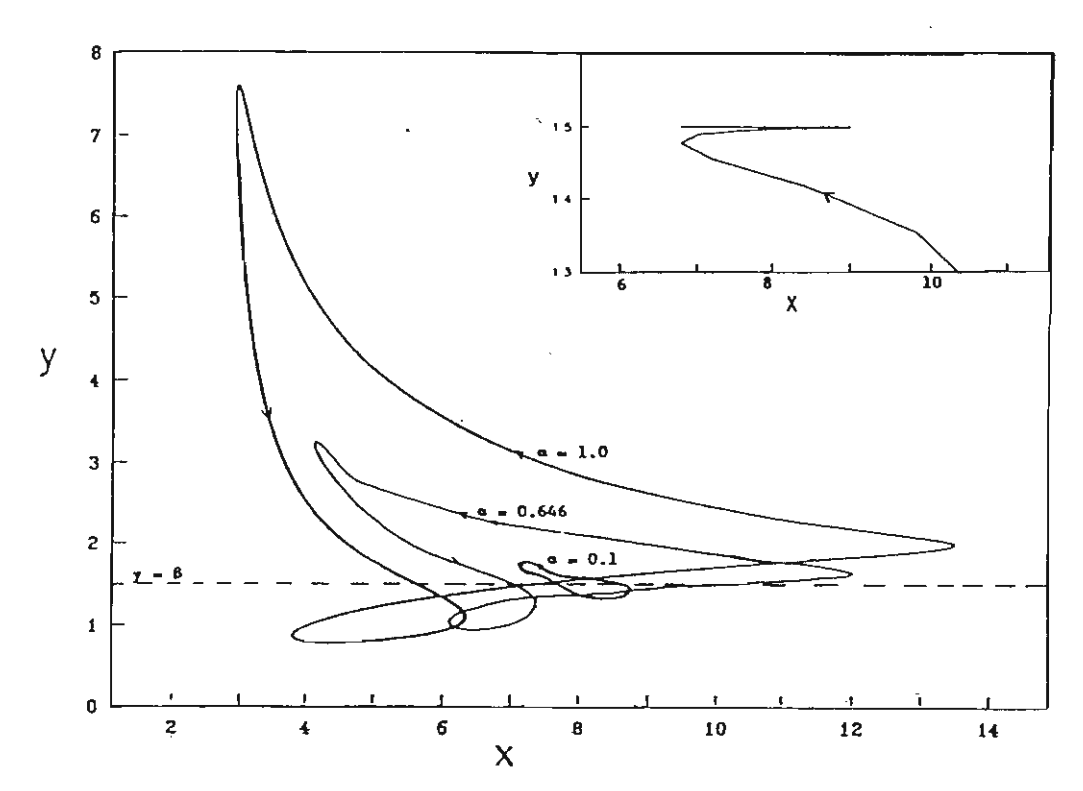


Fig. 4. The effect of varying the field density constant α . In the inset, where $\alpha = 0$, the solution trajectory is seen to approach and lie on the plane $y = \beta$ as time progresses.

r,

In Figure 2, we present a computer simulation of the model equations (14) - (18) with $\alpha \neq 0$ and parametric values chosen to satisfy the bifurcation requirements (31) - (34). The solution trajectory is seen to approach the closed curve on the surface of a 2-torus surrounding the steady state $(x_s, y_s, z_s, u_s, v_s) = (7.875, 1.5, 1.5, 0, 0)$ in the 5-dimensional phase space, seen here projected onto the (x, y) - plane. The time course of cells concentration is shown in Figure 3 exhibiting alternatively low and high peaks which compares well with experimental data mentioned earlier (Figure 1). When different parametric values were tried, we have been able to generate different oscillatory patterns resembling those observed in experimental data of continuous cultures under different operating parameters $\{1, 10\}$.

ASYMPTOTIC BEHAVIOR AND STABILITY ANALYSIS

On multiplying equation (14) by y, equation (15) by x, and adding, we obtain the equation

$$\frac{dw}{dT} = (\alpha u - 1)w + \beta(w + \rho)\frac{z}{M + z}$$
 (47)

where w = xy. We see that equations (16) and (47) involve only the two variables w and z, and therefore can be solved without the help of equation (14). Letting (\hat{w} (T), \hat{z} (T)) be the solution to equations (16) and (47), equation (14) may then be written as

$$\frac{dx}{dT} = F(T) - x \tag{48}$$

where $F(T) = (\widehat{w}(T) + \rho) \frac{\widehat{z}T}{M + \widehat{z}T}$ is a known function of T. Equation (48) can be solved directly for the solution $x = \widehat{x}(T)$.

Moreover, on substituting z = 0 in (16), we find that

$$\frac{dz}{dT}\Big|_{z=0} = z_0 > 0$$

which means that

$$z(T) \ge 0$$
 for all $T \ge 0$ (49)

Considering equation (47) with w = 0, we also have

113

$$\frac{dw}{dT}\Big|_{w=0} = \frac{\beta \rho z}{M+z} \ge 0$$

for positive parametric values. Thus,

$$x(T)y(T) \ge 0 \text{ for all } T \ge 0$$
 (50)

Using (49) and (50) in (48), we again have

$$x(T) \ge 0$$
 for all $T \ge 0$ (51)

Therefore, we conclude that all solutions to our system model remain in the positive octant of the (x, y, z) space.

Further, with (49), (50) and (51), equation (15) can be written as

$$\frac{dy}{dT} = -\alpha u(y - \beta) - (y - \beta)G(T) - \alpha \beta u \qquad (52)$$

where G(T) = $\frac{(\hat{x}(T)\hat{y}(T) + \rho)\hat{z}(T)}{(M + \hat{z}(T))\hat{x}(T)}$ is a known function which satisfies

$$G(T) \ge 0 \text{ for all } T \ge 0$$
 (53)

Using the Liebnitz' formula to solve equation (52), we obtain

$$y(T) - \beta = e^{-\alpha v(T) - h(T)} \left\{ c - \alpha \beta \int_{0}^{T} e^{\alpha v(\tau) + h(\tau)} u(\tau) d\tau \right\}$$
 (54)

where $h(T) = \int_0^{\pi} G(\tau) d\tau$ and c is a constant of integration. Since (53) holds h(T) is increasing with T. Also, $e^{\pm cv(T)} \le e^{\alpha}$ since $-1 \le v(T) \le 1$. Thus, we have

$$\left| e^{-h(T)} \int_{0}^{T} e^{h(\tau)} u(\tau) d\tau \right| \leq e^{2\alpha - h(T)} e^{h(T)} \left| \int_{0}^{T} u(\tau) d\tau \right| \leq e^{2\alpha}$$

Thus, letting $T \rightarrow \infty$ in (54) we find

y(T) -
$$\beta$$
 \rightarrow $\alpha\beta e^{2\alpha}\,y_p$ (T) as T \rightarrow ∞

where $y_p(T)$ is a bounded function. In other words, with $\alpha = 0$, all solutions to the system of equations (14)-(16) approach and lie, as time passes, on the plane $y = \beta$ in the (x, y, z) space.

Figure 4 shows the effect of varying the field density constant α on the position and shape of the solution trajectory. The solution trajectories for smaller α are closer to the plane $y=\beta$

With regards to the stability of these periodic solutions, one can apply various stability criteria (see, for example, [11]) on the system of equations (16) and (47) with $\alpha=0$ which describes the solution curve ($\widehat{w}(T)$, $\widehat{z}(T)$). It turns out to be very laborous calculation if one allows complete generality for the system parameters. However, for the case $\rho=0$ and $\beta=1$, equations (16) and (47) may be written as

$$\frac{dx_1}{dT} = \Pi(x_2)x_1 - x_1 \tag{55}$$

$$\frac{dx_2}{dT} = -\Sigma(x_2)x_1 + x_2 \tag{56}$$

where $x_1 = \frac{W}{z_0}$, $x_2 = 1 - \frac{z}{z_0}$,

$$\Pi(x_2) = \frac{(1-x_2)}{1+\Phi-x_2}$$
 (57)

and

$$\Sigma(x_2) = \frac{\Pi(x_2)}{1 + \Psi - x_2} \tag{58}$$

with
$$\phi = \frac{M}{z_0}$$
, and $\psi = \frac{d}{z_0}$

By making use of the Poincare's criterion and Friedrichs' bifurcation theory, the following condition for orbitally stable periodic solution of equations (55) and (56) can be found [8]:

$$3\Sigma'''(x_{2s}^*) x_{2s}^* < \Sigma''(x_{2s}^*) \left[1 + \frac{4\Pi''(x_{2s}^*) x_{2s}^*}{3\Pi'(x_{2s}^*)} \right]$$
 (59)

where x_{2s}^* is the value of $x_{2s} = 1 - \frac{z_s}{z_0}$ at the critical value δ_c of δ . That is, from (24) and (29),

$$x_{s2}^* = 1 - \frac{1}{z_0} \left[\frac{\delta}{\gamma(2 - \theta)} - d \right]$$

Using (57) and (58) in (59), we find that the bifurcated periodic solution will be stable if

$$F(\phi, \psi) = \left[1 - x_{2s}^* - \phi\theta(1 + \theta)\right] \left\{9 \frac{x_{2s}^*}{\theta} - 1 - \frac{\theta}{3} x_{2s}^*\right\} - 9\phi x_{2s}^* \theta^2 < 0$$
 (60)

where

$$\theta = \frac{(1 + \Psi - x_{2s}^{*})}{(1 + \Phi - x_{2s}^{*})}$$

Therefore, the bifurcation originating at the critical value δ_c of δ is stable if F<0 and unstable if F>0. Moreover, it can be shown that a stable bifurcated periodic solution surrounds an unstable critical point. If it surrounds a stable critical point, it is unstable.

CONCLUSIONS

A model of three ordinary differential equations is used to describe, under certain simplifying hypotheses, a membrane permeability rensitive chemostat system. Depending on the values of the system parameters, the model system may exhibit sustained regular oscillation in the form of a one frequency limit cycle, or a more irregular oscillation in the form of a solution trajectory on the surface of a torus surrounding a non-washout steady state. Thus, by incorporating the effect of membrane permeability variation, the model is shown to be capable of exhibiting oscillatory behavior which compares well with observed experimental data. A stability investigation shows that if the quantity $F(\phi, \psi)$ has positive value then the bifurcated solutions are repelling and if it is negative then the solutions are attracting.

Factors such as electric and magnetic forces have been proposed to have significant effects on cytoplasmic membrane permeability inducing oscillatory pattern in permeability which in turn causes the rhythmicity in the microbial growth patterns. Some investigations have been carried out in that direction [2, 7]. Nontheless, relatively little efforts have been made, up to date, to model such effects of rhythmic variation in membrane permeability

on microbial culture, in order that their biochemical impact may be better understood and appreciated. More in depth studies of the causes and mechanism of the rhythmicities are clearly needed, the repercussions of these kind of studies in the large scale fermentation industry being significant indeed.

ACKNOWLEDGEMENT

Appreciation is rendered to the National Research Council and the Thailand Research Fund for their financial support.

REFERENCES

- Borzani, W., Gregori, R.E., and Vairo, M.L.R., Some observations on oscillatory changes in the growth rate of Saccharamyces cerevisiae inaerobic continuous undisturbed culture. Biotech. Biotech. Biotech. 19, 1363-1374 (1979).
- 2. Yerushalmi, L., Volesky, B., Votruba, J., and Molnar, L., Circadian rhythicity in a fermentation process. Appl. Microbiol. Biotechnol., 30, 460-474 (1989).
- 3. Thomas, D.S., and Rose, A. H., Inhibitory effect of ethanol on growth and solute accumulation by Saccharomyces cerevisiae as affected by plasma-membrane lipid composition. Arch. Microbiol., 122, 49 (1979).
- Herrero, A.A., and Gomez, R.F. Development of ethanol tolerance in Clostridium thermocellum, 40, 571 (1980).
- 5. Panchal, C.J., and Stewart, G.G., Regulatory factors in alcohol fermentations. Proc. Int. Yeast Symp., 5, 9 (1981).
- Hong, F.T., Photoelectric and magneto-orientation effects in pigmented biological membranes. J. Colloid and Interface Sci., 58, 471 (1977).
- 7. Dubrov, A.P., The Geomagnetic Field and Life, Plenum Press, New-York (1974), p. 20.
- 8. Agrawal, P., Lee, C. Lim, H.C., and Ramkrishna, D., Theoretical Investigations of Dynamic Behavior of Isothermal Continuous Stirred Tank Biological Reactors *Chemical Engineering Science*, 37(3), 453-462 (1982)
- 9. Lenbury, Y., Novaprateep, B., and Wiwatpataphee, B., Dynamic behavior classification of a continuous bio-reactor subject to product inhibition. *Mathematical and Computer Modelling*, 19, 107-117 (1994).
- 10. "aruleka, S. J., Semones, G.B., Rolf, M. J., Lievense, J.C., and Lim. H.C., Induction and Elimination of Oscillations in Continuous Cultures of *Saccharomyces cerevisiae Biotech Biotech*, 28 (5),700-710 (1986).
- 11. Hassard, B.D., Kazarinoff, N.D., and Wan, Y.H., Theory and Applications of Hopf Bifurcation, Cambridge University Press, Cambridge (1981), p. 16

1.2 ผู้วิจัยยังได้ทคลองปรับปรุงแบบจำลอง เพื่อพิจารณาผลกระทบของ geomagnatic field variation ที่มีต่อ permeability ต่อไป โดยคิดให้ specific growth rate เป็นฟังก์ชันของ Monod โดยตลอด และการเปลี่ยนแปลงใน premeability นั้นให้มีผลกระทบต่อ yield coefficient เพียงอย่าง เดียว จึงได้แบบจำลองเป็นสมการ 3 สมการ ต่อไปนี้

$$\frac{dS}{dt} = -\frac{(c_1 x P + c_2)S}{(S + K_m)y} - D(S_F - S)$$
 (15)

$$\frac{\mathrm{dx}}{\mathrm{dt}} = \frac{\mu_{\mathrm{m}} S x}{S + K_{\mathrm{m}}} - D x \tag{16}$$

$$\frac{dP}{dt} = -\gamma \cos(w_0 t) P - \frac{(\gamma_2 - P) \mu_m S}{S + K_m}$$
(17)

ผู้วิจัยสามารถพิสูจน์ทฤษฎีบทต่อไปนี้ได้

ทฤษฎีบทที่ 2 ถ้า

$$\eta > 1 \tag{18}$$

$$\rho > \beta x_{S} > 0 \tag{19}$$

โดยที่

$$\eta = \frac{\mu_m}{D}$$

$$\rho = -\frac{c_2}{\mu_m}$$

$$\beta = \frac{\gamma_2 c_1}{\mu_m}$$

และ x_S คือค่าของ x ที่ steady state แล้วระบบสมการ (15)-(17) จะมีคำตอบเป็นคาบ ซึ่ง bifurcate จาก non-washout steady state สำหรับค่าของ δ ในช่วง (δ_c , δ_c + ϵ) โดยที่

$$\delta = \frac{x_S}{z_S + K_m} \tag{20}$$

$$\delta_{c} = \frac{x_{S}}{(\rho - \beta x_{S})(\eta - 1)} \tag{21}$$

ยิ่งไปกว่านั้น ผู้วิจัยได้สร้าง bifurcation diagram โดย plot ค่าของ

$$H_n = \xi_n - \frac{M_{\alpha} + m_{\alpha}}{2}$$
 , $n = 1, 2, ..., 40$

โดยที่

$$M_{\alpha} = \max_{n} \, \xi_{n}$$

$$m_\alpha = \underset{n}{mix} \ \xi_n$$

$$\xi_{\alpha} = \log z(T_n)$$
 , $n = 1, 2, ..., 40$

ag 1

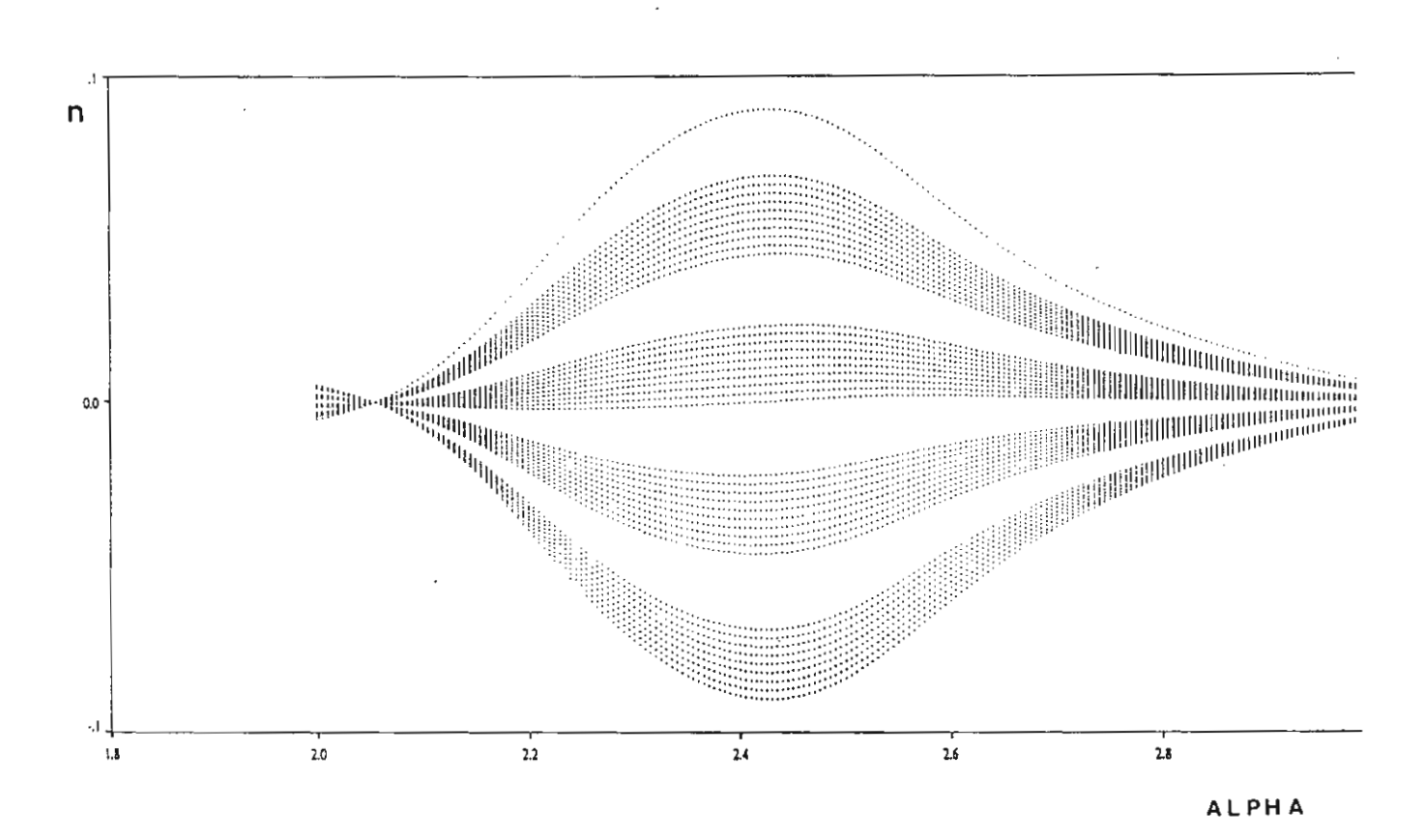
$$T_n = T_0 + \frac{2 n \pi}{w}$$
, $n = 1, 2, ..., 40$

สำหรับค่า α หนึ่งค่า จะได้ว่า H_n 40 ค่า ซึ่งผู้วิจัยใช้ค่า α ในช่วง [0,3] ได้เป็น bifurcation diagram คังที่แสดงในรูปที่ 6 แสดงว่าเมื่อ α มีค่าอยู่ในช่วง

$$2.1 < \alpha < 3$$

จุด 40 จุด จะ scatter ออกเป็น 5 กลุ่ม แสดงว่าคำตอบของระบบสมการ (15)-(17) มีคำตอบ ที่สับสนเป็น chaotic region ซึ่งควรจะหลีกเลี่ยงในการควบคุมปฏิกรณ์การขจัดสารพิษจากโรงงาน อุตสาหกรรมต่าง ๆ

ผู้วิจัยได้นำผลงานวิจัยแบบจำลองซึ่งประกอบด้วย สมการ (15), (16) และ (17) ที่กล่าวข้าง ต้นเขียนเป็น paper และได้รับ published แล้วในวารสาร Mathematical and Computer Modelling คังที่ได้แนบ manuscript คังกล่าวมาด้วยต่อไปนี้



รูปที่ 6 Bifurcation diagram

Bifurcation and Chaos in a Membrane Permeability Sensitive

Model for a Continuous Bioreactor



Mathl. Comput. Modelling Vol. 24, No. 9, pp. 37-48, 1996
Copyright©1996 Elsevier Science Ltd
Printed in Great Britain. All rights reserved
0895-7177/96 \$15.00 + 0.00

PII: S0895-7177(96)00152-5

Bifurcation and Chaos in a Membrane Permeability Sensitive Model for a Continuous Bioreactor

Y. LENBURY*, B. SUKPRASONG AND B. NOVAPRATEEP
Department of Mathematics, Faculty of Science
Mahidol University, Bangkok, Thailand

(Received February 1995; accepted November 1995)

Abstract—In this paper, we investigate the dynamic behavior of a continuous stirred tank reactor modelled by cells and substrate balance equations which have been extended to incorporate the effect of external forces on the cell membrane permeability. Bifurcation analysis done on the system of three ordinary nonlinear differential equations which comprises the model shows that it can simulate oscillatory behavior and more complex dynamic behavior which have been frequently observed in experimental data. Investigation is carried out to identify parametric ranges for which we can expect undesirable complex situations that can compromise the quality of the effluent.

Keywords—Bifurcation, Limit cycles, Continuous bioreactor, Membrane permeability, Chaotic behavior.

NOMENCLATURE

C_1	Proportionality constant, hr ⁻¹
C_2	Constant of integration, g/ℓ
D	Dilution rate, hr^{-1}
K_m, k 's	Constants, g/ℓ
n	Number of active transport sites, hr^{-1}
P	Measure of membrane permeability
\boldsymbol{s}	Substrate concentration in the fermentation vessel, g/ℓ
$S_{m F}$	Substrate concentration in the feeding solution, g/ℓ
t,	Time, hr
X	Cell concentration in the fermentation vessel, g/ℓ
Y	Yield coefficient for cell formation from the limiting substrate
γ 's	Proportionality constants, hr^{-1}
μ	Specific growth rate, hr^{-1}
μ_m	Maximum specific growth rate for the Monod model, hr^{-1}
ω_0	External force field frequency, hr^{-1}

1. INTRODUCTION

Continuous stirred tank reactors (CSTRs) are often used in wastewater treatment and biological technologies, since they represent one of the simplest approaches to continuous processes [1].

Appreciation is rendered to the Thailand Research Fund and The National Research Council of Thailand for their financial support.

^{*}Author to whom all correspondence should be addressed.

Activated sludge processes and the oxidation of some dangerous compounds usually take place in well-mixed continuous reactors at ambient temperature. Most of these biological reactions, described with Michaelis-Menton kinetics, exhibit chaotic behavior as shown by Agrawal et al. [2] in their work on the theoretical investigations of isothermal continuous stirred tank biological reactors. The appearances of limit cycles which can degenerate to chaos for certain values of the control parameters of CSTRs have been more recently reported and discussed in [1,3]. Although the mechanisms for this oscillatory behavior are not yet fully understood, it is clear that such behavior affects the performance of the process and complicates its proper design and optimization. Not only are these phenomena undesirable from the point of view of process control, they can also give rise to potentially dangerous situations in the case of toxic compound treatment. It is, therefore, necessary to investigate in depth the factors that cause such rythmicities in order to better understand the underlying mechanisms and learn how best to avoid this undesirable dynamic behavior.

Basically, microbial kinetics have varied in diverse ways from a model due to Monod fashioned after Michaelis-Menton kinetics for single enzyme-substrate reactions [1]. This model portrays microbial growth as conversion of a fixed amount of substrate (or nutrient) to biomass occurring autocatalytically in the presence of pre-existing biomass. The yield coefficient, determined by the amount of fresh biomass produced per unit mass of nutrient, remains fixed during the growth process. The mass balance equations on cells and the limiting substrate can be expressed as

$$\frac{dX}{dt} = -DX + \mu(S)X,\tag{1}$$

$$\frac{dX}{dt} = -DX + \mu(S)X,$$

$$\frac{dS}{dt} = D(S_F - S) - \frac{\mu(S)}{Y}X,$$
(1)

where X denotes the concentration of cells, S the substrate concentration, $\mu(S)$ the specific growth rate, S_F the feed substrate, and D denotes the dilution rate. Monod's model regards the yield coefficient Y as a constant and simply does not admit any periodic behavior. The most obvious departure of the predictions of the Monod's model is in the variability of the stoichiometric coefficient Y, which has led to damped as well as sustained oscillations [4]. Other workers have also theoretically studied the continuous reactor for the cases in which the specific growth rate responds with time lag to changes in pH, or the Monod's equation holds for growth limitation, and the case where growth inhibitors are formed during the process [5]. In [6], Lenbury et al. made a theoretical study on the dynamic behavior of a single-vessel continuous bioreactor subject to a growth inhibition at high concentration of the rate limitation substrate. Bifurcation and stability analysis showed oscillatory behavior and complexity in terms of steady-states multiplicity and characteristics.

Recent studies of the parameters affecting the cell physiology of C. acetobutylicum showed a high sensitivity of growth and solvent production to the cytoplasmic membrane permeability [7]. A high permeability of the cytoplasmic membrane promotes the growth of the microbial culture, the utilization of the substrate, and the biosynthesis of the solvents. The opposite result is obtained with low permeability of the cell membrane. The controlling action of the cellular membrane permeability on the activities in many continuous processes has been frequently observed. Examples include the influence of plasma-membrane lipid composition and membrane fluidity on growth and solute accumulation by S. cerevisiae [8], growth of Clostridium thermocellum [9], and growth and production of ethanol and glycerol by yeast cultures [10].

In this paper, we consider a mathematical model which incorporates this sensitivity to the cellular membrane permeability, the specific rate of change of which is assumed to vary in a sinusoidal fashion. Bifurcation analysis of the model shows that it can exhibit oscillatory behavior in the form of a closed orbit on the surface of a 2-torus for certain ranges of parametric values. Further investigation shows that chaotic behavior can result for values of a control parameter which correspond to the windows of chaos.

2. SYSTEM MODEL

One physical mechanism which has been proposed to exert its biological effect on the variability of the cytoplasmic membrane is the geomagnetic field variation [7]. Due to its crystalline structure, the performance of the cell membrane is influenced by such external forces. This concept has been extensively investigated and is well supported by experimental evidence [11,12]. Attempts to incorporate the effects of external forces on the cell membrane permeability into a model of the continuous bioreactor was carried out by Yerushalmi et al. [7] who asserted that, as a result of the influence of the geomagnetic field, the cellular membrane permeability can follow an oscillatory pattern which will in turn cause the complexed oscillatory behavior in the bioreactor.

The geomagnetic field can exert its biological effect by introducing an "order" in the composition of the cytoplasmic membrane. It is well documented [7] that the rodlike molecules in a liquid crystal can orient themselves in a magnetic field which will increase the anisotropy of the liquid crystals, making the cellular membrane more compact, resulting in a decrease in its permeability. The opposite effect is observed when the external force is not so strong.

Studying the relationship between the magnetic field strength and the anisotropy of liquid crystals, which is indirectly related to the cytoplasmic membrane permeability, it was found in [7] that the variation of the membrane permeability P with time can be described by the following equation:

$$\frac{dP}{dt} = -\gamma_1 \cos(\omega_0 t) P,\tag{3}$$

where γ_1 is a proportionality constant which is related to the intensity of the external force field that varies in a sinusoidal fashion (with a period of approximately 24 hours for the geometric field variation).

Equation (3) describes the periodic changes in the cytoplasmic membrane permeability when there is no cell growth. Growth of the cells contributes to an increase in the apparent permeability of the cell population due to the newly formed cells which possess a thin cell membrane with high permeability. Thus, the variations in the permeability of the cell population can be described by the following equation:

$$\frac{d(PX)}{dt} = -\gamma_1 \cos(\omega_0 t) PX + \gamma_2 \frac{dX}{dt},\tag{4}$$

where γ_2 is a proportionality constant. The second term in equation (4) describes the increase in the apparent permeability due to the growth of the culture and the formation of new cells.

Eliminating X from both sides of (4) results in the following equation for the dynamics of the cells membrane permeability:

$$\frac{dP}{dt} = -\gamma_1 \cos(\omega_0 t) P + (\gamma_2 - P) \mu, \tag{5}$$

where μ is the specific growth rate. More detailed discussions on the derivation of the above equations may be found in [7], where the inhibitory effect of butanol was also incorporated, but which will be considered negligible here, however.

The rate of nutrient utilization in the continuous culture is proportional to the number of active sugar transport sites which results in the following equation for nutrient uptake rate:

$$\frac{dS}{dt} = -\frac{n'S}{S + K_m}X + D(S_F - S),\tag{6}$$

where n' = kn, k being a proportionality constant, while the direct relationship between the number of active transport sites and the membrane permeability can be expressed as

$$\frac{d(nX)}{dt} = k_p \frac{d(PX)}{dt}. (7)$$

Thus, integrating (7), we find that equation (6) reduces to

$$\frac{dS}{dt} = -\frac{(C_1 X P + C_2)S}{S + K_m} + D(S_F - S),\tag{8}$$

where $C_1 = kk_P$ and C_2 is a constant of integration.

Thus, our model system consists of equations (1), (5), and (8), where the Monod model will be assumed for the specific growth rate, that is

$$\mu(S) = \frac{\mu_m S}{S + K_m}. (9)$$

3. BIFURCATION ANALYSIS

For the following analysis, it is convenient to introduce new variables. Namely, we define T=Dt, $\alpha=\gamma_1/D$, $\beta=\gamma_2C_1/\mu_m$, $\eta=\mu_m/D$, $\omega=\omega_0/D$, $\rho=-C_2/\mu_m$, $M=K_m$, x=X, $y=C_1P/\mu_m$, z=S, $z_0=S_F$, $u=\cos(\omega_0t)$, and $v=\sin(\omega_0t)$.

In these variables, our model equations (1), (5), and (8) become

$$\frac{dx}{dT} = \frac{\eta zx}{z + M} - x,\tag{10}$$

$$\frac{dy}{dT} = -\alpha uy + (\beta - y)\frac{\eta z}{z + M},\tag{11}$$

$$\frac{dz}{dT} = -(xy - \rho)\frac{\eta z}{z + M} + (z_0 - z),$$
(12)

$$\frac{du}{dT} = -\omega v,\tag{13}$$

$$\frac{dv}{dT} = \omega u. \tag{14}$$

The above system has a steady state solution $(x_S, y_S, z_S, u_S, v_S)$ obtained from equating the right sides of equations (10)-(14) to zero, namely

$$\frac{\eta z_S x_S}{z_S + M} - x_S = 0, \tag{15}$$

$$(\beta - y_S) \frac{\eta z_S}{z_S + M} = 0, \tag{16}$$

$$-(x_S y_S - \rho) \frac{\eta z_S}{z_S + M} + (z_0 - z_s) = 0,$$

$$u_S = 0, \qquad v_S = 0.$$
(17)

from which we obtain

$$z_S = \frac{M}{n-1},\tag{18}$$

$$y_S = \beta$$
, and (19)

$$x_S = \frac{(z_0 - z_s) + \rho}{\beta}. (20)$$

If we let

$$\delta = \frac{x_S}{z_S + M},\tag{21}$$

then the Jacobian matrix J of the system of equations (10)-(14) evaluated at the steady state $(x_S, y_S, z_S, u_S, v_S)$ can be written as

$$J = \begin{bmatrix} 0 & 0 & \frac{M\eta\delta}{z_S + M} & 0 & 0 \\ 0 & -1 & 0 & -\alpha\beta & 0 \\ -\beta & -x_S & -\left(\beta - \frac{\rho}{x_S}\right) \frac{M\eta\delta}{z_S + M} - 1 & 0 & 0 \\ 0 & 0 & 0 & 0 & -\omega \\ 0 & 0 & 0 & \omega & 0 \end{bmatrix}.$$

The five eigenvalues of J are found to be

$$\lambda_{1,2} = \frac{1}{2}\Gamma(\delta) \pm \frac{1}{2}\Delta^{1/2}(\delta),$$

$$\lambda_{3} = -1,$$

$$\lambda_{4,5} = \pm i\omega,$$

$$(22)$$

where

$$\Gamma(\delta) = -\left(\beta - \frac{\rho}{x_S}\right) \frac{M\eta\delta}{z_s + M} - 1,\tag{23}$$

$$\Delta(\delta) = \Gamma^2(\delta) - 4(\eta - 1)\delta\beta. \tag{24}$$

Due to the complex conjugate eigenvalues $\pm i\omega$, the linearized model will have a periodic solution for appropriate parametric values. In particular, if the parametric values are such that the eigenvalues λ_1 and λ_2 both have negative real parts, then we will observe the solution trajectories tending toward a periodic orbit in the phase space. This is the oscillatory behavior caused by sinusoidal variation in the cellular membrane permeability due to the influence of the external force field. We can show, however, that the system also possesses a natural frequency, which when compounded with the forced frequency, can give rise to a more complicated dynamic behavior. To do this, we consider the system of equations (10)-(12) with $\omega = 0$, for which the eigenvalues are also λ_1, λ_2 , and λ_3 . Letting

$$\delta_C = \frac{x_S}{(\rho - \beta x_S)(\eta - 1)},\tag{25}$$

then, according to Hopf bifurcation theory [13], if a value δ_C can be found such that

- (i) Re $\lambda_1(\delta_C) = 0$,
- (ii) $\lambda_1(\delta_C)$ and $\lambda_2(\delta_C)$ are complex conjugates,
- (iii) Im $\lambda_1(\delta_C) \neq 0$,
- (iv) Re $\lambda'_1(\delta_C) \neq 0$,
- (v) all other eigenvalues have negative real parts,

then a Hopf bifurcation occurs and the system will have a family of periodic solutions for values of δ in some open interval $(\delta_C, \delta_C + \varepsilon)$. The result can be stated as in the following theorem.

THEOREM. If

$$\eta > 1, \tag{26}$$

$$\rho > \beta x_S > 0,\tag{27}$$

then the system of equations (10)–(14) with $\omega = 0$ will have periodic solutions bifurcating from a nonwashout steady state for values of δ in some open interval $(\delta_C, \delta_C + \varepsilon)$, where δ_C is given by equation (25).

PROOF. First, we note that if η and ρ are chosen to satisfy (26) and (27), then $\delta_C > 0$. Substituting δ_C into δ in (23) and using (18), we find $\Gamma(\delta_C) = 0$, so that $\operatorname{Re} \lambda_1(\delta_C) = 0$, which is the requirement (i). Also, at $\delta = \delta_C$, we have

$$\Delta(\delta_C) = -4(n-1)\delta_C\beta < 0,$$

so that $\lambda_1(\delta_C)$ and $\lambda_2(\delta_C)$ are complex conjugates, and moreover,

$$\operatorname{Im} \lambda_1(\delta_C) \neq 0.$$

Differentiating Re $\lambda_1(\delta_C)$ with respect to δ , we find

$$\lambda_1'(\delta_C) = -\left(\beta - \frac{\rho}{x_S}\right) \frac{M\eta}{z_S + M} \neq 0,$$

Ν

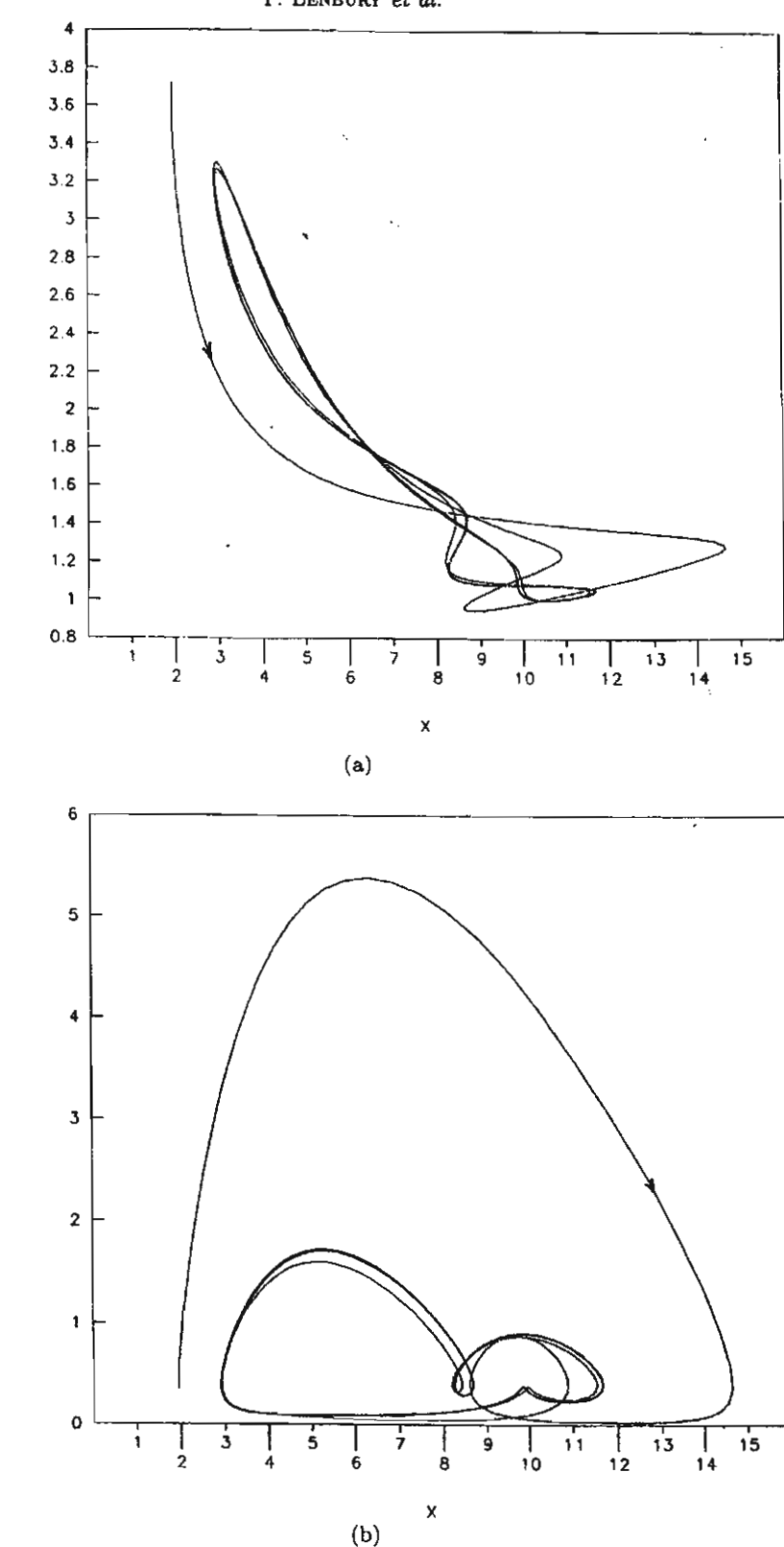


Figure 1. Computer simulation of model equations (10)–(14) with $\alpha=1.1$, $\beta=1.5$, $\rho=11$, $\eta=6$, $\delta=0.241$, M=2, $\omega=1.256$, $z_0=0.2$, $z_S=0.5$, $y_S=1.5$, and $z_S=0.05$. The solution trajectory approaches and eventually lies on a 2-torus, seen here projected onto the coordinate planes.

and finally, $\lambda_3 = -1 < 0$. Thus, all requirements for Hopf bifurcation are met. For δ in some open interval $(\delta_C, \delta_C + \varepsilon)$, the system of equations (10)–(12) with $\omega = 0$ will have a periodic solution bifurcating from its steady state (x_S, y_S, z_S) . For the system of equations (10)–(14) with $\omega \neq 0$, this means that if conditions (26) and (27) are satisfied, a Hopf bifurcation occurs on top

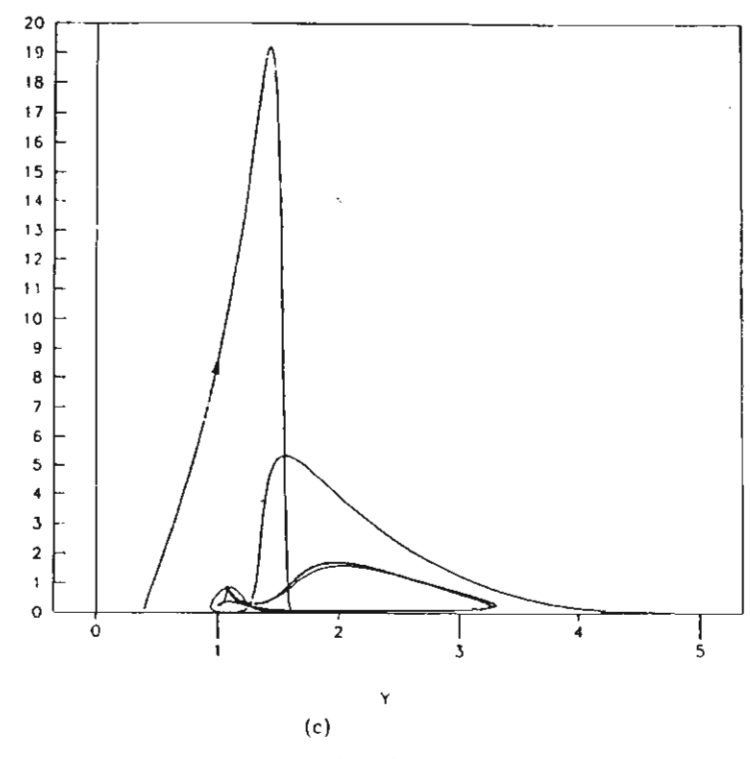


Figure 1. (cont.)

of the existing periodic solution, due to the eigenvalues $\pm i\omega$, giving rise to solution trajectories on a 2-torus in the five-dimensional phase space.

Now, with the above choice of parametric values, Hopf bifurcation occurs at a nonwashout steady state (x_S, y_S, z_S) , namely $y_S = \beta > 0$, and from (20),

$$z_S = z_0 + (\rho - \beta x_S) > 0,$$

while $x_S > 0$ by (27). In fact, the solution trajectory of the model equations (10)-(12) remains in the first octant $(x \ge 0, y \ge 0, z \ge 0)$ of the (x, y, z) space since, on substituting z = 0 into equation (12), we find

$$\frac{dz}{dT} = z_0 > 0, (28)$$

here. Also, on the (x, z) plane y = 0 so that

$$\frac{dy}{dT} = \beta > 0,$$

and on the plane x = 0, we have

$$\frac{dx}{dT} = 0,$$

so that the solution trajectory does not cross the coordinate planes.

In Figure 1, we present a computer simulation of the model equations (10)-(14) with $\omega \neq 0$ and parametric values chosen to satisfy the bifurcation requirements (26) and (27), that is, $\eta = 6$, $\beta = 1.5 = y_S$, $x_S = 0.5$, and $\rho = 11$. Then, from (25), we find

$$\delta_C = 0.125.$$

Thus, we chose $\delta = 0.241 > \delta_C$, which gives $z_S = 0.05$, M = 2, while $\omega = 1.256$, $\alpha = 1.1$, and $z_0 = 0.2$. The solution trajectory is observed to approach the closed curve on the surface of a 2-torus surrounding the steady state $(x_S, y_S, z_S, u_S, v_S) = (0.5, 1.5, 0.05, 0, 0)$ in the 5-dimensional phase space, seen here projected onto the coordinate planes.

4. FORCE FIELD INTENSITY AND BIFURCATION DIAGRAM

We now investigate the influence of the force field intensity α on the dynamic behavior of the model system (10)-(14) by first showing that the smaller the force field intensity α , the closer to the plane $y = \beta$ will the solution trajectory on the 2-torus lie.

Letting

$$G(T) \equiv \frac{\eta z(T)}{z(T) + M},\tag{29}$$

we see by (28) that G(T) > 0 for all T. Thus, equation (12) can be written as

$$\frac{d(y-\beta)}{dT} = [-\alpha u - G(T)](y-\beta) - \alpha \beta u. \tag{30}$$

Using the Leibnitz' formula, we then find

$$y(T) - \beta = e^{\int_0^T (-\alpha u - G(\tau))d\tau} \left\{ \int_0^T e^{-\int_0^T (-\alpha u - G(u))du} (-\alpha \beta u)d\tau + C \right\}. \tag{31}$$

Letting

$$h(T) = \int_0^T G(\tau) d\tau, \tag{32}$$

it is easily seen that h(T) is an increasing function, and therefore, we have

$$y(T) - \beta = e^{-\alpha v(T) - h(T)} \left\{ C - \alpha \beta \int_0^T e^{\alpha v(\tau) + h(\tau)} u(\tau) d\tau \right\},\,$$

where $e^{-h(T)} \to 0$ as $T \to \infty$.

Since $e^{h(\tau)} \le e^{h(T)}$, $0 \le \tau \le T$, we have

$$\left|e^{-\alpha v(T)-h(T)}\int_0^T e^{\alpha v(\tau)+h(\tau)}u(\tau)\,d\tau\right| \leq e^{-\alpha v(T)-h(T)}e^{h(T)}\left|\int_0^T e^{\alpha v(\tau)}u(\tau)\,d\tau\right| = 1.$$

Therefore,

$$|y(T) - \beta| \le \alpha \beta$$
, as $T \to \infty$, (33)

which means that for small α , the time course of y(T) tends to a value close to β as time passes. In fact, if $\alpha = 0$, then we have

$$y(T) \to \beta$$
, as $T \to \infty$,

and the bifurcating solution trajectory eventually lies on the plane $y = \beta$. The expression (33), in fact, gives us a bound for the extent to which y will be perturbed from the value β .

Now, we have shown that the critical point (x_S, y_S, z_S) of the system of equations (10)–(12) with $\omega = 0$ loses its stability and a Hopf bifurcation occurs when the two complex conjugate eigenvalues λ_1 and λ_2 cross the imaginary axis. In other words, at the value δ_C of our bifurcation parameter δ , the two eigenvalues λ_1 and λ_2 have a vanishing real part. Figure 2 shows the stability region in the (x_S, δ) plane for a continuous stirred tank reactor modelled by equations (10)–(14) under the conditions $\beta = 1.5$, $\rho = 11$, and $\eta = 6$. The region is the union of two sets S_1 and S_2 , where

$$S_1 = \{(x_S, \delta) \mid 0 < x_S < \rho \beta^{-1}, 0 < \delta < \delta_C\},$$

$$S_2 = \{(x_S, \delta) \mid \rho \beta^{-1} < x_S\}.$$

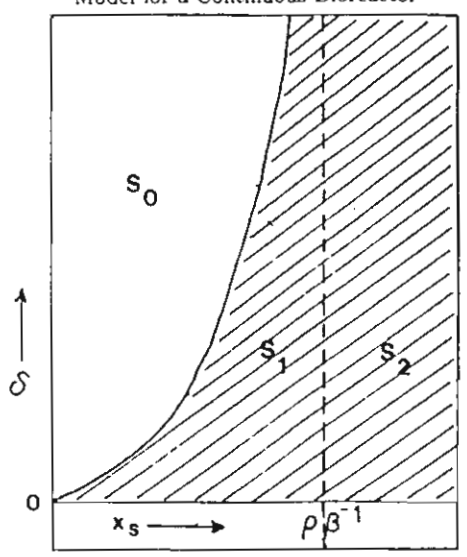


Figure 2. Stability diagram in the (x_S, δ) plane for the model system (10)-(14).

In $S_1 \cup S_2$, solution trajectories near the steady state solution $(x, y, z) = (x_S, y_S, z_S)$ remain close to that point as time passes.

On the other hand, in the instability region given by

$$S_0 = \{(x_S, \delta) \mid 0 < x_S < \rho \beta^{-1}, \delta_C < \delta < \infty\},$$

the reactor can exhibit bifurcation or chaotic behavior. The set is thus to be avoided from a control point of view. The transition from periodic orbits to chaos is known to occur after a cascade of period doubling, followed by the appearance of chaos windows. Following the work presented by Schaffer [14] on how nonlinear dynamics can elucidate mechanisms in ecology and epidemiology, we create a bifurcation diagram, shown in Figure 3, in the following manner. For each value of the force field intensity α , the simulation of the model equations (10)-(14), for parametric values in the region S_0 , is allowed to run for a sufficiently long period of time, then 40 data points $z(t_n)$, $n=1,2,\ldots,40$, are collected every interval of $2\pi/\omega$, the period of the external force field. That is,

$$T_n = T_0 + \frac{2n\pi}{\omega}, \qquad n = 1, 2, \dots, 40,$$

where $T_0=100$ in Figure 3. The values $\xi_n=\log z(T_n),\ n=1,2,\ldots,40$, are then plotted against α which ranges from 0 to 3. All other parametric values are the same in all computer simulations which generate the points in this figure. We see here that the solution is periodic for small α ; all 40 data points for each value of α apparently fall on the same spot in the (α,ξ) plane. Windows of chaos are observed for α in the approximate ranges $1.2 < \alpha < 1.9$ and $2.1 < \alpha < 3$, although the chaotic scatter of data points is more pronounced in the second range. The data points for each value of α no longer fall on the same spot, a characteristic which is markedly different from the behavior in the range where α is small.

In Figure 4, we investigate the behavior in the range $2.1 < \alpha < 3$ more closely. Here, we plot

$$H_n \equiv \xi_n - \frac{M_\alpha + m_\alpha}{2}, \qquad n = 1, 2, \dots, 40,$$

where

$$M_{\alpha} = \max_{n} \xi_{n}, \qquad m_{\alpha} = \min_{n} \xi_{n},$$

against α . We observe that at $\alpha = 2.1$, approximately, the 40 data points apparently fall on the same spot. As α increases, however, they bifurcate into two groups, one of which bifurcates

46

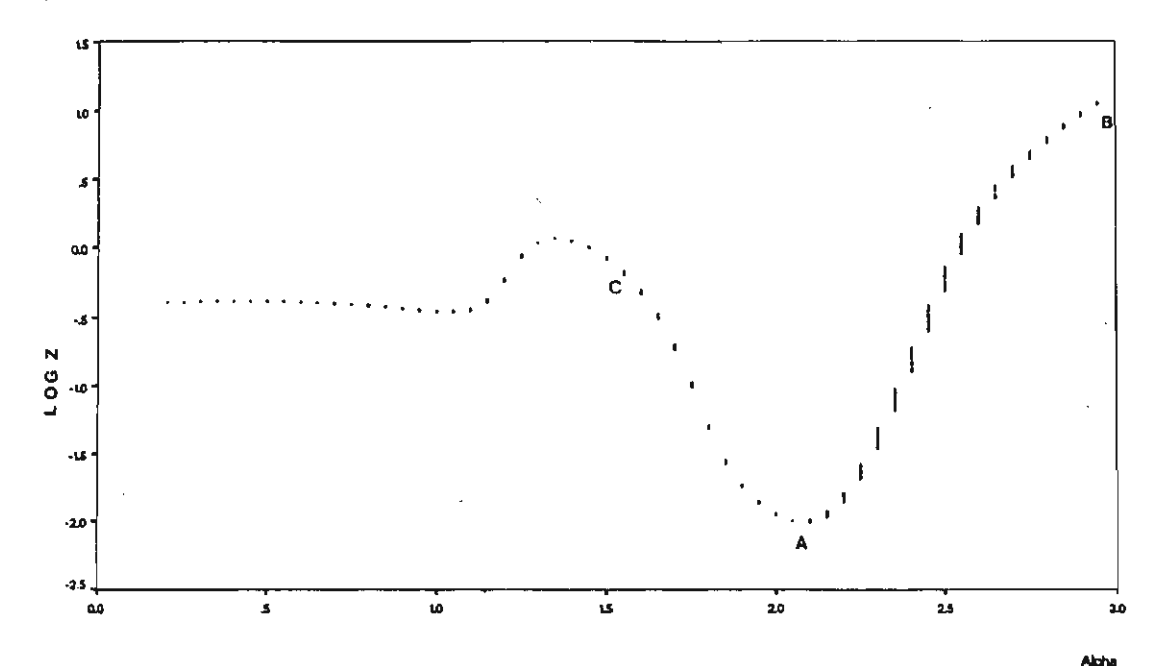


Figure 3. Bifurcation diagram of the model system (10)-(14) with parametric values in the region S_0 ; $\beta=1.5$, $\rho=11$, $\eta=6$, $\delta=0.241$, M=2, $\omega=1.256$, $z_0=0.2$, $x_S=0.5$, $y_S=1.5$, $z_S=0.05$: plot of $\log(z_n)$ versus α .

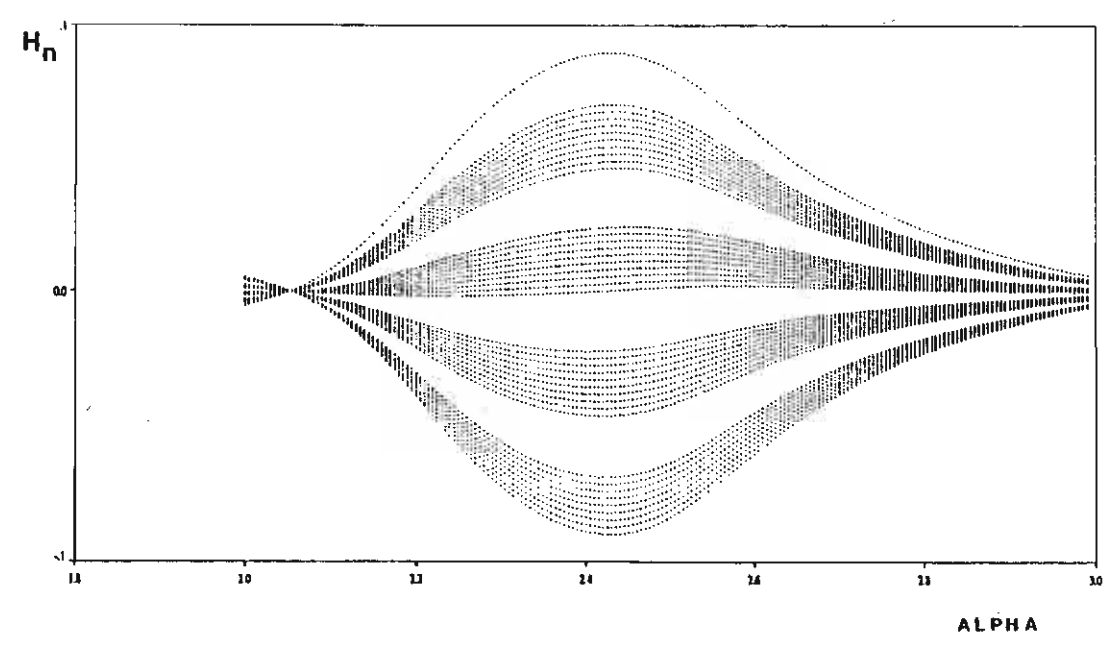


Figure 4. Bifurcation diagram of the CSTR modelled by equations (10)-(14) in the range $2 < \alpha < 3$ with parametric values of Figure 3: plot of H_n versus α .

further into four. For α around 2.45, the solution is apparently no longer periodic. We do not obtain the same value of z(T) every interval of $2\pi/\omega$. A similar chaos window can be observed for α between the values 1.2 and 1.9, approximately, although not so marked. Periodicity is recaptured, however, at α around 2.1 and 3.0 (points A and B, respectively).

Finally, Figure 5 shows the time course of z(T) for parametric values of Figure 3, but with $\alpha = 1.5$, inside the range of a chaos window (point C). The solution is no longer periodic, as is born out by the bifurcation diagram in Figure 3. Similar dynamic behavior of this type has previously been observed in a model for the spread of measles reported in [14], where an increase

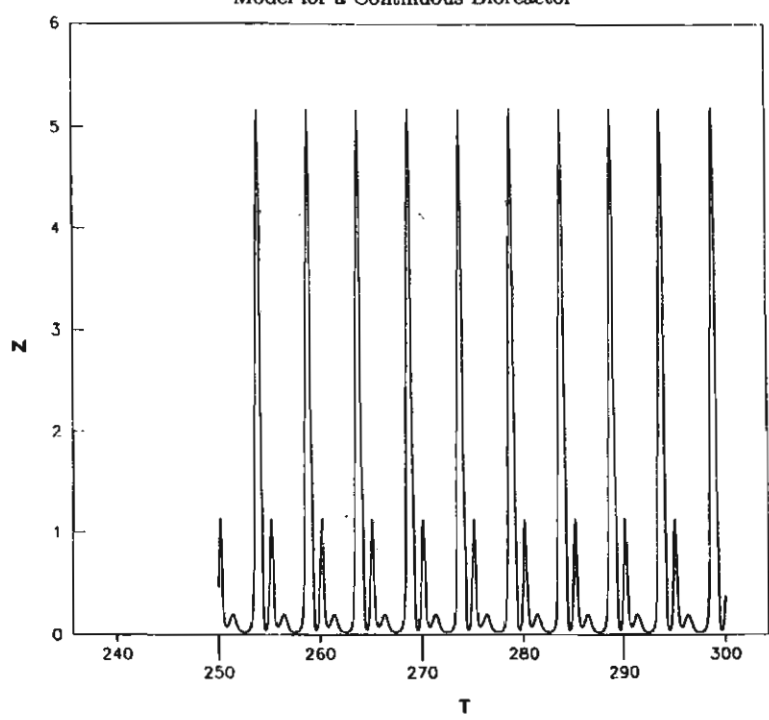


Figure 5. The time course of the simulated substrate concentration z with $\alpha = 1.5$ and other parametric values as in Figure 3.

in the amplitude of an external factor can drive the system into behaving in such an unpredictable manner.

5. CONCLUSIONS

We have investigated the dynamic behavior of a continuous stirred tank reactor modelled by cells and substrate balance equations which have been extended to incorporate the effect of external forces, such as the earth's magnetic field, on the cell membrane permeability. From considerations of the relationship between the anisotropy of the liquid crystals and the permeability of the cytoplasmic membrane, it is deduced that the membrane permeability varies with time in a sinusoidal fashion. The equation for the dynamics of variation in the permeability is then derived, taking into account also the increase in the apparent permeability due to the newly-formed cells.

The balance equation for the nutrient uptake rate is also adjusted to take into account the direct relationship between the membrane permeability and the number of active transport sites.

Bifurcation analysis done on the resulting model equations shows that, for suitable ranges of parametric values, the model system admits oscillatory behavior as a result of a Hopf bifurcation on top of the existing periodic solution due to the sinusoidal variation in the membrane permeability. Consequently, if parametric values satisfy the conditions put down in the theorem, the model system will have a solution whose phase space trajectory eventually lies on the surface of a 2-torus.

Particular attention is then devoted to the identification of the operating zones in which it is possible to carry out the continuous process while avoiding undesirable complex dynamic behavior. Owing to the importance of the process and the hazardous nature of the compounds which might be involved, we have attempted to identify the ranges of control parameters (δ and x_S , specifically) to be avoided since they correspond to the region where complex dynamic behavior is possible. The appearance of chaos windows for ranges of the external force field intensity identified in the bifurcation diagrams is not only undesirable for control and design problems, it can also give rise to potentially dangerous situations in the case where toxic compounds are involved, such as in the operation of wastewater treatment processes. Clearly, further theoret-

ical studies must be carried out to shed more light onto this complicated, but most frequently observed dynamic behavior.

REFERENCES

- 1. O. Paladino, Transition to chaos in continuous processes: Applications to wastewater treatment reactors, *Environmetics* 5, 57-70 (1994).
- 2. P. Agrawal, C. Lee, H.C. Lim and D. Ramkrishna, Theoretical investigations of dynamic behavior of isothermal continuous stirred tank biological reactors, *Chemical Engineering Science* 37, 453-462 (1982).
- 3. L. Pellegrini and G. Biardi, Chaotic behavior of a controlled CSTR, Computers and Chemical Engineering 14, 1237-1247 (1990).
- 4. J. Cheng-Fu, Existence and uniqueness of limit cycles in continuous cultures of micro-organisms with non-constant yield factor. Universita degli studi di Bari, Italy, (preprint).
- 5. T. Yano, Dynamic behavior of the chemostat subject to substrate inhibition, Biotechnology and Bioengineering 11, 130-153 (1960).
- Y. Lenbury, B. Novaprateep and B. Wiwatpataphee, Dynamic behavior classification of a model for a continuous bio-reactor subject to product inhibiton, Mathl. Comput. Modelling 19 (12), 107-117 (1994).
- L. Yerushalmi, B. Volesky, J. Votruba and L. Molnar, Circadian rhythmicity in a fermentation process, Appl. Microbiol. Biotechnol. 30, 460-474 (1989).
- 8. D.S. Thomas and A.H. Rose, Inhibitory effect of ethanol on growth and solute accumulations by Saccharomyces cerevisiae as affected by plasma-membrane lipid composition, Arch. Microbiol. 122, 49 (1979).
- 9. A.A. Herrero and R.F. Gomez, Development of ethanal tolerance in clostridium thermocellum: Effects of growth temperature, Appl. Environ. Microbiol. 40, 571 (1980).
- C.J. Panchal and G.G. Stewart, Regulatory factors in alcohol fermentations, Proc. Int. Yeast Symp. 5, 9 (1981).
- F.T. Hong, Photoelectric and magneto-orientation effects in pigmented biological membranes, J. Colloid and Interface Sci. 58, 471 (1977).
- 12. A.P. Dubrov, The Geomagnetic Field and Life, Plenum Press, New York, pp. 20-45, (1974).
- 13. J.E. Marsden and M. McCracken, The Hopf Bifurcation and its Applications, Springer-Verlag, New York, pp. 65-135, (1976).
- S. Schaffer and W.M. Can, Nonlinear dynamics elucidate mechanisms in ecology and epidemiology, IMA J. Math. Appl. Med. Biol. 2, 221-252 (1985).

1.3 แฟกเตอร์ที่สามที่ผู้วิจัยคำนึงถึงอีกแฟกเตอร์หนึ่งคือ ผลผลิต (product) ของขบวน การหมัก ซึ่งเมื่อ product นี้ มีปริมาณมากขึ้นก็สามารถมีผลทำให้อัตราการเพิ่มจำนวนของ x ลดลง ได้ เช่น ขบวนการในปฏิกรณ์ต่อเนื่อง (continuous bio-reactors) จะพบว่า product เป็นก๊าซ เช่น ethanol หรือเป็น cells killing products อื่น ๆ ซึ่งเป็นผลพวงของขบวนการนั้น ๆ จะสามารถ inhibit การเจริญเติบโต หรือการขยายพันธุ์ของ x ได้ ในขณะที่ระดับของเหยื่อ หรือสารอาหารที่มีสูงเกินไป ก็สามารถ inhibit การขยายพันธุ์ของ x ได้เช่นกัน

ผู้วิจัยจึงได้นำ model ค้นแบบ (2) และ (3) มาปรับเปลี่ยนเพิ่มเคิมสมการที่สามซึ่งคิดถึงการ เปลี่ยนแปลงในระดับของ product P(t) และได้เป็นระบบสมการไม่เชิงเส้น 3 สมการ ดังนี้

$$\frac{dS}{dt} = D(S_F - S) - \frac{\mu x}{Y}$$
 (22)

$$\frac{\mathrm{dx}}{\mathrm{dt}} = \mu \mathbf{x} - \mathbf{D}\mathbf{x} \tag{23}$$

$$\frac{dP}{dt} = \eta_0 \mu x - DP \tag{24}$$

โดยที่

$$\mu = \frac{kSe^{-\frac{S}{K_S}}}{\left\{1 + \frac{P}{K_P}\right\}} \tag{25}$$

โดยการวิเคราะห์ด้วย singular perturbation technique เราสามารถแสดงได้ว่า ถ้าเงื่อนไข ต่อไปนี้เป็นจริง

$$a > 1 \tag{26}$$

$$\beta > 1 - \frac{1}{a} - \frac{1}{a^2} \tag{27}$$

$$e^{a} < \frac{\omega}{d_{2}} < ae \left[\frac{\varepsilon \eta d_{1}}{\gamma d_{3}} \left(1 - \frac{1}{a} \right) \left(\frac{1}{a} + \beta \right) + 1 \right]$$
 (28)

ແຄະ

$$\frac{\eta d_1 \beta}{\gamma d_2} > \frac{1}{ae} \tag{29}$$

ระบบสมการ (22)-(25) จะมีคำตอบที่เป็นคาบ ซึ่งผลงานในขั้นต้นนี้ได้นำเสนอในการประชุมวิชาการ นานาชาติ International Conference on Dynamical Systems and Differential Equations ที่ Southwest Missouri State University ณ ประเทศสหรัฐอเมริกา และได้รับตีพิมพ์ใน Proceedings ของการประชมแล้ว ดังเอกสารที่ได้แนบมาต่อไปนี้

ทั้งนี้ผู้วิจัยยังได้ดำเนินการวิจัยต่อให้ละเอียด และสมบูรณ์ขึ้น แล้วนำเขียนขึ้นเป็น paper และ submitted for publication ในวารสาร Mathematical Modelling of Systems แล้ว ดังที่จะสามารถอ่าน ดูรายละเอียดของการวิเคราะห์วิจัยได้ในเอกสารที่แนบมาด้วยนี้เช่นกัน A Singular Perturbation Analysis of a Product Inhibition

Model for Continuous Bio-Reactor

A SINGULAR PERTURBATION ANALYSIS OF A PRODUCT INHIBITION MODEL FOR CONTINUOS BIO-REACTORS

Y. LENBURY Bangkok, Thailand. Department of Mathematics, Faculty of Science, Mahidol University,

N. TUMRASVIN Bangkok, Thailand.

Department of Mathematics, Faculty of Science, Mahidol University,

ABSTRACT

A model of a continuous bio-reactor subject to product inhibition is considered where a one hump substrate-limited specific growth rate is used. Analysis of the model is carried out through singular perturbation arguments which allow us to derive explicit conditions on the parameters that identify different dynamic behavior of the system, and specifically ascertain the existence of a limit cycle composed of a concatenation of catastrophic transitions occurring at different speeds. Moreover, the interactions between the limiting substrate and the growing microorganisms can give rise to high-frequency oscillations, which can arise during the transients toward the attractor or during the low-frequency cycle. This periodic burst of high-frequency oscillations develops as a result of the effective product inhibitory mechanisms. The analysis helps us in identifying the safe operating region in which undesirable complexed dynamic behavior may be avoided.

1 INTRODUCTION

Viewing the behavior of microbial cultures within the framework of lumped kinetic models, a multitude of models have been proposed and theoretically studied in diverse ways since the model due to Monod [1] fashioned after Michaelis-Menten kinetics for single enzyme-substrate reactions.

In [2], Yano and Koga made a theoretical study on the behavior of a single-vessel continuous fermentation subject to a growth inhibition at high concentration of the rate limiting substrate S. They used the following expression for their continuous fermentation system:

$$\mu = \frac{\mu_{m}}{(K_{s}/S) + 1 + \sum_{j=1}^{n} (S/K_{j})^{j}}$$
(1)

where μ_m and the K's are positive constants and n is a positive integer. Other workers [3-5] have adopted simpler specific growth rate functions involving less control parameters but exhibiting similar necessary characteristics as the usual substrate inhibition model, for example the one hump substrate inhibition function

$$\mu = kSe^{-S/K_s} \tag{2}$$

where k and K_s are positive constants.

Later, Yano and Koga discussed in [6] the nature of the chemostat in which the specific growth rate depends on the concentrations of both a substrate and an inhibitory product of a microorganism. They assumed the specific growth rate equation as follows;

$$\mu = \frac{\mu_{\rm m}S}{(K_{\rm s} + S) \left\{ 1 + \left(\frac{P}{K_{\rm p}}\right)^{\rm n} \right\}}$$
(3)

They showed, with the analog computer, that when the product formation was negatively growth-associated, diverging as well as damped oscillations appeared. No oscillations could be observed, on the other hand, when the product formation was either completely growth-associated, or partially growth-associated. Oscillation phenomena are, however, not unusual in continuous cultures [3]. Since such penchant for periodicity is undesirable from the point of view of process control, it is necessary to identify the safe operating regions in which complexed dynamic behavior may be avoided.

In [4], the dynamic behavior of a chemostat subject to product inhibition was analyzed and classified in terms of multiplicity and stability of steady states and limit cycles. The substrate was assumed to be in sufficient supply so that the model was reduced to a system of two nonlinear differential equations involving only the cells and product concentrations.

In this paper, we consider the full three-variable product inhibition model consisting of the following nonlinear differential equations (described in more detail in [6]):

$$\frac{dS}{dt} = D(S_F - S) - \frac{\mu}{Y}X$$
(4)

$$\frac{dX}{dt} = \mu X - DX \tag{5}$$

$$\frac{dP}{dt} = \eta_0 \mu X - DP \tag{6}$$

where X(t) denotes the cells concentration at time t; S(t) the substrate concentration at time t; P(t) the product concentration at time t; S_F the concentration of the feed substrate; Y the cells to substrate yield; P(t) the dilution rate; and P(t) the constant for product formation. Equations (4) and (5) are based on the well known Monod's model for cells and substrate interaction, described in more detail in reference [1]. To take into account the inhibitory effects of the substrate as well as the product increase in the chemostat, however, we adopt the following expression for the specific growth rate function:

$$\mu = \frac{kSe^{-\frac{S}{K_s}}}{1 + \frac{P}{K_p}} \tag{7}$$

Further, the cells to substrate yield Y is assumed to vary linearly with the substrate level at any time t, allowing for the positively-growth associated situation; namely

$$y = AS + B \tag{8}$$

Such substrate dependent yield has been used previously by several other workers in this field [3-5].

Equation (6) describes the change in the product concentration as X and S change. The first term on the right of this equation is the contribution to the rate of change in P, which is assumed to vary directly as the rate at which X increases, η_0 being the positive constant of variation. The cells X, substrate S, and product P are extracted from the chemostat at a constant dilution rate D, and hence the terms -DS, -DX, and -DP in the three model equations (4) through (6).

The analysis of the model is done through a singular perturbation argument, assuming that the substrate concentration exhibits fast dynamics. The time responses of the different components in the system are assumed to decrease dynamically from top to bottom. The structure of the corresponding attractors and the nature of the transients are then analyzed. It is shown that the model system can exhibit low-frequency cycles in which periodic bursts of high-frequency oscillations may develop giving rise to more complexed dynamical behavior for specified ranges of the system parameters.

2 SYSTEM MODEL

In order to analyze the model system of equations (4), (5) and (6), together with (7) and (8) through the singular perturbation technique, we scale the dynamics of the three hierarchical components of the system by means of two small dimensionless positive parameters ε and δ ;

$$\begin{split} &\text{namely, we let } x = \frac{S}{S_F}, \, y = X, \quad z = \frac{P}{\epsilon K_P} \,\,, \,\, d_1 = D, \,\, d_2 = \frac{D}{\epsilon} \quad, \,\, d_3 = \frac{D}{\epsilon \delta} \quad, \quad \omega = \frac{k S_F}{\epsilon}, \\ &\eta = \frac{\eta_0 \omega}{\epsilon \delta K_P}, \gamma = \frac{k}{A S_F} \quad, \,\, \beta = \frac{B}{A S_F} \quad, \,\, \text{and} \,\, a = \frac{S_F}{K_S} \,\,. \end{split}$$

We are led to the following system of differential equations:

$$\frac{\mathrm{d}x}{\mathrm{d}t} = d_1(1-x) - \frac{\gamma x e^{-ax} y}{(x+\beta)(1+\varepsilon z)} \equiv f(x,y,z) \tag{9}$$

$$\frac{dy}{dt} = \varepsilon y \left[\frac{\omega x e^{-ax}}{1 + \varepsilon z} - d_2 \right] \equiv \varepsilon g(x, y, z)$$
 (10)

$$\frac{dz}{dt} = \varepsilon \delta \left[\frac{\eta x e^{-ax}}{1 + \varepsilon z} y - d_3 z \right] \equiv \varepsilon \delta h(x, y, z)$$
(11)

Thus, with ε and δ small, the equation of the substrate concentration represents the fast system, while that of the cells and product concentrations represent the intermediate and the slow systems respectively. Under suitable regularity assumptions, the singular perturbation method allows us to approximate the solution of the system (9)-(11) with a sequence of simple dynamic transitions along the various equilibrium manifolds of the system and occurring at different speeds. The resulting path, composed of all such transitions, approximates the solution of the system in the sense that the real trajectory is contained in a tube around these transients, and that the radius of the tube goes to zero with ε and δ . The formal proof of this is not given because it is long and trivial and has already been discussed and extensively used in the literature [7-10].

3 EXISTENCE OF LIMIT CYCLE

We now show that if ε and δ are sufficiently small and

$$a > 1 \tag{12}$$

$$\beta > 1 - \frac{1}{a} - \frac{1}{a^2} \tag{13}$$

$$e^{a} < \frac{\omega}{d_{2}} < ae \left[\frac{\varepsilon \eta d_{1}}{\gamma d_{3}} \left(1 - \frac{1}{a} \right) \left(\frac{1}{a} + \beta \right) + 1 \right]$$
 (14)

$$\frac{\eta d_1 \beta}{\gamma d_3} > \frac{1}{ae} \tag{15}$$

then a limit cycle exists for the model system (9)-(11).

We first prove that inequalities (12)-(15) guarantee that the geometry of the manifolds f = 0, g = 0 and h = 0 is as in Fig. 1.

Manifold f = 0

We observe that this manifold is given by the equation

$$y = \frac{d_1}{\gamma} (1 - x)(x + \beta)(1 + \varepsilon z) \frac{e^{ax}}{x}$$
 (16)

which defines a surface $y = \varphi(x, z)$ which intersects the (x, y) plane along the curve

$$y = \frac{d_1}{\gamma} (1 - x)(x + \beta) \frac{e^{ax}}{x}$$
 (17)

From equation (16), it is seen that the manifold intersects the (x,z) plane along the line x = 1 as shown in Fig. 1.

The slope of the curve in (17) is given by

$$\frac{\mathrm{d}y}{\mathrm{d}x} = \frac{\mathrm{d}_1}{\gamma} \frac{\mathrm{e}^{\mathrm{a}x}}{\mathrm{x}^2} F(x) \equiv \frac{\mathrm{d}_1}{\gamma} \frac{\mathrm{e}^{\mathrm{a}x}}{\mathrm{x}^2} \Big[-x^3 + (a - a\beta - 1)x^2 + a\beta x - \beta \Big] \tag{18}$$

which may vanish for some values of x < 1.

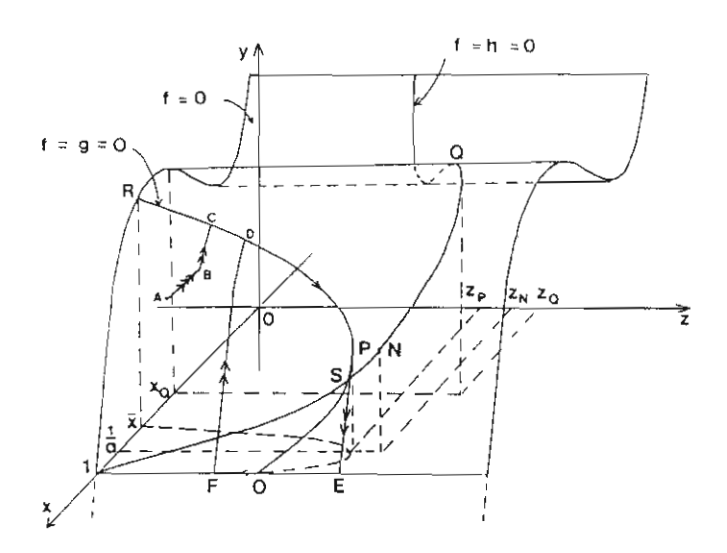


Figure 1 Equilibrium manifolds of the model system (9)-(11). In this case, transitions of different speeds develop into a closed cycle, where one, two and three arrows indicate transitions at low-, intermediate-, and high-speed, respectively.

Manifold g = 0

This manifold consists of 2 parts; the trivial manifold y = 0 and the nontrivial manifold given by the equation

$$\frac{xe^{-ax}}{1+\epsilon z} = \frac{d_2}{\omega} \tag{19}$$

which defines a surface $z = \psi(x)$. We observe that at $x = \frac{1}{a}$

$$\frac{dz}{dx} = 0$$

and so inequality (12) ensures that the point $P(x_p, y_p, z_p)$ in Fig. 1 is located on the manifold f = 0 at the point where $x_p = \frac{1}{a} < 1$.

We also need the point P to be located on the stable part of the manifold f = 0. This is guaranteed by requiring that

$$F\left(\frac{1}{a}\right) < 0 \tag{20}$$

which is equivalent to inequality (13)

The manifolds f = 0 and g = 0 intersect along the curve given by

$$y = \frac{d_1\omega}{d_2\gamma}(1-x)(x+\beta)$$

reaching a maximum at the point $M(x_M, y_M, z_M)$ where

$$x_{M} = \frac{1-\beta}{2}$$

Finally, the curve f = g = 0 intersects the (x, z) plane at the point $O(x_0, y_0, z_0)$ where $x_0 = 1$ and, from (19),

$$z_{0} = \frac{1}{\varepsilon} \left(\frac{\omega}{d_{2}e^{a}} - 1 \right) \tag{21}$$

We see, therefore, that the left side of inequality (14) guarantees that $z_0 > 0$.

Thus, the manifold f = g = 0 is shaped as shown in Fig. 1. We note that the point R may be located on the unstable part of the manifold f = 0. However, the transients also develop into a limit cycle in the case that inequalities (12)-(15) are satisfied.

Manifold h = 0

This manifold is given by the equation

$$z = \frac{\eta x y e^{-ax}}{d_3(1 + \varepsilon z)} \tag{22}$$

which defines a surface $z = \rho(x, y)$. This intersects the manifold f = 0 along the curve

$$z = \frac{\eta d_1}{\gamma d_1} (1 - x)(x + \beta) \tag{23}$$

using equation (16). Thus , z reaches a maximum along this curve at the point $Q(x_Q, y_Q, z_Q)$ where $x_Q = \frac{1}{2}(1-\beta) = x_M$

Also, the curve f = h = 0 intersects the (x,z) plane at the point (1,0,0) as seen in Fig. 1. If we let $N(x_N, y_N, z_N)$ be the point on the curve f = h = 0 with $x_N = \frac{1}{a}$, then from equation (23) we find that

$$z_{N} = \frac{\eta d_{1}}{\gamma d_{2}} \left(1 - \frac{1}{a} \right) \left(\frac{1}{a} + \beta \right) \tag{24}$$

while, from equation (19), we find that

$$z_{\mathbf{p}} = \frac{1}{\varepsilon} \left(\frac{\omega}{\text{aed}_2} - 1 \right) \tag{25}$$

Therefore, so that the equilibrium point S where the curves f = g = 0 and f = g = 0 intersect should be located on the unstable part of the manifold f = g = 0, we require

$$Z_p < Z_N$$

which is exactly the right side of inequality (14).

Finally, along this curve f = h = 0 given by equation (23),

$$z = \frac{\eta d_1}{\gamma d_3}$$

when x = 0, and therefore inequality (15) guarantees that the curve f = h = 0 crosses the curve f = g = 0 only once at the point S.

Now, starting from a point A = (x(0), y(0), z(0)) (see Fig. 1 where low-, intermediate-, and high-speed trajectories are indicated, respectively, with one, two, and three arrows) at first a high-speed transition develops at constant y and z while only the fast system

$$\dot{x} = f(x(t), y(0), z(0))$$

is active and the intermediate (y) and slow (z) variables are frozen at their initial values y(0) and z(0). The high speed transition brings the system to the point B on the stable part of the fast manifold f=0, at which point the intermediate system has now become active. A second intermediate-speed transition takes place on the manifold at constant x (segment AB in Fig. 1) until the point C is reached. A slow transition is then made along the curve f=g=0 until the point P is reached where the stability of the equilibrium manifold g=0 is lost and a quick transition then takes the state of the system to the equilibrium point E on the stable trivial manifold y=0. A slow transition then develops along this manifold until a point is reached where the stability is again lost at some point F beyond O (see Fig. 1). The proof of the existence and location of such a point F is lengthy and can be found in Schecter and Osipove et al. [11,12]. At this point a quick jump again takes us back to the point D on the stable manifold f=g=0, resulting in a closed cycle DPEF lying on the equilibrium manifold f=0.

Fig. 2 shows numerical simulation of the model equations (9)-(11) with parametric values chosen to satisfy inequalities (12)-(15). The trajectory is seen here to develop into a low-frequency limit cycle as theoretically predicted. The time courses of the three variables in this case are shown in Fig. 3.

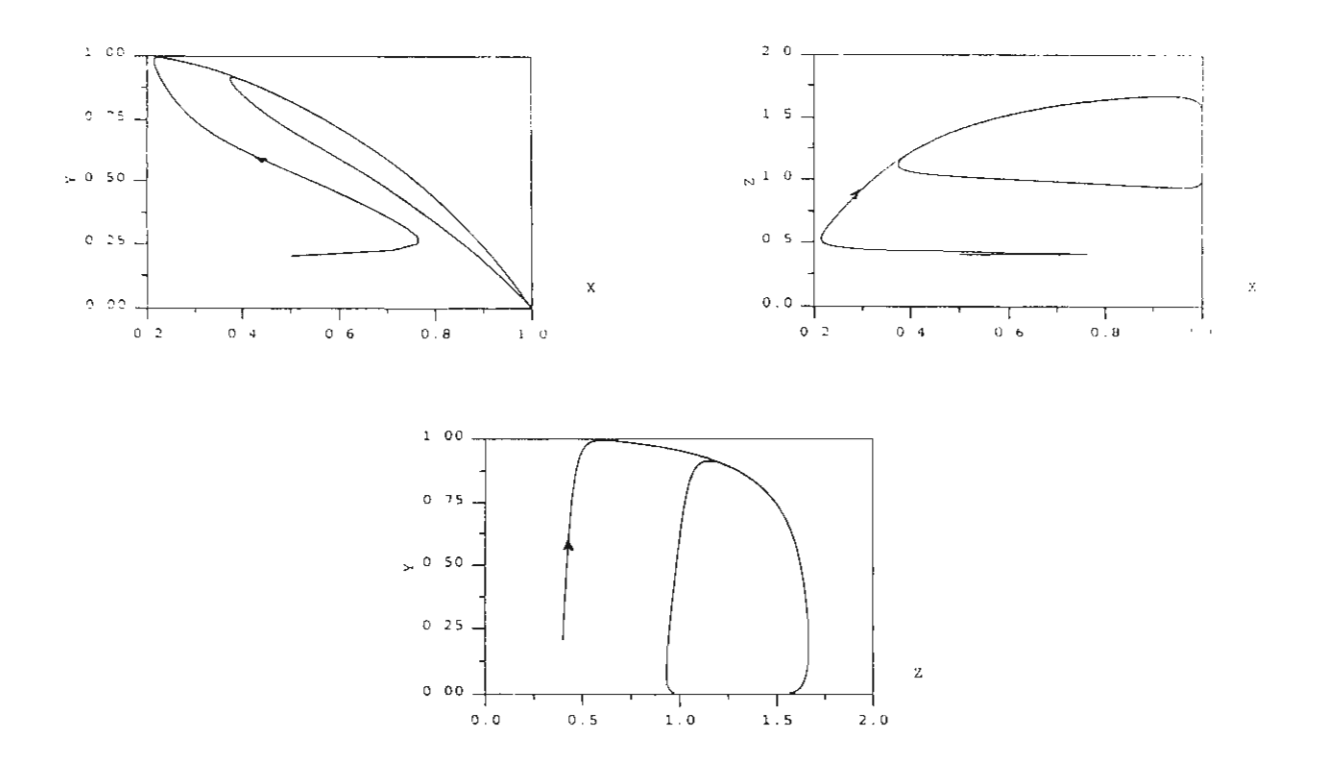
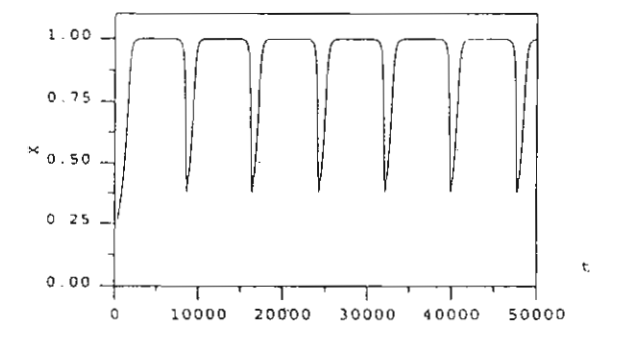
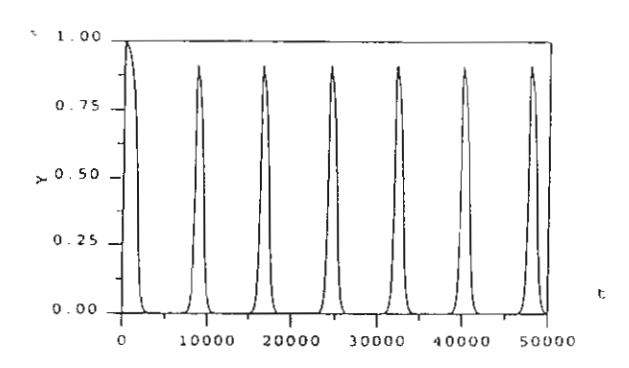


Figure 2 Numerical simulation of the model equations (9)-(11) where the parametric values have been chosen to satisfy inequalities (12)-(15), so that the solution trajectory tends toward a low-frequency limit cycle as theoretically predicted. Here, $\varepsilon = 0.1$, $\delta = 0.01$, $\beta = 0.8$, $\gamma = 2.0$, $\eta = 10.0$, $\omega = 3.0$, $\alpha = 1.5$, $\alpha = 0.25$, $\alpha = 0.3$, $\alpha = 0.1$, $\alpha = 0.25$, $\alpha = 0.3$, $\alpha = 0.1$, $\alpha = 0.25$, $\alpha = 0.25$, $\alpha = 0.3$, $\alpha = 0.1$, $\alpha = 0.25$, $\alpha = 0.25$, $\alpha = 0.3$, $\alpha = 0.1$, $\alpha = 0.25$, $\alpha = 0.25$, $\alpha = 0.3$, $\alpha = 0.1$, $\alpha = 0.25$, $\alpha = 0.25$, $\alpha = 0.3$, $\alpha = 0.1$, $\alpha = 0.25$, $\alpha = 0.25$, $\alpha = 0.3$, $\alpha = 0.1$, $\alpha = 0.25$, $\alpha = 0.25$, $\alpha = 0.3$, $\alpha = 0.1$, $\alpha = 0.25$, $\alpha = 0.25$, $\alpha = 0.3$, $\alpha = 0.1$, $\alpha = 0.25$, $\alpha = 0.25$, $\alpha = 0.3$, $\alpha = 0.1$, $\alpha = 0.25$, $\alpha = 0.25$, $\alpha = 0.3$, $\alpha = 0.1$, $\alpha = 0.25$, $\alpha = 0.25$, $\alpha = 0.3$, $\alpha = 0.1$, $\alpha = 0.25$, $\alpha = 0.25$, $\alpha = 0.3$, $\alpha = 0.1$, $\alpha = 0.25$, $\alpha = 0.25$, $\alpha = 0.3$, $\alpha = 0.1$, $\alpha = 0.25$, $\alpha = 0.25$, $\alpha = 0.1$, $\alpha = 0$





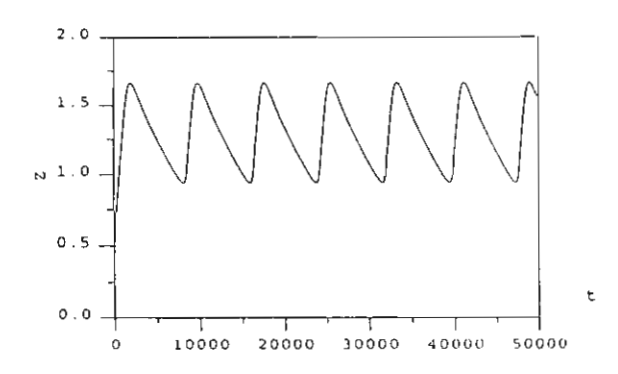


Figure 3 The time courses of the three variables x(t), y(t), and z(t) are shown here corresponding to the case seen in Fig. 2. Here, $\epsilon = 0.1$, $\delta = 0.01$, $\beta = 0.8$, $\gamma = 2.0$, $\eta = 10.0$, $\omega = 3.0$, $\alpha = 1.5$, $\alpha = 0.25$, $\alpha = 0.3$, $\alpha = 0.1$, $\alpha = 0.25$, $\alpha = 0.3$, $\alpha = 0.1$, $\alpha = 0.25$, $\alpha = 0.3$, $\alpha = 0.1$, $\alpha = 0.25$, $\alpha = 0.3$, $\alpha = 0.1$, $\alpha = 0.25$, $\alpha = 0.3$, $\alpha = 0.1$, $\alpha = 0.25$, $\alpha = 0.3$, $\alpha = 0.1$, $\alpha = 0.25$, $\alpha = 0.3$, $\alpha =$

4 BURSTS OF HIGH-FREQUENCY OSCILLATIONS

For the occurrence of periodic burst of high-frequency oscillations during each low-frequency cycle, we further require that the manifold f = 0 has an unstable portion. This is equivalent to requiring that the slope given by equation (18) is positive at some value of x < 1, say $x = \frac{1}{3}$.

Letting $x = \frac{1}{3}$ in (18) leads to the following inequality

$$\beta < \frac{3a - 4}{27 - 6a} \tag{26}$$

which ensures that the curve $y = \phi(x,0)$ has positive slope on some interval containing the point $x = \frac{1}{2}$.

Combining inequalities (13) and (26) leads to the requirement that

$$1 - \frac{1}{a} - \frac{1}{a^2} < \beta < \frac{3a - 4}{27 - 6a} \tag{27}$$

It is also necessary to have

$$F(\bar{x}) > 0 \tag{28}$$

so that the point R should be located now on the unstable branch of the manifold f = 0. This is easily accomplished by letting

$$\overline{\mathbf{x}} = \frac{1}{3} - \theta \tag{29}$$

for a sufficiently small θ , then simply set

$$\frac{d_2}{\omega} = \overline{x}e^{-\overline{x}} = (\frac{1}{3} - \theta)e^{-(1/3 - \theta)}$$
(30)

Finally, in order that the transition goes back into high-frequency oscillations in each low-frequency cycle, we require $z_0 < z_M$, which is equivalent to

$$e^{-a} < \frac{1-\beta}{2} e^{-a(1-\beta)/2} \tag{31}$$

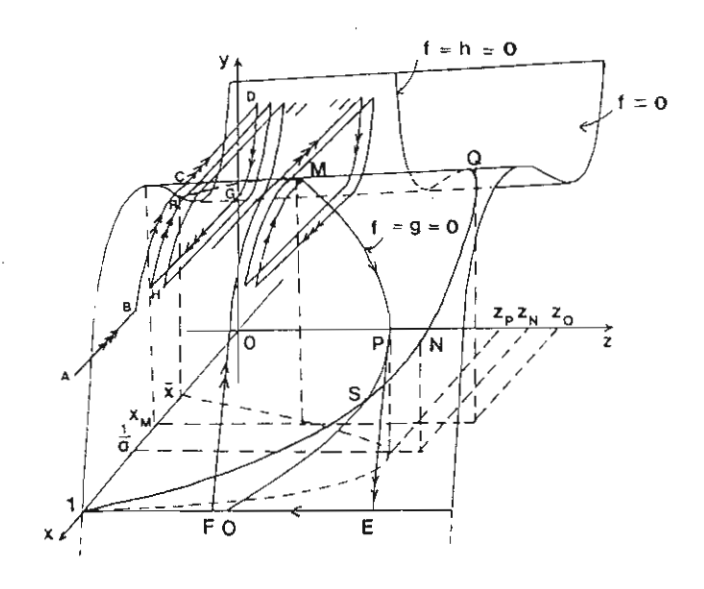


Figure 4 Equilibrium manifolds of the model system (9)-(11). In this case, transitions of different speeds develop into a low-frequency cycle with a period of high-frequency oscillation as identified in the text.

With all the above inequalities being satisfied, the equilibrium manifolds are shaped as shown in Fig. 4. Starting from the point A, a fast transition takes us, as explained earlier, to the point B on f = 0. An intermediate transition develops on this manifold until C is reached where the stability of the equilibrium fast manifold is lost. A fast transition then takes the system to the stable equilibrium point D. An intermediate speed transition is then made along this branch of manifold until G is reached where the stability is again lost and a quick jump brings us to the stable point H. This almost closes up the cycle but just misses the point B. The slow system has become active and z has been slowly increasing since $\dot{z} > 0$ here. Transitions then develop following the same pattern but with slowly varying z as seen in Fig. 4 until M is reached, at which point the trajectory develops into a slow cycle which goes back into the fast cycles since inequality (31) guarantees that $z_F < z_M$.

Thus, we have proved, by the above discussions, the following theorem

THEOREM If inequalities (12), (14), (15), (27), (30) and (31) hold then the system of equations (9)-(11) has a periodic solution which will be a low-frequency limit cycle containing high-frequency oscillations if ε , δ , and θ are sufficiently small.

Fig. 5 shows numerical simulation of the model equations (9)-(11) with parametric values chosen to satisfy all inequalities mentioned in the above theorem. The corresponding time courses of the three variables are shown in Fig. 6, where the burst of high frequency oscillations is observed in each low-frequency cycle.

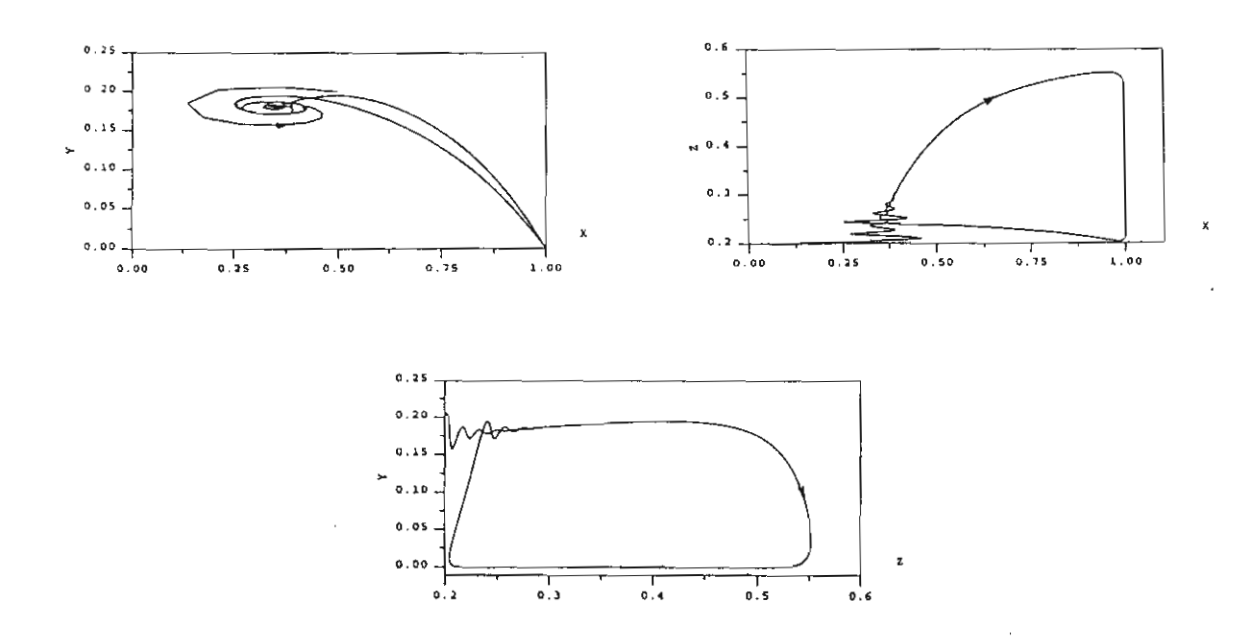
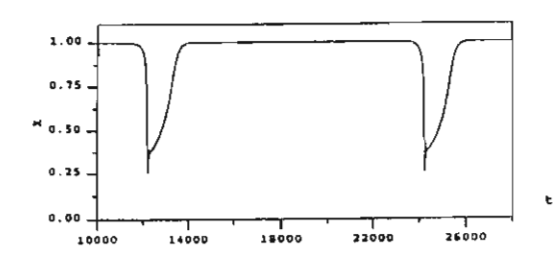
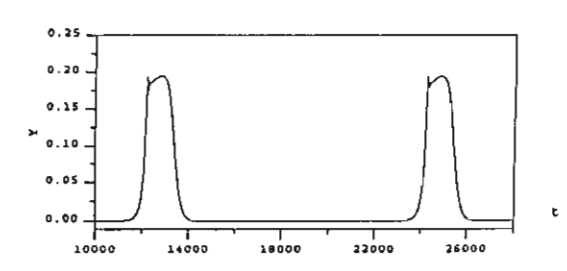


Figure 5 Numerical simulation of the model equations (9)-(11) where the parametric values have been chosen to satisfy all the inequalities set out in the Theorem. The solution trajectory is a low-frequency limit cycle which contains a period of high-frequency oscillations. Here, $\epsilon=0.1$, $\delta=0.01$, $\beta=0.02$, $\gamma=2.0$, $\eta=10.0$, $\omega=3.0$, a=1.5, $d_1=0.25$, $d_2=0.5$, $d_3=0.1$, x(0)=0.5, y(0)=0.2, and z(0)=0.2.





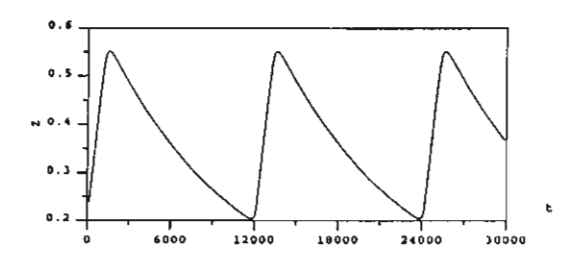


Figure 6 The time courses of the three varibles x(t), y(t), and z(t) corresponding to the case seen in Fig. 4 are shown here, where periodic bursts of high-frequency oscillations are clearly observed. Here, $\epsilon=0.1$, $\delta=0.01$, $\beta=0.02$, $\gamma=2.0$, $\eta=10.0$, $\omega=3.0$, a=1.5, $d_1=0.25$, $d_2=0.5$, $d_3=0.1$, x(0)=0.5, y(0)=0.2, and z(0)=0.2.

5 CONCLUSION

The dynamic behavior of a continuous bio-reactor described by equations (9)-(11) has been investigated in this paper. Assuming that the time responses of the three components are highly diversified, increasing from bottom to top, we were able to use standard singular perturbation analysis to describe the nature of the transients and the attractors of the system.

Complexed oscillatory behavior is extremely undesirable not only for control and design problems, but also for its potential for dangerous situations which may result in the case where toxic compounds are involved, such as in the operation of toxic waste treatment processes. Insights that can be gained from this type of analysis described above should prove most valuable in the light of such considerations.

ACKNOWLEDGMENT

Appreciation is rendered to the Thailand Research Fund for the financial support which made possible this research project.

REFERENCES

- 1. J. Monod, recherces pur la croessance des cultures bacteriennes, Hermann et Cie, Paris (1942).
- 2. T. Yano. and S. Koga, Dynamic Behavior of the Chemostat Subject to Substrate Inhibition, *Biotechnology and Bioengineering*. 11: 139-153 (1969).
- 3. P. Agrawal, C. Lee, H.C., Lim and D. Ramkrishna, Theoretical Investigations of Dynamic Behavior of Isothermal Continuous Stirred Tank Biological Reactors, *Chemical Engineering Science*. 37(3): 453-462 (1982).
- 4. Lenbury, Y., Novaprateep, B., and Wiwatpataphee, B., Dynamic Behavior Classification of Model for a Continuous Bio-Reactor Subject to Product Inhibition, *Mathl. Comput. Modelling*, 19(12): 107-117 (1994).
- 5. J. Cheng-Fu, Existence and uniqueness of limit cycles in continuos cultures of microorganisms with non-constant yield factor, Universita degli studi di Bari, Italy (Preprint).
- 6. T.Yano and S. Koga, Dynamic Behavior of the Chemostat Subject to Product Inhibition, J. Gen. Appl. Microbiol. 19: 97-114 (1973).
- 7. F. Hoppensteadt, Asymptotic stability in singular perturbation problems II: Problems having matched asymptotic expansions, *J. Differential Equations*. 15:510-512 (1974).
- 8. P.S. Crooke, C.J. Wee and R.D. Tanner, Continuous fermentation model, *Chem. Eng. Commun.* 6: 333-347 (1980).
- 9. S. Muratori, An Application of the Separation Principle for Detecting Slow-Fast Limit Cycles in a Three-Dimensional System, *Appl. Math. and Comput.* 43: 1-18 (1991).
- 10. S. Muratori and S. Rinaldi, Remarks on Competitive Coexistence, SIAM J. APPL. MATH. 49 (5): 1462-1472 (1989).
- 11. S. Muratori and S. Rinaldi, Low- and High-frequency Oscillations in Three Dimensional Food Chain Systems, SIAM J. APPL. MATH. 52(6): 1688-1706 (1992).
- 12. S. Schecter, Persistence unstable equilibria and closed orbits of a singularly perturbed equation, *J. Differential Equations*. 60, : 131-141 (1985).
- 13. A.V. Osipove, G. Soderbacka and T. Eirold, On the Existence of Positive Periodic Solutions in Dynamical System of Two Predator-One Prey Type, *Viniti Deponent n.*4305-B86 [In Russian].

Modelling Effects of High Product and Substrate Inhibition on Oscillatory Behavior in Continuous Bioreactors

MODELLING EFFECTS OF HIGH PRODUCT AND SUBSTRATE INHIBITION ON OSCILLATORY BEHAVIOR IN CONTINUOUS BIOREACTORS

Yongwimon Lenbury*

Apichat Neamvong

Somkid Amornsamankul

Pannee Puttapiban

Department of Mathematics

Faculty of Science, Mahidol University

Rama 6 Rd., Bangkok 10400, Thailand

scylb@mahidol.ac.th

^{*} to whom all correspondences should be addressed.

MODELLING EFFECTS OF HIGH PRODUCT AND SUBSTRATE INHIBITION ON OSCILLATORY BEHAVIOR IN CONTINUOUS BIOREACTORS

ABSTRACT

In this study we consider a model for continuos bioreactors which incorporates the effects of high product and substrate inhibition on the kinetics and biomass and product yields. We theoretically investigate the possibility of various dynamic behavior in the bioreactor over different ranges of operating parameters to determine the delineating process conditions which may lead to oscillatory behavior. Application of the singular perturbation technique allows us to derive explicit conditions on the system parameters which specifically ascertain the existence of limit cycles composed of concatenation of catastrophic transitions occurring at different speeds. We discover further that the interactions between the limiting substrate and the growing microorganisms can give rise to high frequency oscillations which can arise during the transients toward the attractor or during the low-frequency cycle. Such study can not only more fully describe the kinetics in a fermentor but also assist in formulating optimum fermentor operating conditions and in developing control strategy for maintaining optimum productivity.

Key words: continuous bioreactors, product inhibition, substrate inhibition, singular perturbation, oscillation.

NOMENCLATURE

- X concentration of cells in bioreactor, g/ℓ
- S concentration of substrate in bioreactor, g/ℓ
- S_F concentration of substrate in the feeding solution, g/ℓ
- P concentration of product in biorector, g/ℓ
- T time, h
- K_S , K_p positive constants, g/ℓ
- D dilution rate, h-1
- Y yield coefficient, g cell/g substrate
- μ specific growth rate, h-1
- μ_{m} maximum specific growth rate, h-1

INTRODUCTION

The growth of microorganisms is an unusually complicated phenomenon. Viewing the behavior of microbial cultures within the framework of lumped kinetic models, a multitude of models have been proposed and theoretically studied in diverse ways since the model due to Monod [9] fashioned after Michaelis-Menten kinetics for single enzyme-substrate reactions.

In ethanol fermentation, instantaneous biomass yield of the yeast $Saccharomyces\ cerevisiae$ was found by Thatipamala $et\ al.$ in [15] to decrease with the increase in ethanol concentration (P), indicating a definite relationship between biomass yield and product inhibition. It was also found in [15] that substrate inhibition occurs when substrate concentration (S) is above 150 g/ ℓ . Figure 1 shows experimental data taken from the work of Thatipamala $et\ al.$ [15] indicating the effect of substrate inhibition on the specific growth rate at low ethanol concentrations. Figure 2, on the other hand, shows the effect of product inhibition on the specific growth rate, with data taken from the same source [15].

A number of simple kinetic expressions have been suggested in the literature for specific growth rate μ incorporating product and/or substrate inhibition [2-4,16]. Mainly, four types of inhibition correlations have been suggested based on experimental observations: linear, exponential, hyperbolic, and parabolic. In [16], Yano and Koga made a theoretical study on the behavior of a single-vessel continuous fermentation subject to a growth inhibition at high concentration of the rate limiting substrate S. They used the following expression for their continuous fermentation system:

$$\mu = \frac{\mu_{\rm m}}{(K_{\rm s}/S) + 1 + \sum_{\rm j=1}^{\rm n} (S/K_{\rm j})^{\rm j}}$$
(1)

where μ_m and the K's are positive constants and n is a positive integer. Other workers [1,8] have adopted simpler specific growth rate functions involving less control parameters but exhibiting similar necessary characteristics as the usual substrate inhibition model, for example the one hump substrate inhibition function

$$\mu = kSe^{-S/K_s} \tag{2}$$

where k and K_s are positive constants

Later, Yano and Koga discussed in [17] the nature of the chemostat in which the specific growth rate depends on the concentrations of both a substrate and an inhibitory product of a microorganism. They assumed the specific growth rate equation as follows;

$$\mu = \frac{\mu_{\rm m}S}{(K_{\rm s} + S) \left\{ 1 + \left(\frac{P}{K_{\rm p}}\right)^{\rm n} \right\}}$$
(3)

They showed, with the analog computer, that when the product formation was negatively growth-associated, in which the rate of product formation decreases with the increase in the cells concentration, diverging as well as damped oscillations appeared. No oscillations could be observed, on the other hand, when the product formation was either completely growth-associated, or partially growth-associated. Oscillation phenomena are, however, not unusual in continuous cultures [1]. Since such penchant for periodicity is undesirable from the point of view of process control, it is necessary to identify the safe operating regions in which complexed dynamic behavior may be avoided.

In [14], Ramkrishna et al. presented a chemostat model which assumed that viable cells (X) interact with a substrate (S) so as to produce the new viable cells and a cell-killing product (P). This product interacts with viable cells to form dead cells, in the process of which the cell-killing product may be released.

In [8], the dynamic behavior of a chemostat subject to product inhibition was analyzed and classified in terms of multiplicity and stability of steady states and limit cycles. The substrate was assumed to be in sufficient supply so that the model was reduced to a system of two nonlinear differential equations involving only the cells and product concentrations.

In this paper, we consider the full three-variable product inhibition model consisting of the following nonlinear differential equations:

$$\frac{\mathrm{dX}}{\mathrm{dt}} = \mu X - \mathrm{DX} \tag{4}$$

$$\frac{dS}{dt} = D(S_F - S) - \frac{\mu}{Y}X$$
 (5)

$$\frac{\mathrm{d}P}{\mathrm{d}t} = \eta_0 \mu X + \eta_1 P - \mathrm{D}P \tag{6}$$

where X(t) denotes the cells concentration at time t; S(t) the substrate concentration at time t; P(t) the product concentration at time t; S_F the concentration of the feed substrate, while D is the dilution rate at which the feed substrate is being fed into the reactor and the content of the bio-reactor is being removed, and η_0 is the constant for product formation. The term $\eta_1 P$ in equation (6) takes into account the release of the cell-killing product during the product's interaction with viable cells to form dead cells, following the suggestion of Ramkrishna *et al.* in their earlier mentioned paper [14]. Here, we assume that the production rate is directly proportional to the amount of the product present, with $\eta_1 < D$ being the positive constant of variation.

We also adopt the following expression for the specific growth rate function:

$$\mu = \frac{kSe^{-a\frac{S}{S_F}}}{1 + \frac{P}{K_P}} \tag{7}$$

where a and k are positive constants, to take into account the inhibitory effects of both the substrate and the product increase in the chemostat.

Further, the cells to substrate yield Y defined as

$$Y \equiv \frac{\text{amount of cells produced}}{\text{amount of substrate consumed}}$$

is assumed to vary linearly with the substrate level at any time t, allowing for the positively-growth associated situation; namely

$$Y = A + BS \tag{8}$$

Such substrate dependent yield has been used previously by several other workers in this field [1, 8].

The analysis of the model is done through a singular perturbation argument, assuming that the substrate concentration exhibits fast dynamics. The time responses of the different components in the system are assumed to decrease dynamically from top to bottom. The structure of the corresponding attractors and the nature of the transients are then analyzed. It is shown that the model system can exhibit low-frequency cycles in which periodic bursts of high-frequency oscillations may develop giving rise to more complexed dynamical behavior for specified ranges of the system parameters.

SYSTEM MODEL

In order to analyze the model system of equations (4), (5) and (6), together with (7) and (8) through the singular perturbation technique, we assume that the substrate has fast dynamics, while the cells and product have intermediate and slow dynamics respectively, and scale the time responses of the three hierarchical components of the system by means of two small dimensionless positive parameters ϵ and δ ; namely, we let $x = \frac{S}{S_F}$, y = X, $z = \frac{P}{\epsilon K_P}$, $d_1 = D$, $d_2 = \frac{D}{\epsilon}$, $d_3 = \frac{D - \eta_1}{\epsilon \delta}$, $\omega = \frac{kS_F}{\epsilon K_P}$, $\eta = \frac{\eta_0 \omega}{\epsilon \delta}$, $\gamma = \frac{k}{AS_F}$, and $\beta = \frac{A}{BS_F}$. We are led to the following system of differential equations:

$$\frac{dx}{dt} = d_1(1-x) - \frac{\gamma x e^{-ax} y}{(x+\beta)(1+\epsilon z)} = f(x,y,z)$$
 (9)

$$\frac{\mathrm{d}y}{\mathrm{d}t} = \varepsilon y \left[\frac{\omega x \mathrm{e}^{-ax}}{1 + \varepsilon z} - \mathrm{d}_2 \right] = \varepsilon \mathrm{g}(x, y, z) \tag{10}$$

$$\frac{\mathrm{d}z}{\mathrm{d}t} = \varepsilon \delta \left[\frac{\eta x \mathrm{e}^{-\mathrm{a}x}}{1 + \varepsilon z} y - \mathrm{d}_3 z \right] = \varepsilon \delta \mathrm{h}(x, y, z) \tag{11}$$

Thus, with ε and δ small, the equation of the substrate concentration represents the fast system, while that of the cells and product concentrations represent the intermediate and the slow systems, respectively. Under suitable regularity assumptions, the singular perturbation method allows us to approximate the solution of the system (9)-(11) with a sequence of simple dynamic transitions along the various equilibrium manifolds of the system and occurring at different speeds. The resulting path, composed of all such transients, approximates the solution of the system in the sense that the real trajectory is contained in a tube around these transients, and that the radius of the tube goes to zero with ε and δ . The formal proof of this is not given because it is long and trivial and has already been discussed and extensively used in the literature [7,10-12].

Two-dimensional dynamics

By means of singular perturbation analysis, the solution of the system of equations (9)-(11) can be approximately found for small values of ϵ and δ . First, the slow (z) and intermediate (y) variables are frozen at their initial values z(0) and y(0), and the evolution of the fast component of the system is determined by solving the 'fast system' consisting of equation (9) with z set equal to z(0). If, for simplicity of the following analysis, we assume that the starting value of z is comparatively small, since δ is small, the value of z remains small during the initial phase. The evolution of the system components can then be approximately determined by first setting $\delta = 0$ and z = 0 in the equations (9)-(11). Thus, we are led to the following system:

$$\frac{dx}{dt} = d_1(1-x) - \frac{\gamma x e^{-ax} y}{(x+\beta)}$$
 (12)

$$\frac{\mathrm{dy}}{\mathrm{dt}} = \varepsilon y \left[\omega x \mathrm{e}^{-\mathrm{a}x} - \mathrm{d}_2 \right] \tag{13}$$

which is a fast-slow second-order system for which the dynamical behavior can be analyzed and existence of limit cycles detected through the singular perturbation principle. The results are summarized in Figure 3, where two cases of interest can be identified. The conditions on the parameters identifying the two cases are as follows.

Case 1

The system (12) has an equilibrium manifold where $\dot{x} = 0$ given by

$$y = (1 - x)(x + \beta) \frac{e^{ax}}{x} \equiv \phi(x)$$
 (14)

which intersects the x-axis at the point x = 1 as shown in Figure 3. The slope of the curve in (14) is given by

$$\frac{dy}{dx} = \frac{e^{ax}}{x^2} F(x) = \frac{e^{ax}}{x^2} \left[-x^3 + (a - a\beta - 1)x^2 + a\beta x - \beta \right]$$
 (15)

Letting $x = \frac{1}{3}$ in (15) leads to the following inequality

$$\beta < \frac{3a-4}{27-6a} \tag{16}$$

which ensures that the curve $y = \varphi(x)$ has positive slope on some interval containing the point $x = \frac{1}{3}$.

The equilibrium manifold of the intermediate system (13) consists of 2 parts, the trivial manifold y = 0 and the nontrivial manifold given by the equation

$$xe^{-ax} = \frac{d_2}{\omega} \tag{17}$$

In Case 1, the curve (17) intersects the graph of (14) at the point R in the Figure 3 where $x = \overline{x}$ for which

$$F(\bar{x}) > 0 \tag{18}$$

which means that the point R is located on the unstable branch of the manifold f = 0. This is easily accomplished by letting

$$\overline{\mathbf{x}} = \frac{1}{3} - \theta \tag{19}$$

for a sufficiently small θ , then simply set

$$\frac{d_2}{\omega} = \bar{x}e^{-\bar{x}} = (\frac{1}{3} - \theta)e^{-(1/3 - \theta)}$$
 (20)

Thus, Case 1 is identified by the inequality (18) with (19) and (20).

Case 2

This case is then identified by the opposite inequality to (18), namely

$$F(\bar{x}) < 0 \tag{21}$$

However, since the nontrivial intermediate manifold is given by (17),

$$\bar{x} > \frac{d_2}{\omega} \tag{22}$$

We see that (21) will be satisfied if $\frac{d_2}{\omega}$ is sufficiently large as well as satisfying

$$\frac{d_2}{\omega} < 1 \tag{23}$$

to allow for \overline{x} to be located to the left of the point x = 1 where the fast manifold crosses the x-axis.

Thus, in Figure 3 where transitions of low, intermediate, and high speeds are indicated by one, two, and three arrows, respectively, if we start from the point marked by the number 1 above the curve $\dot{x}=0$, then $\dot{x}<0$ here and a fast transition develops toward the point 2 on the stable manifold (section AB), while y still remains frozen at the initial value y(0). (If we start from the point 1 below the curve $\dot{x}=0$, then $\dot{x}>0$ here and so a fast transition will develop toward point 3 on section CD of the manifold). Since the manifold is stable here, a transition of intermediate speed is made along the curve as the intermediate system becomes active. From point 2, the transition develops along the direction of decreasing y since $\dot{y}<0$ on the left of the curve g=0. Once the point B is reached, the manifold loses its stability and a fast transition is made towards the point D on the stable section CD of the manifold. Transition of intermediate speed upwards along this curve ends if either a stable equilibrium R is reached in Case 2, or a quick jump brings the trajectory back to the section AB completing a closed cycle ABDC in Case 1.

Three-dimensional dynamics

As z increases, the slow system (11) becomes active. We now show that, for suitable values of the parameters and for ε and δ sufficiently small, the system (9)-(11) has a unique attractor that is either a stable equilibrium or a low-

frequency limit cycle which may exhibit high-frequency oscillations during a finite interval of time.

To do this, we observe that the manifold

$$f(x,y,z) = 0 (24)$$

intersects the nontrivial intermediate manifold along the curve

$$f = g = 0 \tag{25}$$

given by the equation

$$\frac{xe^{-ax}}{1+\epsilon z} = \frac{d_2}{\omega} \tag{26}$$

which defines a surface $z = \psi(x)$. We observe that at $x = \frac{1}{a}$

$$\frac{\mathrm{dz}}{\mathrm{dx}} = 0$$

Thus, to ensure that the point $P(x_P, y_P, z_P)$ in Fig. 4 is located on the stable part of the manifold f = 0 at the point where $x_P = \frac{1}{a} < 1$, we require

$$F\left(\frac{1}{a}\right) < 0 \tag{27}$$

or equivalently,

$$\beta > 1 - \frac{1}{a} - \frac{1}{a^2} \tag{28}$$

and

$$a > 1 \tag{29}$$

Combining the inequalities (16) and (28), we arrive at the requirement that

$$\frac{3a-4}{27-6a} > \beta > 1 - \frac{1}{a} - \frac{1}{a^2} \tag{30}$$

Now, the curve (25) is given by the equation

$$y = \frac{d_2}{\omega}(1-x)(x+\beta)$$

which reaches a maximum at the point $M(x_M, y_M, z_M)$ where

$$x_{M} = \frac{1-\beta}{2}$$

Finally, the curve f = g = 0 intersects the (x,z)-plane at the point $O(x_0,y_0,z_0)$ where $x_0 = 1$ and, from (26),

$$z_{o} = \frac{1}{\varepsilon} \left(\frac{\omega}{d_{2}e^{a}} - 1 \right) \tag{31}$$

We therefore require that

$$e^{a} < \frac{\omega}{d_{2}} \tag{32}$$

to ensure that $z_0 > 0$.

We now analyze each of the two cases separately.

Case 1

We observe that in this case the point R is located on the unstable part of the manifold f = 0 and the curve f = g = 0 remains on the unstable part, as shown in Figure 4, until the point M is reached. The curve then stretches along the stable part of the manifold f = 0 until either the point S is reached in the cases 1(a) and 1(b), or the point P is reached first in the cases 1(c) and 1(d). Thus, four subcases can be identified as follows.

<u>Case1(a)</u> This case is identified by the inequality

$$a < 1 \tag{33}$$

so that the turning point P is below the (x,z)-plane. Thus, starting from an initial point A in Figure 4, a fast transient takes us to the point B on the stable part of the fast manifold f = 0. Transition of intermediate speed is then made along this manifold in the direction of increasing y until the point C is reached where stability is lost. A fast jump is made to the point D on the other stable branch of the manifold f = 0 from which point a transition of intermediate speed develops until stability is lost again at the point G. A quick jump back to H almost closes up the cycle. However, z has been slowly increasing in the meantime so that the same cycling transitions are repeated in the direction of increasing z, densely covering the surface f = 0, until the point M is reached. The transient now follows the curve f = g = 0 until the point S is reached in the case f = 0. In this case, the point S where f = 0 is on the stable part of the manifold f = 0 and thus the transitions end at this stable equilibrium point.

Case 1(b) This is the case identified by the inequality

$$a > 1 \tag{34}$$

so that the point P is located on f = 0 above the (x,z)-plane as shown in Figure 4 (b). This case is also identified by the fact that the point S, where f = g = h, is located on the stable part of the curve f = g = 0. This situation is guaranteed by requiring that

$$z_{P} > z_{N} \tag{35}$$

where $N(x_N, y_N, z_N)$ is the point on the curve f = h = 0 with $x_N = \frac{1}{a}$. From equating f and h to zero, we find that

$$z_{N} = \frac{\eta d_{1}}{\gamma d_{3}} \left(1 - \frac{1}{a} \right) \left(\frac{1}{a} + \beta \right) \tag{36}$$

while, from equation (26), we have

$$z_{P} = \frac{1}{\varepsilon} \left(\frac{\omega}{\text{aed}_{2}} - 1 \right) \tag{37}$$

Therefore, so that S is located on the stable part of f = g = 0, we require

$$\frac{\omega}{d_2} > ae \left[\frac{\varepsilon \eta d_1}{\gamma d_3} \left(1 - \frac{1}{a} \right) \left(\frac{1}{a} + \beta \right) + 1 \right]$$
 (38)

which guarantees that (35) holds.

In this case 1(b) then, the transition also reaches the point S first and ends there since it is a stable equilibrium point where $\dot{x} = \dot{y} = \dot{z} = 0$. Moreover, along The curve f = h = 0 we have

$$z = \frac{\eta d_1}{\gamma d_3}$$

when x = 0. Therefore we must also require that

$$\frac{\eta d_1 \beta}{\gamma d_3} > \frac{1}{ae} \tag{39}$$

to ensure that the curve f = h = 0 intersects the curve f = g = 0 only once.

Case 1(c) This case is identified by inequality (34) and the opposite inequality to (38), that is

$$\frac{\omega}{d_2} < ae \left[\frac{\varepsilon \eta d_1}{\gamma d_3} \left(1 - \frac{1}{a} \right) \left(\frac{1}{a} + \beta \right) + 1 \right]$$
 (40)

which guarantees that the point P is reached first during the transition from the point M in Figure 4(c). At the point P, there is a loss of stability and a quick jump to E takes place. A slow transition develops now along this manifold where x = 1 until a point is reached where stability in again lost at some point F. A transition of intermediate speed will develop along the fast manifold f = 0 back to the point L which completes the limit cycle in the case 1(c).

Case 1(d) In order that the transition goes back into high-frequency oscillations in each low-frequency cycle, we need to require that $z_0 < z_M$, which is equivalent to

$$e^{-a} < \frac{1-\beta}{2}e^{-a(1-\beta)/2}$$
 (41)

Thus, starting from the point A in Figure 4(d), a fast transition takes us, as explained earlier, to the point B on f = 0. An intermediate transition develops on this manifold until C is reached where the stability of the equilibrium fast manifold is lost. A fast transition then takes the system to the stable equilibrium point D. An intermediate speed transition is then made along this branch of manifold until G is reached where the stability is again lost and a quick jump brings us to the stable point H. This almost closes up the cycle but just misses the point B. The slow system has becomes active and z has been slowly increasing since $\dot{z} > 0$ here. Transitions then develop following the same pattern but with slowly varying z as seen in Figure 4(d) until M is reached, at which point the trajectory develops into a slow cycle which goes back into the fast cycles since inequality (41) guarantees that $z_0 < z_M$.

Case 2

We observe that in this case the point R is located on the stable part of the fast manifold f = 0 as shown in Figure 5. Mainly 3 subcases can therefore be identified here.

Case 2(a) If (21) as well as (33) hold then starting from the point A in Figure 5(a), a fast transition develops to the point B, followed by a transient of intermediate speed to C, from which point a slow transient takes us to the stable equilibrium point S where the transition ends.

Case 2(b) If (21) holds as well as (38) then, similarly to Case 2(a), transients develop toward the stable equilibrium point S where $\dot{x} = \dot{y} = \dot{z} = 0$ and the transition ends.

Case 2(c) Finally, if (21) holds as well as (40) then, from the point C in Figure 5(c), the point P is reached first where the stability is lost. A quick jump to E, followed by a transition at slow speed from E to F, then at intermediate speed back to D, closes the trajectory up into a low-frequency limit cycle for this case 2(c).

The above analysis can be summarized by the following theorem.

Theorem If ε and δ are sufficiently small, and if (16), (30), (32), and (39) hold, then system (9)-(11) has a global attractor which is a stable equilibrium if (18) and (33) hold, or (18), (34) and (38) hold, or if (21) and (33) or (38) hold. It is a low-frequency limit cycle if (21) and (40) hold, or if (18), (34) and (40) hold. Moreover, if (18), (34) and (40) as well as (41) hold, then the attractor is a low-frequency limit cycle which contains a period of high frequency oscillations.

NUMERICAL RESULTS AND DISCUSSION

Figure 6(a) shows a numerical simulation of the model equations (9)-(11) with parametric values chosen to satisfy inequalities (18), (30), (32), (34), (39) and (40). This is therefore the case 1(c) and the solution trajectory develops into a low-frequency limit cycle as predicted. The corresponding time courses of the three variables are shown in Figure 7(a).

Figure 6(b) shows a numerical simulations of the model equations (9)-(11) with parametric values chosen to satisfy inequalities (18), (30), (32), (34), (39), (40) as well as (41). This is therefore Case 1(d). The solution trajectory develops into a low-frequency limit cycle which contains high frequency oscillations as predicted in the above theorem. The corresponding time courses of the three variables are shown in Figure 7(b). Such underlying high frequency cycles in the biomass concentration profile have frequently been observed by a number of investigators [16-18]. In [16], the total budding cells count in their bioreactor data shows oscillatory behavior closely resembling our result of case 1(d) shown in Figure 7(b). Experimenting with different values for the system parameters such as β , d₃, a, and so on, shows that the frequencies and amplitude of oscillations can be appropriately adjusted to fit different chemostat conditions.

We observe that the constant a plays an important role in the kinetics of the chemostat under study. Considering the model in equation (7), a is in fact an indicator of how late or how soon the substrate inhibition sets in. In Figure 1, substrate inhibition seems to set in approximately half way to the maximum substrate level, suggesting that a should by around 2. Thus, the numerical results presented in Figures 6(a) and 6(b) can be considered as corresponding to the case where substrate inhibition is late in setting in (a < 2). In Figure 6(c), we present a numerical simulation of equations (9)-(11) in which a = 2.5, thus corresponding to the situation where the inhibition sets in rather early (a > 2). With this value of a, inequality (32) is violated and a = 2.5. Therefore, the transition develops from the

point E (in Figure 4(c) or 5(c)) all the way to the point (1, 0, 0) on the x-axis which is a stable washout steady state of the system. Figure 7(c) shows the corresponding time courses of the state variables in this case, where both the cells and product levels are seen to decrease toward zero, while the substrate level tends toward the maximum level $(S = S_F)$.

Also, it is numerically found that solution trajectories can still develop as theoretically predicted even though the values of ϵ and δ are not so small, and the assumption that the three components of the system carry highly diversified dynamics can be relaxed to a certain extent.

CONCLUSION

The appearance of sustained oscillations in bioreactor variables in continuous cultures indicates the complex nature of microbial systems, and the difficulties which may arise in bioprocess control and optimization.

In this paper, the dynamic behavior of a continuous bioreactor described by equations (9)-(11) has been investigated, incorporating the inhibitory effect at high levels of product and substrate concentrations. Assuming that the time responses of the three components are highly diversified, increasing from bottom to top, we were able to use standard singular perturbation analysis to describe the nature of the transients and the attractors of the system.

Complexed oscillatory behavior is extremely undesirable not only for control and design problems, but also for its potential for dangerous situations which may result in the case where toxic compounds are involved, such as in the operation of toxic waste treatment processes. Insights that can be gained from this type of analysis described above should prove most valuable in the light of such considerations.

ACKNOWLEDGMENT

Appreciation is rendered to the Thailand Research Fund for the financial support which made possible this research project.

FIGURE CAPTIONS

- FIGURE 1. Effect of substrate inhibition on specific growth rate at low ethanol concentration. (Data points taken from reference [15]).
- FIGURE 2. Effect of product inhibition on specific growth rate. (Data points taken from reference [15]).
- FIGURE 3. Two possible cases of trajectory development for the two dimensional fast-slow system (12), (13). Trajectories go toward a limit cycle ABDC in Case 1, and toward a stable equilibrium point R in Case 2.
- FIGURE 4. Trajectories of the model system (9)-(11) in Case 1 exhibiting four possible subcases 1(a), 1(b), and 1(c) identified in the text.
- FIGURE 5. Trajectories of the model system (9)-(11) in Case 2 exhibiting three possible subcases 2(a), 2(b), and 2(c) identified in the text.
- FIGURE 6. Numerical simulation of the model equations (9)-(11). Here, $\epsilon = 0.1$, $\delta = 0.01$, $\gamma = 2.0$, $\eta = 10.0$, $\omega = 3.0$, $d_1 = 0.25$, $d_2 = 0.25$, and $d_3 = 0.1$. In 6(a), the parametric values satisfy the inequalities of Case 1(c), with $\beta = 0.8$, a = 1.5, and the solution trajectory tends toward a low-frequency limit cycle as theoretically predicted. In 6(b), the parametric values satisfy the inequalities of Case 1(d), with $\beta = 0.2$, a = 1.5, and the solution trajectory tends toward a low-frequency limit cycle which contains a period of high-frequency oscillations. In 6(c), $\beta = 0.2$, and $\alpha = 0.2$, which corresponds to the situation where substrate inhibition is early in setting in.
- FIGURE 7. The time courses of the state variables x(t), y(t) and z(t) are shown here corresponding to the three respective cases seen in Figure 6.

 represents x(t) + 2.2 in 7(a), x(t) + 0.4 in 7(b), and x(t) in 7(c).

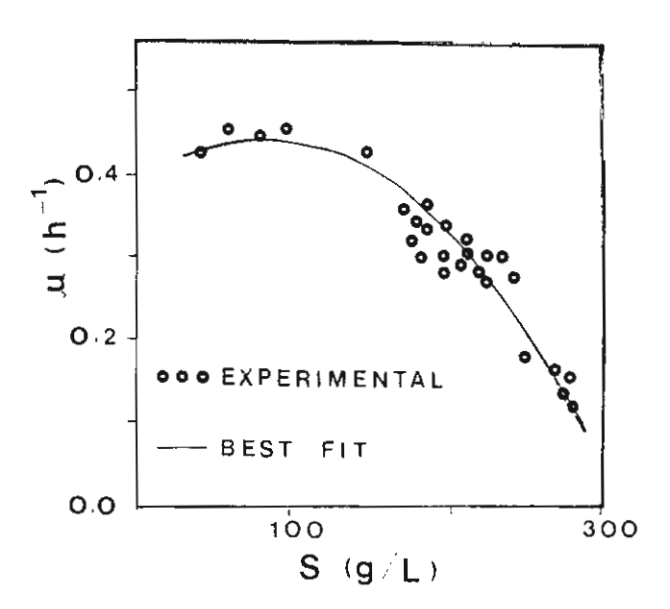
 o—o represents y(t).

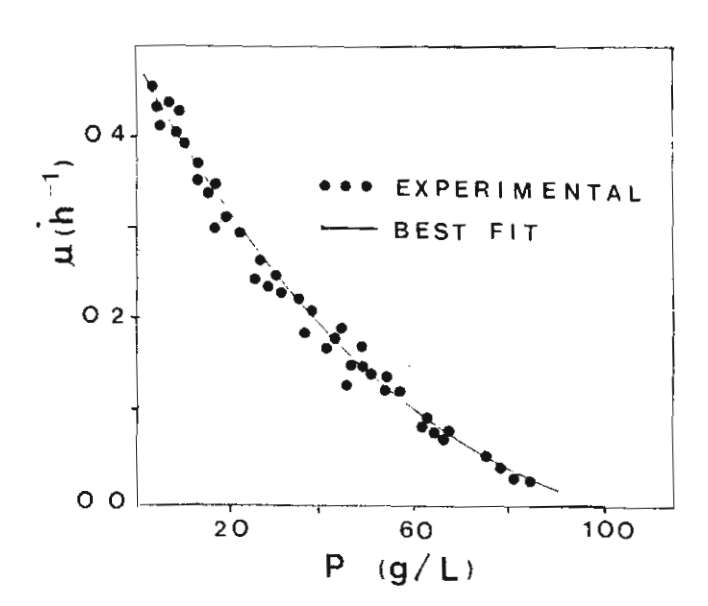
 ×—× represents z(t) + 0.3 in z(t) in z(t) in z(t) and z(t) in z(t) and z(t).

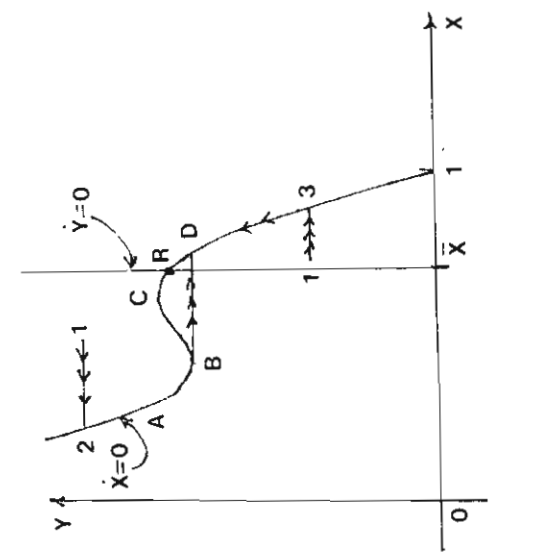
REFERENCES

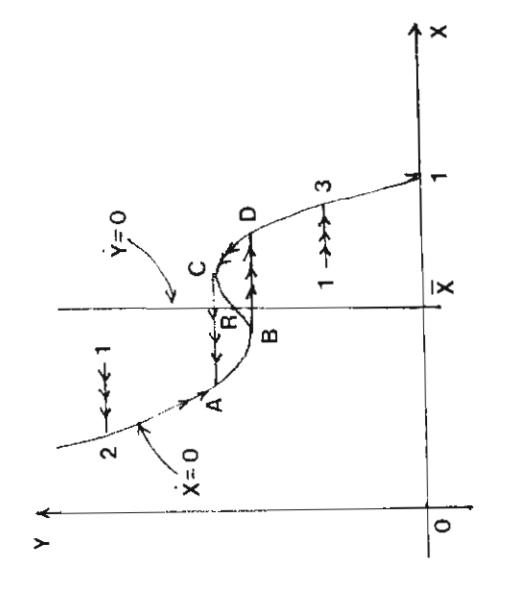
- 1. Agrawal, P., Lee, C., and Lim, H.C.: and Ramkrishna, D., Theoretical Investigations of Dynamic Behavior of Isothermal Continuous Stirred Tank Biological Reactors. *Chemical Engineering Science*. 37 (1982)3, pp. 453-462.
- 2. Aiba, S., and Shoda, M.: Reassesment of the product inhibition of alcohol fermentation. *J. Ferment. Technol.* 47 (1969) pp. 790-799.
- 3. Andrews, J. F.: A mathematical model for the continuous culture of microorgnisms utilizing inhibitory substrates. *Biotechnology and Bioengineering*. **10** (1968) pp. 707-723.
- 4. Bazua, C. D., and Wilke, C. R.: Ethanol effects on the kinetics of a continuous fermentation with Saccharomyces cerevisiae. Biotechnology and Bioengineering Symp. 7 (1977) pp. 105-118.
- 5. Ching-I Chen, and McDonald, K. A.: Oscillatory Behavior of *Saccharomyces* cerevisiae in Continuous Culture: I Effects of pH and Nitrogen Levels. *Biotechnology and Bioengineering*. **36** (1990) pp. 19-27.
- 6. Ching-I Chen, and McDonald, K. A.: Oscillatory Behavior of *Saccharomyces cerevisiae* in Continuous Culture: II Analysis of Cell Synchronization and Metabolism. *Biotechnology and Bioengineering*. **36** (1990) pp. 28-38.
- 7. Hoppensteadt, F.: Asymptotic stability in singular perturbation problems II: Problems having matched asymptotic expansions. *J. Differential Equations.* 15 (1974) pp. 510-512.
- 8. Lenbury, Y., Novaprateep, B. and Wiwatpataphee, B.: Dynamic Behavior Classification of a Model for a Continuous Bio-Reactor Subject to Product Inhibition. *Mathl. Comput. Modelling.* 19 (1994) 12, pp. 107-117.
- 9. Monod, J.: recherces pur la croessance des cultures bacteriennes, Hermann et Cie, Paris, 1942.

- Muratori, S.: An Application of the Separation Principle for Detecting Slow-Fast Limit Cycles in a Three-Dimensional System. Applied Mathematics and Computation. 43 (1991) pp. 1-18.
- 11. Muratori, S. and Rinaldi, S.: Remarks on Competitive Coexistence, SIAM J. APPL. MATH. 49 (1989) 5, pp. 1462-1472.
- Muratori, S. and Rinaldi, S.: Low- and High-frequency Oscillations in Three Dimensional Food Chain Systems. SIAM J. APPL. MATH. 52 (1992) 6, pp. 1688-1706.
- Olsvik, E. S., and Kristiansen, B.: Influence of Oxygen Tension, Biomass Concentration, and Specific Growth Rate on the Rheological Properties of a Filamentous Fermentation Broth. *Biotechnology and Bioengineering*. 40 (1992) pp. 1293-1299.
- 14. Ramkrishna, D., Fredrickson, A.G., and Tsuchiya, H.M.: Dynamics of Microbial Propagation: Models Considering Inhibitors and Variable Cell Composition, *Biotech. Bioeng.* 9 (1967) p. 129-170.
- Thatipamala, R., Rohani, S., and Hill, G. A., Effects of High Product and Substrate Inhibitions on the Kinetics and Biomass and Product Yields During Ethanol Batch Fermentation, *Biotechnology and Bioengineering*. 40 (1992) pp. 289-297.
- 16. Yano, T., and Koga, S.: Dynamic Behavior of the Chemostat Subject to Substrate Inhibition. *Biotechnology and Bioengineering*. 11 (1969) pp. 139-153.
- 17. Yano, T. and Koga, S.: Dynamic Behavior of the Chemostat Subject to Product Inhibition. J. Gen. Appl. Microbiol. 19 (1973) pp. 97-114.





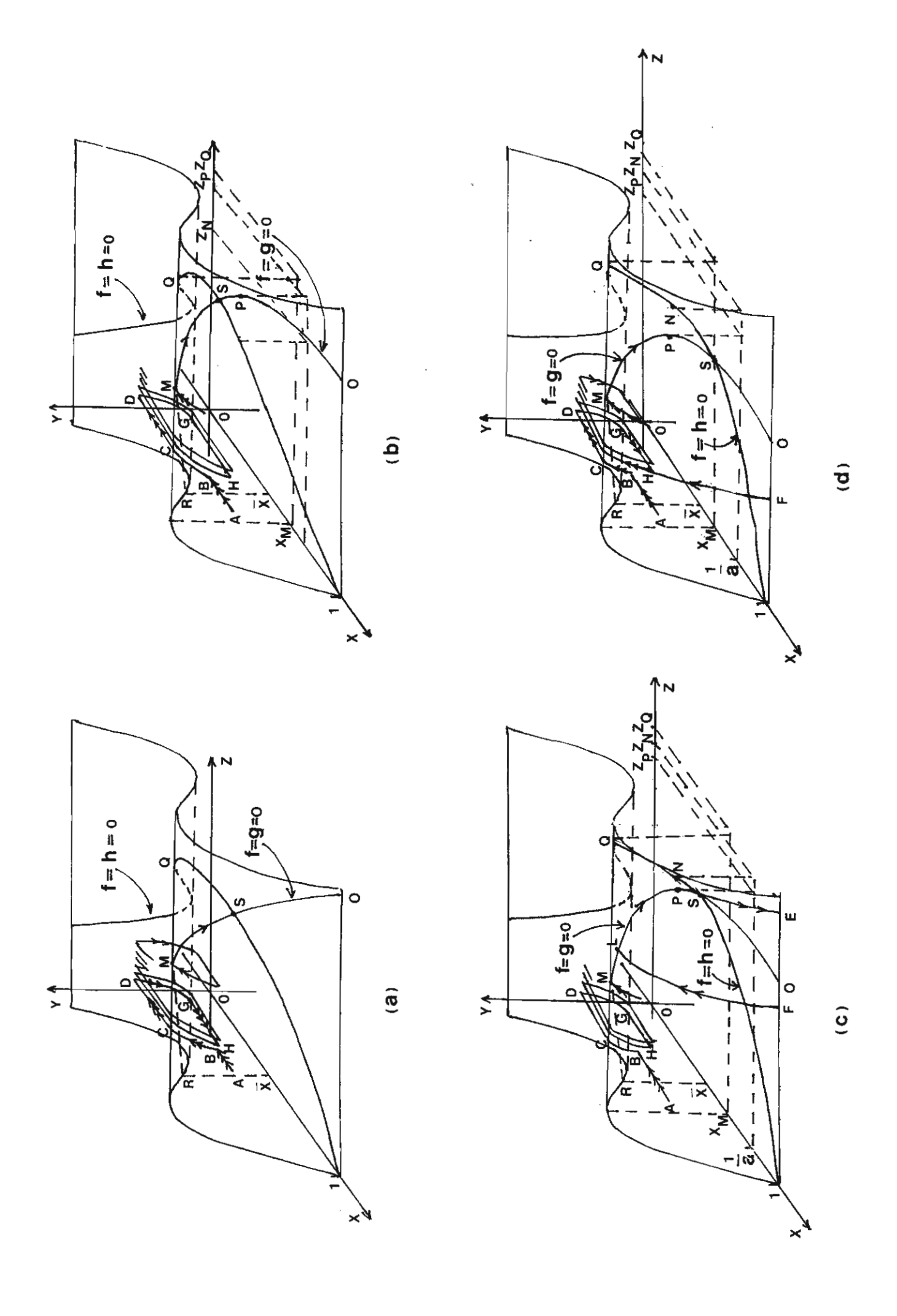


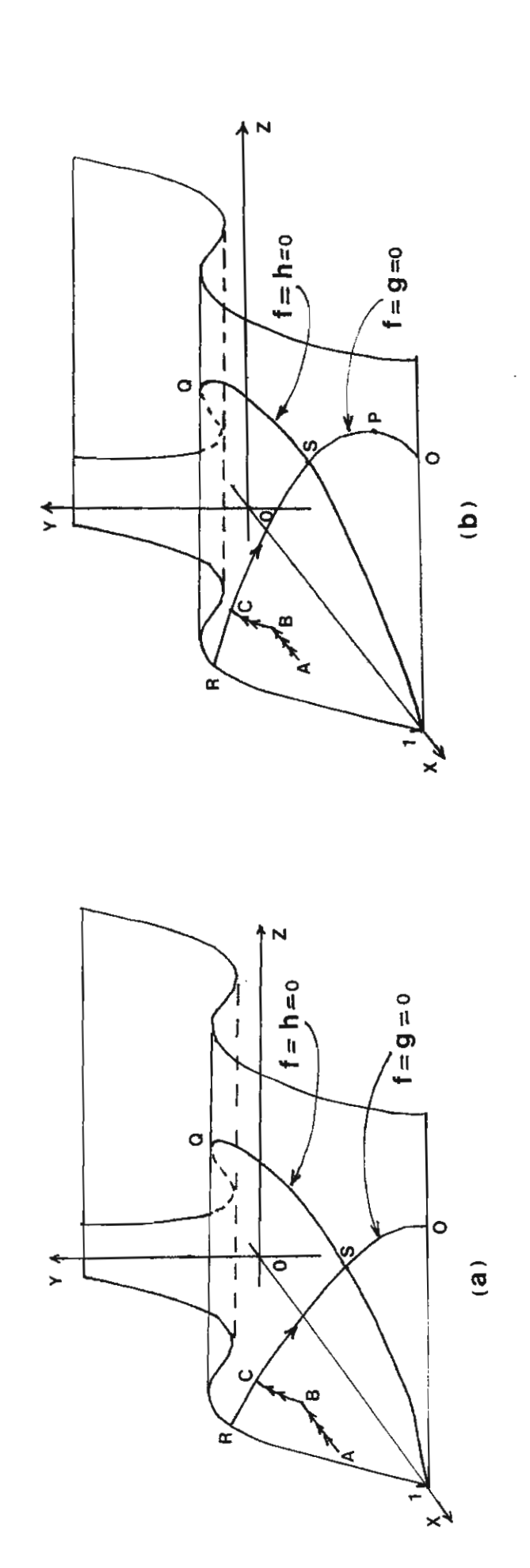


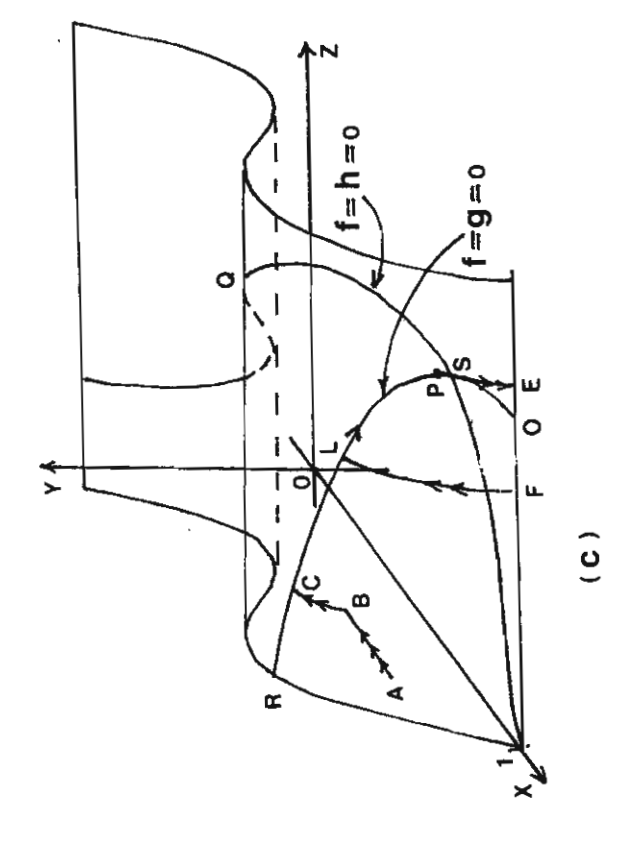
CASE 2

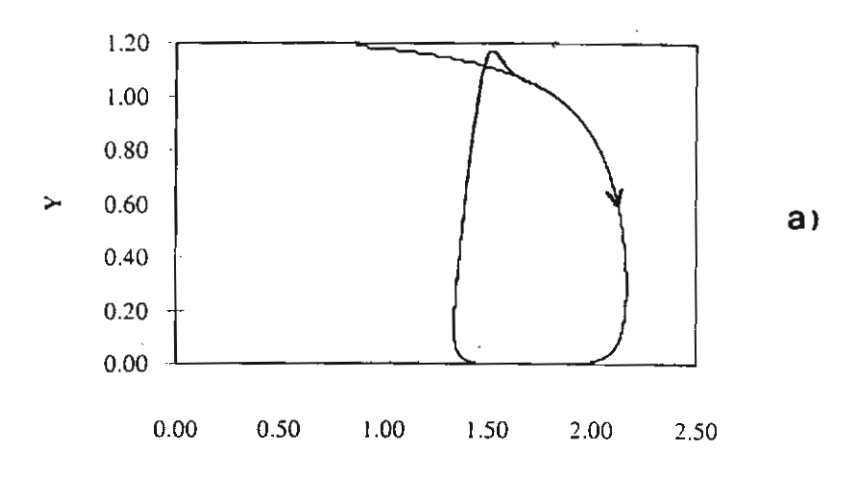
CASE 1

, -

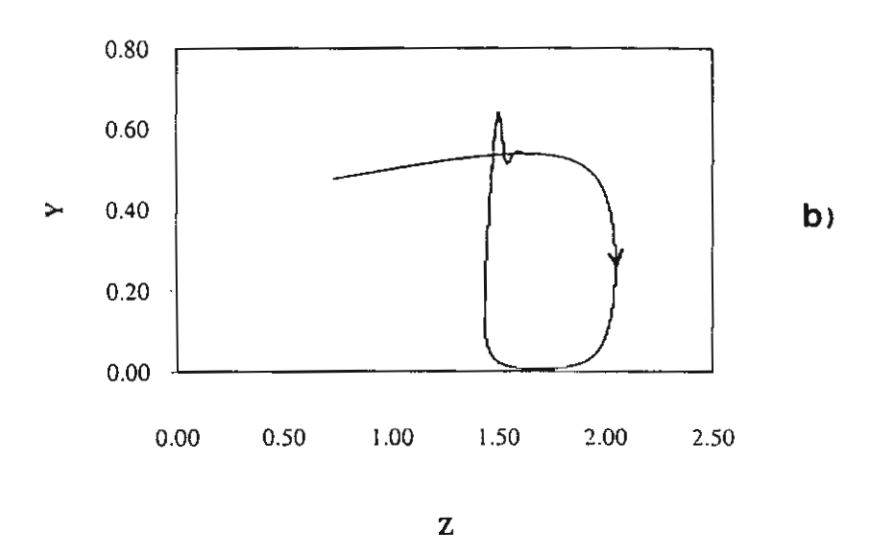


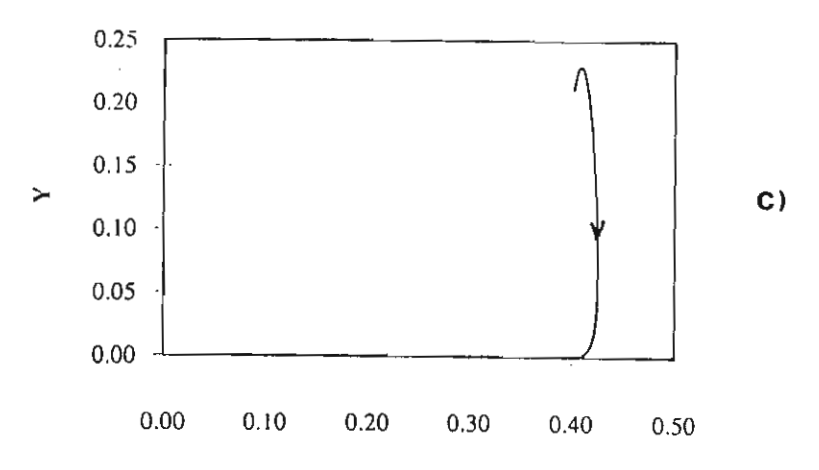


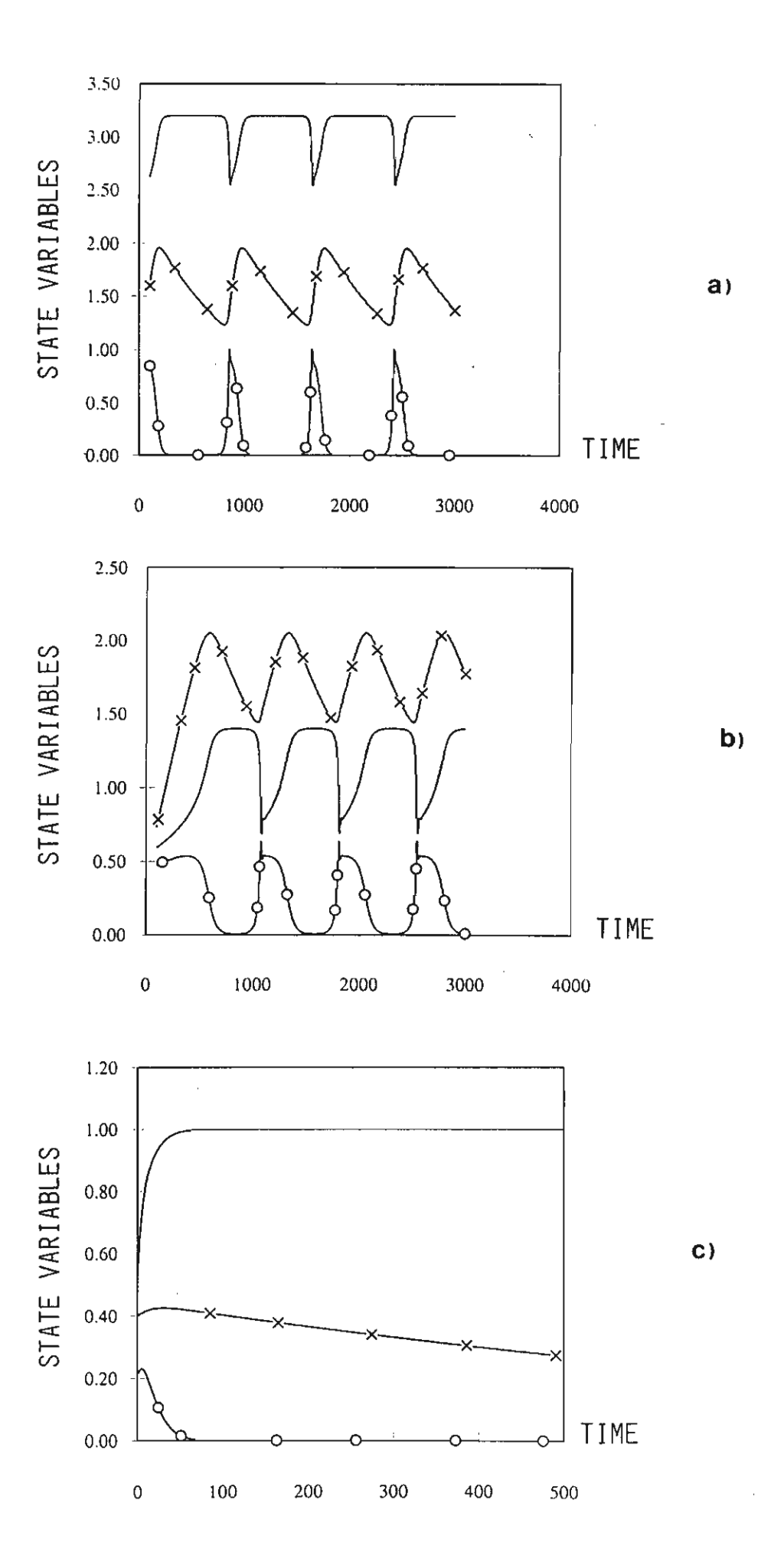




Z







การวิจัยช่วงที่ 2

ในช่วงที่สองนี้ ผู้วิจัยได้นำแบบจำลองค้นแบบ (2) และ (3) มาดัดแปลง โดยกิดแบ่ง prey population ออกเป็นสองกลุ่ม คือ กลุ่มเหยื่อที่ติดพยาธิหรือเชื้อโรคแล้ว (infective prey) กับกลุ่มเหยื่อ ที่ยังไม่มีพยาธิ (susceptible prey) ซึ่งกลุ่มที่ติดพยาธิแล้วย่อมมีความสามารถลดลงในการรอดพ้นจาก การถูกผู้ล่าจับกินเป็นอาหาร เพราะผลของพยาธิอาจทำให้เหยื่อมีระบบการรับรู้แสงสว่างที่ผิดปกติ เช่น ปลาก็จะแยกแยะระดับแสงได้ไม่ดีเท่าเดิม ทำให้ไม่ว่ายหลบแสงสว่างอยู่ตามใต้โขดหิน จึงถูกผู้ ล่า เช่น หมื จับกินเป็นอาหารได้ง่ายขึ้น ดังนี้เป็นต้น

ผู้วิจัยจึงทำการวิเคราะห์แบบจำลองที่ประกอบด้วยสมการอนุพันธ์ไม่เชิงเส้น 3 สมการ ดังนี้

$$\dot{S} = B(S+I) - D_1 S - \beta_0 S - \frac{\alpha_0 S z}{k+S}$$
 (30)

$$\dot{\mathbf{I}} = \beta_0 \mathbf{S} - \mathbf{D}_2 \mathbf{I} - \gamma \mathbf{I} \mathbf{z} \tag{31}$$

$$\dot{z} = z \left(-a_0 - b_0 z - \frac{c_0}{d+z} + \frac{\ell_0 S}{k+S} + \eta_0 I \right)$$
 (32)

โดยที่ S คือ ปริมาณของ susceptible prey

I คือ ปริมาณของ infective prey

z คือ ปริมาณของ predator

B คือ natural birth rate ของ prey

D₁ คือ natural death rate ของ susceptible prey

D₂ คือ natural death rate ของ infective prey

 β_0 คือ rate of infection

ผู้วิจัยกิดให้ predator เป็นสัตว์ชนิด social ซึ่งคำรงชีวิตได้ดีเมื่อยู่กันเป็นฝูง เช่น หมาใน เป็นค้น แล้วทำการวิเคราะห์ด้วย singular perturbation technique ซึ่งทำให้สามารถพิสูจน์ได้ว่า ถ้า $\alpha=\alpha_0\epsilon,\,\beta=\beta_0\epsilon,\,\eta=\eta_0\epsilon,\,a=a_0\epsilon\delta,\,b=b_0\epsilon\delta,\,c=c_0\epsilon\delta,\,\ell=\ell_0\epsilon\delta$ สำหรับค่าของ ϵ และ δ ที่มีค่าเล็กพอ และ

$$\ell > a + \frac{c}{d} \tag{33}$$

$$b < \frac{c}{d^2} \tag{34}$$

$$D + \beta - B > 0 \tag{35}$$

$$\alpha > \frac{B}{\sqrt{\frac{c}{b} - d}} \left(k + S_A\right) \left(\frac{I_B}{S_A} - \frac{D_2 + \beta - B}{B}\right)$$
(36)

$$\frac{D+\beta+B}{B} < \frac{\beta'}{D} \tag{37}$$

โดยที่

$$S_{A} = k \frac{(a - \eta I_{A}) + 2\sqrt{bc} - bd}{\ell - (a - \eta I_{A}) - 2\sqrt{bc} + bd}$$
(38)

$$I_{A} = \frac{\beta' S_{A}}{D + \gamma Z_{A}} \tag{39}$$

$$z_{A} = \sqrt{\frac{c}{b}} - d \tag{40}$$

$$I_{B} = \frac{\beta' k}{D} \left[\frac{(a - \eta I_{B}) + \frac{c}{b}}{\ell - (a - \eta I_{B}) - \frac{c}{b}} \right]$$
(41)

แล้วระบบสมการ (30)-(32) จะมีคำตอบเป็นคาบ

นอกจากนั้นยังได้แบ่งแยกพฤติกรรมของคำตอบในลักษณะต่าง ๆ ที่เราสามารถจะพบได้ใน สมการแบบจำลอง (30)-(32) เมื่อค่าพารามิเตอร์อยู่ในช่วงต่าง ๆ กัน ซึ่งผลการวิจัยทั้งหมดได้นำเขียน ขึ้นเป็น paper และได้รับ published เรียบร้อยแล้ว ในวารสาร *BioSystems* ซึ่งจะสามารถอ่านราย ละเอียดของการวิเคราะห์วิจัยได้ใน manuscript ที่แนบมาด้วยในหน้าถัดไป

นอกไปจากนั้น ผู้วิจัยยังได้นำเสนอผลงานการวิจัยต่าง ๆ ในการประชุมวิชาการนานาชาติ
The Second Asean Mathematical Conference ที่ Suranaree University of Technology เป็น invited paper ซึ่งได้รับพิมพ์ใน Proceedings ของการประชุมเรียบร้อยแล้ว ดังที่ได้แนบมาด้วยเช่นกัน

Singular Perturbation Analysis of a Model for a Predator-prey System Invaded by a Parasite



BioSystems 39 (1996) 251-262



Singular perturbation analysis of a model for a predator-prey system invaded by a parasite

Yongwimon Lenbury

Department of Mathematics, Faculty of Science, Mahidol University, Rama 6 Rd., Bangkok 10400, Thailand

Received 4 October 1995; revised 18 April 1996; accepted 8 May 1996

Abstract

A model of the predator-prey dynamics, as modified by the action of a parasite, is considered in which the prey population is divided into two classes, the susceptible and the infective members. The predator population is assumed to be of a social type, and have very fast dynamics, with all of its members infected by the parasite. Analysis of the model is carried out through singular perturbation arguments which allow us to derive explicit conditions on the parameters that identify different dynamic behavior of the system, and specifically ascertain the existence of a limit cycle composed of a concatenation of catastrophic transitions occurring at different speeds.

Keywords: Parasite-host interaction; Singular perturbation; Limit cycles

1. Introduction

Many different researchers (Holmes and Bethel, 1972; Moore and Lasswell, 1986; Dobson, 1988) have reported and extensively discussed the ability of parasites to change the behavior of infected hosts. It is well documented that the physiological interactions between parasites and their hosts often lead to changes in the behavior of infected animals which are usually beneficial to the pathogen and often detrimental to the host. According to Dobson (1988), the induced changes in host behavior have the effect of increasing the rate of parasite transmission. To achieve this effect, however, it is observed that the mechanisms involved in turns influence the host's survival, and occasionally they also affect its fecundity. This

establishes a conflict of interest between the parasite and its host. It is now recognized that parasites and pathogens are important factors in determining both the density and long-term population dynamics of many population (Anderson and May, 1979; Dobson, 1988). While previous workers have mainly considered predation and competition as important factors influencing both the individual and social behavior of various animal species, more recent studies (Anderson and May, 1979; 1986; Dobson, 1988) have now considered this interaction between parasites and their host to have significant effects on both ecological and evolutionary time scales (Dobson, 1988). Anderson and May (1986) proposed that parasites and pathogens can be divided, according to the response of the host to their presence, into

0303-2647/96/\$15.00 © 1996 Elsevier Science Ireland Ltd. All rights reserved PII S0303-2647(96)01622-X

two broad classes: the microparasites and the macroparasites. The former is characterised by their ability to produce a sustained immunological response in the host. These include the viruses, bacteria and protozoa. The latter, on the other hand, tends not to induce a sustained immunological response, and includes the helminths and other metazoan parasites.

Holmes and Bethel (1972) suggested four ways in which the parasite may modify infected members of the prey population: reduced stamina, increased conspicuousness, disorientation, and altered responses. In their earlier work, Arme and Owen (1967) reported on sticklebacks, infected by plerocercoids (Schistocephalus solidus), tending to swim closer to the surface of lakes and making themselves more susceptible to predation by birds. It has also been documented (Tiner, 1953) that the presence of larvae of Ascaris columnaris Leidy in mice and squirrels produces incoordination, blindness and loss of fear of larger animals. In other specific examples such as the moose-wolf system on Isle Royale (Freedman, 1990), this parasite-host interaction has been discovered to be necessary in the survival of the predator population.

In Dobson's seminal work (1988), various simple mathematical models were described which allowed the author to examine the demographic and evolutionary consequences, leading to the determination of how changes in the behavior of individual host affect both the net reproductive success of the parasite and the population dynamics of the parasite-host interaction.

More recently, Freedman (1990) studied a model of predator-prey dynamics as modified by the action of parasite. All predators in his model are invaded by the parasite, while the prey population is divided into two classes, the susceptible and the infectives. Anderson and May (1979) have previously shown that invasion of a resident predatorprey system by a new strain of parasite could cause destabilization in the sense that limit cycles may appear and extinction becomes possible. Freedman (1990) showed the opposite effect that an unstable (in the sense of extinction) system could be stabilized. He was also able to derive the criteria for persistence and discuss the stability of an interior equilibrium.

In this paper, we consider an adapted version of Freedman's model, so that the density-dependent death rate of the predator describes a social population which tends to survive better in herds or packs. Analysis of the model is carried out by applying a singular perturbation technique. We derive explicit conditions on the system parameters which identify different dynamical behavior exhibited by the system. When the predator population is assumed to have very fast dynamics with respect to prey, the analysis can be carried out through singular perturbation arguments which are based on simple geometric characteristics of the equilibrium manifolds of the fast, intermediate and slow variables of the system, allowing one to derive explicit conditions that guarantee the existence of a limit cycle in the extreme case of very fast very slow dynamics. The resulting limit cycle is composed by the alternate concatenation of two slow and two fast transitions and has interesting biological interpretations leading to better understanding of the system under study.

2. The model

In his study, Freedman (1990) considered the following model system of three ordinary differential equations:

$$\dot{S}(t) = B^*(X(t)) - \frac{S(t)D^*(X(t))}{X(t)} - \left[\beta_0 + \beta_1 z(t)\right]S(t) - \frac{S(t)p_1(X(t))z(t)}{X(t)}$$
(1)

$$\dot{I}(t) = [\beta_0 + \beta_1 z(t)]S(t) - \frac{I(t)D^*(X(t))}{X(t)}$$

$$-\frac{I(t)p_2(X(t))z(t)}{X(t)} \tag{2}$$

$$-\frac{I(t)p_2(X(t))z(t)}{X(t)}$$

$$\dot{z}(t) = z(t) \left[-\gamma^*(z(t)) + c \left(\frac{S(t)p_1(X(t)) + I(t)p_2(X(t))}{X(t)} \right) \right]$$
(2)

with $S(0) \ge 0$, $I(0) \ge 0$, $z(0) \ge 0$, where S(t), I(t), X(t) = S(t) + I(t), z(t), $t \ge 0$, are the susceptible, infective, total prey, and predator population densities, respectively. Here, $B^*(X)$ and $D^*(X)$ are, respectively, the birth rate and the natural death rate of the prey population, $\gamma^*(z)$ is the death rate of the predator in the absence of prey, while $p_1(X)$ and $p_2(X)$ are the functional responses of the susceptible and infective prey, respectively, assumed by Freedman (1990) to depend on λ alone. The constant c is the rate of increase of predator per unit prey uptake.

For our specific purpose, we will make the reasonable assumption that the birth rate $B^*(X)$ and the natural death rate $D^*(X)$ of the prey population both vary directly as the total prey population X, namely;

$$B^*(X) \equiv B_0 X \tag{5}$$

where B_0 is a constant, and similarly for $D^*(X)$. We further assume that β_1 , which is the rate per unit predator of prey infection due to parasitic reproduction in the predator population, is negligible ($\beta_1 = 0$), while the infection rate of susceptible prey in the absence of predator is $\beta_0 \neq 0$. For

regularity reason, if $\beta_1 > 0$ in the system model, the solution should not be very much different from what we shall find here under the assumption that β_1 is zero, as long as β_1 is not too large.

The density-dependent death rate $\gamma^*(z)$ of the predator in the absence of prey is assumed to have the form

$$\gamma^*(z) \equiv a_0 + b_0 z + \frac{c_0}{d+z} \tag{6}$$

the graph of which can be seen in Fig. 1. Such a mortality curve would describe the death rate of social predators, such as wolves or hyenas, which survive somewhat better by staying in a pack, so that the mortality rate decreases initially as the number of predators in the pack increases. When the population density is too high then its mortality rate begins to rise as described by the graph of the function in Eq. (6). Field studies which support this form of $\gamma^*(z)$ can be found in the work by Barton and Whiten (1993) which described feeding competition among female olive baboons. It was stated

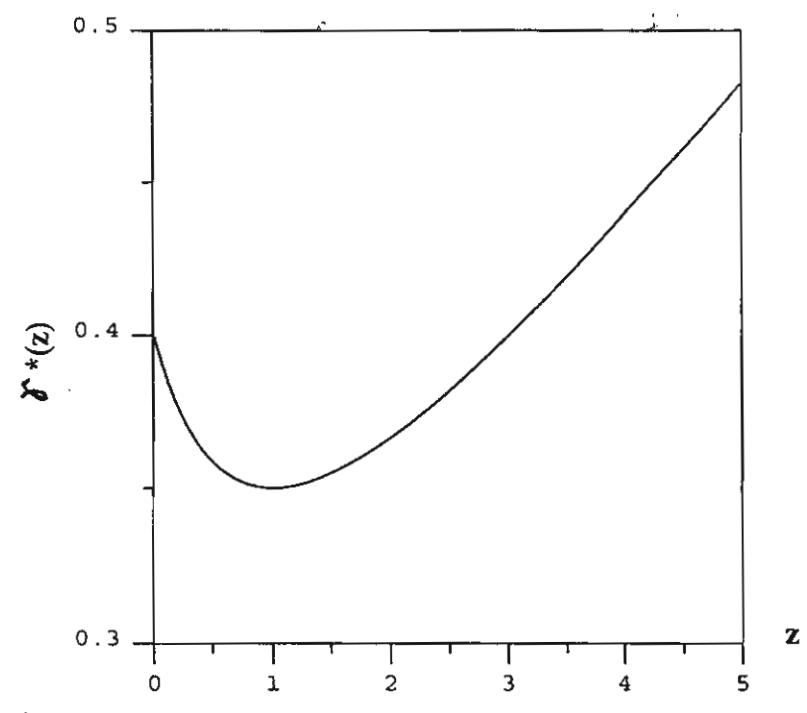


Fig. 1. The graph of the density-dependent death rate of the predator described by Eq. (6). Here, a = 0.2, b = 0.05, c = 0.2, d = 1.0.

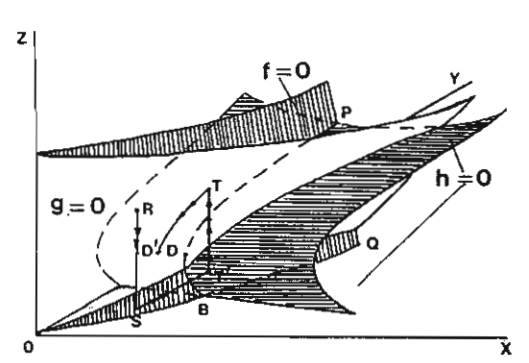


Fig. 2. The three equilibrium manifolds f = 0, g = 0, h = 0. The intermediate manifold g = 0 separates the line DP from the line OO.

that group-living is, on the one hand, a mutualistic or cooperative solution to predation pressure or resource acquisition. On the other hand, once the group exists, characteristic patterns of interactions between individuals within the group may then reflect the social partitioning of resources; competition for food and mates. Brault and Caswell (1993) also did a study on pod-specific demography of killer whales. They investigated the suggestion that, in social animals, group structure influences the vital rates and the fitness of members of the group or 'pod'.

Finally, the predator functional responses in Eq. (3) are modified so that the functional response of the susceptible population follows the Michaelis Menten kinetics, while that of the infected population varies directly as the density of the total prey population (X). Namely, we let

$$p_1 \equiv \frac{\alpha_0 X}{k + S}$$

where α_0 is the maximum predation rate and k is the half saturation constant, while

$$p_2 = \gamma X$$

where γ is a positive constant of variation.

We are thus led to the following system of differential equations:

$$\dot{S} = B_0(S+I) - D_1 S - \beta_0 S - \frac{\alpha_0 S z}{k+S}$$
 (7)

$$\dot{I} = \beta_0 S - D_2 I - \gamma I z \tag{8}$$

$$\dot{z} = z \left[-a_0 - b_0 z - \frac{c_0}{d+z} + \frac{l_0 S}{k+S} + \eta_0 I \right]$$
 (9)

where the infected prey has an increasingly higher functional response, owing to the action of the parasites, than the uninfected prey.

3. Singular perturbation analysis

To analyze the predator-prey dynamics as modified by the action of a parasite, we consider then the model equations (7)-(9) and scale the dynamics of the three hierarchical components of the system by means of two small dimensionless positive parameters ε and δ , namely; we let x=I, y=S, $\beta=\beta_0\varepsilon$, $B=B_0\varepsilon$, $\beta'\equiv\beta/\varepsilon$, $D=D_1\varepsilon=D_2$, $\alpha=\alpha_0\varepsilon$, $a=a_0\varepsilon\delta$, $b=b_0\varepsilon\delta$, $c=c_0\varepsilon\delta$, $l=l_0\varepsilon\delta$, and $\eta=\eta_0\varepsilon\delta$. We are led to the following system of differential equations:

$$\dot{x} = \beta' y - Dx - \gamma xz \equiv f(x, y, z) \tag{10}$$

$$\varepsilon \dot{y} = B(x+y) - Dy - \beta y - \frac{\alpha yz}{k+y} \equiv g(x, y, z)$$
 (11)

$$\varepsilon \delta \dot{z} = z \left[-a - \dot{b}z - \frac{c}{d+z} + \frac{ly}{k+y} + \eta x \right]$$

$$\equiv h(x, y, z) \tag{12}$$

which shows that during transitions, when the right sides of Eqs. (10–12) are finite but different from zero, $|\dot{y}|$ is of the order $1/\varepsilon$ and $|\dot{z}|$ is of the order $1/\varepsilon$ 0. This means that, if ε and δ are small, the growth of infected population is slower than the growth of the susceptible one, and the predator population has, in comparison, very fast dynamics. These assumptions are satisfied in many predator-prey systems found in nature which are effected by the host-parasite interactions.

We shall first show that if certain conditions on the parametric values are satisfied then the equilibrium manifolds of the system of Eqs. (10-12) will be shaped as in Fig. 2. Transients of varying speeds along these manifolds will form a path which results in a closed cycle in this case. Such a path approximates the exact solution to the model system Eqs. (10-12) in the sense that the solution trajectory will be contained in a tube around that path and the radius of the tube goes to zero along

with ε and δ . Consideration of the various regions in the parameter plane, as delineated by the above mentioned conditions on the parameters, then allows us to gain a better insight into the effect of parasite invasion on the stability of the predator-prey system and the survival of the species.

As is well known (Muratori, 1991; Muratori and Rinaldi, 1992), the system Eqs. (10-12), with ε and δ small, can be analyzed with the singular perturbation method which, under suitable reguarity assumptions, allows approximating the solution of the system Eqs. (10-12) with a sequence of simple dynamic transitions along the equilibrium manifolds of the system and occurring at different speeds. First, the slow (x) and intermediate (y) variables are frozen at their initial values x(0) and y(0), and the evolution of the fast component of the system is determined by solving the 'fast system'

$$\dot{z}(t) = h(x(0)), y(0), z(t)) \tag{13}$$

Thus, z(t) eventually tends toward a stable equilibrium of z(x(0),y(0),z(0)) of Eq. (13), assuming here that the system has unique stable equilibrium. Then keeping x frozen at x(0), we look at the 'intermediate system' which has now become active, namely;

$$\dot{y}(t) = g\bigg(x(0), y(t), \tilde{z}(x(0), y(t), z(0))\bigg)$$
(14)

where $\tilde{z}(x(0),y(0),z(0))$ is a stable equilibrium of the fast system (Eq. (13)) with y(0) substituted by y.

In Fig. 2, where low-, intermediate-, and high-speed trajectories are indicated, respectively, with one, two, and three arrows, the three equilibrium manifolds of the system Eqs. (10-12) are shown. The intermediate manifold g=0 is seen here to separate the line DP from the line OQ. Here, the line DP lies along the intersection of the slow manifold f=0 and the nontrivial fast manifold given by an equation of the form $y=\phi(x,z)$ on which h=0. The line OQ lies along the intersection of the slow manifold f=0 and the trivial fast manifold z=0 on which z=0 as well.

At first a high-speed transition develops at constant x and y and brings the system from (x(0),y(0),z(0)) (point R in Fig. 2) to a stable equilibrium of the fast manifold h=0 (point S in Fig. 2). Then, the intermediate system having now

become active, a second intermediate-speed transition takes place on the manifold at constant x (segment ST' in Fig. 2) until a point is reached (point T' in Fig. 2) where the stability of the equilibrium manifold h = 0 is lost and a quick transition then takes the state of the system to the equilibrium point on a stable part of the manifold, which will be the point T in Fig. 2. A transition of intermediate speed then develops along this part of the manifold to the point D' of Fig. 2.

The proof of the existence and location of the point T' can be found in Schecter (1985) and Osipove et al. (1986). The direction of transition along the line ST' or T' depends on the sign of \dot{y} namely g(x,y,z). Thus, let us assume that for suitable values of the parameters the intermediate (stable) manifold g = 0 separates the trivial manifold z = 0 from the part of the non-trivial manifold h = 0 on which the line TD' and CD lie (see Fig. 2), and that g is positive below the manifold g = 0 and negative above it. Under these conditions the system moves toward point D' along the line TD', and when D' is reached we have a saddle-node bifurcation of the fast system: the variable z at point D' is not at a stable equilibrium anymore and a catastrophic transition from D' to A' occurs at a very high speed. This almost closes the cycle but for the fact that during this time the variable x has been increasing very slowly, assuming that we have started on the side of the manifold f = 0 where f >

Once the system is at A', a slow motion develops again from A' in the direction of increasing y because g is positive here. The same cycling is repeated, densely covering the manifold h = 0 while the variable x increases slowly until the equilibrium point B' on the manifold f = 0 is reached where $\dot{x} = 0$. A high-speed transient brings the state of the system back onto the non-trivial manifold h = 0 at the point C along the line of intersection between the manifold h = 0 and f = 0. A transition of intermediate speed to D then takes place along this line followed by a catastrophic transition from D to A. An intermediate speed transition from A then brings us back to B', resulting in a closed cycle AB'CD lying on the manifold f = 0. (see Fig. 3a)

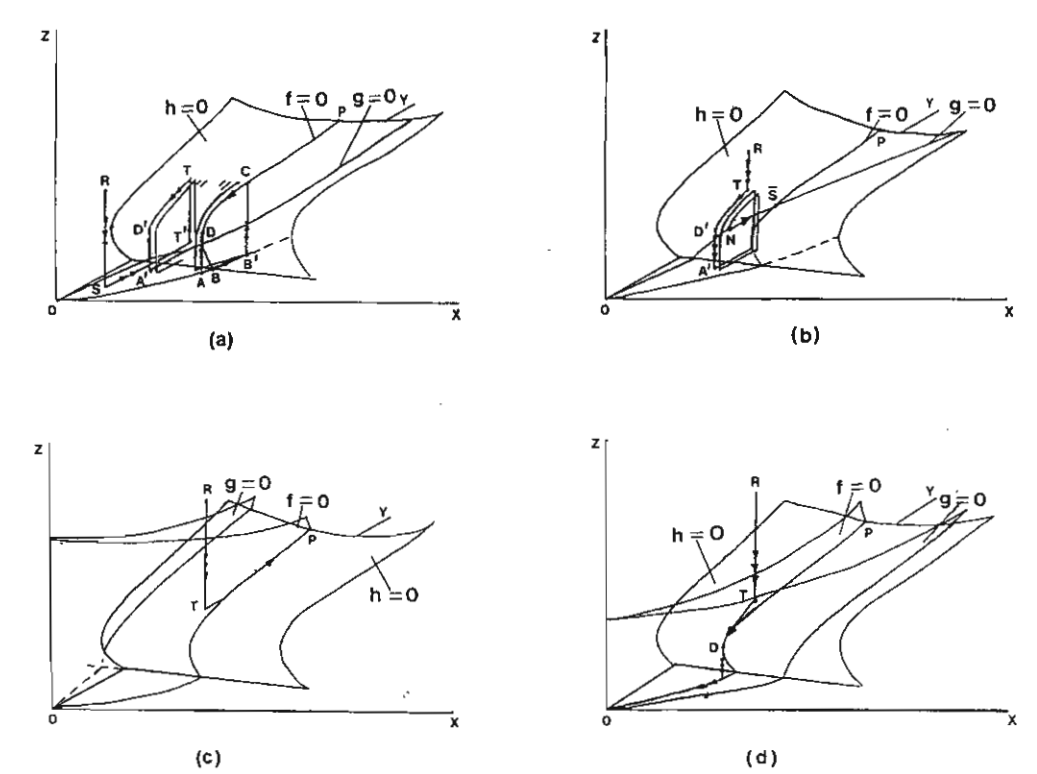


Fig. 3. Four possible cases identified in the text according to the relative positions of the three equilibrium manifolds.

4. Existence of limit cycle

We now show that if ε and δ are sufficiently small and

$$l > a + c/d$$
 (15)
 $b < c/d^2$ (16)

$$h < c/d^2 \tag{16}$$

$$D + \beta - B > 0 \tag{17}$$

$$\alpha > \frac{B}{\sqrt{c/b} - d} (k + y_A) \left(\frac{x_B}{y_A} - \frac{D + \beta - B}{B} \right)$$
 (18)

$$\frac{D+\beta-B}{B} < \frac{\beta'}{D} \tag{19}$$

where

$$y_A = k \frac{(a - \eta x_A) + 2\sqrt{bc - bd}}{l - (a - \eta x_A) - 2\sqrt{bc + bd}}$$
(20)

$$x_A = \frac{\beta' y_A}{D + \gamma z_A} \tag{21}$$

$$z_A = \sqrt{\frac{c}{b}} - d \tag{22}$$

$$x_{B} = \frac{\beta' k}{D} \left[\frac{(a - \eta x_{B}) + \frac{c}{d}}{l - (a - \eta x_{B}) - \frac{c}{d}} \right]$$
 (23)

then a limit cycle exists for the model system Eqs. (10-12).

We first prove that Eqs. (15-19) guarantee that the geometry of the manifolds f = 0, g = 0, and h = 0 is as in Figs. 2 and 3a.

Manifold h = 0

We observe that the manifold h = 0 consists of 2 parts; the trivial manifold z = 0 and the non-trivial manifold given by the equation

$$a + bz + \frac{c}{d+z} = \frac{ly}{k+y} + \eta x \tag{24}$$

Eq. (24) defines a surface $y = \phi(x,z)$ which intersects the (x,y) plane at

$$y_B = k \frac{(a - \eta x) + \frac{c}{d}}{l - (a - \eta x) - \frac{c}{d}}$$
(25)

so that $y_B > 0$ for some values of x > 0 if

$$\frac{a + \frac{c}{d}}{l - a - \frac{c}{d}} > 0 \tag{26}$$

using the fact that y_B is a continuous function of x in the neighbourhood of x = 0.

Eq. (26) holds if Eq. (15) is satisfied. Further, differentiating Eq. (24) with respect to y, we find that, for a fixed x,

$$b - \frac{c}{(d+z)^2} = \frac{lk}{(k+y)^2} \frac{d\varphi}{dz}$$

so that Eq. (16) implies that $d\phi/dz$ for z = 0. Thus, the manifold $y = \phi(x,z)$ is shaped as in Fig. 2, and the function $y = \phi(x,z)$ has a minimum at point D with

$$z_D = \sqrt{\frac{c}{d}} - d \tag{27}$$

which is positive due to Eq. (16), and independent of x. Therefore, we find that

$$y_{A'} = y_{A} = \varphi(x_{A}, z_{D})$$

$$= k \frac{(a - \eta x_{A}) + 2\sqrt{bc} - bd}{l - (a - \eta x_{A}) - 2\sqrt{bc} + bd}$$
(28)

Manifold f = 0

This manifold is given by

$$x = \frac{\beta' y}{D + \gamma z}$$
Thus, $x > 0$ for all $y > 0$ and

$$\frac{\partial x}{\partial y} = \frac{\beta'}{D + \tau z} \tag{30}$$

which is positive for y = 0 so that the manifold is as in Figs. 2 and 3a. Moreover,

$$\frac{\partial f}{\partial x} = -D - \gamma z < 0$$

for all positive values of z and of the parameters, so that the equilibria of the intermediate system Eq. (11) with y frozen are always stable.

The manifold f = 0 intersects the manifold h = 0 along the curve characterized by the value of x_B given in Eq. (23).

Manifold g = 0

The manifold g = 0 is given by the equation

$$x = \rho(y, z) = \left(\frac{D + \beta - B}{B}\right)y + \frac{\alpha yz}{B(k + y)}$$
(31)

so that Eq. (17) implies that ρ is increasing with y as well as with z. The manifold is thus shaped as seen in Figs. 2 and 3a, and x increases from C to D along line DQ. The manifold $x = \rho(y,z)$ is therefore below the line segment CD if

$$\rho(y_D, z_D) > x_C \tag{32}$$

But $x_C = x_B$ and $y_D = y_A$, therefore, Eq. (32) is guaranteed by

$$\rho(y_A, z_D) > x_B \tag{33}$$

Using Eqs. (27) and (28) in Eq. (33) we arrive at Eq. (18) which guarantees that the manifold $x = \rho(y,z)$ is below the line CD of Fig. 3a.

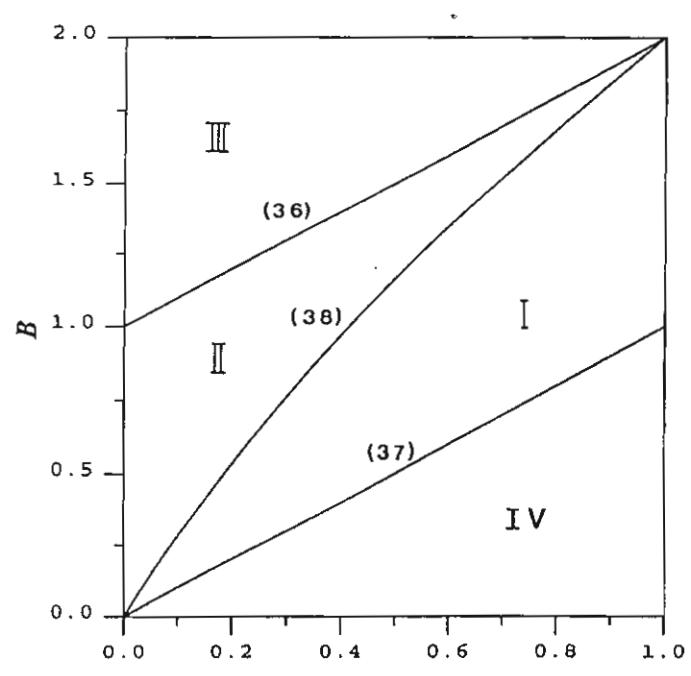


Fig. 4. Four regions in the (D,B) parameter plane delineated by Eqs. (35-37) where different dynamic behavior can be expected. Here, $a=0.1,\ b=0.025,\ c=0.1,\ d=1.0,\ l=0.3,\ k=1.0=0.8=0.2=0.2=0.1$, and =0.025.

Finally, along the line OB

$$\frac{x}{y} = \frac{\beta'}{D + \gamma z} \bigg|_{z=0} = \frac{\beta'}{D} \tag{34}$$

while the intersection of manifold f = 0 with the (x,y) plane (z = 0) is given by

$$\frac{x}{y} = \frac{D + \beta - B}{B} \tag{35}$$

We also observe, considering Eqs. (30) and (31), that the slope $\partial x/\partial y$ decreases with z along the manifold f=0 but the slope of $\partial x/\partial y$ the manifold g=0 increases with z. Therefore, the requirement that the line formed by Eq. (34) is below the line formed by Eq. (35) will be assured if Eq. (19) is satisfied.

Thus, the manifold g = 0 separates the line segment AB from the line segment DC of Fig. 3a and the transitions of various speeds can develop

as argued in the previous section. Starting from the point C, a transition slowly develops along PD towards the point D, since g < 0 here, where a saddle-node bifurcation occurs. A catastrophic transition from D to A then takes place followed by a slow transition from A towards B, since the line segment AB is below the manifold g = 0 so that g > 0 and y is increasing along this line. Once a point B' is reached a quick jump back to C closes up the transition AB'CD, resulting in a limit cycle composed of the concatenation of transitions occurring at two different speeds.

5. Parameter space classification of dynamic behavior

We now discuss the different cases into which the transitions can develop according to different regions in the parameter space. For fixed values of

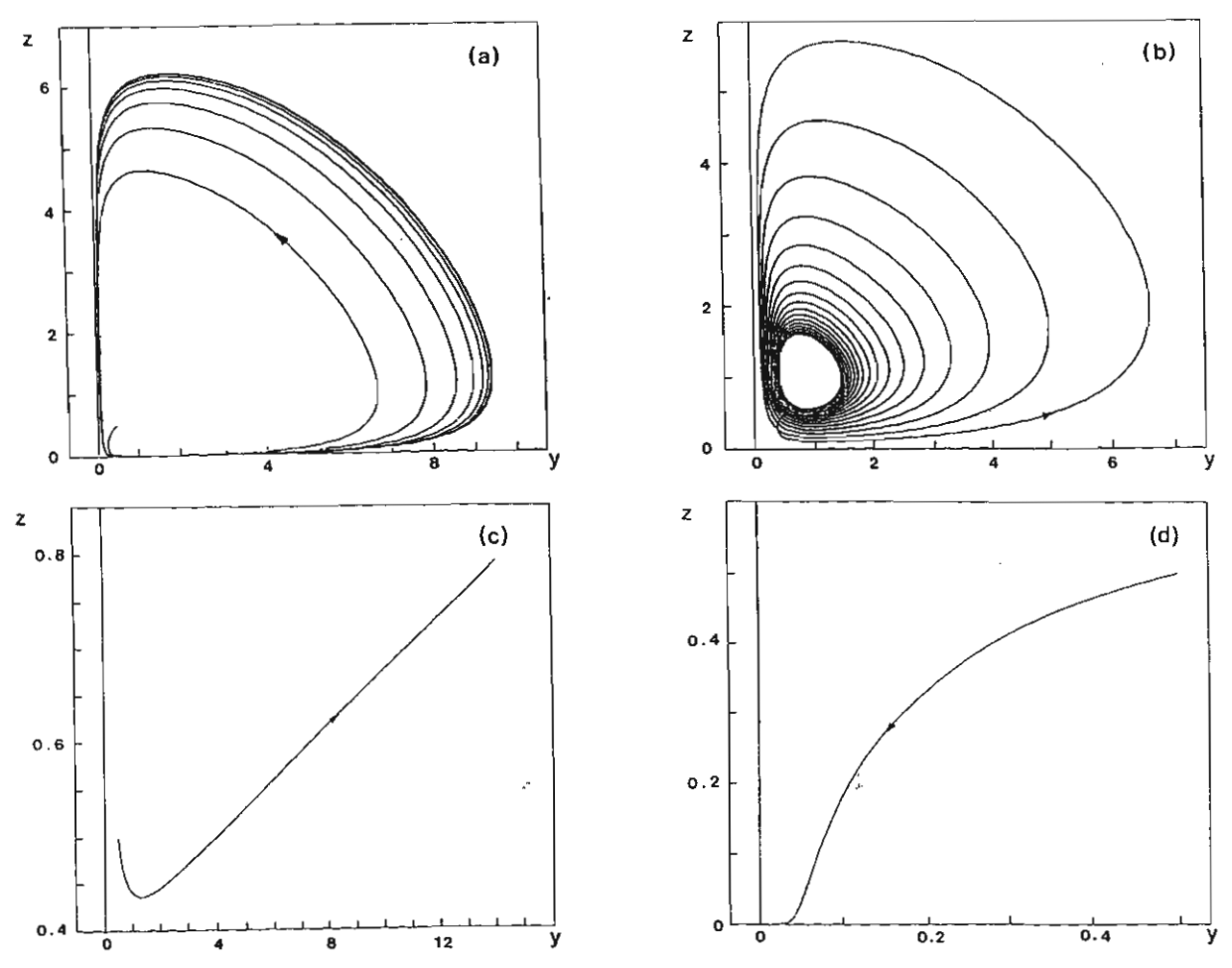


Fig. 5. Computer simulations of the model system Eqs. (10-12) with a = 0.1, b = 0.025, c = 0.1, d = 1.0, l = 0.3, k = 1.0 = 0.8, = 0.2 = 0.2 = 0.1 = 0.025 = 1.0 = 0.5 0. In Figures (a), (b), (c), and (d), the point (D,B) is located in Regions I, II, III, and IV of Fig. 4, respectively.

the parameters a, b,c,d,k,l, α , β , β' , γ , and η , the graphs of equations

$$D + \beta - B = 0 \tag{36}$$

$$\frac{D+\beta-B}{B} = \frac{\beta'}{D} \tag{37}$$

and

$$\alpha = \frac{B}{\sqrt{c/b} - d} (k + y_A) \left(\frac{x_B}{y_A} - \frac{D + \beta - B}{B} \right)$$
 (38)

divide the (D,B) space into four regions as shown in Fig. 4.

In region I, inequalities (15-19) are satisfied, and

therefore, the transitions are as in Fig. 3a and the solution trajectories develop into a limit cycle which is guaranteed by the discussions in the previous section. Fig. 5a presents a computer simulation of the model system Eqs. (10-12) with (D,B)=(0.1,0.2) in this region I, showing the predicted limit cycle seen here projected onto the (y,z) plane.

In region II, inequality (18) is violated which means that the requirement that the manifold f = 0 is below CD cannot be guaranteed. The positions of the manifolds can be as in Fig. 3b, in which case the intersection point \bar{s} of the three manifolds f = 0, g = 0 and h = 0, (the steady state) is located on the

stable portion of the manifold h = 0. When the transitions reaches the point N on the line of intersection between the manifolds f = 0 and h = 0, a slow motion develops along this line in the direction of increasing y and the transition ends once the point \bar{s} in Fig. 3b is reached. Thus the solution trajectory is expected to spiral towards this stable equilibrium point \bar{s} . Fig. 5b presents a computer simulation of the model system for this case with (D,B) = (0.00002,0.2) in region II, showing the solution trajectory spiralling towards the stable equilibrium state.

In region III, inequalities (17) and (18) are violated. The property of the manifold g = 0 that $\rho(y,z)$ increases with y is not guaranteed and it is possible for the manifolds to be positioned in this case as in Fig. 3c in which the line segment DP is in the region where g > 0. This means that, once the state of the system reaches the point T transition of intermediate speed will develop in the direction of increasing x toward the point P. We therefore, have in this case an overflow in all three populations. Fig. 5c shows an example of solution trajectory in this case with (D,B) = (0.0002,0.8) in region III.

Finally, in region IV inequality (19) is now violated and it can not be guaranteed that the manifold g=0 is above the line segment AB. It is then possible for the manifolds to be positioned as shown in Fig. 3d. Here, along OB we have g < 0, and once the state of the system reaches the point T, a slow transition will develop in the direction of decreasing y along TDO towards the point O. In this case, we have extinction of all three populations in the system under study. Fig. 5d shows a computer simulation of the system model in this case with (D,B) = (0.14, 0.08) in region IV and the solution trajectory is observed to approach the origin as time passes as expected.

6. Discussion

From the above analysis of our model system Eqs. (10-12), we can immediately make the following observations and comments.

The 'stable' region II is located between the lines given by Eqs. (36) and (37). In the case that $\beta = \beta'$,

this means that for a stabilized situation, it is necessary that we have

$$D < B < D + \beta \tag{39}$$

In other words, the birth rate of the susceptible prey must not be less than its death rate, but should not exceed the sum of its death rate and the rate of infection β . This is not surprising and no more than what we should expect.

Moreover, inequality (18) says that in order to drive the system into the stable region II, the value of the constant α in the response function of uninfected prey should not be too large. In fact, it must be smaller than the quantity on the right hand side of inequality (18). This is again a reasonable condition for parasite-host dynamics in which the uninfected prey has lower functional response than the infected prey. If, on the other hand, α becomes too high, the system can destabilize and limit cycles appear.

The interesting feature of the limit cycle which is discovered to be composed of transitions of two different speeds fits well with the host-parasite dynamics observed in nature. When the number of the predator'is low, susceptible and infected preys grow relatively slowly for a long period until they reach a biomass at which the situation becomes so attractive to members of the predator population that we have an abrupt increase in the number of the predator in a very short space of time. This is then followed by a second long period during which the prey biomass slowly decays. As a result, the predator population also decreases smoothly until it reaches a critical density at which point its own mortality mechanisms destabilize it. The predator population then collapses quickly to almost extinction.

We also observe that if the parasite is no longer present, which will be the case if $\beta = \beta' = 0$ then Eqs. (17) and (19) cannot be satisfied simultaneously. This means analytically that the stable region (Region II) no longer exists and neither does Region I. The system may destabilize to extinction. If, on the other hand, β and β' are non-zero, then the stable region II exists and the prey and predator populations can tend toward the stable steady state values as time progresses. In the case where inequalities (15–19) are satisfied, the population densities

will oscillate close to these steady state values. This seems to indicate that stable existence of the predator population depends, to a certain extent, on the presence of the parasites. In other words, the invasion of the parasite can stabilize the system resulting in persistence and the survival of the predator. This is in agreement with the observations made by several other authors who have done extensive research work in this field (Peterson, 1977; Rau and Caron, 1979).

7. Conclusion

In this paper, singular perturbation arguments have been used to detect limit cycle behavior as well as describe other dynamical situations which are observed in the predator-prey interaction which is modified by the action of a parasite. Implicit conditions have been derived which identify the ranges of parametric values for which, in particular, the existence of a parasite ($\beta_0 > 0$) can cause destabilization and the appearance of limit cycles (Region I of Fig. 4). On the other hand it is possible to stabilize an unstable (in the sense of extinction) system by driving the system into Region II of Fig. 4.

The method of analysis is based on purely geometric arguments which is an extension of a known method used to study relaxation oscillations in second order systems (Hoppensteadt, 1974). Examples where the method were applied can be found in the work on a mathematical model of a food chain by Muratori and Rinaldi (1992) and more recently in the work of Lenbury and Kamnungkit (1995). The method allows us to describe and identify different transients and attractors which develop in our system in the case where it is assumed that the predator population has infinitely faster dynamics than that of the prey. Nevertheless, experimenting with simulations has shown that the limit cycle behavior is preserved even though this assumption is not strictly satisfied and ε and δ are not necessarily small.

The analysis of our model seems to indicate that in the absence of the parasites, the predator may not be able to survive on the prey, given unfavourable conditions. The absence of the parasites can result in the persistence of the predator population, in which case a paradoxical situation arises. On the one hand, the parasites are an obligate mutualist of the predator (Freedman, 1990); that is, survival of the predator population is to some extent dependent on the presence of the parasites in the prey. On the other hand, the parasites cost the predator some energy, causing detrimental effects such as reduced fitness or reduced life span. This paradox of mutualism remains a complex topic for future research.

Acknowledgements

Appreciation is rendered to the Thailand Research Fund for the financial support which has made possible this research project.

Nomenclature

- a_0 Basic mortality rate of predation.
- b_0z Surplus mortality rate of predation.
- c_0 , d parameters accounting for effect of groupliving on mortality rate.
- c Rate of increase of predator per unit uptake of prey.
- k Half saturation constant.
- p_1 Functional response of susceptible prey.
- p_2 Functional response of infective prey.
- t Time.
- z Predator population density.
- B^* Birth rate of prey population.
- B_0 Specific birth rate of prey.
- D* Death rate of prey population.
- D_0 Specific death rate of prey.
- I Infective prey density.
- Susceptible prey density.
- X Total prey density.
- α_0 Maximum predation rate in function p_1 .
- β_0 Infection rate of susceptible prey in the absence of predator.
- β_1 Rate per unit predator of prey infection due to parasitic reproduction in the predator population.
- ε, δ Scaling parameters, assumed small.
- y constant of variation in function p_2 .
- γ^* Death rate of predator in absence of prey.

References

- Anderson, R.M. and May, R.M., 1979, Population biology of infectious diseases: Part 1. Nature 280, 361-367.
- [2] Anderson, R.M. and May, R.M., 1986, The invasion, persistence and spread of infectious diseases within animal and plant communities. Proc. Soc. Lond., B, 314, 533-570.
- [3] Arme, C. and Owen, R.W., 1967, Infections of the threespined stickleback, Gasterosteus aculeatus L., with the plerocercoid larvae of Scistocephalus solidus (Muller, 1776), with special reference to pathological effects. Parasitology 57, 301-314.
- [4] Barton, R.A. and Whiten, A., 1993, Feeding competition among female olive baboons, *Papio anubis*. Anim. Behav. 46, 777-789.
- [5] Brault, S. and Caswell, H., 1993, Pod-specific demography of killer whales (*Orcinus Orca*). Ecology 74 (5), 1444-1454.
- [6] Dobson, A.P., 1988, The population biology of parasiteinduced changes in host behavior. Q. Rev. Biol. 62, 2, 139-165.
- [7] Freedman, H.I., 1990, A model of predator-prey dynamics as modified by the action of parasite. Math. BioSci. 99, 143-155.
- [8] Holmes, J.C. and Bethel, W.M., 1972, Modification of Intermediate Host Behaviour by Parasites, in: Behavioural Aspects of Parasite Transmissions, E.V. Cunning and C.A. Wright (eds.). Zool. J. Linnean Soc. 51 (Suppl. 1), 123-149.

- [9] Hoppensteadt, F., 1974, Asymptotic stability in singular perturbation problems II: problems having matched asymptotic expansions. J. Diff. Equations 15, 510-521.
- [10] Lenbury, Y. and Kumnungkit, K., 1995, Detection of slow-fast limit cycles in a model for electrical activity in the pancreatic-cell. IMA J. Math. Appl. Med. Biol. (in press).
- [11] Moore, J. and Lasswell, J., 1986, Altered behavior in isopods (Armadillidium vulgare) infected with the nematode (Dispharynx nasuta). J. Parasitol. 72, 186-189.
- [12] Muratori, S., 1991, An application of the separation principle for detecting slow-fast limit cycles in a three-dimensional system. Appl. Math. Comput. 43, 1-18.
- [13] Muratori, S. and Rinaldi, S., 1992, Low- and high-frequency oscillations in three-dimensional food chain systems. SIAM J. Appl. Math. 52, 6, 1688-1706.
- [14] Osipov, A.V., Soderbacka, G., and Eirold, T., 1986, On the existence of positive periodic solutions in a dynamical system of two predator-one prey type. Viniti Deponent n 4305-B86 (Russian).
- [15] Peterson, R.O., 1977, Wolf ecology and prey relationships on isle royale. Natl. Park Serv. Sci. Monogr. 11.
- [16] Rau, M.E. and Caron, F.R., 1979, Parasite-induced susceptibility of moose to hunting. Can. J. Zool. 57, 2466– 2468
- [17] Schecter, S., 1985, Persistence unstable equilibria and closed orbits of a singularly perturbed equation. J. Diff. Equations 60, 131-141.
- [18] Tiner, J.D., 1953, The migration, distribution in the brain, and growth of ascarid larvae in rodents. J. Infect. Dis. 92, 2, 105-113.

How Can Nonlinear Dyanmics Elucidate Mechanisms Relevant to

Issues of Environmental Managemant and Global Change

HOW CAN NONLINEAR DYNAMICS ELUCIDATE MECHANISMS RELEVANT TO ISSUES OF ENVIRONMENTAL MANAGEMENT AND GLOBAL CHANGE

ABSTRACT

To illustrate how nonlinear dynamics can help elucidate mechanisms in ecological and biotechnological processes relevant to the environmental issues, we discuss recent work where bifurcation theory and singular perturbation theory are applied to matnematical models of predator-prey systems invaded by parasites and continuous bio-reactor in order to classify various dynamic behavior to be expected in our systems according to different ranges of the system parameters. Through bifurcation and stability analysis, we show that a model for a continuous bio-reactor subject to product inhibition can exhibit complexed dynamic behavior in which up to 5 possible invariants can occur in a phase plane. Owing to the importance of the process often used in waste water treatment, and the hazardous nature of the compounds which might be involved, particular attention must be given to the identification of the operating zone in which it is possible to carry out the process while avoiding undesirable complexed dynamic behavior. We resort to the use of singular perturbation techniques, however, to identify limit cycle behavior in a model for a predator-prey system modified by the action of parasites.

INTRODUCTION

The theory of dynamical systems has had an impact in many areas including physics, chemistry, and engineering. Not the less significant is its contribution to the field of biology, where key issues in environmental management and global change have engaged the interests of administrators, academics and researchers world wide. How do we deal with environment-genotype interactions? What factors regulate populations? How important are competitive interactions? What determines community diversity and stablity? How does trophic structure evolve? Are there general food web patterns which apply across the planet? What is the role of competition in determining community patterns? How do we couple knowledge of flows within ecosystems to build knowledge of global-scale processes? How do we couple processes acting on vastly different temporal and spatial scales to address important problems of environmental management? These are only a few of the key biological questions being put forward in the scientific world.

To illustrate how nonlinear dynamics can help elucidate mechanisms in ecological and biotechnological processes relevant to the environmental issues, we discuss recent work where bifurcation theory and singular perturbation theory are applied to mathematical models of predator-prey and continuous bio-reactor in order to classify various dynamic behavior to be expected in our systems according to different ranges of the system parameters.

CONTINUOUS BIO-REACTOR SUBJECT TO PRODUCT INHIBITION

A model for such a chemostat in which the growth of a microorganism is inhibited by its product was presented and theoretically studied in a paper by Yano and Koga [1] where the specific growth rate was assumed to have the form

$$\mu = \frac{\mu_{m}S}{(K_{S} + S) [1 + (P/K_{p})^{n}]}$$
 (1)

in order to cover wider problems of product inhibition. If the growth limiting substrate (S) is supplied in sufficient amount so that $S \gg K_S$ at any moment, then the concentration change of S has little effect on the rates of change of cells concentration (X) and product concentration (P). The product inhibition system may then be described by the following two - variable system:

$$\frac{dX}{dt} = \mu X - DX \tag{2}$$

$$\frac{dP}{dt} = \frac{\mu}{Y_P} X - DP \tag{3}$$

where D is the dilution rate. If the yield Yp is assumed constant, it can be shown [2] that the system of Equations (2) and (3) will not admit periodic behavior. It was also shown by Lenbury and Chiaranai [3] that if Yp is a linear function of the product concentration, sustained oscillation in X and P is possible due to a Hopf bifurcation in the system of differential equations which comprises the model. In this paper, we shall therefore consider the system of Equations (2) and (3) with

$$Yp = A - BP (4)$$

where A and B are constants, allowing for the negatively-growth associated situation. We also adopt for simplicity the function

$$\mu = \mu_0 (1 + P/k_m - P^2/k_p)$$
 (5)

where m₀, k_m, and k_p are positive constants, which results for linearizing the exponential term in the 'one hump' product inhibition model

$$\mu = k(P+1) \exp(-P/K)$$
 (6)

Introducing appropriate dimensionless variables will reduce the Equations (2) through (5) to

$$\frac{dx_1}{dt} = -x_1 + Da M(x_2) x_1 \tag{7}$$

$$\frac{dx_2}{dt} = -x_2 + Da M(x_2) x_1 / y(x_2)$$
 (8)

where
$$y(x_2) = (\beta - x_2)/\beta \tag{9}$$

$$M(x_2) = 1 + x_2 - \alpha x_2^2 \tag{10}$$

Letting

$$\Sigma(x_2) = M(x_2) / y(x_2)$$
 (11)

$$f_1(x_1, x_2, Da) = -x_1 + Da M(x_2)x_1$$
 (12)

$$f_2(x_1x_2, Da) = -x_2 + Da \Sigma(x_2)x_1$$
 (13)

Equations (7) and (8) may be recast in vector form as

$$dx / dT = f(x, Da)$$
 (14)

Solving the equation

$$\mathbf{f}(\mathbf{x}_{S}, \mathbf{D}\mathbf{a}) = 0 \tag{15}$$

for $\mathbf{x}_S = (\mathbf{x}_{S_1}, \mathbf{x}_{S_2})$, we obtain the steady state solutions as

- (a) trivial (washout) steady state : $x_{S_1} = x_{S_2} = 0$, and
- (b) nontrivial steady state (s): $x_{S_1} = y(x_{S_2}) x_{S_2}$, $M(x_{S_2}) = 1/Da$

The Hopf bifurcation occurs at a steady state \mathbf{x}_{S}^{\star} if the Jacobian matrix J of (14) evaluated at \mathbf{x}_{S}^{\star} has purely imaginary eigenvalues, which requires that

$$\det J > 0 \text{ and } \operatorname{tr} J = 0. \tag{16}$$

Applying conditions (16) to the functions in Equations (12) and (13), we find that for positive det J the following condition must be satisfied

$$1-2\alpha x_{S_{3}}^{*} < 0 \tag{17}$$

while tr J = 0 is equivalent to the requirement that

$$g(x_{S_2}^*) = (1 - \alpha \beta) (x_{S_2}^*)^2 + 2x_{S_2}^* - \beta = 0$$
 (18)

the other factors in tr J being always positive.

The function $g(x_{S_2}^*)$ will have two distinct positive real roots $x_{S_2}^* = r_1$ and r_2 , with $r_1 < r_2$, if

$$1/\beta > \alpha\beta - 1 > 0 \tag{19}$$

On the other hand, if $\alpha\beta$ -1 < 0 then g $(x_{S_2}^*)$ has only one positive real root r_1 . In fact, $M'(x_{S_2}^*)$, and correspondingly det J, changes signs when

$$\alpha \beta - 1 = 0 \tag{20}$$

Finally, onset of instability of steady states x_S is realized when tr J = 0 and (tr J)' = 0 which, from Equation. (18), occurs when

$$\alpha \beta^2 - \beta - 1 = 0 \tag{21}$$

Applying the Poincare's criterion and Friedrich's bifurcation theory [4], we may derive the following condition for the stability of the periodic solution which bifurcates from the point $x_{S_2} = x_{S_2}^*$:

$$9[(1-\alpha\beta)x_{S_2}^*+1](x_{S_2}^*)^2 < \frac{(\beta-x_{S_2}^*)^2(3-14\alpha x_{S_2}^*)}{3-6\alpha x_{S_2}^*}$$
 (22)

It can be shown that a limit cycle bifurcating from the bifurcation point $\alpha x_{S_2}^* = r_2$ is always stable.

Substituting the appropriate root r_1 in (22), we find that a loss of stability of the periodic solution which bifurcates from $x_{S_2} = r_1$ occurs when

$$\beta = \frac{(1-c)(-14c^2 + 68c - 54)}{(3c^2 - 38c + 27)}$$
 (23)

where $c = \sqrt{1 - \beta(\alpha\beta - 1)}$.

Thus, it is clear from the above discussions that the two system parameters α and β determine the stability regions of bifurcating periodic solutions. Figure 1 shows the (α, β) plane divided into 5 regions by the graphs of Equations (20), (21), (23) and the equation

$$\alpha\beta = \frac{1+2\alpha}{1+\alpha} \tag{24}$$

which holds when r_1 is equal to the value $1/\alpha$ exactly.

Following the representation used by Uppal *et al.* [5] we show in Figure 2 typical steady state and limit cycle plots of x_{S_2} versus w for each region, where

$$w = 1 - 1/Da$$

There can be as many as eleven different types of qualitative phase plane which are possible for different ranges of w, and correspondingly the Damkohler numbers. These are labelled A through K in Table 1.

In Region I, there is no bifurcation $(\alpha \beta^2 - \beta - 1 > 0)$. Three types of phase plane are possible: A, B and C.

Region II is bounded above by the line $\alpha\beta^2 - \beta - 1 = 0$ and below by the graph of Equation (24). This region is also above the graph of Equation (23). Therefore unstable bifurcation originates at the Damkohler number Da_1^* corresponding to the lower w^* value w_1^* , with stable bifurcation originating at the Damkohler number Da_2^* corresponding to the upper w^* value w_2^* . In this region, two cases are possible, IIa and IIb, permitting seven types of phase plane, A through G.

Region III is bound above by the graph of equation (24) and below by that of equation (23). Here, r_1 lies below the value $1/\alpha$ and there can be two cases, IIIa and IIIb, in this region admitting eight types of phase planes, A through C, E, and H through K.

Region IV is one of stable bifurcation at the Damkohler number Da_1^* . Therefore, five types of phase plane trajectories are possible, A through C, E and I. Figure 3 shows a computer simulation of the system model for $\alpha=0.273997$ and $\beta=3.9$ in this region IV and Da=1.891370559 of the type E, showing the predicted asymptotically stable limit cycle surrounding the unstable steady state .

Finally, in Region V $\alpha\beta$ -1 < 0 and no bifurcation occurs. Tr J becomes positive at x_{S_2} for which $M'(x_{S_2})$ < 0 so that the non-washout steady states are always unstable. Thus, there are 3 possible types of phase plane in this region, A, G and K.

PREDATOR-PREY SYSTEM INVADED BY A PARASITE

Holmes and Bethel [6] suggested four ways which the parasite may modify infected members of the prey population: reduced stamina, increased conspicuousness, disorientation, and altered responses. In [7], Arme and Owen reported on sticklebacks, infected by plerocercoids [Schistocephalus solidus], tending to swim closer to the surface of lakes and making themselves more susceptible to predation by birds. It has also been documented that the presence of larvae of Ascaris columnaris Leidy in mice and squirrels produces incoordination, blindness and loss of fear of larger animals. In other specific examples, this parasite-host interaction is even discovered to be necessary to the survival of the predator population.

In this paper, we consider an adapted version of the Freedman's model proposed in his recent work [8], where the density-dependent death rate of the predator describes a social population which tends to survive better in herds or packs. Analysis of the model is carried out by applying the singular perturbation technique. We derive explicit conditions on the system parameters which identify different dynamical behavior exhibited by the system. When the predator population is assumed to have very fast dynamics with respect to prey, the analysis can be carried out through singular perturbation arguments which are based on simple geometric characteristics of the equilibrium manifolds of the fast, intermediate and slow variables of the system, allowing one to derive explicit conditions that guarantee the existence of a limit cycle in the extreme case of very fast very slow dynamics. The resulting limit cycle is composed by the alternate concatenation of two slow and two

fast transitions and has interesting biological interpretations leading to better understanding of the system under study.

The reference model, after we have scaled the dynamics of the three hierarchical components of the system by means of two dimensionless positive parameters ϵ and δ , is the following system of differential equations:

$$\dot{\mathbf{x}} = \beta' \mathbf{y} - \mathbf{D} \mathbf{x} - \gamma \mathbf{x} \mathbf{z} \equiv \mathbf{f}(\mathbf{x}, \mathbf{y}, \mathbf{z}) \tag{25}$$

$$\varepsilon \dot{y} = B(x+y) - Dy - \beta y - \frac{\alpha yz}{k+y} \equiv g(x,y,z) \tag{26}$$

$$\varepsilon \delta \dot{z} = z \left[-a - bz - \frac{c}{d+z} + \frac{ly}{k+y} + \eta x \right] \equiv h(x,y,z)$$
 (27)

where x(t), y(t), and z(t) are the susceptible prey, infective prey, and the predator population, respectively. Here $\beta = \epsilon \beta'$ is the rate of infection, D the natural death rate of the infectives and the susceptibles, and B is the birth rate of the susceptible prey. The density-dependent death rate $\gamma^*(z)$ of the predator in the absence of prey is assumed to have the form

$$\gamma^*(z) \equiv a + bz + \frac{c}{d+z}$$
 (28)

Such a mortality curve would describe the death rate of social predators, such as wolves or hyenas, which survive somewhat better by staying in a pack.

As is well known [9], the system (25)-(27), with ε and δ small, can be analyzed with the singular perturbation method which, under suitable regularity assumptions, allows approximating the solution of the system (25)-(27) with a sequence of simple dynamic transitions along the equilibrium manifolds of the system and occurring at different speeds. First, the slow (x) and intermediate (y) variables are frozen at their initial values x(0) and y(0), and the evolution of the fast component of the system is determined by solving the "fast system"

$$\dot{z}(t) = h(x(0), y(0), z(t)) \tag{29}$$

Thus z(t) eventually tends toward a stable equilibrium $\overline{z}(x(0),y(0),z(0))$ of (29), assuming here that the system has unique stable equilibrium. Then keeping x frozen at x(0), we look at the "intermediate system" which has now become active, namely;

$$\dot{y}(t) = g(x(0), y(t), \overline{z}(x(0), y(t), z(0)))$$
 (30)

where $\overline{z}(x(0), y(t), z(0))$ is a stable equilibrium of the fast system (29) with y(0) substituted by y.

Referring to Figure 4, where low-, intermediate-, and high-speed trajectories are indicated, respectively, with one , two , and three arrows, at first a high-speed transition develops at constant x and y and brings the system from (x(0),y(0),z(0)) (point R in Fig. 4) to a stable equilibrium of the fast manifold h=0 (point S in Fig. 4). Then a second intermediate-speed transition takes place on the manifold at

constant x (segment ST' in Fig. 4) until a point is reached (point T' in Fig. 4) where the stability of the equilibrium manifold h=0 is lost and a quick transition then takes the state of the system to the equilibrium point on a stable part of the manifold, which will be the point T in Fig. 4. A transition of intermediate speed then develops along this part of the manifold to the point D' of Fig. 4.

The resulting curve RST'TD' approximates the solution of the system, in the sense that the real trajectory is contained in a tube arround that curve with the radius of the tube going to zero with ϵ and δ .

The direction of transition along the line ST' or TD' depends on the sign of \dot{y} namely g(x, y, z). Thus, let us assume that for suitable values of the parameters the intermediate (stable) manifold g=0 separates the line ST' on the trivial manifold z=0 from the line TD' on the nontrivial manifold h=0 (see Fig. 4) and that g is positive below the manifold g=0 and negative above it. Under this conditions the system moves toward point D' along the line TD', and when D' is reached we have a saddle-node bifurcation of the fast system: the variable z at point D' is not at a stable equilibrium anymore and a catastrophic transition from D' to A' occurs at a very high speed. This almost closes the cycle but for the fact that during this time the variable z has been increasing very slowly, assuming that we have started on the side of the manifold z0 where z0.

Once the system is at A', a slow motion develops again from A' in the direction of increasing y because g is positive here. The same cycling is repeated, densely convering the manifold h=0 while the variable x increases slowly until the equilibrium point B' on the manifold f=0 is reached where $\dot{x}=0$. A high-speed transient bring the state of the system back onto the nontrivial manifold h=0 at the point C along the line of intersection between the manifold h=0 and f=0. A transition of intermediate speed to D then takes place along this line followed by a catastophic transition from D to A. An intermediate speed transition from A then brings us back to B', resulting in a closed cycle AB'CD lying on the manifold f=0. (See Fig. 4.)

It can be shown, from the above discussion, that if ϵ and δ are sufficiently small and

$$l > a + \frac{c}{d} \tag{31}$$

$$b < \frac{c}{d^2} \tag{32}$$

$$D + \beta - B > 0 \tag{33}$$

$$\alpha > \frac{B}{\sqrt{c/b-d}}(k+y_A)(\frac{x_B}{y_A} - \frac{D+\beta-B}{B})$$
 (34)

$$\frac{D+\beta-B}{B} < \frac{\beta'}{D} \tag{35}$$

where

$$y_A = k \frac{(a - \eta x_A) + 2\sqrt{bc} - bd}{l - (a - \eta x_A) - 2\sqrt{bc} + bd}$$
 (36)

$$x_{A} = \frac{\beta' y_{A}}{D + \gamma z_{A}} \tag{37}$$

$$z_{A} = \sqrt{\frac{c}{h}} - d \tag{38}$$

$$x_{B} = \frac{\beta' k}{D} \left[\frac{(a - \eta x_{B}) + \frac{c}{d}}{l - (a - \eta x_{B}) - \frac{c}{d}} \right]$$
(39)

then a limit cycle exists for the model system (25)-(27).

Figure 5 shows a computer simulation of the model system (25)-(27) when the inequalities (31)-(35) are satisfied showing the solution trajectory tending toward a stable limit cycle as predicted.

We observe that if the parasite is no longer present, which will be the case if $\beta = \beta' = 0$, then conditions (33) and (35) cannot be satisfied simultaneously. The system may destabalize to extinction. This seems to indicate that stable existence of the predator population depends, to a certain extent, on the presence of the parasites. In other words, the invasion of the parasite can stabalize the system resulting in persistence and the survival of the predator. This is in agreement with the observations made by several other authors who have done extensive research work in this field.

CONCLUSION

We have illustrated, by way of two examples of mathematical models of important biological processes, how the theories of nonlinear dynamics may be applied to gain insightful information concerning the systems under study. The results of such theoretical analysis lead to significant advances in the field of theoretical biology, and have come a long way in the attempt at answering key biological questions of environmental concerns that will engage the attention of scientists, researchers, and administrators in the years to come.

ACKNOWLEDGEMENT

Appreciation is rendered to the Thailand Research Fund and the National Research Council for the financial support which has made this research project possible.

Table 1. Typical phase plots

	A	В	C	D	E	F	G	H	Ι	J	K
Stable washout (node)	1	1	0	0	0	0	1	1	1	1	1
Unstable washout (saddle point)	0	0	1	1	1	1	0	0	0	0	0
Stable normal (saddle pt. or focus)	0	1	1	1	0	1	0	1	0	1	0
Unstable normal (saddle pt. or focus)	0	1	0	0	1	0	1	1	2	1	2
Stable limit cycle	0	0	0	1	1	0	0	1	1	0	0
Unstable limit cycle	0	0	0	1	0	1	0	1	0	1	0
Total invariants	1	3	2	4	3	3	2	5	4	4	3

REFERENCES

- [1] T. Yano and S. Koga, Dynamic Behavior of the Chemostat Subject to Product Inhibition. J. Gen. Appl. Microbiol. 19 (2), 97-114 197).
- [2] Y. Lenbury and C. Chiaranai, Bifurcation Analysis of a Product Inhibition Model of a Continuous Fermentation Process. *Appl. Microbiol. Biotechnol.* **25**: 532-34 (1987).
- [3] Y. Lenbury and C. Chiaranai, Direction of the Sustained Oscillation Trajectoriy in the Cell - Product Phase Plane Describing Product Inhibition on Continuous Fermentation Systems. *Acta Biotechnol*. 7 (5) 433-437 (1987).
- [4] Poore, B. A., A model Equation Arising from Chemical ReactorTheory. *Arch. Rat. Mech. Anal.* 52, 358 388 (1973).
- [5] A. Uppal, W. H. Ray and A. B. Poore, On the Dynamic Behavior of Continuous Stirred Tank Reactors. *Chem. Engng. Sci.* 29, 967 985 (1974).
- [6] Holmes, J. C. and Bethel, W. M. Modification of intermediate host behaviour by parasites, in *Behavioural Aspects of Parasite Transmissions*, E. V. Cunning and C. A. Wright. Eds., Sppl. No. 1 to the *Zool. J. Linnean Soc.* 51 (1972) 123-149.
- [7] Arme, C. and Owen, R. W. Infections of the three-spined stickleback, Gasterosteus aculeatus L., with the plerocercoid larvae of Scistocephalus solidus (Muller, 1776), with special reference to pathological effects. Parasitology. 57 (1967) 301-314.
- [8] Freedman, H. I. A Model of Predator-Prey Dynamics as Modified by the Action of Parasite. *Mathematical BioSciences.* **99** (1990) 143-155.
- [9] Muratori, S. An Application of the Separation Principle for Detecting Slow-Fast Limit Cycles in a Three-Dimensional System. *Applied Mathematics and Computation.* **43** (1991) 1-18.

FIGURE CAPTION

Figure 1. The (α, β) plane delineated by graphs of Equations. (20)-(21), (23), and (24) into 5 regions of qualitatively different dynamic behavior.

Figure 2. Typical plots of w versus x_{S_2} for each region in the (α, β) plane.

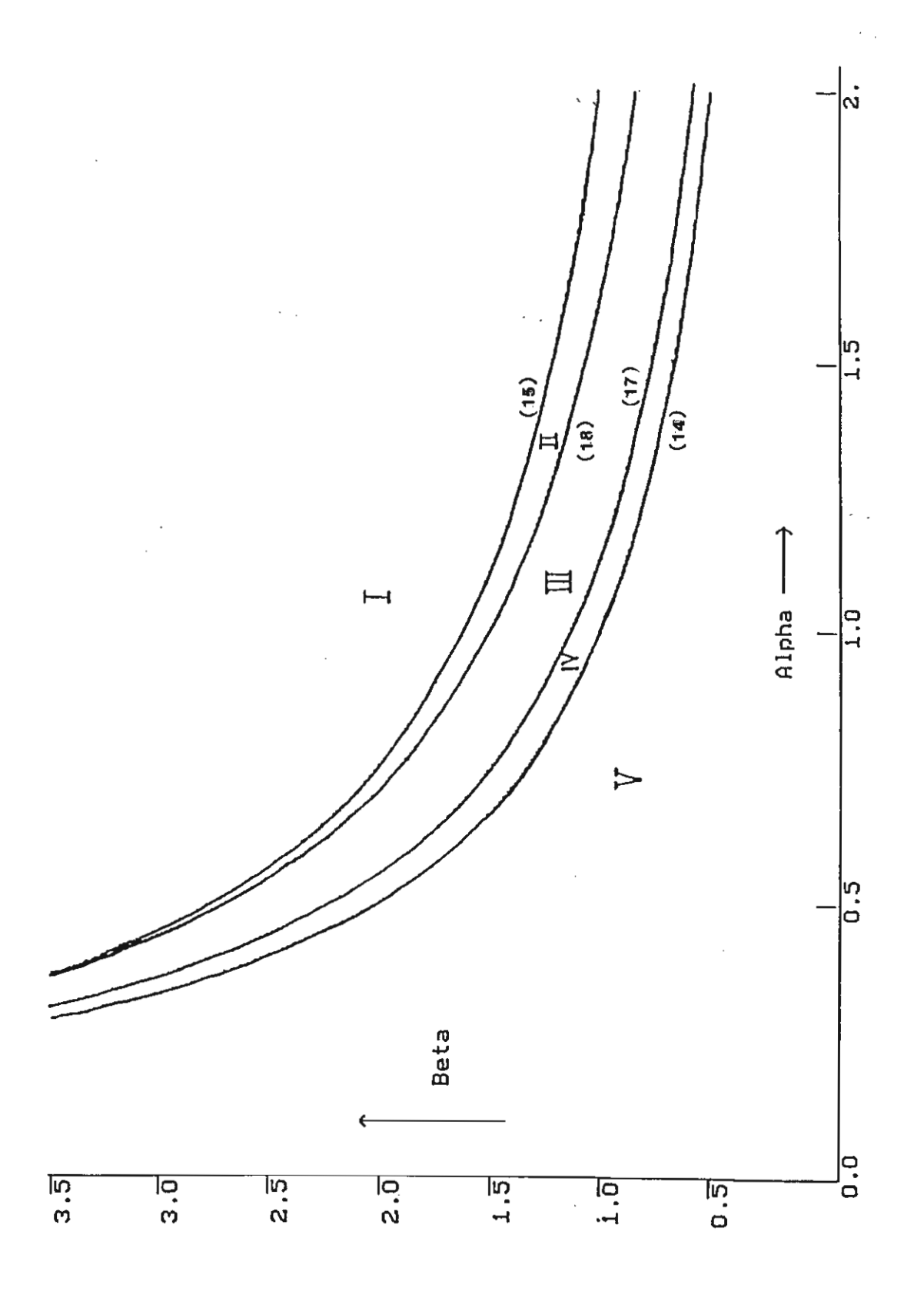
stable steady state,
unstable steady state,
stable limit cycles,

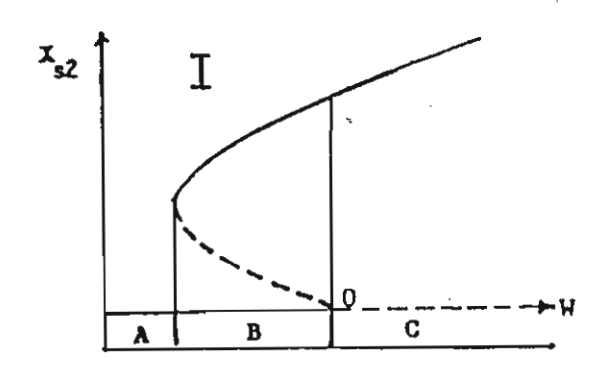
oooooo unstable limit cycles.

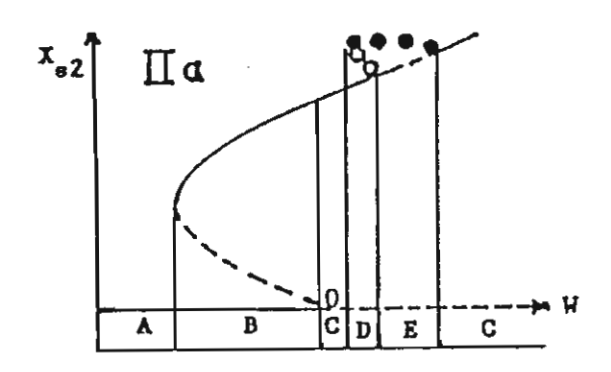
Figure 3. Computer simulation of the model system (2) and (3) with parametric values in Region IV (type I), showing solution trajectories tending away from the saddle point towards the stable limit cycle or the stable washout.

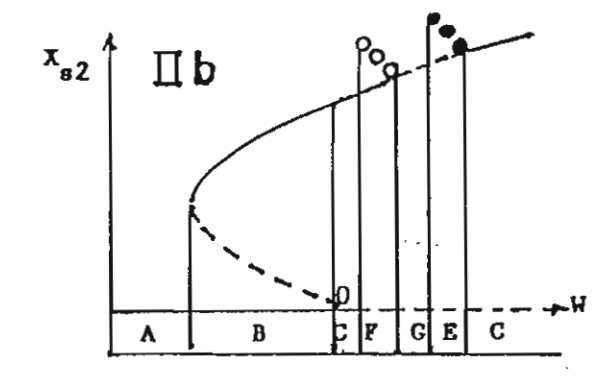
Figure 4. The three equilibrium manifolds f = 0, g = 0, h = 0. The intermediate manifold g = 0 separates the line DP from the line OQ.

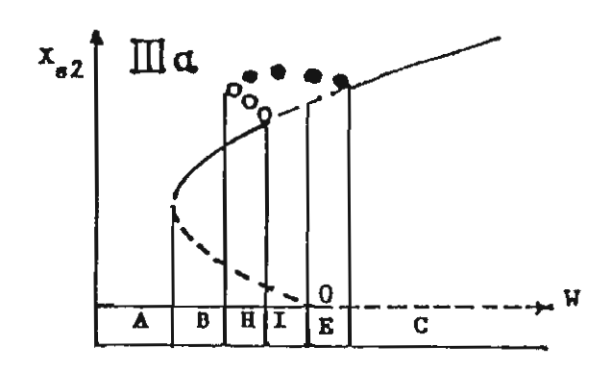
Figure 5. Computer simulations of the model system (25)-(28) when all the conditions identified in the text for the existence of a limit cycle are satisfied.

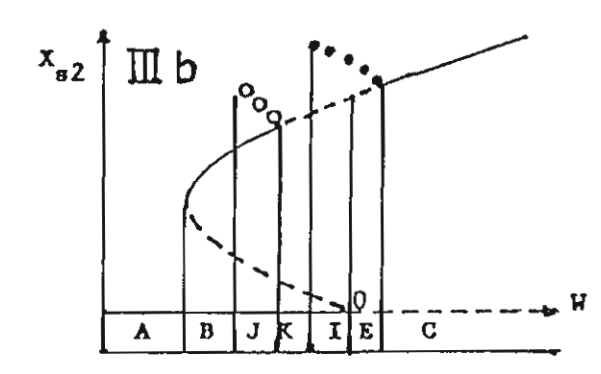


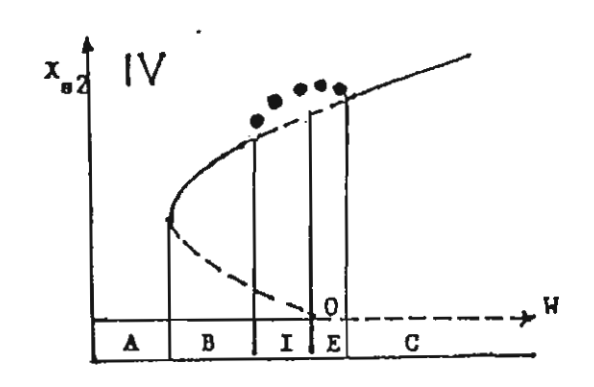


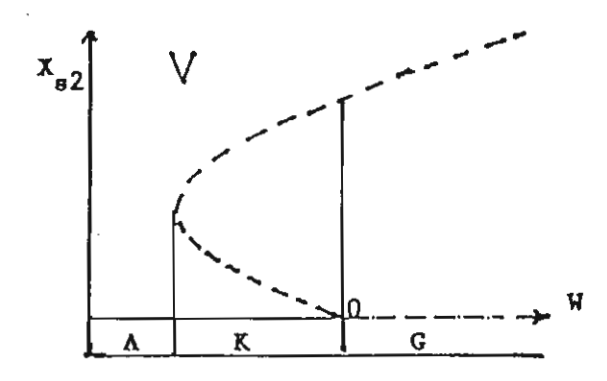




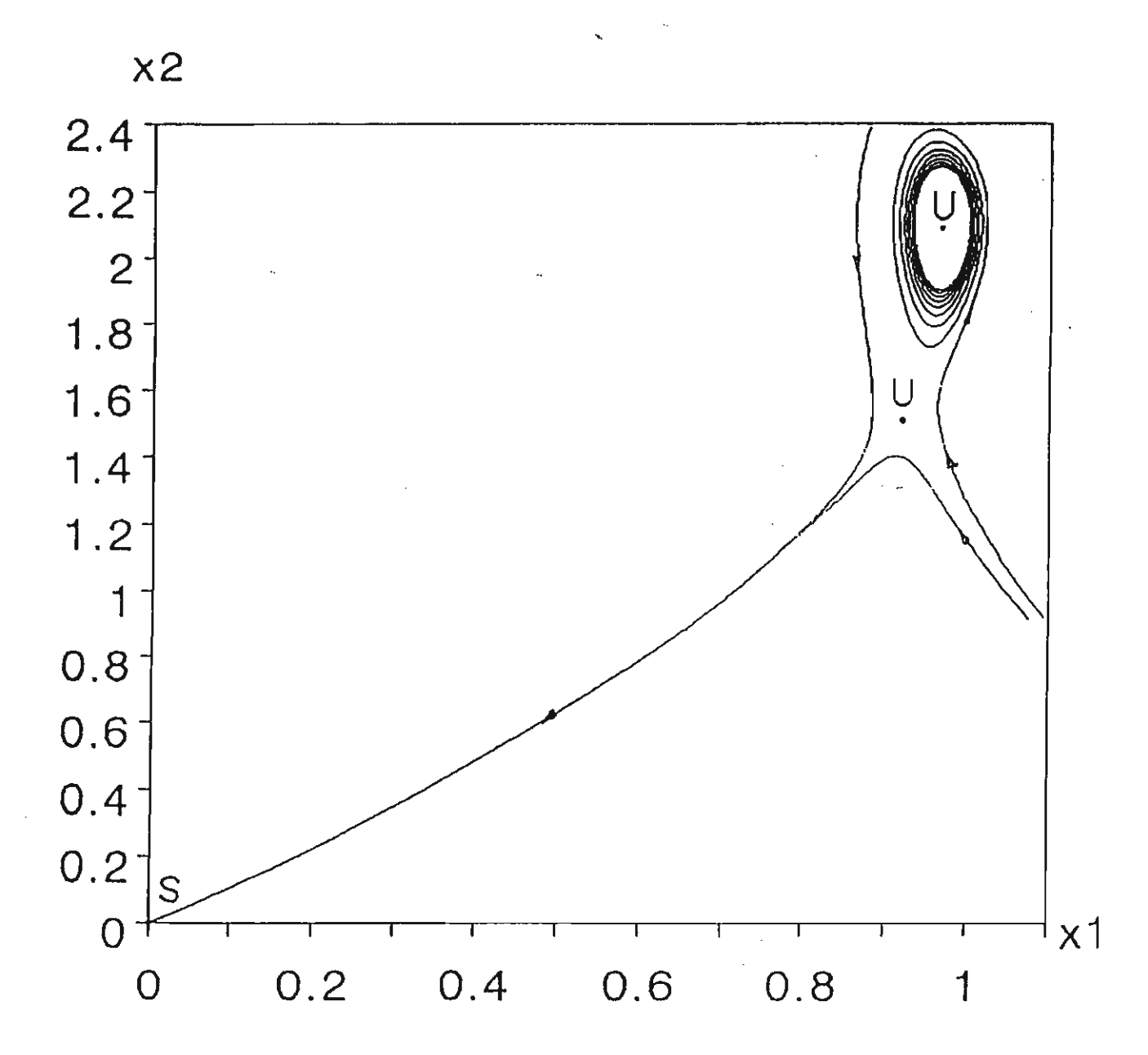




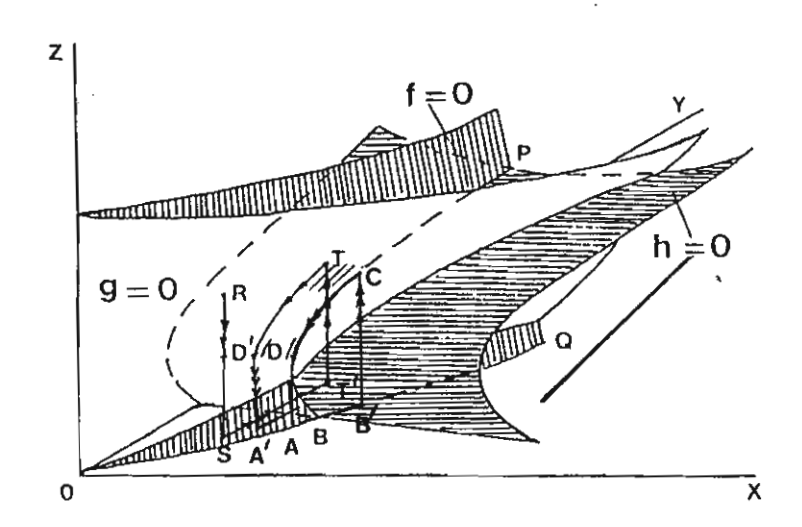


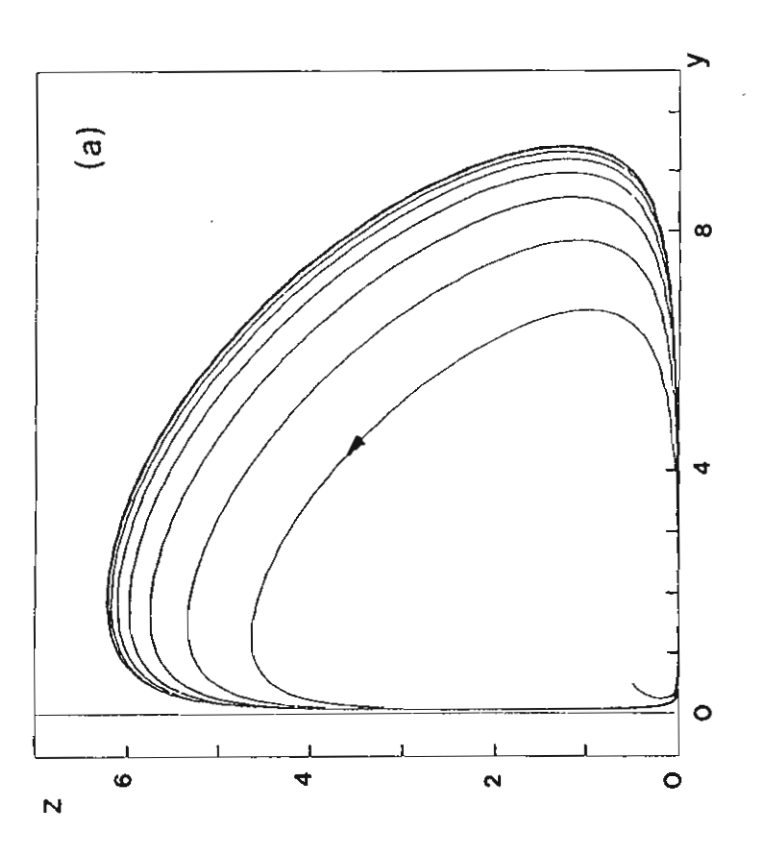


F16.2



F16. 3





การวิจัยช่วงที่ 3

ในการวิจัยช่วงนี้ ผู้วิจัยได้ปรับเปลี่ยนแบบจำลองพื้นฐาน (2) และ (3) ให้ผู้ล่าถูกแบ่งเป็น 2 กลุ่ม คือ susceptible predator และ infective predator ซึ่งผู้ล่าซึ่งติดพยาธิย่อมมีความสามารถในการ ไล่ล่าด้อยลง จึงได้เป็นสมการอนุพันธ์ไม่เชิงเส้น 3 สมการต่อไปนี้

$$\frac{dP}{dt} = P \left(B(1-rP) - D_P - \frac{\alpha S}{P+\ell} - \frac{\gamma I}{P+k} \right)$$
 (42)

$$\frac{dS}{dt} = \frac{aSP}{P+\ell} - D_SS + c_1I - \beta SI$$
 (43)

$$\frac{\mathrm{dI}}{\mathrm{dt}} = \mathrm{I}\left(\beta \,\mathrm{S} - \mathrm{D}_{\mathrm{I}} + \frac{\mathrm{c}_2 \,\gamma \,\mathrm{P}}{\mathrm{P} + \mathrm{k}}\right) \tag{44}$$

โดยที่ P คือ ปริมาณของ predator

S คือ ปริมาณของ susceptible predator

I คือ ปริมาณของ infective predator

 $D_P,\ D_S$ และ D_I คือ natural birth rate ของ $P,\,S,\,$ และ I ตามลำดับ

S ล่าจับ P เป็นอาหารด้วยอัตรา

$$\frac{\alpha \,\mathrm{S}\,\mathrm{P}}{\mathrm{P} + \ell} \tag{45}$$

I ล่าจับ P เป็นอาหารด้วยอัตรา

$$\frac{\gamma I P}{P + k} \tag{46}$$

ซึ่งมี $\gamma < \alpha$ และ $\ell < k$ โดยใช้ response functions แบบ Holling's type ทั้งหมด ส่วน

β คือ infection rate

c₁ คือ recovery rate

และ B คือ natural birth rate ของ prey

เมื่อคำเนินการวิเคราะห์เชิงทฤษฎีด้วย singular perturbation analysis ผู้วิจัยสามารถพิสูจน์ ได้ว่า ระบบสมการ (42)-(44) จะมีคำตอบที่มี dynamical behavior ที่แตกต่างกันไปได้เป็น 5 กรณี ดังต่อไปนี้ โดยกำหนดให้

$$S' = \frac{D_I}{\beta}$$

$$\overline{S} = \frac{(B - D_P)\ell}{\alpha}$$

$$P_{l} = \frac{D_{l}k}{c_{2}\gamma - D_{l}} \tag{47}$$

$$P_2 = \frac{B - D_P}{Br} \tag{48}$$

$$P_3 = \frac{B - D_P - Br \ell}{2Br} \tag{49}$$

$$P_4 = \frac{D_S \ell}{a - D_S} \tag{50}$$

$$I_{R} = \frac{c_{2} k}{c_{2} \gamma - D_{I}} \left(B - D_{P} - \frac{r B D_{I} k}{c_{2} \gamma - D_{I}} \right)$$
 (51)

$$I_{1} = \frac{k}{\gamma} \left(B - D_{P} - \frac{\alpha D_{I}}{\beta l \ell} \right)$$
 (52)

$$I_{2} = \frac{-\theta + \sqrt{\theta^{2} + 4\beta_{2}\ell^{2}\gamma k(B - D_{P})}}{2\beta_{2}\ell\gamma}$$
(53)

โคยที่ $\theta = \alpha c_1 k + \ell \gamma D_S - \ell \beta_2 k (B - D_P)$

กรณีที่ 1 ถ้า

$$I_R > 0 \tag{54}$$

$$P_3 > 0, \quad \overline{S} > S' \tag{55}$$

$$P_3 > P_4 \tag{56}$$

$$I_2 > I_1 \tag{57}$$

$$P_2 > P_1 > P_4 > 0 (58)$$

ระบบสมการ (42)-(44) จะมีคำตอบเป็นคาบ

กรณีที่ 2 ถ้า (54), (55), (57), (58) เป็นจริง และ

$$0 < P_3 < P_4 \tag{59}$$

ระบบสมการ (42)-(44) จะมี solution trajectory ซึ่งลู่เข้าสู่ steady state solution ซึ่งมีเสถียร ซึ่งใน กรณีนี้ เราจะได้ persistence of the species นั่นคือ ทั้ง P, S, และ I จะมีระดับคงที่ และไม่สูญพันธุ์ ไป **กรณีที่ 3** ถ้า (54), (55), (57), (58) เป็นจริง และ

$$P_3 < 0 < P_4$$
 (60)

ระบบสมการ (42)-(44) จะมี solution trajectory ซึ่งลู่เข้าสู่ steady state solution ซึ่งมีเสถียร ซึ่งใน กรณีนี้ เราจะได้ persistence of the species เช่นกัน นั่นคือ ทั้ง P, S, และ I จะมีระดับคงที่ และไม่ สูญพันธุ์ไป

กรณีที่ 4 ถ้า (54), (55), (57) เป็นจริง และ

$$0 < P_2 < P_4 < P_1 . (61)$$

ระบบสมการ (42)-(44) จะมี solution trajectory ซึ่งคู่เข้าสู่ steady state $(P,S,I)=(P_2,0,0)$ ซึ่ง predator population จะสูญพันธุ์ ส่วน prey population จะ persist

กรณีที่ 5 ถ้า (54), (56)-(58) เป็นจริง แต่

 $P_3 > 0$

 $\overline{S} < S'$

ແລະ

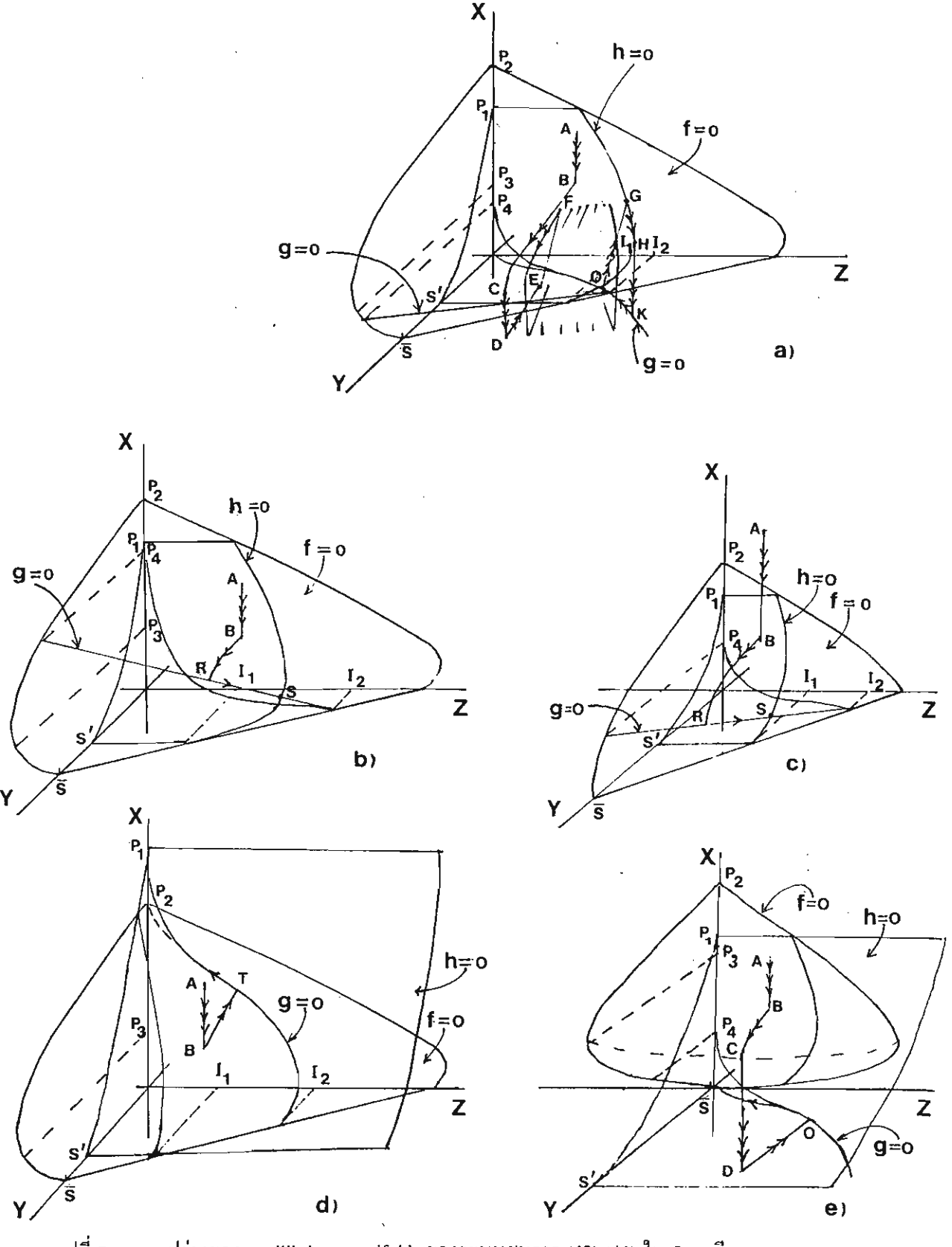
 $\overline{S} \ll 1$

ระบบสมการ (42) - (44) จะมี solution trajectory ซึ่งคู่เข้าสู่ washout steady state (P,S,I) = (0,0,0) ซึ่ง prey และ predator population จะสูญพันธุ์

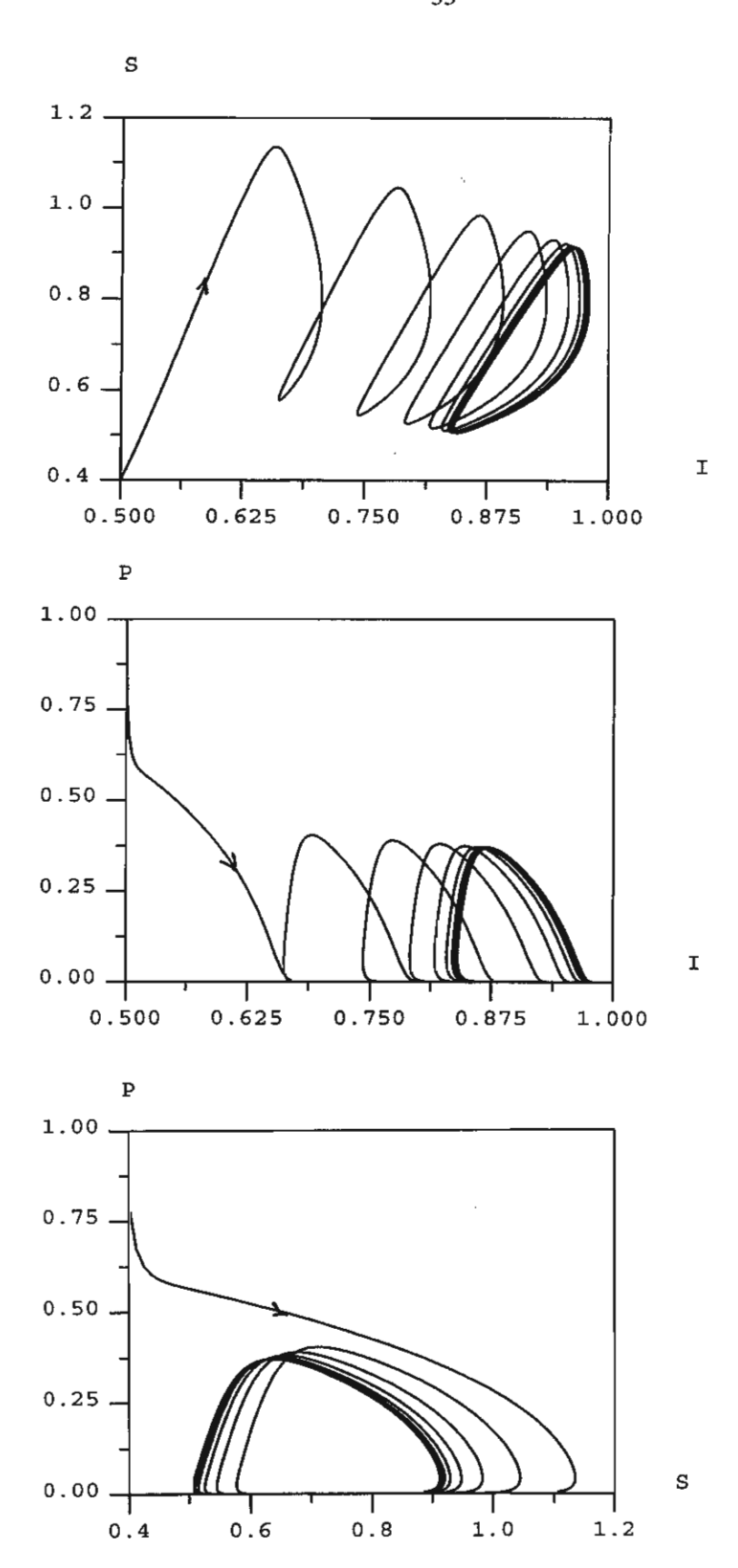
ทั้งนี้ความเป็นไปได้ทั้ง 5 กรณี ที่กล่าวมาข้างต้น เกิดขึ้นตามตำแหน่งและรูปร่างของ equilibrium manifolds และ transients บน manifolds ซึ่งแยกแยะและวาดได้เป็น 5 กรณี ตามที่เห็นได้ในรูปที่ 7

เมื่อทำการ simulate สมการ (42)-(44) ด้วยคอมพิวเตอร์ โดยกำหนดค่าของพารามิเตอร์ให้ สอดกล้องกับเงื่อนไขในแต่ละกรณีแล้ว ก็จะพบว่าคำตอบเชิงตัวเลขได้เป็นจริงตามที่คาดคะเนไว้ใน ทางทฤษฎี ดังที่เห็นได้ในรูปที่ 8-10

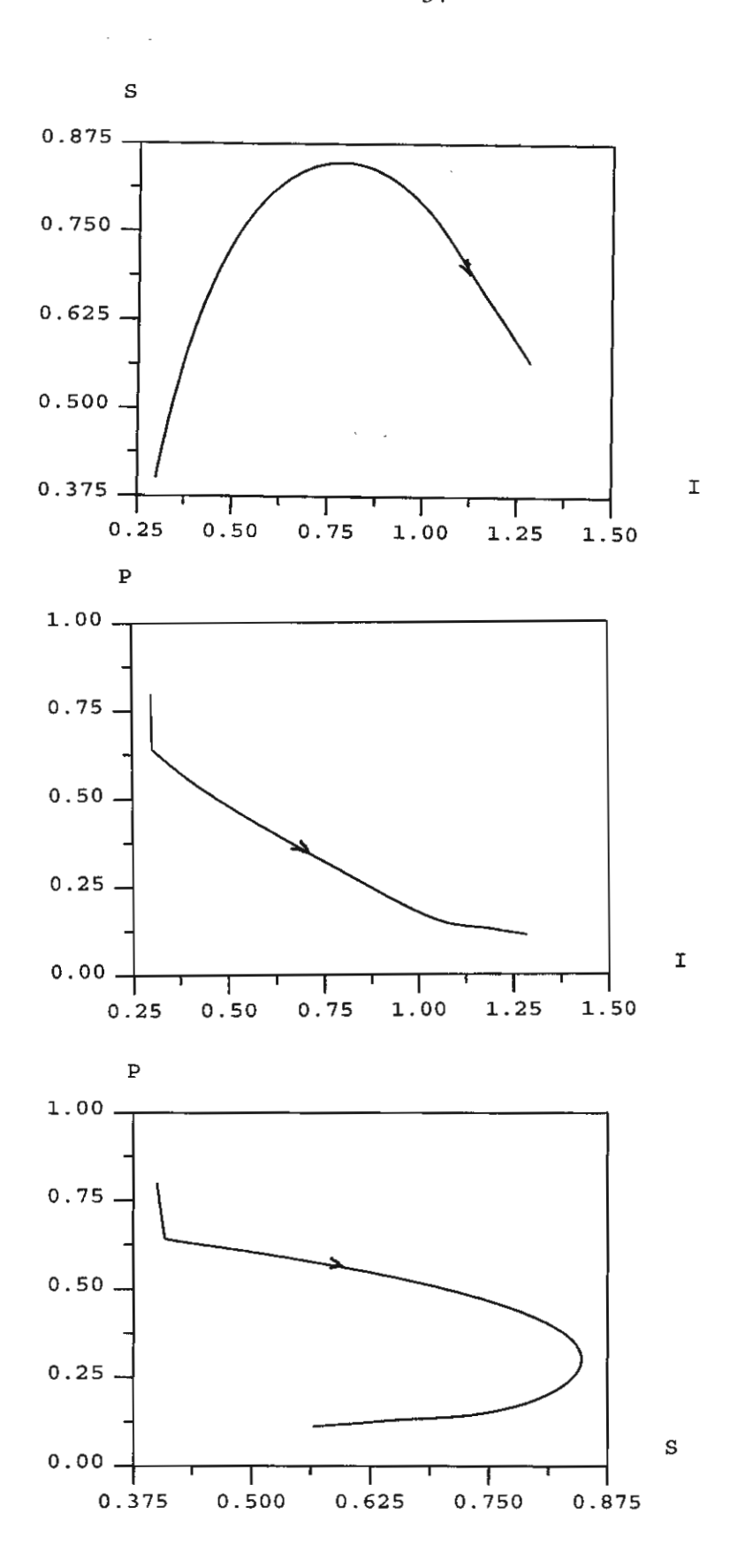
ผลงานของการวิจัยในช่วงนี้อยู่ในระหว่างการนำเขียนขึ้นเป็น paper เพื่อ submit for publication ในวารสารนานาชาติต่อไป



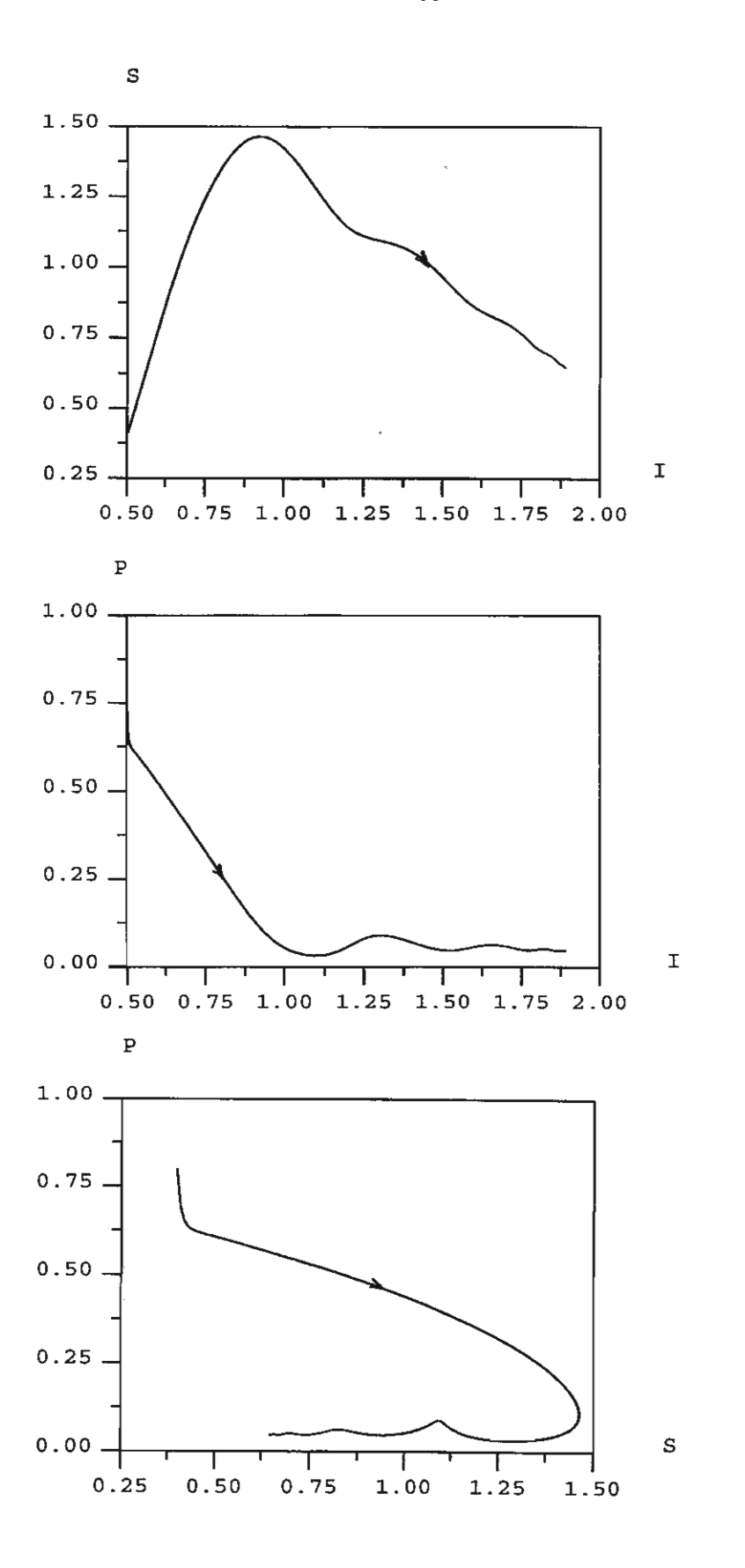
รูปที่ 7 รูปร่างของ equilibrium manifolds ของระบบสมการ (42)-(44) ใน 5 กรณี ที่กล่าวไว้ในเนื้อหา



รูปที่ 8 คำตอบเชิงตัวเลขของระบบสมการ (42)-(44) เมื่อเลือกค่าพารามิเตอร์ ให้สอดกล้องกับเงื่อนไขของกรณีที่ 1



รูปที่ 9 คำตอบเชิงตัวเลขของระบบสมการ (42)-(44) เมื่อเลือกค่าพารามิเตอร์ ให้สอดคล้องกับเงื่อนไขของกรณีที่ 2



รูปที่ 10 คำตอบเชิงตัวเลขของระบบสมการ (42)-(44) เมื่อเลือกค่าพารามิเตอร์ ให้สอดกล้องกับเงื่อนไขของกรณีที่ 3

การวิจัยในช่วงที่ 4

4.1 ในช่วงที่ 4 นี้ ผู้วิจัยได้นำสมการแบบจำลอง (1) มาเพิ่มสมการที่คำนึงถึงผลกระทบ ของแฟกเตอร์ภายนอก นั่นคือระดับของสารพิษในสิ่งแวคล้อม ต่อความสามารถในการสืบพันธุ์ (birth rate) และการดำรงชีวิตอยู่ของประชากรในสิ่งแวคล้อมปิด (closed environment) ซึ่งเขียนได้ เป็นระบบสมการต่อไปนี้

$$\frac{dX}{dt} = R(T)x - \frac{r_0x^2}{K(T)}$$
(62)

$$\frac{dT}{dt} = -\delta_0 T - \alpha_1 x T + f(X, U) \tag{63}$$

$$\frac{dU}{dt} = -\delta_1 U + \alpha_1 x T - \gamma_1 x U \tag{64}$$

โดยที่ $x(t) = \frac{\text{concentration of the population biomass}}{\text{mass(or volume) of the total environment where the population lives}}$

 $T(t) = \frac{\text{concentration of the toxicant in the environment}}{\text{mass(or volume) of the total environment where the population lives}}$

 $U(t) = \frac{\text{concentration of the toxicant in the total population}}{\text{mass(or volume) of the total environment where the population lives}}$

R = birth rate

K = carrying capacity

 δ_0 , δ_1 = natural depletion rate of T and U, respectively

 α_1 = rate of toxicant intake by the population

 γ = removal rate

f(X,U) = fraction of toxicant in the population which returns to the environment = $\pi \gamma_1 X U + \beta U \ (\pi > 0, \ \gamma_1 > 0, \ \beta > 0)$

ผู้วิจัยได้ใช้ singular perturbation technique ทำการวิเคราะห์ model ที่ได้นี้ จนได้เงื่อนไขบน ค่าของพารามิเตอร์ ซึ่งจะทำให้ระบบสมการ (62)-(64) มีคำตอบที่มี dynamical behavior แตกต่างกัน ไป โดยสามารถแบ่งแยกได้เป็น 5 กรณีใหญ่ ๆ ด้วยกัน ดังที่จะสามารถอ่านรายละเอียดได้จาก manuscript ที่แนบมาด้วยนี้ ซึ่งผู้วิจัยได้นำเสนอใน International Conference on Nonlinear Systems in Biology and Medicine ณ เมือง Veszprem ประเทศ Hungary และได้รับตีพิมพ์แล้ว ในวารสาร Mathematical and Computer Modelling ซึ่งจะตีพิมพ์เป็น special issue สำหรับ Proceedings ของการประชุมดังกล่าว

Singular Perturbation Analysis of a Model for the Effect of Toxicant in Single-Species Systems

SINGULAR PERTURBATION ANALYSIS OF A MODEL FOR THE EFFECT OF TOXICANT IN SINGLE-SPECIES SYSTEMS

Yongwimon Lenbury*
Nardtida Tumrasvin

Department of Mathematics, Faculty of Science

Mahidol University, Rama 6 Rd.

Bangkok 10400, Thailand

scylb@mahidol.ac.th

^{*}To whom all correspondences should be addressed

SINGULAR PERTURBATION ANALYSIS OF A MODEL FOR THE EFFECT OF

TOXICANT IN SINGLE-SPECIES SYSTEMS

ABSTRACT

We consider a mathematical model for the effect of toxicant levels on a single-species ecosystem in the case where there is an initial instantaneous introduction of toxicant into the environment. The population birth-rate as well as the carrying capacity are assumed to be directly effected by the level of toxicant in the environment as it is absorbed by the population. The toxicant level in the population can be depleted at a constant specific rate, a part of which amount may return to the environment. Through a singular perturbation analysis, we are able to identify different dynamical behavior which may be possible to the system, including the existence of sustained oscillation in the levels of toxicant in the population and in the environment.

Key words: Toxicants, singular perturbation, sustained oscillation, single-species, mathematical model.

INTRODUCTION

In the past decade or so, there has been a burst in the number of literatures concerned with the study of effects of pollutants and toxicants on ecological communities simply because such studies are not only of great interest from environmental and conservational points of view, but also bear great relevance to

the decision making process of any abiding policy makers in matters of environmental regulation and control.

Case studies and field observations have yielded a number of insightful articles such as the study by Nelson [1] on the problem of oil pollution of the sea, and the work by Woodman and Cowling [2] on the effect of airborne chemicals on forest health. From a physiological point of view, many researchers have carried out studies on the effects of toxic substances on the human body and other living organisms. Examples include the article by Chen and Hsu [3] on the polychlorinated biphenyl poisoning from toxic rice-bran oil in Taiwan, and the paper by J.J. Ryan [4] concerning the variation of dioxins and furans in human tissues. These studies lead to a number of valuable efforts to describe and analytically study the effects of toxicants and pollutants on various ecosystems, and on the human population or other living organisms, by utilizing mathematical models. Examples of such work include a series of papers by Hallam and his coworkers [5-8], a paper by Shukla et al. [9] on a mathematical model for the degradation and subsequent regeneration of a forestry resource, and a series of papers by Carrier et al. [10-11] attempting to model the toxicokinetics of Polychlorinated Dibenzo-p-dioxins and Dibenzofurans in mammalians, including humans.

More recently, Freedman and Shukla [12] proposed a model for the effect of toxicant in single-species systems and one for predator-prey polluted systems. So that their model should be more viable, they modelled the interactions of the populations and the toxicants in the population and in the environment by means of ordinary differential equations in terms of their concentrations with respect to mass or volume of the total environment in which the population lives.

In their model for a single-species system, the amount of toxicant in the population is depleted due to their death, some of which re-entering the environment in proportion to the population biomass. Such a model was found to exhibit no oscillatory behavior in the case that there is no more dumping of

toxicants after the initial instantaneous introduction. It was shown that provided that the pollutant concentration was not sufficient to kill all the population, eventually the toxicant would be removed and the population would recover to its former level. However, cases have often been found in nature in which this is not so, and persistence of toxicant levels in the population and the environment have been observed such as the incidents described in the paper by Xober and Papke [13] on their study of the concentrations of PCDDs and PCDFs in human tissues 36 years after accidental dioxin exposure.

Such toxic substances are persistent and bioaccumulate and therefore contaminate air, water, soil, and most living organisms, including humans. Accidental intoxication of humans by these substances can result in chronic effects [11] and the possible toxicological consequences are of great concern.

The uncertainties inherent to the conventional response assesment make it difficult to determine realistic allowable exposure limits for these substances, and the debate on how such toxic substances should be regulated continues for governments around the world [11]. More extensive studies which elucidate quantitatively the toxicokinetics and dynamics of these substances are needed to provide a credible basis for reducing the uncertainties involved in the response assesments and regulation decision making.

In this paper, we therefore consider single-species in a closed homogeneous environment, in which the carrying capacity and the population birth-rate are both affected by the exogeneous introduction of toxicant. By modifying the model proposed by Freedman and Shukla [12], we allow the toxicant in the population to re-enter the environment, a part of which amount varies directly as the toxicant level in the population alone.

We are interested in determining the different dynamics that may result from the effects of toxicants on such a closed ecosystem. If the population is assumed to have a very fast dynamics, as compared to the toxicant levels in the population and in the environment, and the time responses of the different state variables are assumed to increase from bottom to top, a singular perturbation approach can be utilized and the structures of corresponding attractors and the nature of the transients can be analyzed geometrically. Explicit conditions are derived which separate the various dynamic structures and identify, in particular, the limit cycles in the case of extreme dynamics.

DESCRIPTION OF THE MODEL

Based on a model by Freedman and Shukla [12], we let

 $x(t) = \frac{\text{concentration of the population biomass}}{\text{mass(or volume) of the total environment where the population lives}}$

 $T(t) = \frac{\text{concentration of the toxicant in the environment}}{\text{mass(or volume) of the total environment where the population lives}}$

 $U(t) = \frac{\text{concentration of the toxicant in the total population}}{\text{mass(or volume) of the total environment where the population lives}}$

It is assumed that the population growth is logistic. The absorbtion of the toxicant in the environment by the population causes the birth-rate r of x to diminish, and we shall therefore assume that r depends explicitly on T with the following properties:

$$r(0) = r_0 > 0$$

$$r'(T) < 0$$
 for $T \ge 0$

and $r(\overline{T}) = 0$ for some \overline{T} .

The carrying capacity K(T) of the environment also decreases with the increase in T and has the following general properties:

$$K(T) = K_0 > 0$$

and K'(T) < 0 for $T \ge 0$.

The following system of ordinary differential equations can be derived.

$$\dot{x} = r(T)x - \frac{r_0 x^2}{K(T)}$$
 (1)

$$\dot{T} = -\delta_0 T - \alpha_1 x T + \pi \gamma_1 x U + \beta_1 U \tag{2}$$

$$\dot{\mathbf{U}} = -\delta_1 \mathbf{U} + \alpha_1 \mathbf{x} \mathbf{T} - \gamma_1 \mathbf{x} \mathbf{U} \tag{3}$$

where δ_0 and δ_1 are the depletion rates of toxicant in the environment, and in the population, respectively; α_1 is the depletion rate of toxicant in the environment due to its intake by the population; γ_1 the depletion rate of toxicant in the population due to their death or removal; and π the fraction of the toxicant which re-enters the environment due to death. The term $\beta_1 U$ in equation (2) takes into account of the portion that is returned to the environment even in the absence of x, since even though all population has died out, toxicants in their remains can still keep re-entering the environment ($\dot{T} > 0$ when x = 0 and T = 0).

SINGULAR PERTURBATION ANALYSIS

In order to carry out the analysis, we introduce the following change of variables and system parameters : $d_0 = \frac{\delta_0}{\epsilon} \;,\;\; \alpha = \frac{\alpha_1}{\epsilon} \;,\;\; d_1 = \frac{\delta_1}{\epsilon \delta} \;,\;\; \gamma = \frac{\gamma_1}{\epsilon \delta} \;,$ $\beta = \frac{\beta_1}{\epsilon \delta} \;,\;\; y = \epsilon T \quad \text{and} \quad z = \epsilon \delta U \;. \quad \text{We are led to the following system of differential equations.}$

$$\dot{x} = R(y)x - \frac{x^2}{k(y)} \equiv f(x, y) \tag{4}$$

$$\dot{y} = \varepsilon \left[-d_0 y - \alpha x y + \pi \gamma x z + \beta z \right] = g(x, y, z) \tag{5}$$

$$\dot{z} = \varepsilon \delta \left[-d_1 z + \alpha x y - \gamma x z \right] \equiv h(x, y, z) \tag{6}$$

where
$$R(y) \equiv r(T)$$
 and $k(y) \equiv \frac{K(T)}{r_0}$.

Thus, during the transients, when the right hand sides of equations (4)-(6) are finite but different from zero, $|\dot{y}|$ is of the order ε and $|\dot{z}|$ is of the order $\varepsilon\delta$. This means that, for small values of ε and δ , the change in the toxicant level in the population takes place more slowly than that in the environment, and the population has, in comparison, a very fast dynamics. This is quite a reasonable assumption in view of the field observations reported in the previously mentioned studies.

So that the following analysis may be carried out explicitly in a simple manner, we shall consider the case where the population birth-rate R has the form

$$R(y) \equiv A - By \tag{7}$$

where A and B are positive constants, while the effect of the toxicant level on the carrying capacity is negligent (k = constant).

Under the above assumptions, for small values of ϵ and δ , the solution of the system (4)-(6) for given initial conditions can be approximately found by means of singular perturbation analysis [13, 14]. First, the slow (z) and intermediate (y) variables are frozen at their initial values z(0) and y(0), and the evolution of the fast component of the system is determined by solving the "fast system"

$$\dot{\mathbf{x}} = \mathbf{f}(\mathbf{x}, \mathbf{y}(0)) \tag{8}$$

The fast variable x tends asymptotically to one of the stable equilibria of the fast system on which $\frac{\partial f}{\partial x} < 0$. Figure 1 shows how a fast transient develops toward an equilibrium manifold f = 0 of the fast system. Here, slow, intermediate, and fast transients are indicated by one, two, and three arrows, respectively.

Once the state of the system has reached the fast manifold f=0, the variable with intermediate speed begins to become active and we can now consider the "intermediate system".

$$\dot{\mathbf{y}}(t) = \mathbf{g}(\mathbf{x}(t), \mathbf{y}(t), \mathbf{z}(0)) \tag{9}$$

As before, the variable y(t) tends to a stable point of its equilibrium manifold g = 0. Thus, it is seen in Figure 1 that the trajectories start from the point B of the fast manifold and tend toward a stable point C of the intermediate manifold at intermediate speed.

At this point, a slow transient develops subject to the constraints

$$f(x,y) = g(x,y,z) = 0$$
 (10)

and brings us to a stop at a stable equilibruim point D where f = g = h = 0 or reaches the point U where the manifold f = g = 0 becomes unstable and a saddle-node bifurcation occurs. A catastrophic transition at a very high speed takes place from U to a stable point E on an equilibrium manifold.

The directions in which the transitions take place are determined by the signs of f, g, or h as each state variable becomes active. If ϵ and δ remain small, the resulting trajectory composed of all such transients of different speeds represents a close approximation to the actual solution trajectory of the model equations in the sense that the solution trajectory will lie in a small tube about these transients and the radius of the tube tends to zero with ϵ and δ .

More detailed description of the singular perturbation technique can be found in [13] and [14], while examples of its application to mathematical models can be found in [15] and [17].

DESCRIPTION OF THE EQUILIBRIUM MANIFOLDS

In order to determine the structure of the attractors and the nature of the transients, we now identify the various equilibrium manifolds.

The Fast Manifolds

The manifold f = 0 has 2 parts; namely, the trivial manifold x = 0 and the nontrivial one which is a surface parallel to the z axis given by the equation

$$x = a - by \tag{11}$$

where a = Ak and b = Bk

The surface in (11) crosses the (x,z)-plane along the line

$$y = \frac{a}{b} \tag{12}$$

as seen in Figure 2.

Since

$$\frac{\partial f}{\partial x} = \frac{1}{k} [(a - by) - x] - \frac{1}{k}$$
 (13)

it is clear that $\frac{\partial f}{\partial x} < 0$ on the surface given by the equation [11], and thus the nontrivial fast manifold is always stable.

The Intermediate Manifold

This manifold is given by the equation g = 0 which defines a surface

$$z = \rho(x, y) \tag{14}$$

It intersects the nontrivial fast manifold along the curve

$$z = \rho(a - by, y) = \frac{(d_0 + a\alpha)y - \alpha by^2}{(\beta + \pi a\gamma) - \pi b\gamma y}$$
(15)

We observe that this curve intersects the (x,y)-plane (z=0) at the points where

$$y = 0$$

and

$$y = \frac{a}{b} + \frac{d_0}{b\alpha} \tag{16}$$

Thus, the curve f = g = 0 reaches the (y,z)-plane in the first octant if

$$d_0 > 0 \tag{17}$$

Now, differentiating (15) with respect to y, we find that the numerator of $\frac{dz}{dy}$ along the curve f = g = 0 is

$$Num\left(\frac{dz}{dy}\right)_{f=g=0} = (d_0 + a\alpha)(\beta + \pi a\alpha) - 2b\alpha(\beta + \pi a\gamma)y + \pi b^2\alpha\gamma y^2$$
 (18)

Therefore the curve f = g = 0 has a stationary point when the left hand side of (18) vanishes. However, we find that the two roots of (18) are

$$y_{1,2} = \frac{2b\alpha(\beta + \pi a \gamma) \pm \Delta}{2\pi b^2 \alpha \gamma} = \frac{a}{b} + 2b\alpha\beta \pm \Delta$$
 (19)

where

$$\Delta = 2b \left[(\beta + \pi a \gamma) \left(\alpha^2 \beta - \pi \alpha \gamma d_0 \right) \right]^{\frac{1}{2}}$$
 (20)

Thus, for $y_{1,2}$ to be real, we require that

$$\beta > \frac{\pi \gamma \delta_0}{\alpha} \tag{21}$$

Moreover, for at least one root to be less than $\frac{a}{b}$, we need

$$2b\alpha\beta - 2b\left[(\beta + \pi a\gamma)\left(\alpha^2\beta - \pi\alpha\gamma d_0\right)\right]^{\frac{1}{2}} < 0$$
 (22)

Squaring and rearranging (22) lead to the requirement that

$$\beta > \frac{\pi a \gamma d_0}{a \alpha - d_0} \tag{23}$$

provided

$$a\alpha - d_0 > 0 \tag{24}$$

At this point, we note that since

$$\frac{\pi a \gamma d_0}{a \alpha - d_0} > \frac{\pi \gamma d_0}{\alpha} \tag{25}$$

the conditions (21) and (23) are quaranteed by the requirement that (23) and (24) hold.

The Slow Manifold

This is the surface h = 0 which defines a surface

$$z = \varphi(x, y) \tag{26}$$

that intersects the fast manifold f = 0 along the curve given by

$$z = \varphi(a - by, y) = \frac{a\alpha y - b\alpha y^{2}}{(d_{1} + a\gamma) - b\gamma y}$$
 (27)

for which z = 0 when y = 0 and $y = \frac{a}{b}$ (see Figure 2).

Thus, we can identify essentially 5 cases of different dynamical behavior as follows.

Case 1

This case is identified by the inequalities (23) and (24). The shape of the fast manifold is therefore as shown in Figure 2(a) and the curve f = g = 0 has a stationary point P above the (y, z)-plane and intersects the (y, z)-plane at the point H in the first octant.

Now, to also guarantee that the point S where f = g = h = 0 is below the point P we need that at $y = y_2$ we have

$$\frac{a\alpha y_2 - b\alpha y_2^2}{(d_1 + a\gamma) - b\gamma y_2} > \frac{(d_0 + a\alpha)y_2 - \alpha by_2^2}{(d_1 + \pi a\gamma) - \pi b\gamma y_2}$$
(28)

using (15) and (27).

Inequality (28) means that the part of the curve f = g = 0 from C to P lies "above" the surface h = 0 while the line DG lies "below" the surface h = 0. Looking at the sign of h, we see that h > 0 along CP and h < 0 along DG which determines the directions of the transients along these curves as shown in Figure 2(a). Moreover, for the curve f = g = 0 and f = h = 0 to be located with respect to each other as shown in Figure 2(a) we require that at y = 0, the slope along the curve f = g = 0 should be less than that along the curve f = h = 0. That is, we need

$$\frac{\mathrm{d}z}{\mathrm{d}y}\Big|_{\mathbf{f}=\mathbf{g}=\mathbf{0}} < \frac{\mathrm{d}z}{\mathrm{d}y}\Big|_{\mathbf{f}=\mathbf{h}=\mathbf{0}}$$

which leads to the inequality

$$\frac{d_0+a\alpha}{\beta+\pi a\gamma}<\frac{a\alpha}{d_1+a\gamma}$$

$$\beta > \frac{(d_0 + a\alpha)(d_1 + a\gamma)}{a\alpha} - \pi a\gamma \tag{29}$$

Starting from some initial point, say A (see Figure 2(a)), if A is above the nontrivial fast manifold, f < 0 here and a high speed transition will develop in the direction of decreasing x towards the stable fast manifold (point B). As B is approached, the intermediate system has become active and, since g < 0 here, a

transition of intermediate speed will develop along the fast manifold towards point C on the curve f = g = 0. As mentioned above, along this portion of the curve, h > 0 and so a slow transition develops in the direction of increasing z until the point P is reached, at which point the stability of the manifold is lost. A transition at a very high speed then takes place which brings us to the point D on the trivial manifold x = 0. Since we are now in the region where h < 0, transition develops slowly along the line $y = \frac{b}{a}$ until a point E is reached where the stability is again lost. The existence of such a point E in a similar system has been shown in a previous work by Osipov *et al.* [18]. For the point E to be to the right of G as in Figure 2(a), we further require that the second coordinate y_E of this point is positive, namely

$$y_{E} > 0 \tag{30}$$

However, considering (16), this is easily accomplished if b is made sufficiently small.

A quick jump from E will then take us back to the point F on the curve f = g = 0 which completes the closed cycle FPDEF in this case.

Thus, this is the case where the attractor is a limit cycle composed of a concatenation of catastrophic transitions occurring at different speeds, corresponding to the situation where persistence in the toxicant levels and the population density is observed exhibiting sustained oscillations in all three state variables.

Case 2

This case is shown in Figure 2(b), identified by the inequalities (24), (29) and the one opposite to (23), namely

$$\frac{\pi a \gamma d_0}{a \alpha - d_0} > \beta \tag{31}$$

This last inequality means that, in this case, the stationary point of the curve f = g = 0 is below the (y, z)-plane and the position of the manifolds are as shown in Figure 2(b).

Starting at an initial point A, transitions will develop as described before until C is reached, from which point a slow transition brings us to a stop at the stable equilibrium point S where f = g = h = 0.

This therefore corresponds to the case where population density and both toxicant levels attain stable equilibrium values as time passes.

Case 3

This case is identified by inequalities (23), (24) and the one opposite to inequality (29), namely

$$\beta < \frac{(d_0 + a\alpha)(d_1 + a\gamma)}{a\alpha} - \pi a\gamma \tag{32}$$

Thus, in this case, once we are at the point B on the fast manifold (see the Figure 2(c)), h < o here and a slow transition will develop along the curve f = g = 0 in the direction of decreasing z instead. This takes us to a stop on the x-axis (y = z = 0)

This is therefore the case where toxicants eventually get depleted and the population re-establishes itself as time passes.

Case 4

This case is identified by the inequalities (23), (24), (29), and the opposite to inequality (28), namely

$$\frac{a\alpha y_2 - b\alpha y_2^2}{(d_1 + a\gamma) - b\gamma y_2} < \frac{(d_0 + a\alpha) - \alpha b y_2^2}{(d_1 + \pi a\gamma) - \pi b\gamma y_2}$$
(33)

This last inequality means that the point S is above P on the curve f = g = 0 as seen in Figure 2(d).

Again the transitions develop from A to B then to C as before. However, a slow transition from C will stop at the point S since here f = g = h = 0. This is also the case where each state variable attains an equilibrium value as time progresses.

Case 5

This last case is identified by (23), (24), (29), and

$$y_{E} < 0 \tag{34}$$

However, considering (16), condition (34) can be satisfied if b is made sufficiently large.

The manifolds are then positioned as shown in Figure 2(e). The transitions, once P is reached, will make a quick jump to the point D on the (y, z)-plane. Since the trivial manifold is stable troughout the line DG in this case, the slow transition from D will continue until G is reached where g < 0. Transition is then made toward the origin. This then corresponds to the case where the population becomes extinct and the toxicant in the population of course gets depleted as a result, while the toxicant level in the environment reaches a high level then slowly depletes itself as time passes.

By the above analysis, we have proved the following theorem.

Theorem If ε and δ are sufficiently small and inequalities (21) and (24) hold, then the system (4)-(6) has a unique global attractor in the first octant. The attractor will be a stable equilibrium point if (23), (29) and (33) hold or (29), and (31) hold, while it will be a limit cycle if inequalities (23), (28), (29) and (30) hold.

Numerical simulations of the system (4) - (6) when the parametric values are chosen to satisfy the requirements in each of the 5 cases are shown in Figure 3.

CONCLUSION

In this paper, we have analyzed a model for the effects of a toxin introduced into the environment of a single-species system. The population growth is logistic, while the time responses of the different state variables are assumed to increase from bottom to top. We have been able to identify five separate cases in which different dynamic behavior can be observed.

It has been shown that if the rate β at which the toxicant in the population re-enters the environment is higher than the levels given by inequilities (21) and (23) then toxicant will not get depleted to allow the population to recover its former level. If this is further compounded by the condition where the effect of toxicant on the birth-rate is too high (b>>1) then we can expect extinction of the species which is case 5 identified above.

Thus, the model has proved to be quite versatile and fits well with field observations, yielding greater insights into this perplexing problem of interactions among the population and the toxicants in the environment which is of great concern to us all.

ACKNOWLEDGEMENT

Appreciation is extended toward the National Research Council and the Thailand Research Fund for their financial support, without which this research effort would not have been possible.

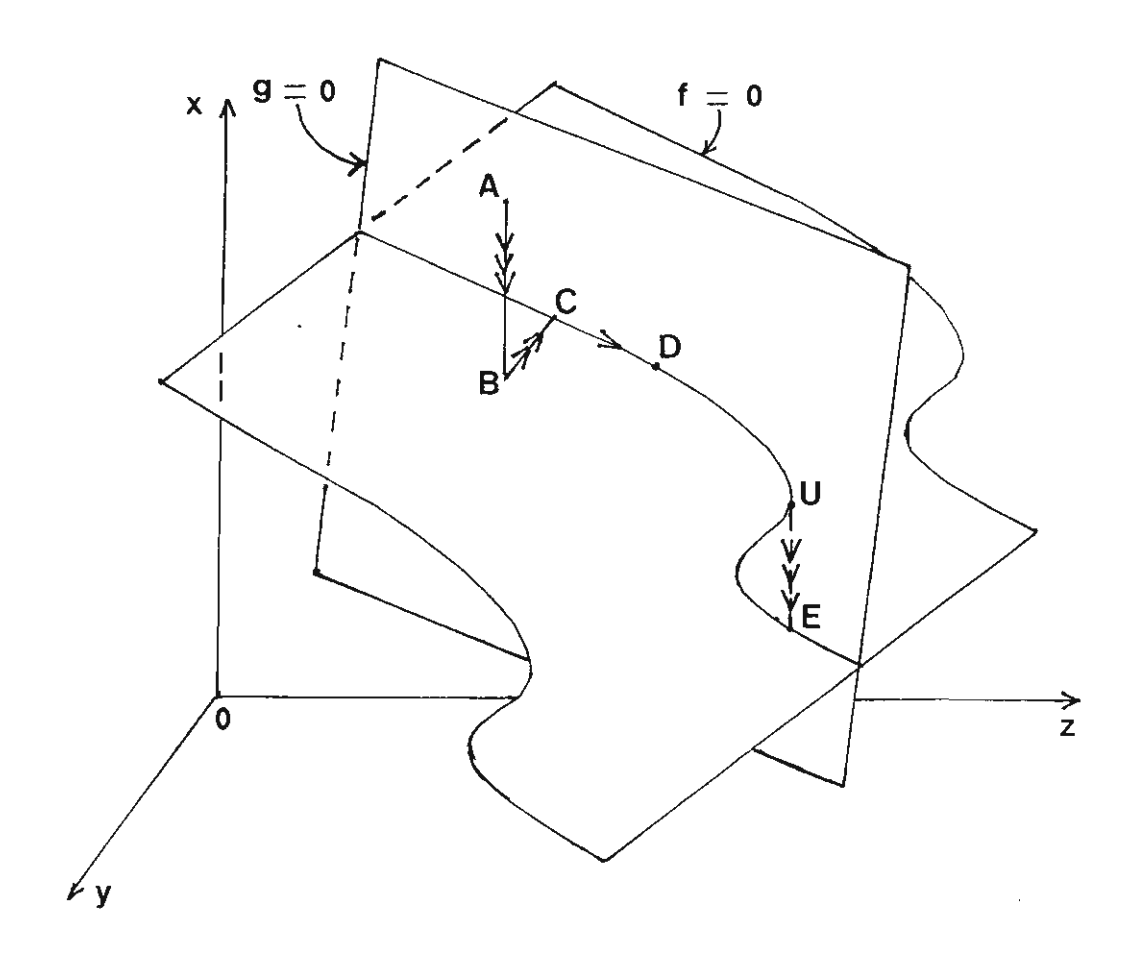
REFERENCES

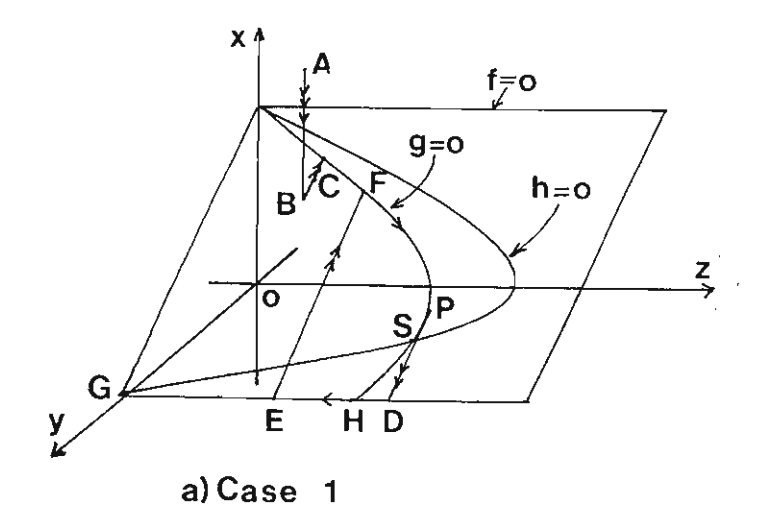
- [1] Nelson, S. A. (1970) The problem of oil polution of the sea. In: *Advances* in Marine Biology. London: Academic Press. pp.215-306.
- [2] Woodman, J. N., Cowling, E. B. Airborne chemicals and forest health. Environ. Sci. Technol. 21(1987)120-126.
- [3] Chen, P. H., Hsu, S.-T. (1987) PCB poisoning from toxic rice-bran oil in Taiwan. In: *PCBs and the Environment* (J. S. Waid, Ed.), Vol. III. Boca Raton: CRC Press. pp. 27-37.
- [4] Ryan, J. J. Variation of dioxins and furans in human tissues. Chemosphere. 15(1986)1585-1593.
- [5] Hallam, T. G., Clark, C. E., Lassiter, R. R. Effects of toxicants on populations: a qualitative approach I. Equilibrium environmental exposure. *Ecolog. Model.* **18**(1983)291-304.
- [6] Hallam, T. G., Clark, C. E., Lassiter, R. R. Effects of toxicants on populations: a qualitative approach II. First order kinetics. J. Math. Biol. 18(1983)25-37.
- [7] Hallam, T. G., Clark, C. E., Lassiter, R. R. Effects of toxicants on populations: a qualitative approach III. Environmental and food chain pathways. *J. Theor. Biol.* **109**(1984)411-429.
- [8] Luna, de J. T., Hallam, T. G. Effects of toxicants on populations: a qualitative approach IV. Resource-consumer-toxicant models. *Ecilog. Model.* 35(1987249-273.
- [9] Shukla, J. B., Freedman, H. I., Pal, V. N., Misra, O. P., Agrawal, M., Shukla, A. Degradation and subsequent regeneration of a forestry resource: a mathematical model. *Ecolog. Model.* 4(1989)219-229.

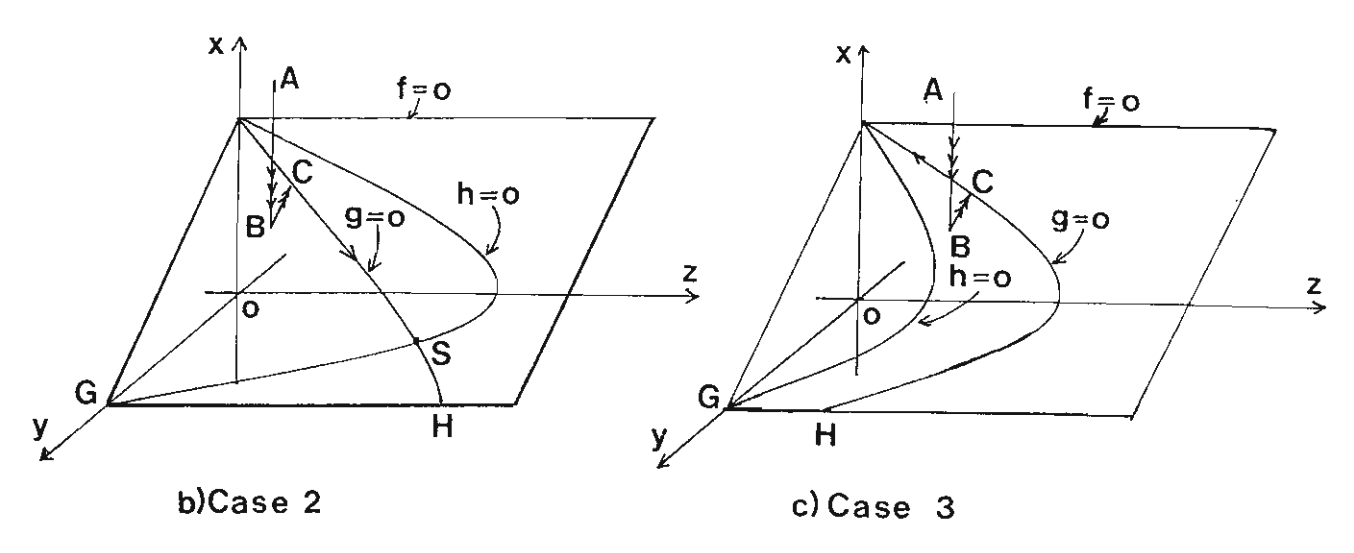
- [10] Carrier, G., Brunet, R., Brodeur, J. Modeling of the Toxicokinetics of Polychlorinated Dibenzo-p-dioxins and Dibenzofurans in Mammalians, Including Humans I. Nonlinear Distribution of PCDD/PCDF Body Burden between Liver and Adipose Tissues. *Toxicol. and Appl. Pharmacol.* 131(1995)253-266.
- [11] Carrier, G., Brunet, R., Brodeur, J. Modeling of the Toxicokinetics of Polychlorinated Dibenzo-p-dioxins and Dibenzofurans in Mammalians, Including Humans II. Kinetics of Absorbtion and Disposition of PCDDs/PCDFs. Toxicol. and Appl. Pharmacol. 131(1995)267-276.
- [12] Freedman, H. I., Shukla, J. B. Models for the effect of toxicant in single-species and predator-prey systems. *J. Math. Biol.* **30**(1991)15-30.
- [13] Zober, A., Papke, O. Concentrations of PCDDs and PCDFs in human tissue 36 years after accidental dioxin exposure. Chemosphere. 27(1993)413-418.
- [14] Muratori, S. An Application of the Separation Principle for Detecting Slow- Fast Limit Cycles in a Three-Diemnsional Systems. Appl. Math. Comput. 43(1991)1-18.
- [15] Muratori, S., Rinaldi, S. Low and High Frequency Oscillations in Three Dimensional Food Chain Systems. SIAM J. Appl. Math. 52 (1992) 1688-1706.
- [16] Muratori, S., Rinaldi, S. Remarks on Competitive Coexistence. SIAM J. Appl. Math. 49(1989)1462-1472.
- [17] Lenbury, Y., Likasiri, C., Novaprateep, B. Low- and High-Frequency Oscillations in a Food Chain Where One of the Competing Species Feeds on the Other. *Mathl. Comput. Modelling.* 20(1994)71-89.
- [18] Osipov, A. V., Soderbaka, G. Eirola, T. On the Existence of Positive Periodic Solutions in a Dynamical System of Two Predators-One Prey Type. Viniti Deponent n. 4305-B86. [In Russian].

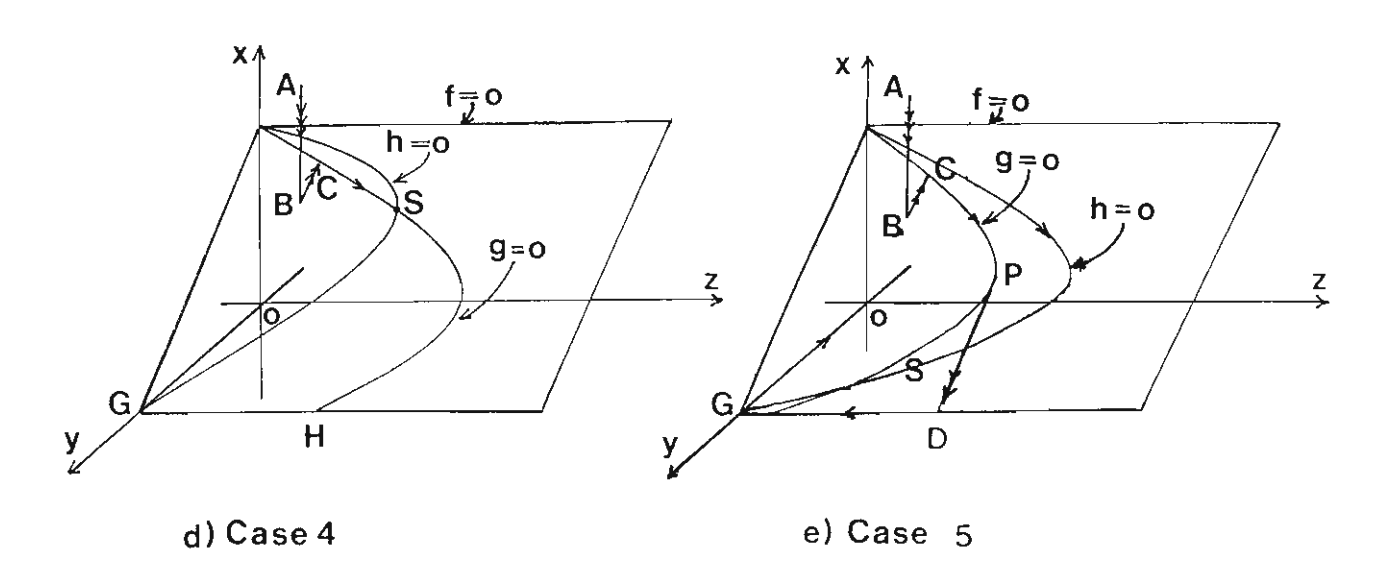
FIGURE CAPTION

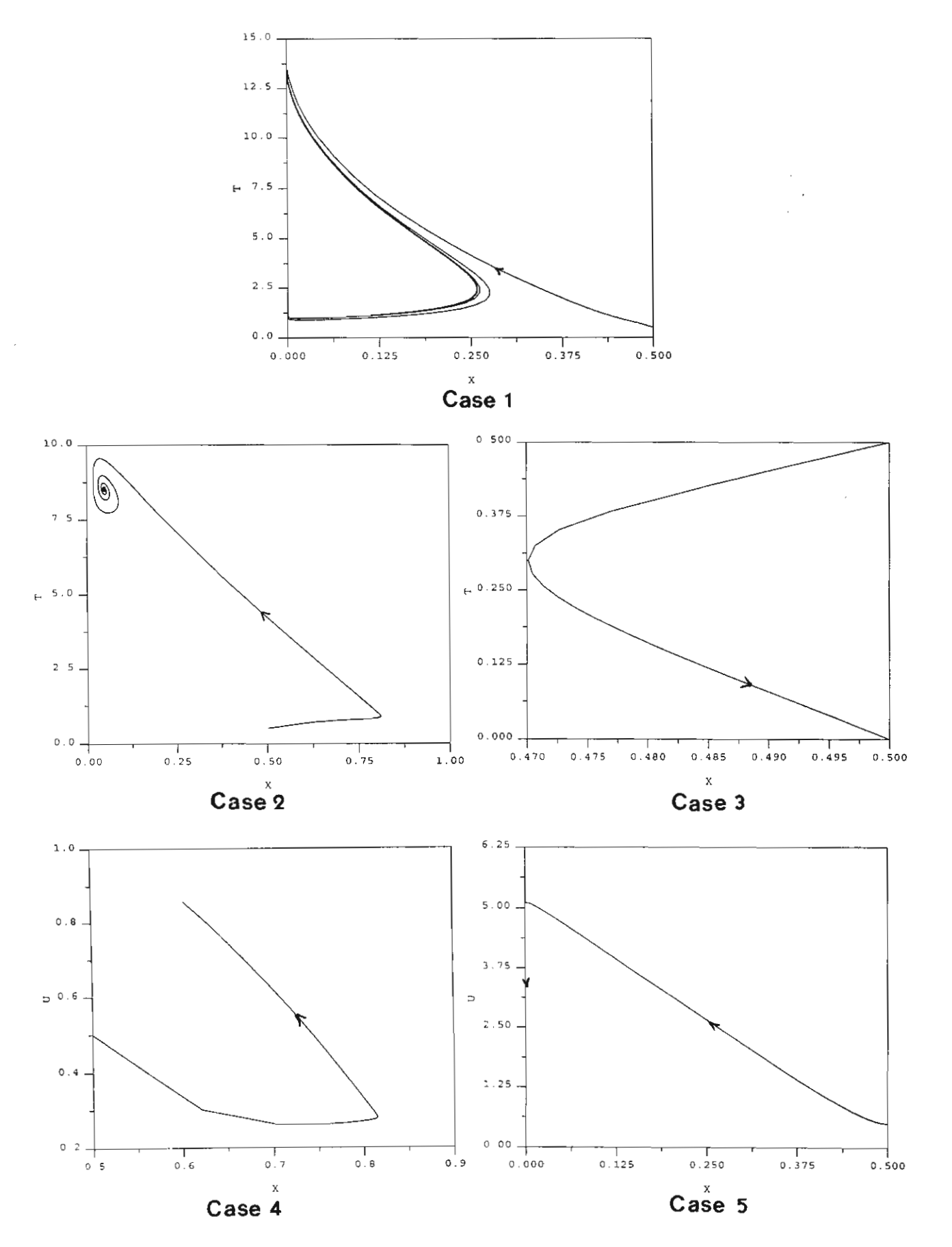
- Figure 1: A fast (f = 0), intermediate (g = 0), and slow (h = 0) equilibrium manifolds, with the fast (triple arrow), intermediate (double arrow) and slow (single arrow) transients.
- Figure 2: The solution trajectories of the system (4)-(6) in the five cases identified in the text. The attractor is a limit cycle in Case 1, and an equilibrium in Case 2, or 4. The population recovers itself in Case 3, but becomes extinct in Case 5.
- Figure 3: Numerical simulations of the system (4)-(6) for each of the five cases identified in the text. Here, $\varepsilon=\delta=k=1$; Case1: a=0.5, b=0.1, $\alpha=0.9$, $\beta=0.9$, $\gamma=0.9$, $\pi=0.9$, $d_0=0.3$, $d_1=0.01$; Case 2: a=0.9, b=0.1, $\alpha=0.5$, $\beta=0.9$, $\gamma=0.9$, $\pi=0.9$, $d_0=0.4$, $d_1=0.01$; Case 3: a=0.5, b=0.1, $\alpha=0.9$, $\beta=0.5$, $\gamma=0.9$, $\pi=0.1$, $d_0=0.3$, $d_1=0.01$; Case 4: a=0.9, $d_0=0.1$, $d_1=0.5$; Case 5: $d_0=0.5$, $d_0=0.1$, $d_1=0.5$; $d_0=0.001$, $d_1=0.01$.











4.2 ผู้วิจัยยังได้ทำการวิเคราะห์ model system (62)-(64) โดยใช้ bifurcation analysis เพื่อพิจารณาแบ่งแยก phase space ลักษณะต่าง ๆ ตามจำนวนของ transients และ attractors ได้เป็น phase space 11 แบบที่แตกต่างกัน

ผลงานวิจัยในส่วนนี้ได้นำเขียนขึ้นเป็น paper และได้รับตีพิมพ์แล้วใน The Mahidol University Journal ตามเอกสารที่แนบมาด้วยต่อไปนี้

Dynamical Modelling of the Effect of Toxicants on a Single-Species Ecosystem

DYNAMICAL MODELLING OF THE EFFECT OF TOXICANTS ON A SINGLE-SPECIES ECOSYSTEM

Yongwimon Lenbury*
Siriporn Hongthong
Nardtida Tumrasvin

Department of Mathematics
Faculty of Science, Mahidol University
Rama 6 Rd., Bangkok 10400
Thailand
scylb@mahidol.ac.th

^{*} to whom all correspondences should be addressed.

DYNAMICAL MODELLING OF THE EFFECT OF TOXICANTS ON A SINGLE-SPECIES ECOSYSTEM

ABSTRACT

We consider a mathematical model of the effect of toxicants on single-species in a closed homogeneous environment. The population birth-rate as well as the carrying capacity are assumed to be directly effected by the level of toxicant in the environment as it is absorbed by the population. The toxicant level in the population can be depleted at a constant specific rate, a part of which amount may return to the environment even in the absence of any living organisms. A Hopf bifurcation analysis is carried out yielding boundary conditions which divide the parametric plane into regions of different dynamical behavior. It is found that when the natural birth rate of the population is too low, no non-trivial equilibrium state exists in the system. At a fixed sufficiently high natural birth rate, the system can settle back to its former stable equilibrium state after the initial dumping of toxicant into the environment, provided that the rate at which the toxicant in the population returns to the environment is not too high. Sustained oscillation in the population and toxicant levels is exhibited for suitable ranges of parametric values. However, if the per capita decay rate or birth rate is too low, the system no longer admits a stable non-trivial equilibrium state if the return rate is too high, and population may become extinct.

Keywords: toxicants, modelling, single species, bifurcation.

INTRODUCTION

The question of effects of pollutants and toxicants on ecological communities has become of grave concern to scientists, environmental agencies and authorities on a global scale, especially in the past decade or so. Toxic substances are persistent and bioaccumulate, and therefore contaminate air, water, and most living organisms, including humans. Accidental intoxication by these substances can result in chronic effects and the possible toxicological consequences can no longer be disregarded. In one of their papers, Xober and Papke [1] reports the incidents where concentrations of Polychlorinated Dibenzo-p-dioxins and Dibenzofurans (PCDDs and PCDFs) in human tissues can be detected 36 years after accidental dioxin exposure.

Several efforts have been made to qualitatively describe and study the effects of toxicants and pollutants on various ecosystems. In a series of papers by Hallam and his coworkers [2-5], analytical study was caried out utilizing various mathematical models. Shukla *et al.* [6] later studied a mathematical model for the degradation and subsequent regeneration of forestry resource. More recently, in papers by Carrier *et al.* [7-8], attempts were made to model the toxicokinetics of PCDDs and PCDFs in mammalians, including humans.

Realistically, a great number of sociological and physiological factors play a part in the dynamics of toxicological pathways in nature. The resulting mathematical model can be quite complexed, handled mainly by powerful computers, and requires a great number of field data for its validation.

A relatively less complicated model involving only a few mathematical equations is often preferred for its capability to give a deep understanding and a great deal to new valuable insights to the system under study, while requiring fewer data for its verification. It can moreover give policy makers the much needed preliminary information to justify their decision or choice of actions concerning important environmental issues.

In [9], Freedman and Shukla proposed a model for the effect of toxicant in single species systems and one for predator-prey polluted systems. The interactions of the population level (X) and toxicants in the population (U) and in the environment (T) are modelled by means of ordinary differential equations in terms of their concentrations with respect to mass or volume of the total environment in which the population lives.

In their model for a single-species system, the amount of toxicant in the population is depleted due to their death, some of which re-entering the environment in proportion to the population biomass. Such a model was found to exhibit no oscillatory behavior in the case that there is no more dumping of toxicants after the initial instantaneous introduction. It was shown that provided that the pollutant concentration was not sufficient to kill all the population, eventually the toxicant would be removed and the population would recover to its former level. However, cases have often been found in nature in which this is not so, and persistence of toxicant levels in the population and the environment have often been observed such as in the earlier mentioned paper by Xober and Papke [1].

In this paper, we therefore consider single-species in a closed homogeneous environment, in which the carrying capacity and the population birth-rate are both affected by the exogeneous introduction of toxicant. By modifying the model proposed by Freedman and Shukla [9], we allow the toxicant in the population to reenter the environment, a part of which amount varies directly as the toxicant level in the population alone. This will account for the portion of toxicant in the population carcasses which may keep re-entering the closed environment even in the dwindling presence ($x \approx 0$) of the living organism.

We are interested in determining the different dynamics that may result from the effects of toxicants on such a closed ecosystem. Application of the Hopf bifurcation analysis allows us to derive boundary conditions which delineate the parametric plane into regions of different dynamic behavior. It is shown that, after an initial dumping of toxicant into the environment, if the toxicant level in the population and the environment keep decaying at a constant per capita degradation rate, the system can settle back to its former stable equilibrium state provided that the rate at which toxicant in the population re-enters the environment is not too high. However, if the natural birth rate is too low, the non-trivial equilibrium state no longer exists. Moreover, even for high natural birth rate, the equilibrium state can become unstable, and sustained oscillation in the population and toxicant levels is observed if the return rate is high enough.

THE SYSTEM MODEL

Following Freedman and Shukla [9], we let

$$X(t) = \frac{\text{concentration of the population biomass}}{\text{mass (or volume) of the total environment where the population lives}}$$

$$T(t) = \frac{\text{concentration of the toxicant in the environment}}{\text{mass (or volume) of the total environment where the population lives}}$$

$$U(t) = \frac{\text{concentration of the toxicant in the total population}}{\text{mass (or volume) of the total environment where the population lives}}$$

It shall be assumed that the population growth is logistic, while the absorbtion of the toxicant in the environment by the population causes the birth-rate (R) of X to diminish. We therefore assume that R depends explicitly on T with the following properties:

$$R(0) = r_0 > 0 (1)$$

$$R(T) < 0 \text{ for } T \ge 0 \tag{2}$$

and
$$R(\overline{T}) = 0$$
 for some \overline{T} . (3)

The carrying capacity K(T) of the environment is also effected by the level of toxicant in the environment and has the following general properties

$$K(T) = K_0 > 0 \tag{4}$$

and
$$K'(T) < 0 \text{ for } T \ge 0.$$
 (5)

The toxicant levels in the environment, and in the population, have natural depletion (or decaying) rates of δ_0 and δ_1 , respectively. The toxicant in the environment is also depleted at a per capita rate α_1 due to its intake by the population. On the other hand, the toxicant in the population is depleted at a per capita rate of γ due to death or removal, a fraction of which amount re-enters the environment. We therefore arrive at the following system of ordinary differential equations.

$$\frac{dX}{dt} = R(T)X - \frac{r_0 X^2}{K(T)}$$
 (6)

$$\frac{dT}{dt} = -\delta_0 T - \alpha_1 X T + f(X, U) \tag{7}$$

$$\frac{dU}{dt} = -\delta_1 U + \alpha_1 XT - \gamma_1 XU \tag{8}$$

where the last term f(X,U) of equation (7) accounts for the fraction of toxicant in the population which returns to the environment. Since this return rate must increase with the increase in X or U, while in the absence of living organisms (X = 0) toxicant can still keep re-entering the environment at a positive rate which necessarily depends on the level of toxicant in the population (U) at that moment in time. The function f(X,U) is thus assumed to have the form

$$f(X,U) = \pi \gamma_1 X U + \beta U \tag{9}$$

where π, γ_1 , and β are positive constants.

STEADY STATES AND THEIR STABILITY

For the following analysis, we shall assume that the population natural birthrate has the form

$$R(T) = r_0 - r_1 T$$
, $r_0 > 0$, $r_1 > 0$. (10)

which satisfies the properties (1)-(3) with $r_0 > and \overline{T} = \frac{r_0}{r_1}$. We will also carry out the analysis for the case where the effect of toxicant on the carrying capacity K is negligible and therefore K = constant.

In order to carry out the stability analysis, we introduce the following change of variables and system parameters : $x=\frac{r_0X}{K},\ y=T,\ z=U,\ a=r_0,\ b=r_1,$ $d_0=\delta_0, \alpha=\frac{K\alpha_1}{r_0}, \gamma=\frac{K\gamma_1}{r_0}, \text{ and } d_1=\delta$

The model equations (6)-(8) with (9) can then be written as

$$\frac{\mathrm{dx}}{\mathrm{dt}} = (a - by)x - x^2 \tag{11}$$

$$\frac{dy}{dt} = -d_0y - \alpha xy + \pi \gamma xz + \beta z \tag{12}$$

$$\frac{dz}{dt} = -d_1 z + \alpha xy - \gamma xz \tag{13}$$

The system of equations (11)-(13) thus admits three steady states, namely

- i) the washout steady state: (x,y,z) = (0,0,0)
- ii) washout of toxicant only: (x,y,z) = (a,0,0)
- iii) the nonwashout steady state(s), $(\bar{x}, \bar{y}, \bar{z})$ satisfying

$$(a - b\overline{y}) - \overline{x} = 0 \tag{14}$$

$$-\mathbf{d}_{0}\overline{\mathbf{y}} - \alpha \overline{\mathbf{x}}\overline{\mathbf{y}} + \pi \gamma \overline{\mathbf{x}}\overline{\mathbf{z}} + \beta \overline{\mathbf{z}} = 0 \tag{15}$$

$$-\mathbf{d}_{1}\overline{\mathbf{z}} + \alpha \overline{\mathbf{x}}\overline{\mathbf{y}} - \gamma \overline{\mathbf{x}}\overline{\mathbf{z}} = 0 \tag{16}$$

Solving equations (14)-(16) for \overline{x} , we find

$$\overline{x}_{1,2} = \frac{\delta \pm \sqrt{\delta^2 - 4(1-\pi)\alpha\gamma d_0 d_1}}{2(1-\pi)\alpha\gamma}$$
(17)

where

$$\delta = \alpha \beta - d_0 \gamma - d_1 \alpha$$

Then

$$\overline{y} = \frac{a - \overline{x}}{b}$$

and

$$\overline{z} \ = \ \frac{\alpha \overline{x} \overline{y}}{d_1 + \gamma \overline{x}} \ = \ \frac{\alpha \overline{x} (a - \overline{x})}{d_1 + \gamma \overline{x}}$$

We note that if

$$\beta < \frac{d_0 \gamma + d_1 \alpha}{\alpha} \tag{18}$$

then $\delta < 0$ and both \bar{x}_1 and \bar{x}_2 are negative and have no physical meaning in our system. Moreover, for values of β such that

$$\delta^2 < 4(1-\pi)\alpha\gamma d_0d$$

the term under the square root sign in (17) is negative. The system therefore admits only the washout steady states until β crosses the critical value

$$\beta_{c} = \frac{1}{\alpha} \left[2\sqrt{(1-\pi)\alpha\gamma d_{0}d_{1}} + d_{0}\gamma + d_{1}\alpha \right]$$
 (19)

at which point the system undergoes a saddle node bifurcation and two more steady states appear which move further apart as β increases. As β increases even further, one of the roots given in (17) becomes negative as shown in Figure 1, and the bigger β gets the roots can become either negative or bigger than a, in which case $\overline{y} = \frac{a - \overline{x}}{b} < 0$, leaving us with only the two washout steady states, as shown in the bifurcation diagram presented in Figure 1.

The Jacobian matrix evaluated at the trivial steady state (0,0,0) is

$$J_{0} = \begin{bmatrix} a & 0 & 0 \\ 0 & -\delta_{0} + \beta & 0 \\ 0 & 0 & -\delta_{1} \end{bmatrix}$$
 (20)

one of whose eigenvalues is always positive (namely a), and one is always negative $(-\delta)$. This means that the washout steady state (0,0,0) is a saddle point for all positive values of the system parameters and thus the dashed line along the β -axis signifying that the trivial steady state $\overline{x} = 0$ is unstable.

The Jacobian matrix of the system (11-(13)) evaluated at the steady state (a,0,0) is

$$J_{\mathbf{a}} = \begin{bmatrix} -\mathbf{a} & -\mathbf{a}\mathbf{b} & 0\\ 0 & -\mathbf{d}_{0} - \alpha\mathbf{a} & \pi \gamma \mathbf{a} + \beta\\ 0 & \alpha\mathbf{a} & -\mathbf{d}_{1} - \gamma \mathbf{a} \end{bmatrix}$$

and the corresponding eigenvalues are -a and

$$\frac{\Delta \pm \sqrt{\Delta^2 - 4[(d_0 + \alpha a)(d_1 + \gamma a) - \alpha a(\pi \gamma a + \beta)]}}{2}$$
 (21)

where

$$\Delta = -d_0 - d_1 - \alpha a - \gamma a.$$

Expanding Δ^2 , we find that the term under the square root sign in (21) is always positive. Moreover, the term will be less than Δ^2 if

$$\beta < \frac{(d_0 + \alpha a)(d_1 + \gamma a)}{\alpha a} - \pi \gamma a \equiv \beta'$$
 (22)

in which case the steady state (a,0,0) will be a stable node since $\Delta < 0$. On the other hand if

$$\beta > \beta'$$
 (23)

then the point will be an unstable saddle point since one of the eigenvalues will be positive.

The Jacobian matrix evaluated at the nontrivial steady state $(\bar{x}, \bar{y}, \bar{z})$, whenever it exists, is

$$\bar{J} = \begin{bmatrix}
-\bar{x} & -b\bar{x} & 0 \\
-\alpha\bar{y} + \pi\gamma\bar{z} & -d_0 - \alpha\bar{x} & \pi\gamma\bar{x} + \beta \\
\alpha\bar{y} - \gamma\bar{z} & \alpha\bar{x} & -d_1 - \gamma\bar{x}
\end{bmatrix}$$
(24)

when \bar{x} , \bar{y} , and \bar{z} satisfy equations (14) through (16). The corresponding characteristic equation is

$$\lambda^3 + a_2 \lambda^2 + a_1 \lambda + a_0 = 0. {(25)}$$

where

$$a_0 = b\overline{x} [(\pi \gamma \overline{z} - \alpha \overline{y})(d_1 + \gamma \overline{x}) + (\pi \gamma \overline{x} + \beta)(\alpha \overline{y} - \gamma \overline{z})]$$
 (26)

$$a_1 = \overline{x} [d_0 + d_1 + (\alpha + \gamma)\overline{x}] + b\overline{x} (\pi \gamma \overline{z} - \alpha \overline{y})$$
 (27)

$$a_2 = d_0 + d_1 + (1 + \alpha + \gamma)\overline{x}$$
 (28)

If we let

$$q = \frac{1}{3}a_1 - \frac{1}{9}a_2^2 \tag{29}$$

$$r = \frac{1}{6}(a_1a_2 - 3a_0) - \frac{1}{27}a_2^3 \tag{30}$$

$$S_1 = [r + (q^3 + r^2)^{\frac{1}{2}}]^{\frac{1}{3}}$$
 (31)

$$S_2 = [r - (q^3 + r^2)^{\frac{1}{2}}]^{\frac{1}{3}}$$
 (32)

In region II, however, $a_0 > 0$ while $a_1 a_2 > a_0$ and the real parts of all 3 eigenvalues are negative. The non-trivial steady state is therefore a stable spiral node in this case. As time passes, all trajectories starting from its neighborhood will spiral toward the equilibrium point where $\bar{x} = \bar{x}_2$.

In region III, $a_0 > 0$ and $a_1a_2 < a_0$ and limit cycle behavior can be observed resulting from a Hopf bifurcation from the steady state solution which has now become unstable. It is found numerically that the bifurcated limit cycle is stable throughout this region.

Schematic diagram of different dynamic behavior and transients which may be observed in each of the 10 ranges of parametric value β ; namely, A through J, are shown in Figure 1. Here, solid lines indicate stability, dashed ones indicate unstability, while closed dots represent stable limit cycles resulting from supercritical bifurcation and increasing in amplitude as β increases. The numbers of possible transients or attractors in each of the 10 ranges, A through J, are given in Table 1.

In fact, substituting (26)-(28) into (40) and (42), we find that Hopf bifurcation occurs for values of β for which $a_1a_2 < a_0$ or equivalently,

$$\beta > \beta_1^* \equiv \frac{a_2 x_2 (\theta_1 + \theta_2) + (a_2 - \theta_1) (\pi \gamma \overline{z}_2 - \alpha \overline{y}_2) b \overline{x}_2}{b \overline{x}_2 (\alpha \overline{y}_2 - \gamma \overline{z}_2)} - \pi \gamma \overline{x}_2$$
 (43)

as well as $a_0 > 0$ which is equivalent to

$$\beta > \beta_2^* \equiv \frac{(\pi \gamma \bar{z}_2 - \alpha \bar{y}_2)\theta_1}{\gamma \bar{z}_2 - \alpha \bar{y}_2} - \pi \gamma \bar{x}_2 \tag{44}$$

where

$$\bar{y}_2 = \frac{a - \bar{x}_2}{b}$$

$$\bar{z}_2 = \frac{\alpha \bar{x}_2 \bar{y}_2}{d_1 + \gamma \bar{x}_2}$$

with

$$\theta_1 = d_0 + \alpha \overline{x}_2$$

$$\theta_2 = d_1 + \gamma \overline{x}_2$$

Thus, Hopf bifurcation occurs for values of β such that

$$\beta > \max(\beta_1^*, \beta_2^*) \tag{45}$$

In Figure 1, four different possibilities in region III are schemetically shown according to the value of β' relative to the values β_c , β_1^* and β_2^* .

Finally, numerical simulations of the model system (11)-(13) in the different cases discussed above are shown in Figure 3, in which parametric values for Figures 3(a), 3(b), and 3(c) are chosen to be in region I, II, and III of Figure 2, respectively. The corresponding time series of the various cases are shown in Figure 4, where sustained oscillation is observed when the paremetric values fall inside the region III where periodic solution has been predicted. In region II, on the other hand, the trajectory is seen to first approach the origin, which is a saddle point, then gets repulsed as the population recovers itself and returns to its equilibrium value at the stable steady state (a, 0, 0). However, if in this region we have a very low degradation rate and birth rate and very high return rate, the population level x is capable of dropping all the way to zero. The toxicant level reaches a high level so fast that the population does not have time to recover itself, in which case the population can become extinct.

CONCLUSION

We have considered a mathematical model of the effect of toxicants on a single species system in a closed homogeneous environment. Application of the Hopf bifurcation analysis led us to the conclusion that if the return rate β , namely the rate at which the toxicant in the population re-enters thee environment is sufficiently low, a stable non-trivial equilibruim state exists in which case the population persists while the toxicant level may degenerate to zero or tend toward an acceptable level. However, for a fixed value of the self degradation rate d_0 and birth rate r_0 , if β increases beyond the critical values β_1^* and β_2^* given in the paper, the system becomes unstable and the toxicant level can rise to an undesirably high level. Through our analysis, we found that the system can exhibit up to 10 different types of phase space, and a possibility of up to 5 transients or attractors.

This study of the various dynamic behavior which is possible in such an important process should serve as a useful tool for trying to understand and efficiently control such interesting but complexed ecosystems.

ACKNOWLEDGEMENT

Appreciation is extended toward the National Research Council and the Thailand Research Fund for their financial support, without which this research effort would not have been possible.

REFERENCES

- [1] Zober, A., Papke, O. Concentrations of PCDDs and PCDFs in human tissue 36 years after accidental dioxin exposure. *Chemosphere* **27** (1993) 413-418.
- [2] Hallam, T.G., Clark, C.E., Lassiter, R.R. Effects of toxicants on populations: a qualitative approach I. Equilibrium environmental exposure. *Ecolog. Model.* **18** (1983) 291-304.
- [3] Hallam, T.G., Clark, C.E., Lassiter, R.R. Effects of toxicants on populations: a qualitative approach II. First order kinetics. *J. Math. Biol.* **18** (1983) 25-37.
- [4] Hallam, T.G., Clark, C.E., Lassiter, R.R. Effects of toxicants on populations: a qualitative approach III. Environmental and food chain pathways. *J. Theor. Biol.* **109** (1984) 411-429.
- [5] Luna, de J.T., Hallam, T.G. Effects of toxicants on populations: a qualitative approach IV. Resource-consumer-toxicant models. *Ecolog. Model* **35** (1987) 249-273.
- [6] Shukla, J.B., Freedman, H.I., Pal, V.N., Misra, O.P., Agrawal, M., Shukla, A. Degradation and subsequent regeneration of a forestry resource: a mathematical model. *Ecolog. Model.* 4 (1989) 219-229.
- [7] Carrier, G., Brunet, R., Brodeur, J. Modeling of the Toxicokinetics of Polychlorinated Dibenzo-p-dioxins and Dibenzofurans in Mammalians, Including Humans I. Nonlinear Distribution of PCDD/PCDF Body Burden between Liver and Adipose Tissues. *Toxicol. and Appl. Parmacol.* 131 (1995) 253-266.

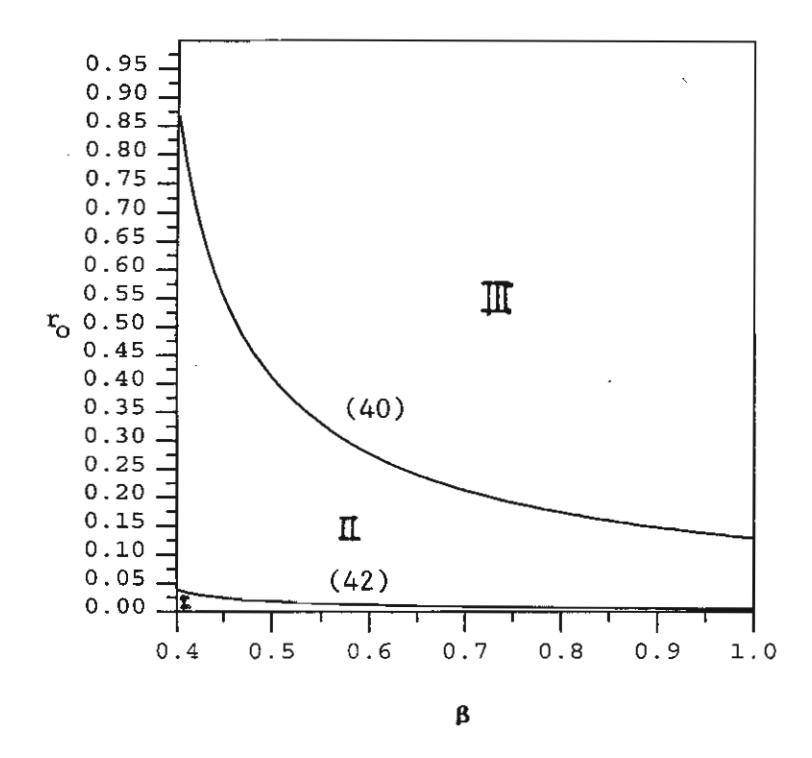
- [8] Carrier, G., Brunet, R., Brodeur, J. Modeling of the Toxicokinetics of Polychlorinated Dibenzo-p-dioxins and Dibenzofurans in Mammalians, Including Humans II. Kinetics of Absorbtion and Diposition of PCDDs/PCDFs Body Burden between Liver and Adipose Tissues. *Toxicol. Parmacol.* 131 (1995) 267-276.
- [9] Freedman, H.I., Shukla, J.B. Models for the effect of toxicant in single-species and predator-prey systems. J. Math. Biol. 30 (1991) 15-30.
- [10] Marsden, J.E., and McCracken M., 1976, The Hopf Bifurcation and its Applications (Springer-Verlag, New York) pp. 65-135.

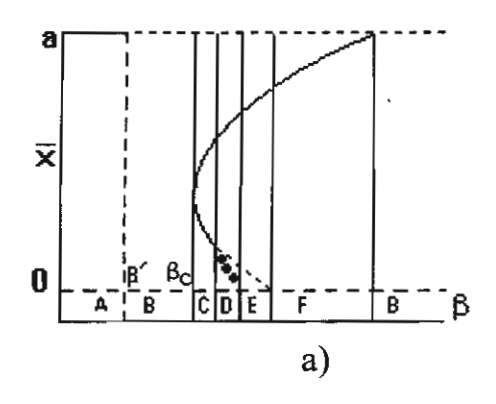
	A	В	С	D	E	F	G	Н	I	J
stable node	1	-	2	\ 1	1	1	3	2	2	2
unstable node	ı	-	-	1	1	-	ı	1	1	-
saddle point	1	2	2	2	2	2	1	1	1	1
limit cycle	-	-	-	1	-	-	-	1	- :	-
Total	2	2	4	5	4	3	4	5	4	3

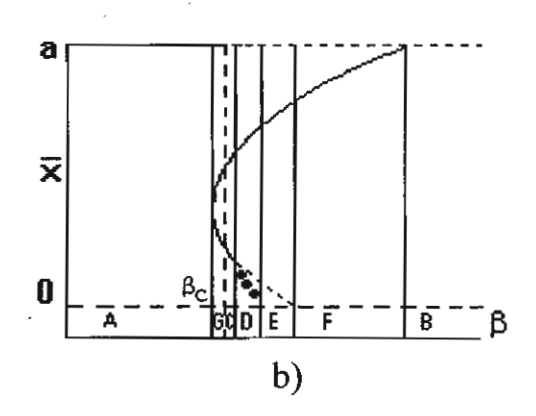
Table 1

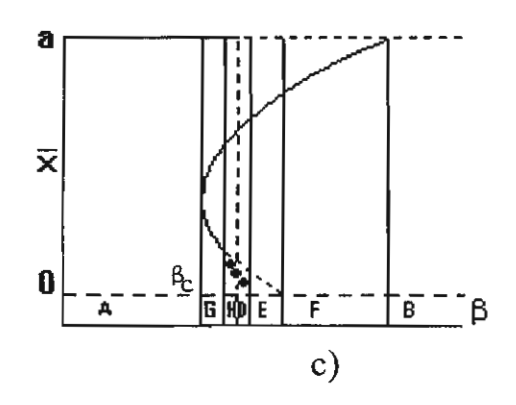
FIGURE CAPTION

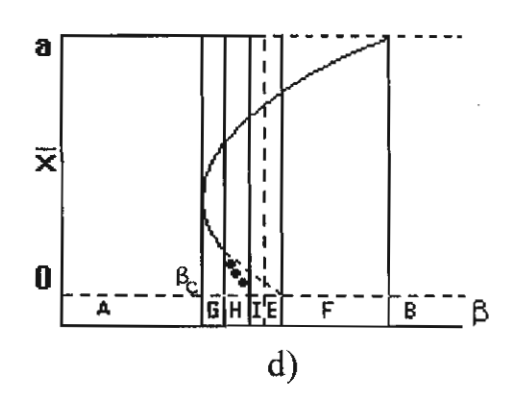
- FIGURE 1. Schemetic diagrams to present \overline{x} as a function of β , showing five different cases which are possible, in the region III of Figure 2, for various values of the parameter β . The dashed lines indicate unstable steady states, the solid lines indicate stable ones, while the closed dots indicate stable limit cycles. The dashed vertical line is the line $\beta = \beta$, whose relative position gives rise to 10 possible types of phase space; A through J.
- FIGURE 2. The graphs of equations (40) and (42) divide the (β, r_0) plane into 3 regions of different dynamic behavior. Here, b=1, $d_0=0.3$, $d_1=0.01$, $\alpha=0.9$, $\pi=0.9$, $\gamma=0.9$.
- FIGURE 3. Numerical simulations of the model system (11)-(13). The parametric values are chosen so that a) $(\beta, r_0) = (0.4, 0.03)$ in Region I of Figure 2, where the solution trajectory is seen to approach the washout steady state, which is a saddle point, then gets repulsed. b) $(\beta, r_0) = (0.36, 0.5)$ in Region II, where the nontrivial steady state S is a stable spiral node, and c) $(\beta, r_0) = (0.55, 0.6)$ in Region III, where a limit cycle is observed as theoretically predicted.
- FIGURE 4. The time series of the solutions to the model equations (11)-(13) in the cases a), b), and c) of Figure 3, respectively.
- TABLE 1. Number of transients or attractors in each of the cases A through J as indicated in Figure 1.

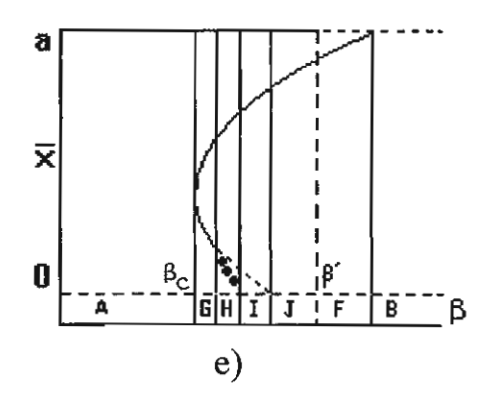


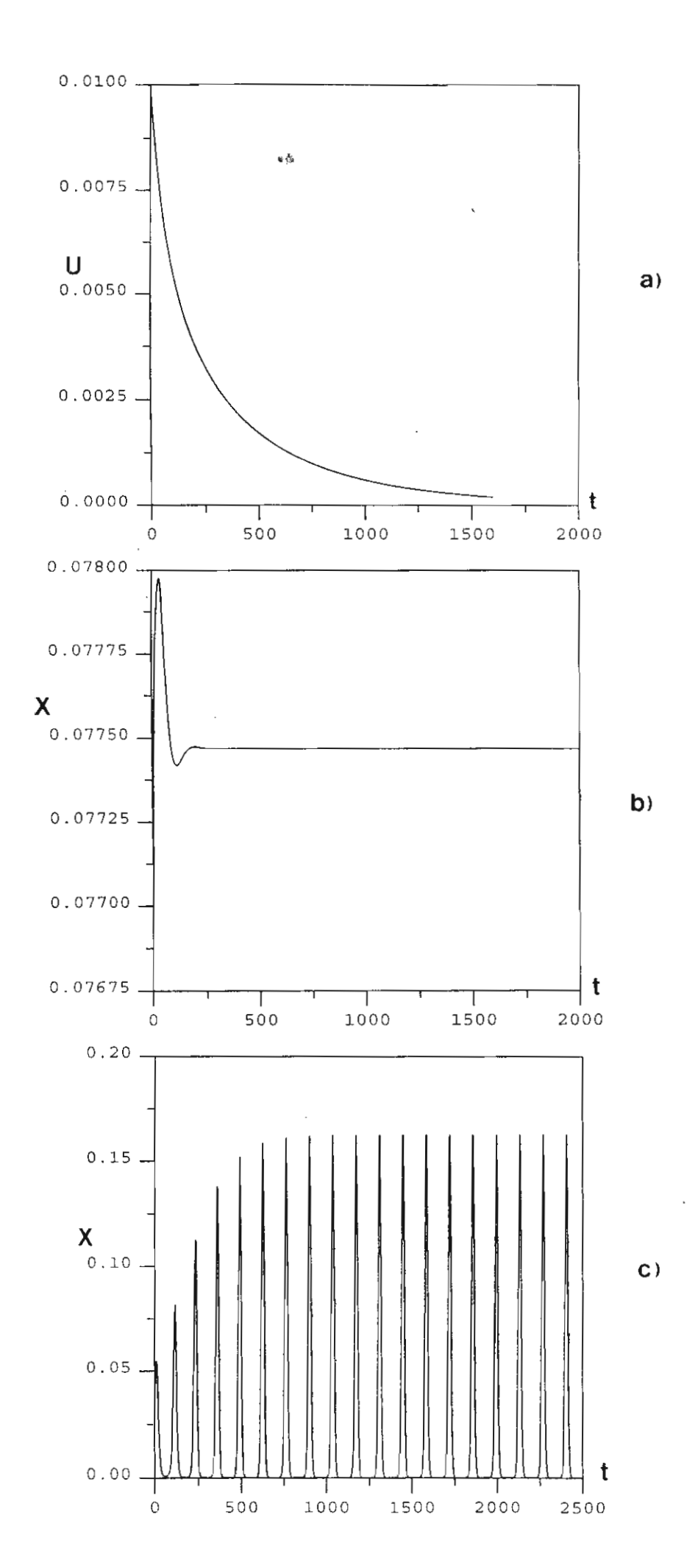




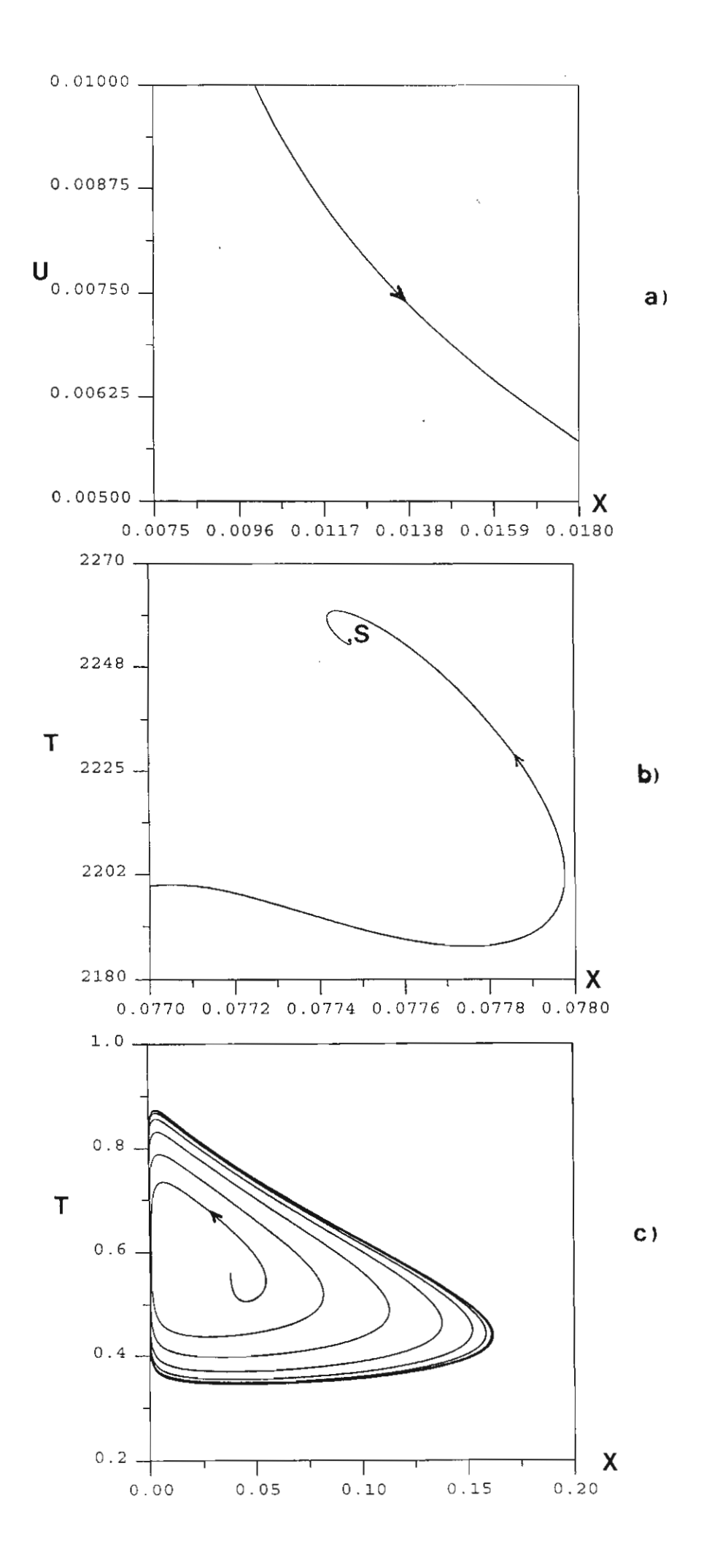








FIG



TIG.

สรุปและข้อเสนอแนะ

โครงการวิจัยนี้ได้บรรลุตามวัตถุประสงค์ที่เสนอไว้ ทั้งยังมีผลงานตีพิมพ์เผยแพร่ในวารสาร มากกว่าจำนวนที่กำหนดไว้ในแบบเสนอโครงการ

ทั้งนี้ทุนที่ผู้วิจัยได้รับจาก สำนักงานกองทุนสนับสนุนการวิจัย เป็นแรงจูงใจและเกื้อ หนุนอย่างดีเยี่ยมที่อำนวยให้ผู้วิจัยมีเวลาว่างจากภาระงาน และความรับผิดชอบด้านครอบครัวและ เศรษฐกิจ และสามารถหันมาใช้เวลาอย่างจริงจังกับงานวิจัย จึงเป็นผลให้ผู้วิจัยมีผลงานลงตีพิมพ์เป็น จำนวนมากกว่าในอดีตที่ผ่านมา โดยที่ภายในระยะเวลา 3 ปี ของการรับทุนของ สำนักงานกองทุน สนับสนุนการวิจัย ผู้วิจัยสามารถมีผลงานตีพิมพ์ และเสนอในที่ประชุมนานาชาติรวม 10 ชิ้น ทั้งที่ เกี่ยวกับโครงการนี้ และนอกเหนือไปจากงานวิจัยในโครงการ

อนึ่งการวิจัยทางด้านคณิตศาสตร์นั้นใช้งบประมาณด้านวัสดุน้อย เพียงแต่ใช้กระดาษ และ ดินสอก็จริง แต่จำเป็นต้องใช้เวลายาวนานในการคิดวิเคราะห์อย่างต่อเนื่อง จึงถือได้ว่าความสนับ สนุนทางด้านเงินอุดหนุนค่าครองชีพจาก สำนักงานกองทุนสนับสนุนการวิจัย เป็นปัจจัยที่สำคัญยิ่งที่ ผลักดันให้ผู้วิจัยได้มีผลงานวิจัยซึ่งมีจำนวนและคุณภาพที่สูงกว่าในอดีต

การวิเคราะห์วิจัยแบบจำลองทางคณิตศาสตร์ ซึ่งอธิบายปรากฏการณ์ในธรรมชาติที่เป็น ระบบนิเวศวิทยาอันสำคัญ ทำให้เกิดความเข้าใจที่ดีขึ้นเกี่ยวกับระบบนั้น และเพิ่มขีดความสามารถให้ แก่หน่วยงานที่เกี่ยวข้องกับปัญหาของสิ่งแวดล้อมทุกรูปแบบที่จะเกิดขึ้นอย่างเลี่ยงเสียมิได้ โดยผู้เกี่ยว ข้องเหล่านี้จะสามารถแก้ไขปัญหาต่าง ๆ นั้นได้อย่างมีประสิทธิภาพ หรือสามารถปรับปรุงระบบการ ผลิตพันธุ์ต่าง ๆ ให้ได้ผลดียิ่งขึ้น ทั้งยังสามารถคิดค้นวิธีการ และเทคโนโลยีใหม่ ๆ ในการจัดการกับ สภาพสิ่งแวดล้อมที่กำลังเสื่อมลง และพันธุ์พืชและสัตว์หลาย ๆ ชนิดที่กำลังจะสูญไป ปัญหาเหล่านี้ ต้องการความเข้าใจที่ดี และสมควรต้องได้รับการศึกษาให้ลึกซึ้งอย่างต่อเนื่องต่อไป

สรุป Output ของโครงการ

Publication ในวารสารวิชาการระดับนานาชาติ

- 1 Lenbury, Y. and Orankitjaroen, S. Dynamic Behavior of Membrane Permeability Sensitive Model for a Continuous Bio-reactor Exhibiting Culture Rhythmcity. J. Sci. Soc. Thailand. 21 (1995) 97-114.
- 2 Lenbury, Y. Singular Perturbation Analysis of a Model for a Predator-prey System Invaded by a Parasite. BioSystems. 39 (1996) 251-262.
- 3 Lenbury, Y., Sukprasong, B. and Novaprateep, B. Bifurcation and Chaos in a Membrane Permeability Sensitive Model for a Continous Bioreactor. *Mathl. Comput. Modelling.* 24 (1996) 37-48.
- 4 Lenbury, Y. and Tumrasvin, N. Singular Perturbation Analysis of a Model for the Effect of Toxicant on a Single-Species System. Mathl. and Comput. Modelling. In press.
- 5 Lenbury, Y., Hongthong, S. and Tumrasvin, N. Dynamical Modelling of the Effect of Toxicants on a Single-Species Ecosystem. The Mahidol University Journal. In press.

วารสารที่คาดว่าจะพิมพ์

- 1 Lenbury, Y., Puttapiban, P. and Amornsamarnkul, S. Modelling Effects of High Product and Substrate Inhibition on Oscillatory Behavior in Continuous Biorecators. *Mathematical Modelling of Systems*. Submitted.
- 2 Lenbury, Y., Rattanamongkonkul S. and Tumrasvin, N. Predator-Prey-Parasite Interaction by Singular Purturbation Analysis. To be submitted for publication in the *Ecological Modelling*.

การเสนอผลงานในที่ประชุมวิชาการ

- 1 Lenbury, Y. How Can Nonlinear Dynamics Elucidate Mechanisms Relevant to Issues of Environmental Management and Global Change? The Second Asean Mathematical Conference. October 17-20, 1996. Suranaree University of Technology.
- 2 Lenbury, Y. Singular Perturbation Analysis of a Product Inhibition Model for Continuous Bio-Reactors. International Conference on Dynamical Systems and Differential Equations. May 29-June 1, 1994. Southwest Missouri State University, U.S.A.
- 3 Lenbury, Y. and Tumrasvin, N. Singular Perturbation Analysis of a Model for the Effect of Toxicant on a Single-Species System. International Conference on Nonlinear Systems in Biology and Medicine. July 17-20, 1996. Veszprem, Hungary.

ผลงานอื่น ๆ

- 1 สามารถผลิตบัณฑิตปริญญาโทสาขาคณิตศาสตร์ประยุกต์ให้สำเร็จการศึกษาไปแล้ว 2 คน โดยนักศึกษาทำงานวิจัยในโครงการนี้ แล้วนำผลการวิจัยเขียนขึ้นเป็นวิทยานิพนธ์
- 2 มีนักศึกษาปริญญาโทที่จะสำเร็จการศึกษาภายในปลายปี พ.ศ. 2540 อีก 2 คน
- 3 มีนักศึกษาสาขากณิตศาสตร์ระดับปริญญาตรีที่ทำ senior project ร่วมในโครงการวิจัยนี้ และ สำเร็จการศึกษาไปแล้ว 2 คน

เป็นการผลิตนักวิจัยรุ่นใหม่ให้กับวงการวิจัยค้านคณิตศาสตร์ประยุกต์ในประเทศ ระหว่างปี พ.ศ. 2538-2540 รวมทั้งสิ้น 6 คน (ปริญญาโท 4 คน, ปริญญาตรี 2 คน)

บรรณานุกรม

- Agrawal, P., Lee, C., and Lim, H.C., and Ramkrishna, D., Theoretical Investigations of Dynamic Behavior of Isothermal Continuous Stirred Tank Biological Reactors. *Chemical Engineering Science*. 37 (1982)3, pp. 453-462.
- 2. Aris, R., 1978, Mathematical Modelling Techniques. (Pitman, London) 127-129.
- 3. Baines, H.A., Hawkes, C.H.H., and Jenkis, S.H., Protozoa as Indicators in Activated Sludge Treatment. Sewage and Industral Wastes. 25 (1953) 9: 1023-1033,
- 4. Begley, S., Service, R., and Underhill, W., 1992, Finding Order in Chaos, Newsweek, May 25: 50-54.
- Borzani, W., Gregori, R.E., and Vairo, M.L.R., Some Observations on Oscillator Changes in the Growth Rate of Sacharomyces Cerevisiae Inaerobic Continuous Undisturbed Culture.
 Biotech. Bioeng. 19 (1979) 1363-1374.
- Canale, R.P., Predator-prey Relationships in a Model for the Activated Process. Biotechnol. Bioeng. 11 (1969) 887-907.
- Canale, R.P., 1970, An Analysis of Models Describing Predator-prey Interaction. Biotechnol. Bioeng. 12 (1970) 353-378.
- Carrier, G., Brunet, R., and Brodeur, J., Modleing of the Toxicokinetics of Polychlorinated
 Dibenzo-p-dioxins and Dibenzofurans in Mammalians, Including Humans I. Nonlinear
 Distribution of PCDD/PCDF Body Burden between Liver and Adipose Tissues. *Toxicol. and Appl. Parmacol.* 131 (1995) 253-266.
- Carrier, G., Brunet, R., and Brodeur, J., Modeling of the Toxicokinetics of Ploychlorinated Dibenzo-p-dioxins and Dibenzofurans in Mammalians, Including Humans II. Kinetics of Absorbtion and Diposition of PCDD/PCDF Body Burden between Liver and Adipose Tissues. Toxicol. and Appl. Parmacol. 181 (1995) 267-276.
- 10. Cheng-Fu, J., Existence and Uniqueness of Limit Cycles in Continuous Cultures of Microorganisms with Non-constant Yield Factor. Universita degli studi di Bari, Italy. (Preprint).
- 11. Connell, J., Ecology 42 (1961) 710
- 12. Dubrov, A.P., 1974, The Geomagnetic Field and Life. (Plenum Press, Niw York.): 20-45.

- 13. Elton, C., and Nicholson, J., J. Anim . Ecol. 11 (1942) 215.
- Freedman, H.I., and Waltman, P., Mathematical Analysis of Some Three-species Food-chain Models. Math. Biosci. 33 (1977) 257-276.
- 15. Freedman, H.I., Math. Biosc. 99 (1990) 143.
- Freedman, H.I., and Shukla, J.B., Models for the Effect of Toxicant in Single-species and Predator-prey System. J. Math. Biol. 30 (1991) 15-30.
- Goldberger, A.L., Regney, D.R., and West, B.J., Chaos and Fractals in Human Physiology.
 Scientific American. (1990) Feb. : 35-41.
- Hallam, T.G., Clark, C.E., and Lassiter, R.R., Effects of Toxicants on Populations: a
 Qualitative Approach I. Equilibrium Environmental Exposure. Ecolog. Model. 18 (1983)

 291-304.
- Hallam, T.G., Clark, C.E., and Lassiter, R.R., Effects of Toxicants on Populations: a
 Oualitative Approach II. First Order Kinetics J. Math. Biol. 18 (1983) 25-37.
- Hallam, T.G., Clark, C.E., and Lassiter, R.R., Effects of Toxicants on Populations: a
 Qualitative Approach III. Environmental and Food Chain Pathways. J. Theor. Biol. 109

 (1984) 411-429.
- Hassard, B.D., Kazarinoff, N.D., and Wan, Y.H., 1981, Theory and Applications of Hopf Bifurcation. (Cambridge University Press, Cambridge.): 16.
- 22. Haukelikian, H., and Gurbaxani, M., Effect of Certain Physical and Chemical Agents on the Bacteria and Protozoa of Activated Sludge. Sewage. Warks Journal. 21 (1949) 5: 811-817.
- Herbert, D., Elsworth, R., and Telling, R.C., The Continuous Culture of Bacteria; a Theoretical and Experimental Study. J. Gen. Microbiol. 14 (1956) 601-622.
- Herrero, A.A., and Gomez, R.F., Development of Ethanal Tolerance in Clostridium
 Thermocellum: Effects of Growth Temperature. Appl. Environ. Microbiol. 40 (1980) 571.
- Hong, F.T., Photoelectric and Magneto-orientation Effects in Pigmented Biological Membranes. J. Colloid and Interface Sci. 58 (1977) 471.
- Hoppensteadt, F., Asymptotic Stability in Singular Perturbation Problems II: Problems
 Having Matched Asymptotic Expansions. J. Differential Equations. 15 (1974) pp. 510-512
- 27. Jenkis, S.H., Role of Protozoa in the Activated Sludge Process. Nature 150 (1942) 607.

- Koch, A.L., Competitive Coexistence of Two Predators Utilizing the Same Prey under Constant Environmental Conditions. J. Theoret. Population Biol. 44 (1974) 387-395.
- 29. Lackey, J.B., Biology of Sewage Treatment. Sewage Works Journal. 21 (1949) 4:649.
- Lenbury, Y., and Chiaranai C., Direction of the Sustained Oscillation Trajectory in the Cell-product Phase Plane Describing Product Inhibition on Continuous Fermentation Systems. Acta Biotechnol. 7 (1987) 6: 433-437.
- Lenbury, Y., and Punpocha, M., The Effect of the Yield Expression on the Existence of Oscillatory Behavior in a Three-Variable Modle of a Continuous Fermentation System Subject to Product Inhibition. *BioSystems*. 22 (1988) 273-278.
- Lenbury, Y., and Punpocha, M., On the Stability of Periodic Solutions for a Product Inhibition Model of Continuous Biological Reactors. J. Gen. Appl. Microbiol. 35 (1989) 269-279.
- Lenbury, Y., and Likasiri C., Low- and High-frequency Oscillations in a Food Chain Where One of the Competing Species Feeds on the Other. Mathematical and Computer Modelling. 20 (1994) 71-89.
- Lenbury, Y., and Siengsanan, M., Coexistence of Competing Microbial Species in a Chemostat Where One Population Feeds on Another. Acta Biotechnol. 13 (1993) 1-18.
- Lenbury, Y., Novaprateep, B., and Wiwatpataphee, B., Dynamic Behavior Classification of a Model for a Continuous Bio-Reactor Subject to Product Inhibition. *Mathl. Comput.* Modelling. 19 (1994) 12: 107-117.
- 36. Lotka, A.J., Essays on Growth and Form, Oxford U. Press, New York (1945).
- Luna, de J.T., and Hallam, T.G., Effects of Toxicants on Populations: a Qualitative
 Approach IV. Resource-consumer-toxicant Models. Ecolog. Model. 35 (1987) 249-273.
- 38. Marsden, J.E., and McGracken, M., 1976, The Hopf Bifurcation and its Applications (Springer-Verlag, New York): 65-135.
- McKinney, R.E., and Gram, A., Protozoa and Activated Sludge. Sewage and Industrial Wastes. 28 (1956) 1219-1231.
- Monod, J., recherces pur la croessance des cultures bacteriennes, Hermann et Cie, Paris, 1942.
- Muratori, S., and Rinaldi, S., Remarks on Competitive Coexistence, SIAM J. APPL.
 MATH. 49 (1989) 5, pp. 1462-1472.

- 42. Muratori, S., and Rinaldi, S., A Separation Condition for the Existence of Limit Cycles in Slow-fast Systems. Report CTS, CNR, Politechnico di Milano, Milano, Italy. (1991).
- 43. Muratori, S., and Rinaldi, S., Low- and High-frequency Oscillations in Three Dimensional Food Chain Systems. SIAM J. APPL. MATH. 52 (1992) 6, 1688-1706.
- 44. Nhung, T.V., and Anh, T.T., preprint IC/93/321 ICTP
- Paladino, O., Transition to Chaos in Continuous Processes: Applications to Wastewater Treatment Reactors. Environmetrics 5 (1994) 57-70.
- Panchal, C.J., and Stewart, G.G., Regulatory Factors in Alcohol Fermentation. Proc. Int.
 Yeast Sysmp. 5 (1981) 9.
- Paruleka, S.J., Semones, G.B., Rolf, M.J., Lievense, J.C.M. and Lim, H.C., Induction and Elimination of Oscillations in Continuous Cultures of Saccharomyces Cerevisiae. *Biotech. Bioeng.* 28 (1986) 5: 700-710.
- Pavlou, S., and Kevrehidis, I.G., On the Coexistence of Competing Microbial Species in a Chemostat under Cycling. Biotechnol. Bioeng. 35 (1990) 224-232.
- Pellegrini, L., and Biardi, G., Chaotic Behavior of Controlled CSTR. Computers and Chemical Engineering. 14 (1990) 1237-1247.
- Rinaldi, S., and Muratori, S., Limit Cycles in Slow-fast Forest-pest Models. J. Theoret.
 Population Biol. 41 (1992) 26-43.
- 51. Rosenzweig, M.L. Science 175 (1992) 564.
- Schaffer, S., and May, W.M., Can Non-linear Dynamics Elucidate Mechanisms in Ecology and Epidemiology. IMA J. Math. Appl. Med. Biol. 2 (1985) 221-252.
- Shukla, J.B., Freedman, H.I., Pal, V.N., Misra, O.P., Agrawal, M., and Shukla, A.,
 Degradation and Subsequent Regeneration of a Forestry Resource: a Mathematical Model.
 Ecolog. Model. 4 (1989) 219-229.
- Thomas, D.S., and Rose, A.H., Inhibitory Effect of Ethanol on Growth Solute Accumulations by Saccharomyces Cerevisiae as Affected by Plasma-membrane Lipid Composition. Arch. Microbiol. 122 (1979) 49.
- Volterra, V., Variazioni e fluctuazioni del numero di individui in speci animali conventi..
 R. Commun. Talassografico Italiano. 131 (1927) 1 142.

- Yano, T., Dynamic Behavior of the Chemostat Subject to Substrate Inhibition.
 Biotechnology and Bioengineering. 11 (1960) 130-153.
- Yano, T., and Koga, S., Dynamic Behavior of the Chemostat Subject to Product Inhibition.
 J. Gen. Appl. Microbiol. 19 (1973) pp. 97-114.
- 58. Yerushalmi, L., Volesky, B., Votruba, J., and Molnar, L., Circadian Rhythmicity in Fermentation Process. *App. Microbiol. Biotchnol.* **30** (1989) 460-474.
- 59. Zober, A., and Papke, O., Concentrations of PCDDs and PCDFs in Human Tissue 36 Years after Accidental Dioxin Exposure. *Chemosphere* **27** (1993) 413-418.

ประวัตินักวิจัย

1. General Information

First name Yongwimon Last Name Lenbury

Maiden name Wiriyawit Date of Birth 23 August 1952

Place of work Department of Mathematics, Faculty of Science, Mahidol University,

Rama 6 Rd., Bangkok 10400. Tel. 274-9893

Address 177 Soi Chantanachart, Bangsue, Bangkok 10800. Tel. 587-7903

2. Qualifications

B.Sc. with A2 Honours (Applied Mathematics) Australian National University, 1976.

M.Sc. (Applied Mathematics) Australian National University, 1978.

Ph.D. (Mathematics) Vanderbilt University, U.S.A., 1985.

3. Honours

1971-1977 Columbo Plan Scholarship, the Australian Government.

1975 The P. Bok Prize for the Best Female Science Student of the year,

Australian National University.

1993 The Outstanding Research Work of the Year Award (in Physical Science),

The National Research Council, Thailand.

1995-1996 Research Award, Thailand Research Fund.

1995-1997 Cited in Marquis Who's Who in the World.

4. Experience

1 Dec. 1977 - 14 Sept. 1987 Lecturer, Department of Physic and Mathematics,

Faculty of Science, Mahidol University.

15 Sept. 1987 - 18 Oct. 1989 Asst. Prof., Department of Physic and Mathematics,

Faculty of Science, Mahidol University.

19 Oct. 1989 - 17 Sept. 1990 Asst. Prof., Department of Mathematics,

Faculty of Science, Mahidol University.

18 Dec. 1990 - Present Assoc. Prof., Department of Mathematics,

Faculty of Science, Mahidol University.

1990 - 1995 Chairman, Master of Science Program in Applied

Mathematics.

1990 - 1994 Asst. Chairman, Department of Mathematics,

Faculty of Science, Mahidol University.

5. List of Publications

 Wiriyawit, Y., 1977, Application of the Galerkin Method to Problems in Two Dimensional Compressible Fluid Flow: M.Sc. Thesis.

- 2. Lenbury, Y., Modelling of Fermentation Processes: Ph.D. Thesis.
- 3. Lenbury, Y., Steppan, J.J., Park, D.-H., Tanner, R.D. Modelling Oscillatory Behavior in Batch Fermentations. *Acta Biotechnol.* **6** (1986)1, 45-53.
- Lenbury, Y., Crooke, P.S., Tanner, R.D. Relating Damped Oscillations to Sustained Limit Cycles Describing Real and Ideal Batch Fermentation Processes. *BioSystems*. 19 (1986), 15-22.
- Lenbury, Y., Crooke, P.S. The Effect of the Specific Growth Rates and the Yield Expressions on Oscillations in a Two-Tank Fermentor. J. Sci. Soc. Thailand. 12 (1986), 171-186.
- Lenbury, Y., Chiaranai, C. Bifurcation Analysis of a Product Inhibition Model of a Continuous Fermentation Process. Appl. Microbiol. Biotechnol. 25 (1987), 532-534.
- Lenbury, Y., Chiaranai, C. Direction of the Sustained Oscillation Trajectory in the Cell-Product Phase Plane Describing Product Inhibition on Continuous Fermentation Systems. Acta Biotechnol. 7 (1987) 6, 433-437.
- Lenbury, Y., Punpocha, M. On the Stability of Periodic Solutions for a Product Inhibition Model of Continuous Biological Reactors. J. Gen. Appl. Microbiol. 35 (1989), 269-279.
- Lenbury, Y., Punpocha, M. The Effect of the Yield Expression on the Existence of Oscillatory Behavior in a Three-variable Model of a Continuous Fermentation System Subject to Product Inhibition. *BioSystems*. 22 (1989), 273-278.

- Lenbury, Y., Roongruangsorakarn, S., Tumrasvin, N. Parameter-Space Classification of the Dynamic Behavior of the Chemostat Subject to Product Inhibition. J. Sci. Soc. Thailand. 15 (1989), 281-291.
- Crooke, P., Tanner, R.D., Lenbury, Y. Investigation of the Volume Effect on a Simple Batch Fermentation Process. Math. Comput. Modelling 12 (1989), 1521-1530.
- 12. Lenbury, Y., Pacheenburawana, P. Modelling fluctuation phenomena in the plasma cortiol secretion system in normal man. *BioSystems*. **26** (1991), 117-125.
- Lenbury, Y., Pacheenburawana, P. Modelling Plasma Cortisol Secretion System in normal Man. 18th Congress on Science and Technology of Thailand. Bangkok, Thailand. 27-29 Oct., 1992. 678-679.
- 14. Lenbury, Y., Siengsanan, M. Dynamics of a Bio-reactor Where One Microbial Population Feeds on Another As Well As the Limiting Nutrient: a Model for the Activated Process. The Second Princess Chularbhorn Science Congress. Bangkok, Thailand. 2-6 Nov., 1992. 166.
- 15. Lenbury, Y., Siengsanan, M. Coexistence of Competing Microbial Species in a Chemostat Where one Population Feeds on Another. *Acta Biotechnol.* **13** (1993), 1.13-200.
 - Lenbury, Y., Novapratheep, B., Wattanapattapee, B. Dynamic Behavior Classification
 of a Model for a Continuous Bio-reactor Subject to Product Inhibition.

 Mathematical and Computer Modelling. 19 (1994), 107-117.
 - Lenbury, Y., Maneesawarng, C. Parameter Space Classification of Solutions to a
 Model for the Cortisol Secretion System in Normal Man. The 2nd Gauss Symposium:
 International Conference in Medical Physics and Mathematics. Munich, Germany.
 2-6 Aug. 1993. 56.
 - Lenbury, Y., Novapratheep, B. Theoretical Investigation of a Product Inhibition Model for a Continuous Culture: Effect of Yield Expression and Specific Growth Rate. J. Sci. Soc. Thailand. 20 (1994), 43-59.
 - Lenbury, Y., Likasiri, C. Low- and High-frequency Oscillations in a Food Chain Where One of the Competing Species Feeds on the Other. *Mathl. Comput. Modelling.* 20 (1994), 71-89.
 - 20. Lenbury, Y., Maneesawarng, C.A. (1994) Parameter Space Classification of

- Solutions to a Model for the Cortisol Secretion System in Normal Man, in Textbook of Biomedical Physics Horizon (Yeiweg Publiching House, Weisbaden, Germany)
 In Press.
- Lenbury, Y., Orankitjaroen, S. Dynamic Behavior of a Membrane Permeability Sensitive Model for a Continuous Bio-reactor Exhibiting Culture Rhythmicity.
 J. Soi. Soc. Thailand. 21 (1995), 97-116.
- Lenbury, Y., Kamnungkit, K. Detection of Slow-Fast Limit Cycles in a Model for Electrical Activity in the Pancreatic β-cell. IMA Journal of Mathematics Applied in Medicine and Biology. 13 (1996), 1-21.
- Lenbury, Y., Sukprasong, B., Novaprateep, B. Bifurcation and Chaos in a Membrane Permeability Sensitive Model for a Continuous Bio-Reactor. *Mathl. Comput. Modelling.* 24 (1996), 9: 37-48.
- Lenbury, Y. Singular Perturbation Analysis of a Model for a Predator-Prey System
 Invaded by a Parasite. BioSystems. 39 (1996), 251-262.
- 25. Lenbury, Y. How can Nonlinear Dynamics Elucidate Mechanisms Relevant to Issues of Environmental Management and Global Change? The Second Asean Mathematical Conference. October 17-20, 1996. Suranaree University of Technology.
- Lenbury, Y. Singular Perturbation Analysis of a Product Inhibition Model for Continuous Bio-Reactors. Proceedings of the International Conference on Dynamical Systems and Differential Equations. May 29 - June 1, 1996. Southwest Missouri State University, U.S.A.
- 27. Lenbury, Y. Singular Perturbation Analysis of a Model for the Effect of Toxicant on a Single-Species System. Special Issue of the Mathl. Comput. Modelling on the Proceedings of International Conference on Nonlinear Systems in Biology and Medicine. July 17-20, 1996. Veszprem, Hungary.

7. Research work presented in international conferences

- Lenbury, Y., Pacheenburawana, P. Modelling Plasma Cortisol Secretion System in normal Man. 18th Congress on Science and Technology of Thailand. Bangkok, Thailand. 27-29 Oct., 1992. 678-679.
- Lenbury, Y., Siengsanan, M. Dynamics of a Bio-reactor Where One Microbial Population Feeds on Another As Well As the Limiting Nutrient: a Model for the Activated Process. The Second Princess Chularbhorn Science Congress. Bangkok, Thailand. 2-6 Nov., 1992. 166.
- Lenbury, Y., Maneesawarng, C. Parameter Space Classification of Solutions to a
 Model for the Cortisol Secretion System in Normal Man. The 2nd Gauss Symposium:
 International Conference in Medical Physics and Mathematics. Munich, Germany.
 2-6 Aug. 1993. 56.
- Lenbury, Y. How can Nonlinear Dynamics Elucidate Mechanisms Relevant to Issues
 of Environmental Management and Global Change? The Second Asean Mathematical
 Conference. October 17-20, 1996. Suranaree University of Technology.
- Lenbury, Y. Singular Perturbation Analysis of a Product Inhibition Model for Continuous Bio-Reactors. International Conference on Dynamical Systems and Differential Equations. May 29 - June 1, 1994. Southwest Missouri State University, U.S.A.
- Lenbury, Y. Singular Perturbation Analysis of a Model for the Effect of Toxicant on a Single-Species. *International Conference on Nonlinear Systems in Biology and Medicine*. July 17-20, 1996. Veszprem, Hungary.